Enhancing chemotherapeutic responses in CNS malignancy through suppression of hyperactive DNA damage repair pathways

By

Marina Mostafizar

A thesis submitted to the Faculty of Graduate Studies of The University of Manitoba in Partial Fulfillment of the requirements for the degree of

MASTER OF SCIENCE

Department of Pharmacology and Therapeutics
Rady Faculty of Health Sciences
University of Manitoba
Winnipeg

ABSTRACT

Current methods to treat medulloblastoma (MB) and malignant glioma (MG) are highly intrusive with three-year survival. Recurrence is high due to chemoradio-resistance. We are targeting DNA repair pathways through inhibitors of DNA repair proteins; Poly (ADP-Ribose) Polymerase (PARP1i), DNA-dependent protein kinase (DNA-PKi) and Ataxia-Telangiectasia Mutated (ATMi) to sensitize tumours to DNA damaging agents. However, differing tumours have variable expression of these enzymes/repair pathway(s) activity, therefore; their identification and inhibition may enhance current treatment efficacy.

High-throughput comet assay revealed enhanced drug-mediated tumour cell death in MB cell lines with TOPI+PARP1i with activation of specific repair pathways. Further, RNA-Seq analysis revealed PARP1 upregulated in DAOYMB and downregulated in D283; while BRCA1 downregulated in DAOYMB and upregulated in D283MB, suggesting defective Homologous recombination (HRR) pathway, hence synthetic lethality in MB cell line (DAOYMB). Therefore, I have identified unique DNA repair enzymes, which may mediate specific differential chemo-radioresistant phenotypes in MB.

ACKNOWLEDGMENTS

First and foremost, I would like to thank my supervisor, Dr. Sachin Katyal for giving me the opportunity to work in his laboratory. I have learned a lot from him and gained research skills that will help me down the road for future research projects. I could not thank him enough for allowing me to develop and share my research knowledge among scientists.

I have had the opportunity to attend several conferences (national and international) and showcase my work. I also had the opportunity to work in collaboration with other laboratories. I have learned not only bench work but also developed networking skills. It would not have been possible without his guidance, immense support, patience and advice.

I would like to thank my committee members, Dr.Spencer Gibson and Dr. Michael Jackson for their help and advice throughout my research programme and for allowing me to finish this project.

I would like to thank my lab members for teaching me basic research skills and for their support. I would like to thank Asha Sinha for all those brainstorming days on High-Throughput Comet assay and Cytation 5. I would like to recognize the immense help, support and guidance from Elizabeth Henson (from Gibson lab) for helping me on my 'Establishment of the stable cell line project' and on flow cytometry. I would like to mention about all those tight hugs on my bad days at work that kept me moving forward. Also, I would like to thank Bozena Kuzio and Ali Saleh for sharing research knowledge with me and the smiles, laughter.

Lastly, I would like to thank my parents for being my backbone and encouraging me through all the ups and downs of life.

TABLE OF CONTENTS

LIST OF TABLES

LIST OF FIGURES

LIST OF ABBREVIATIONS

ACNU	Nimustine
AIF	Apoptosis-inducing factor
ALL	Acute lymphoid leukemia
Alt-NHEJ	Alternative non-homologous end joining
AMT	Absorption-mediated transcytosis
AOA1	Ataxia with oculomotor apraxia 1
AP	Abasic site
AP-1	Activator protein-1
APC	Adenomatous Polyposis Coli
APE1	AP endonuclease-1
APLF	Aprataxin-and-PNK-like factor
A-TLD	Ataxia telangiectasia-like syndrome
ATM	Ataxia Telangiectasia Mutated
ATR	Ataxia Telangiectasia and Rad3-related protein
ATRIP	ATR interaction protein
AXIN 1,2	Axis Inhibition protein 1
BAX	BCL2-associated X protein
BBB	Blood Brain Barrier
BBTB	Blood-Brain Tumour Barrier
BCNU	Carmustine
BM1	Polycomb complex protein
BMPs	Bone morphogenetic proteins
BRCA1	Breast cancer associated gene 1
BRCA2	Breast cancer associated gene 2
BTs	Brain Tumours
CAD	Caspase activated DNAase

CCNU	Lomustine
CCNU	Lomustine
Cdc25	Cell division control 25
CDK6	Cyclin-Dependent Kinase 6
cdKs	Cyclin-dependent kinases
CHK1	Checkpoint Kinase 1
CHK2	Checkpoint Kinase 2
CK2	Casein kinase 2
CLL	Chronic lymphocytic leukemia
C-NHEJ	Classical non-homologous end joining
CNS	Central Nervous System
CNTF	Ciliary neurotrophic factor
CPT	Camptothecin
CPT	Camptothecin
CSCs	Cancer stem cells
CSF	Cerebrospinal Fluid
CSR	Class switch recombination
CtIP	C-terminal region of adenovirus E1A-binding protein
CTNNB1	Catenin β1
CTSCAN	Computed Tomography
DDR	DNA Damage Response
DFF	DNA fragmentation factor
DNA	Deoxyribonucleic acid
DNA LIG	DNA ligases 1
DNAPK	DNA dependent protein kinase
Drp	deoxyribose phosphate
dsDNA	Double-stranded DNA
EGFR	Epidermal Growth Factor

EndoG	Endonuclease G
ER	Endoplasmic reticulum
ERK	Extracellular signal-regulated protein kinase
FA	Fanconi Anemia
FAS	First apoptotic signal
FAT	FRAP-ATM-TRRAP
FATC	FAT C-terminal
FDA	Federal Drug Agency
FDR	False Discovery Rate
FEN1	Flap endonuclease-1
FGF	Fibroblast Growth Factor
GBM	Glioblastoma Multiforme
GG-NER	Global-genome NER
GMT	O6-methylguanine- DNA methyltransferase
Gw8	Gestational week eight
HABH	Human AlkB homologous
HDAC5,9	Histone Deacetylase 5,9
HER2	Human Epidermal Growth Factor Receptor 2
HGF	Hepatocyte Growth Factor
HR	Homologous recombination
ICAD	Inhibitor of caspase-activated DNAase
ICLs	Inter-strand crosslinks
IDH1	Isocitrate dehydrogenase 1
IFP	Interstitial fluid pressure
IGF	Insulin-like Growth Factor
JNK	Jun N-terminal kinase
KCNA	Potassium voltage-gated channel
LEF-1	T cell-specific transcription factor 1

LIF	Leukemia inhibitory factor
MB	Medulloblastoma
MDC1	Mediator of DNA damage checkpoint 1
MDM2	Mouse double minute 2
MDR	Multidrug resistance
MG	Malignant Glioma
MLL23	Myeloid-Lymphoid Leukemia
MMEJ	Microhomology-mediated end-joining
MMR	Mismatch repair
MMS	Methylmethane sulfonate
MRI	Magnetic Resonance Imagin
MRP	MDR associated protein
N7MeG	N7-methylguanine
NADþ	Nicotinamide adenine dinucleotide
NBCCS	Nevoid basal-cell carcinoma syndrome
Nbs	Nijmegen breakage syndrome
NBS1	Nijmegen breakage syndrome1
NER	Nucleotide excision repair
NHEJ	Non-homologous end joining
NMMG	N-methyl-N-nitro-N-nitrosoguanidine
Ns	non-significant
NSC	Neocarzinostatin
NSC	Neural stem cells
O4MeT	O4-methylamine
O6MeG	O6-methylguanine
OPCs	Oligodendrocyte progenitor cells
OS	Overall Survival
PARP	Poly(ADP-ribose) polymerase

PBZ	PAR-binding zinc finger
PCD	Programmed cell death
PCNA	Proliferating cell nucleus antigen
PDGFR	Platelet-derived growth factor receptor
P-gp	P-glycoprotein
PI3K	Phosphoinositol-3 Kinase
PIDD	p53 death domain protein 1
PIK	Phosphoinositol Kinase
PIKKs	Phosphatidylinositol 3-kinase-like protein kinase
PKC	Protein Kinase C
PLD	Potentially lethal damage
PNK	Polynucleotide kinase
PNKP	Polynucleotide Kinase 3'-Phosphatase
Pol-β	DNA polymerase beta
PRD	PIKK regulatory domain
PTCH1	Patched-1
PUMA	p53 upregulated modulator of apoptosis
Rb	Retinoblastoma
RFC	Replication factor
RIN	RNA Integrity Number
ROS	Reactive oxygen specie
ROS	Reactive oxygen species
RPA	Replication Protein
SCAN1	Spinocerebellar ataxia with axonal neuropathy 1
Shh	Sonic HedgeHog
SMC1	Structural maintenance of chromatin 1
SMO	Smoothened
SSA	Single-strand annealing

ssDNA Single-stranded DNA

SUFU Suppressor of Fused

TCF-1 Transcription Factor 1

TC-NER Transcription-coupled NER

TDP1 Tyrosyl-DNA phosphodiesterase 1

TEL2 Telomere maintenance 2

TMN Tumour Node Metastasis

TMZ Temozolomide

TOP1–DSBs TOP1-linked DSBs

TOP1–SSBs TOP1-linked SSBs

TopBP1 Topoisomerase binding protein 1

TOPI DNA Topoisomerase-I

TOPIccs Topoisomerase-I cleavage complexes

TP53 Tumour protein p53

TPA 12-O-tetradecanoyl phorbol-13-acetate

USG Ultrasonography

VEGFR Vascular Endothelial Growth Factor

WHO World Health Organization

XFL XRCC4-like factor

XRCC4 X-ray cross complementing prote

I. INTRODUCTION

1.1. A brief history of the discovery and epidemiology of cancer

Cancer is derived from the Greek word *karkinos*, described by the physician Hippocrates (460–370 B.C) as a carcinoma tumour. The world's oldest record of breast cancer is from ancient Egypt (circa 1500 BC) and even then, it was reported that there is no curative treatment for cancer other than palliative care (1). Cancer is described as a heterogeneous disease due to different cell types originating within a certain tumour type (2). After cardiovascular disease, cancer (1) ranks as the second highest cause of mortality amongst individuals across the world. Cancer is a serious health condition (3); one in four people will die of cancer worldwide. Similarly, it is one of the leading causes of mortality in Canada; accounting for 30% of all death (4). In Canada, the rates of newly diagnosed cases of cancer have increased in the past 10 years. In 2010, it was estimated that one in every two Canadians is likely to develop cancer during their lifetime: 49% of men and 45% of women (4). In 2012, a similar study showed that one out of four Canadians is likely to die from cancer: 28% of men and 24% of women. In 2017, 50% of newly diagnosed cancer cases stratified amongst lung, prostate, colorectal and breast cancer (4). The estimated age-standardized mortality rate for all cancers between 2014-2025, is predicted to be an estimated, 208 to 180 deaths per 100,000 in males and 133 to 120 deaths per 100,000 in females (5).

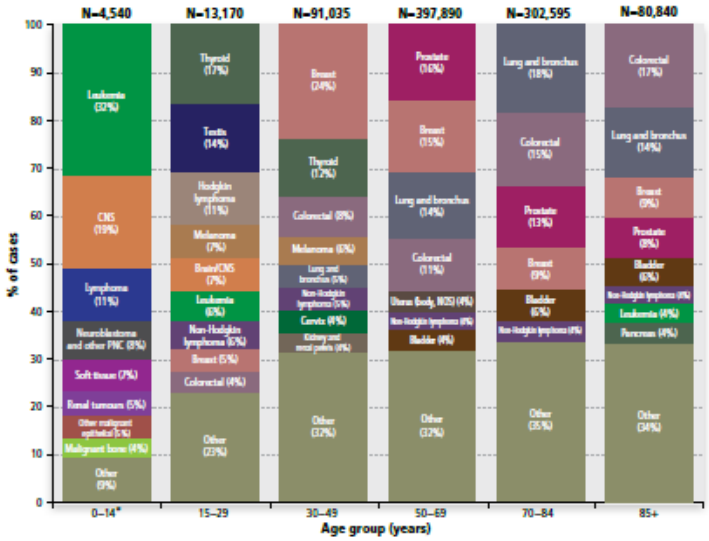

Figure-1.1. Distribution of selected cancers by age group, Canada 2010-2012(4)

For health professionals, dealing with cancer as a disease has been a challenge due to its heterogeneous nature and its various forms and types. Each cancer is considered its own unique disease, each with unique challenges and outcomes thus making effective treatment strategies difficult to elucidate (1). There are a variety of tumour types with differences in prevalence among gender. For example, prostate, lung, bronchus, colon, rectum and urinary bladder cancer are more widespread in men. On the other hand, breast, lung, bronchus, colon, rectum, uterine corpus and thyroid are more prevalent in women (3). This data indicate that prostate cancer is most common among men and breast cancer among women (4). Amongst children; blood, brain and lymph node tumours are common (3).

Genetic considerations, such as familial hereditary predisposition mutations, polymorphisms, and developmentally-acquired defects can account for certain cancer types (1). Furthermore, carcinogenic chemicals found in cigarettes and environmental chemical compounds can contribute to the acquisition of cancer-causing somatic mutations, due to their direct or indirect effect on the cell (1). In addition, some viruses have also been linked to cancer formation, including Hepatitis B or C (liver cancer), Epstein-Barr virus (non-Hodgkin lymphomas and nasopharyngeal cancer), human immunodeficiency virus (HIV: Kaposi Sarcoma and non-Hodgkin lymphoma) (6) and human papillomaviruses (HPVs: cervix, vulva and penile cancers). Bacteria and ionizing radiation are also considered risk factors, accounting for approximately 7% of all cancers (2).

1.2. Hallmarks of cancer

There are six hallmarks of cancer; these are considered as biological drivers during the multistep development of tumourigenesis (7). These include i. sustaining proliferative signaling, ii. evading growth suppressors, iii. resisting cell death (8), iv. enabling replicative immortality, v. inducing angiogenesis, and vi. activating invasion and metastasis. These hallmarks provide a means to understand the complexities of neoplastic disease (9) and targets with which to develop ways to counteract the mechanisms leading to tumour progression/malignancy (7). Genetic instability gives rise to genetically-diverse transformed cells with multiple cancer hallmarks (8). Tumour cells are surrounded by extracellular matrix (ECM), stromal cells, blood vessels, fibroblast, bone marrow-derived inflammatory cells, immune cells, and signaling molecules. All these different cell types make up the cellular environment in which the tumour cells thrive, commonly denoted as the "tumour microenvironment" (10). In addition to tumour cells, normal, non-

malignant/transformed cells contribute to tumourigenesis (the process of formation of cancer) by affecting the ‘‘tumour microenvironment’’. This is a very complex area and currently a major target for cancer therapy (7).

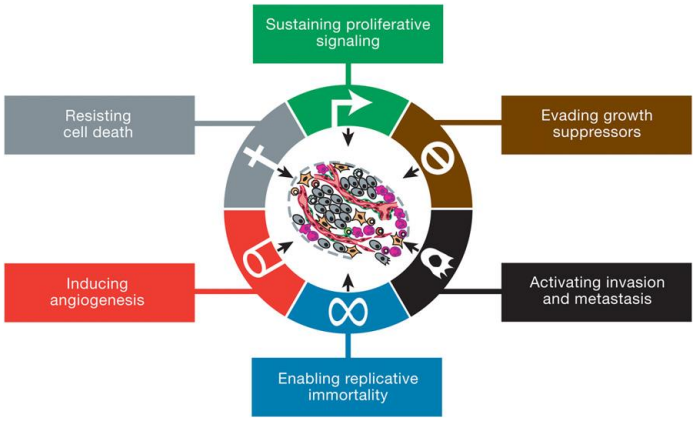

Figure-1.2. Hallmarks of cancer(7)

1.3. Detection and staging of tumours

Early detection of cancer is important for an effective therapeutic response. Pap test was the first cancer screening test developed by George Papanicolaou and was used to detect cervical cancer. Later in the 1960s, mammography was used for breast cancer detection (1). Later more advanced techniques were developed to detect cervix, breast, colon, rectum, endometrium, prostate, thyroid, oral cavity, skin, lymph nodes, testes, and ovaries cancers in clinical practice. Nowadays MRI (Magnetic Resonance Imaging), CTSCAN (Computed Tomography) are used (1).

Staging of a tumour is important in diagnosing cancer in order to track cancer progression and to develop better treatment plans (11). Staging includes parameters such as location and size of a primary tumour, location and number of infiltrated regional lymph nodes and presence of distant metastases. In clinical oncology, the Tumour-Node-Metastasis (TNM) classification figures prominently (Table-1.1). This classification system is useful and informative for solid tumours like colorectal cancer of head and neck, breast cancer etc., but not as informative for tumours of the central nervous system (12).

TNM classification stands for; T (a tumour), N (metastasis in regional lymph nodes), and M (distant metastasis). The level of malignancy is termed as: TX (Tumour cannot be assessed), T0 (No evidence of primary tumour), T1-4 (increasing size or local extent), This (Carcinoma in situ); NX (Regional lymph nodes cannot be assessed), N0 (No regional lymph node metastasis), N1-3 (Increasing involvement of regional lymph nodes); M0 (No distant metastasis), M1 (Distant metastasis) (12)(11).

Descriptor	Values	Meaning
T	0-4, is, X	Extent of the primary tumour
N	0-3, X	Extent of metastasis in regional lymph nodes
M	0-1	Existence of distant metastasis
Prefix to T, N, M	p, c	Clinical (pre-therapeutical) or pathological (post-surgical assessment)
Suffix to pNn	(mi)	Micrometastasis (< 0.2 cm)
Suffix to pNn	(sn)	Sentinel lymph node metastasis
Suffix to pN0 or pM0	(i+), (mol+)	Isolated tumour cells, positive findings
G	X, 1-4	Histopathological grading
Suffix to T	(m)	Multiple primary tumours at a single side
Prefix to c/ p	y	Assessment during multimodal therapy
Prefix to c/ p	r	Recurrent tumour
Prefix to c/ p	a	Assessment during autopsy
L	X, 0-1	Lymphatic invasion
V	X, 0-2	Venous invasion
Pn	X, 0-1	Perineural invasion
C	1-5	Validity of the assessment, can follow each of T, N, M
R	X, 0-2	Residual tumour

Table-1.1. TNM classification descriptors and additional modifiers(12)

1.4. Cancer development and progression

Cancer is a progressive disease usually starting off as a pre-cancerous lesion (benign) (1). Over time, this lesion may increase in size and transform into a malignant lesion (8). Transformation and formation of cancer are well described with the term tumourigenesis. Tumourigenesis is a dynamic cellular process which includes initiation, promotion, and progression, genetic alteration, cytogenetic and epigenetic changes in tumour cells leading to malignancy. The malignant transformation causes tumour cells to metastasize to other parts of the body through the circulatory or lymphatic systems (3). For example, breast cancer cells that seed and grow in the liver are still called breast cancer (1). These transformed cells invade host tissue and continue to proliferate at

an abnormal rate. This property of cancer cells provide a proof of genetic alteration which can be passed from one generation to the next (6).

1.4.1. Cancer is a genetic disease

Acquired and inherited genetic alterations in genes that regulate cell growth, differentiation, is responsible for initiation and progression of a cell towards malignancy. These are mainly induced through activation of proto-oncogenes (oncogenic transformation) and inactivation of tumour suppressors (6). Protooncogenes drive and deliver responses to growth promotor stimulation (13), such as transcription factors, growth factor receptors, and membrane-associated signaling proteins (6). Oncogenes are dysregulated forms of protooncogenes due to chromosomal rearrangement/amplification, mutation and retroviral action (14)(6).

The first cancer-associated oncogenic mutation characterized in humans, c-Ha-ras oncogene, was first identified by Feinberg and Vogelstein (15). Tumour suppressors act as 'gatekeeper genes' which control cell cycle, proliferation, differentiation, and apoptosis. Anecdotally, tumour suppressor genes have protective cell 'brake' functions (to slow cell growth) whereas oncogenes have 'gas' functions (driving cell growth) (6). When tumour suppressor genes are switched off, there are no longer any 'brakes'; inhibiting cell growth is lost. Similarly, when oncogenes are switched on, more 'gas' drives cell growth. Combined, these genetic alterations lead to disruption in balance, causing uncontrolled cell growth and differentiation (6).

Studies have shown that more than one genetic hit (usually 5-8 hits) is required to transform a primary cell into cancerous form (6). For example, individual activation of oncogenes, ras, and myc cannot trigger transformation but, together, they can transform into malignant phenotype: by immortalizing the cell and ras lead to increased proliferation and growth (16). Similarly, activation of an oncogene (ras) and inactivation of a tumour suppressor gene can lead to malignant transformation(p53) (17)(18). Loss of tumour suppressor genes also contribute to the notion because both types of the gene might have opposite function in the same cellular signaling pathway, for example, p16INK4A inactivates cyclin-dependent kinases Cdk4 and Cdk6 while protooncogenes cylinD1 activates them (19).

As mentioned above, genetic alterations lead to activation of oncogenes and inactivation of tumour suppressors. These phenomena are characterized in a number of cancer and can involve chromosomal translocation (gene Bcr and oncogene Abl in chronic blood cancer), point mutation (Ras gene in colon cancer), deletion (Erb-B gene in breast cancer), amplification (N-myc in neuroblastoma) and insertion activation (C-myc in acute blood cancer). Studies have shown that almost 60% of cancers incur mutations in p53, considered a master tumour suppressor (3). The p53 gene play critical roles in cell division, cell death, senescence, angiogenesis, differentiation, and DNA metabolism. Mutation in p53 results in widespread abnormalities amongst these molecular and biological processes contributing to tumour development. It can either promote or inhibit tumour development (3).

p53 is activated by various cellular stress like DNA damage (20)(Figure-1.3) and loss of p53 function during DNA damage result in cell aneuploidy as cells are not being eliminated by p53 dependent apoptosis. It has been observed that in cell culture and mouse studies, that restoring p53 function can result in tumour regression and cell death (21). The anti-cancer function of p53 is active during DNA repair, induction of apoptosis and arresting of the cell cycle in G1/S phase (Figure-1.3); mutation resulting in loss of p53 function leads to progression to malignancy (21).

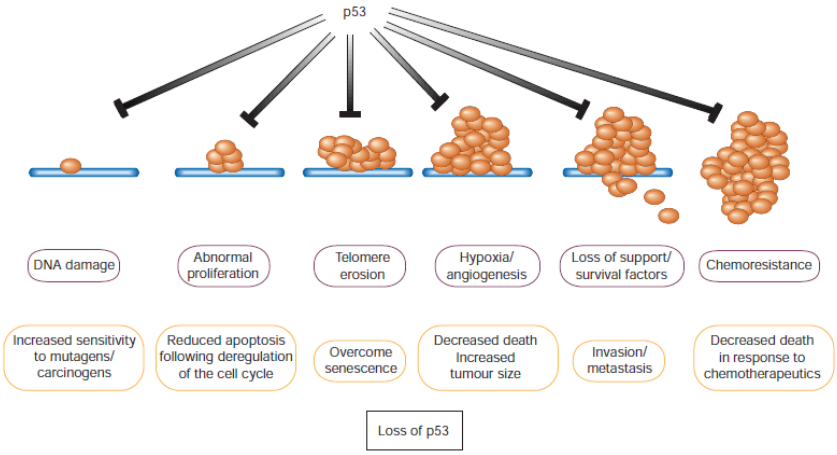

Figure-1.3. Mutagenic loss of tumour suppressor p53(21)

Epigenetics is the study of a cellular mechanism that changes gene expression without affecting the DNA sequence (22). These cellular processes are reversible and heritable (15). There are four known epigenetic modifications: DNA methylation, post-translational modification of histone modifications, chromatin remodeling and nucleosome position (22)(23)(24)(15). These cellular

processes are involved in normal growth and development of cells along with their modification for neoplastic phenotypes. Therefore, an aberration in these mechanisms results in malignant transformation and cancer progression (22). For example, 56% reduction has been observed in 5-methylcytosine and monoacetylated H4K16 mediated histone modification in tumour cells (3).

High-throughput (next generation) techniques have been recently developed to characterize each individual's tumour mutation profile including nonsense, silent and point mutations, deletions, insertions, translocations, epigenetic marks and polymorphisms (15)(2). These techniques are revolutionizing our understanding of cancer and how we approach treatment, particularly using a personalized medicine approach to take advantage of the knowledge of these tumour-specific molecular features to drive therapy. Such characterization is now becoming commonplace and is increasing the precision of treatment regimen.

Cells that make up the cancer mass show heterogenous nature and this give rise to the broad term 'tumour heterogeneity'(25). Heterogeneity among and within a tumour arises giving rise to tumour subtypes, for example, pediatric brain tumour, medulloblastoma have four different subtypes (Sonic hedgehog, Wnt subtype, Group 3 and Group 4) (26). Variability between a tumour is termed as intertumoural heterogeneity while variation within an individual tumour is intratumoural heterogeneity. These tumour cells have diverse function and expression of markers.

There are different theories that have been demonstrated to organize this heterogenous nature of tumour cells and their functional properties (2). Cancer stem cells (CSC) and clonal evolution have emerged as major drivers of intratumoural heterogeneity and responsible for the intrinsic differences in a tumour regenerating capacity (26). Acquisition of tumour intratumoural heterogeneity has been associated with two mechanisms; genetic or epigenetic mutations within a target cell generating different tumour phenotypes and different cell subtypes arising from a cell of origin. Tumour heterogeneity becomes even more complex when tumour cells interact with the stromal micro-environment which further drives malignant growth (27).

1.5. Cancer Therapy

Several cancer treatment strategies have evolved over the last few decades and each has proven to be effective in different tumour types. Surgical resection, radiotherapy, and chemotherapy are the three main cancer treatment modalities (1). They are given either singly or in combination (mainly for secondary tumour), such as radiotherapy followed by chemotherapy, chemotherapy along with

surgical resection (adjuvant chemotherapy and neoadjuvant chemotherapy) (28), radiotherapy followed by surgery or vice-versa and sometimes all three. Most treatment strategies depend on the stage of tumour progression and patient condition. Recently combination therapies and targeted therapy have been made possible due to the development of precision medicine initiatives which are increasingly being used in both research and clinical practice (29).

The limitation of cancer therapy is due to irreversible side effects from radiotherapy and chemotherapy. These therapeutic regimens have enhanced tumour cell death but also exert their toxicity on normal cells of the body. Specifically targeting tumour cells and sparing normal cells is the major goal yet remain a challenge for researchers and clinicians (1). New therapeutic approaches have been adopted to reduce side effects, such as newer combinations of drugs, immunotherapy (29) (liposomal and monoclonal antibody therapy) (29), chemoprotective agents, hormonal therapy (aromatase inhibitors, LHRH analogs are used to treat prostate and breast cancers)(28), stem cell transplants (hematopoietic stem cell transplantation) and drugs being developed to overcome multi-drug resistance (1).

Another class of drugs, defined as targeted therapy, include growth inhibitors (i.e. trastuzumab, gefitinib, imatinib, and cetuximab), drugs that induce apoptosis, endogenous angioinhibitors (i.e. bevacizumab, thrombospondin-1, angiostatin, interferons, endostatin, arrestin, canstatin) and others (1). In the recent phase, specific cellular pathway (cell death, DNA repair, DNA damage response) components are a prime target for drug design (20). Some of these molecules are being tested in preclinical and clinical trials. The aim is to design drugs with maximum therapeutic benefit and minimum side effect.

2.1. CNS tumours incidence and epidemiology

Central nervous system (CNS) tumours are one of the most common solid tumours reported amongst individuals of all ages, with higher proportions in children (30). These are a heterogeneous group of neoplasms and they differ according to the site of origin, morphologic features, genetic alterations, growth potential, the extent of invasiveness, the tendency for progression and recurrence and therapeutic response (31). Primary brain tumours are the most aggressive and lethal form (32) with the often devastating quality of life for patients (33). Brain tumours comprise a small percentage (~ 2%) of all cancer types but account for a high degree of cancer mortality with a survival time as short as 9 months to 5 years (less than 25%) (32).

Survivors often suffer from permanent neurological deficits, either due to the tumour or the treatment (30)(33). In Canada, brain tumours have become a major concern because of an observed increase in the number and proportion of deaths over the past few decades (32).

Approximately 3.7 per 100,000 men and 2.6 per 100,000 women develop primary brain tumours (BTs), respectively (31). Interestingly, statistics have also shown that women develop more non-malignant BTs, primarily meningiomas, compared to men. This rate of BTs is found to be increased in developed countries with 5.8 per 100,000 in men and 4.1 per 100,000 in women, compared to undeveloped/third world countries. Amongst children, BTs are the most common solid tumour type, with peak occurrence by age of 3 (Figure-2.1) (31). In Canada, BTs have been reported to be one of the leading cause of mortality in children (over the age of 1 month), comprising about 20% (34). The most common type of BTs is astrocytoma medulloblastoma, comprising 28% and 25% BT occurrences, respectively. Some BTs like medulloblastoma are common among children, hence denoted as a pediatric brain tumour (Figure-2.1) (31).

BTs are thought to arise from ionizing radiation, inherited genetic mutations, allergies, infections, viruses like polyomavirus like JC virus, BK virus and simian virus, neurocarcinogens, and heavy metals. Studies have shown that high dose radiation, typically used to treat cancer, increases the risk of nerve sheath tumours, meningiomas and gliomas (31).

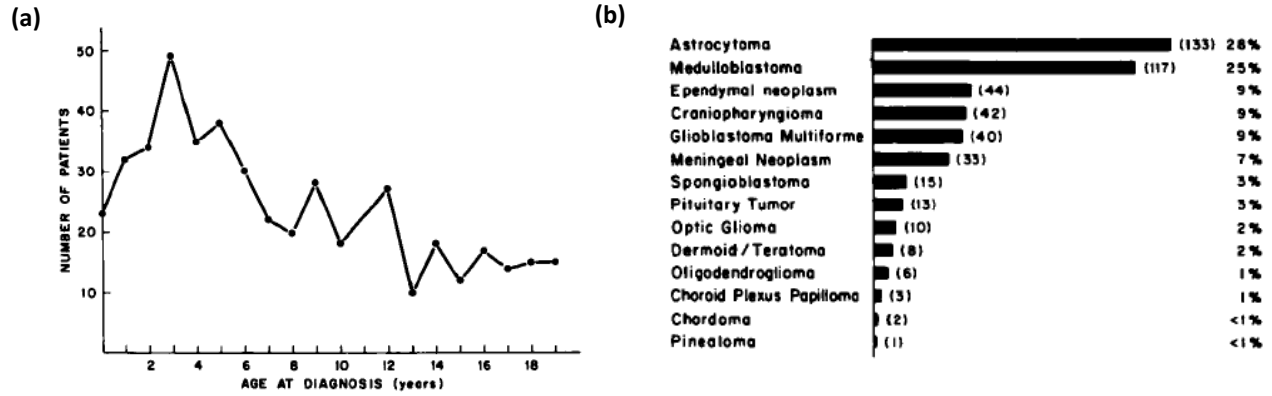

Figure-2.1. (a) denotes the age at diagnosis of children with intracranial tumours which peaks at 3. (b) histopathological distribution of 467 intracranial neoplasms (35)

2.2. Classification of CNS tumours

Brain tumours are classified based on the cell of origin and location in the brain. Based on these criteria, in 2016 the World Health Organization (WHO) classified brain tumours into subtypes: diffuse astrocytic and oligodendroglial tumours, ependymal tumours, choroid plexus tumourous, neuronal and mixed neuronal-glial tumours, tumours of the pineal region, embryonal, tumours of the cranial and paraspinal nerves, meningiomas, mesenchymal non-meningothelial tumours, melanocytic tumours, lymphomas, histiocytic tumours, germ cell tumours, tumour of the sellar region and metastatic tumours (Table-2.1) (36).

Further, BTs are categorized into different grades - from I to IV depending on the extent of tissue abnormality. Tumours are visualized under a microscope using immunohistochemical techniques while molecular techniques are now used to characterize molecular features. Almost half of CNS tumours are gliomas; arising from glial cells. Gliomas are further classified into low-grade astrocytoma (grade I and II), anaplastic astrocytoma (grade III) and glioblastoma multiforme (grade IV) (37).

Diffuse astrocytic and oligodendroglial tumours	
Diffuse astrocytoma, IDH-mutant	9400/3
Gemistocytic astrocytoma, IDH-mutant	9411/3
Diffuse astrocytoma, IDH-wildtype	*9400/3*
Diffuse astrocytoma, NOS	9400/3
Anaplastic astrocytoma, IDH-mutant	9401/3
Anaplastic astrocytoma, IDH-wildtype	*9401/3*
Anaplastic astrocytoma, NOS	9401/3
Glioblastoma, IDH-wildtype	9440/3
Giant cell glioblastoma	9441/3
Gliosarcoma	9442/3
Epithelioid glioblastoma	*9440/3*
Glioblastoma, IDH-mutant	9445/3*
Glioblastoma, NOS	9440/3
Diffuse midline glioma, H3 K27M–mutant	9385/3*
Oligodendroglioma, IDH-mutant and 1p/19q-codeleted	9450/3
Oligodendroglioma, NOS	9450/3
Anaplastic oligodendroglioma, IDH-mutant and 1p/19q-codeleted	9451/3
Anaplastic oligodendroglioma, NOS	*9451/3*
Oligoastrocytoma, NOS	*9382/3*
Anaplastic oligoastrocytoma, NOS	*9382/3*
Other astrocytic tumours	
Pilocytic astrocytoma	9421/1
Pilomyxoid astrocytoma	9425/3
Subependymal giant cell astrocytoma	9384/1
Pleomorphic xanthoastrocytoma	9424/3
Anaplastic pleomorphic xanthoastrocytoma	9424/3
Ependymal tumours	
Subependymoma	9383/1
Myxopapillary ependymoma	9394/1
Ependymoma	9391/3
Papillary ependymoma	9393/3
Clear cell ependymoma	9391/3
Tanycytic ependymoma	9391/3
Ependymoma, *RELA* fusion–positive	9396/3*
Anaplastic ependymoma	9392/3
Other gliomas	
Chordoid glioma of the third ventricle	9444/1
Angiocentric glioma	9431/1
Astroblastoma	9430/3
Choroid plexus tumours	
Choroid plexus papilloma	9390/0
Atypical choroid plexus papilloma	9390/1
Choroid plexus carcinoma	9390/3
Neuronal and mixed neuronal-glial tumours	
Dysembryoplastic neuroepithelial tumour	9413/0
Gangliocytoma	9492/0
Ganglioglioma	9505/1
Anaplastic ganglioglioma	9505/3
Dysplastic cerebellar gangliocytoma (Lhermitte–Duclos disease)	9493/0
Desmoplastic infantile astrocytoma and ganglioglioma	9412/1
Papillary glioneuronal tumour	9509/1
Rosette-forming glioneuronal tumour	9509/1
Diffuse leptomeningeal glioneuronal tumour	
Central neurocytoma	9506/1
Extraventricular neurocytoma	9506/1
Cerebellar liponeurocytoma	9506/1
Paraganglioma	8693/1
Tumours of the pineal region	
Pineocytoma	9361/1
Pineal parenchymal tumour of intermediate differentiation	9362/3
Pineoblastoma	9362/3
Papillary tumour of the pineal region	9395/3
Embryonal tumours	
Medulloblastomas, genetically defined	
Medulloblastoma, WNT-activated	9475/3*
Medulloblastoma, SHH-activated and *TP53*-mutant	9476/3*
Medulloblastoma, SHH-activated and *TP53*-wildtype	9471/3
Medulloblastoma, non-WNT/non-SHH	9477/3*
Medulloblastoma, group 3	
Medulloblastoma, group 4	
Medulloblastomas, histologically defined	
Medulloblastoma, classic	9470/3
Medulloblastoma, desmoplastic/nodular	9471/3
Medulloblastoma with extensive nodularity	9471/3
Medulloblastoma, large cell / anaplastic	9474/3
Medulloblastoma, NOS	9470/3
Embryonal tumour with multilayered rosettes, C19MC-altered	9478/3*
Embryonal tumour with multilayered rosettes, NOS	*9478/3*
Medulloepithelioma	9501/3
CNS neuroblastoma	9500/3
CNS ganglioneuroblastoma	9490/3
CNS embryonal tumour, NOS	9473/3
Atypical teratoid/rhabdoid tumour	9508/3
CNS embryonal tumour with rhabdoid features	*9508/3*
Tumours of the cranial and paraspinal nerves	
Schwannoma	9560/0
Cellular schwannoma	9560/0
Plexiform schwannoma	9560/0

Table-2.1. WHO classification of tumours of the central nervous system(36)

2.3. Diagnosis

Detection and identification of brain tumour type is necessary for proper treatment planning and patient survival. Identification of the tumour type is mediated through cytology, histopathology, immunohistochemistry and genetic analysis (37). Advanced genomic techniques like transcriptomic and methylation profiling have revealed disease heterogeneity within and among tumour types (38). Detection of BTs is mediated through advanced diagnostic imaging techniques such as radiography, ultrasonography (USG), computed tomography (CT), magnetic resonance imaging (MRI), neuronavigation and neuromonitoring (37). Magnetic Resonance Imaging (MRI) is the commonly used technique but this is only utilized to track the presence and progression of the tumour (30) and but not to delineate the tumour grade (37). Newer techniques have been reported in recent years for imaging BTs through use of vibrational spectroscopy (IR and Raman).

This diagnostic tool provides BT imaging along with its morphological and biochemical properties with very high spectral and spatial resolution (37)(39).

BT patients show various signs and symptoms. Common symptoms include a headache and seizures (due to increased intracranial pressure), unilateral weakness or personality changes (due to tissue destruction or compression of specialized regions) (39). Other symptoms include anosmia, apraxia, cognitive delay, drowsiness, dysphagia, hallucinations, memory loss, nausea and vomiting, pain, and stiff neck. In comparison to other cancer types, BTs do not have a standard staging system (39).

2.4. Brain development and cancer

Development of the brain involves the characteristic folding pattern which allows growth and appropriate fitting of the structure within small cranial vaults. The development of brain starts during embryogenesis which continues throughout gestational week eight, or GW8 (40). The basic structure of the brain, spinal cord and peripheral nervous system are all demarcated at the end of the embryonic period. Cortical, subcortical structures and a major component of main fiber pathways are defined during this embryonic development phase (40).

The human brain is composed of >100 billion neurons (41)(40) and neuron production is first observed on embryonic day 42. E42, i.e. 42 days post conception. Neurons migrate to different regions of the brain and continue to make interconnections (a neuron interconnect with more than 1,000 other neurons) (40). The neurons are interconnected through synapses and this interconnection is crucial for the development of information processing networks for thoughts, sensations, feelings, and actions (40). Neocortex and the subcortical nuclei are the largest brain information processing networks. Subcortical nuclei transmit information to and from the neocortex and between the neocortex and rest of the body. The center of the brain consists of the ventricular system which is a series of interconnected cavities. These cavities are filled with cerebrospinal fluid (CSF) and provide cushioning and protection of the brain, removal of waste material and mediate transport of hormones and other substances (40).

The first stage of brain development is the differentiation of neural progenitor cells (43). Progenitor cells generate glia and neurons. Neuronal cells include radial glia (RG) and neural stem cells (NSC) (44). Neural stem cells (NSC) reside in the subventricular zone and hippocampal dentate gyrus. NSC cells differentiate forming neurons through neurogenesis which function in learning,

memory, and mood. NSC in the subventricular zone form astrocytes, oligodendrocytes, and oligodendrocyte progenitor cells and are present throughout the central nervous system (45). Astrocytes regulate neuronal growth, survival, cell migration and axon growth during development along with synapse formation and transmission (46). Astrocyte differentiation is promoted by extracellular signals (33). Epidermal growth factor (EGF), cytokines of the ciliary neurotrophic factor (CNTF)/leukemia inhibitory factor (LIF) family, Bone morphogenetic proteins (BMPs) all act to promote astrocytic differentiation. Unlike other brain cells, astrocytes have the capability of being reactive and dividing, hence retain the ability to differentiate. This justifies why astrocytic tumours are common among brain tumours (46).

It has been shown through molecular and genetic profiling studies that specific cancer-causing genetic mutations induce tumourigenesis resulting in the formation of brain tumours (47). A genetic mutation in components of the cell cycle checkpoints, DNA damage response (DDR) and DNA repair pathways and/or damage to DNA, disrupts the normal cellular functioning of these processes. This result in a proliferation of cells with incurred damage and unresolved mutations. These cells become desensitized to apoptotic signals and multiply at an abnormal rate thus forming hyperplasia. This abnormal mass can surround brain structures and continue to proliferate (48). Normal cell cycle and other cellular processes do not have any effect on this mass. Brain tumour arises when this mass increases in size through rapid proliferation. This mass of tissue has the ability to replace, compressing and invading normal brain cells (48). It has been demonstrated in mouse models that mutation in the tumour suppressor gene p53 and PTEN, or their overexpression of these mutant forms in NSCs with hGFAP-Cre or Nestin-Cre genetic lines result in brain tumour development (glioma). In preclinical studies, mutation of INK4a/Arf and EGFRvIII in cultured neurospheres potentiated glioma in immuno-compromised mice (44).

Advances in transcriptional and genetic profiling of brain tumours revealed the complex interaction between genetic mutations seen with BTs. Also, these newly developed assay also helped to understand the biology of brain tumour development (33).

3.1. Glioblastoma Multiforme (GBM) incidence, epidemiology, and etiology

Gliomas are the most common primary brain tumours of central nervous system and their nomenclature is derived from their cell of origin, similar to oligodendrogliomas, ependymomas, mixed gliomas and astrocytic tumours (astrocytoma, anaplastic astrocytoma and glioblastoma) (Table-3.2) (49). WHO classifies gliomas according to their level of malignancy based on histopathological criteria, from grade I to IV (Table-3.1) (50). Grade I gliomas represent low proliferation (49) tumours and can be removed completely by surgery while Grade II to IV are increasingly aggressive and malignant (51).

Glioblastoma multiforme (GBM) is a highly aggressive Grade IV brain tumour affecting individuals of all ages, comprising of 30% of all tumours of central nervous system and 80% of all malignant brain tumours (52). Malignant glioma is a cerebral tumour and 95% are located in supratentorial region (49). GBMs arise from dysregulated glial cells, particularly astrocytes such as astrocyte progenitor cells (APC), glial-restricted progenitor cells (GPC) and oligodendrocyte progenitor cells (OPC) (52)(53). Although brain tumours are rare events with global incidence of about 10 per 100,000 people, its sensitive disease site and difficult accessibility contributes to its poor prognoses and survival rates, thus, making these tumours the most difficult for therapeutic/clinical management. Despite invasive triple therapy including surgical resection, radiotherapy and adjuvant chemotherapy, recurrence often occurs resulting in a mean patient survival rate of 14 months (54). Factors affecting these outcomes include, a high number of chemo/radio-resistant tumour cells (52)(53), distinct tumour heterogeneity and poor penetrance through the blood-brain-barrier of drugs mitigating access to all the tumour cells.

Type	Grade	Description	Median survival (years)
Astrocytoma	II	Found diffusely infiltrating into surrounding neural tissue; increased hypercellularity, no mitosis	6-8
Oligodendroglioma	II	Occur in the white matter and cortex of the cerebral hemispheres, low mitotic activity, no necrosis	12
Oligoastrocytoma	II	Diffuse mixed tumor with mixed glial background	3 to >10
Anaplastic-astrocytoma/ oligodendroglioma	III	Highly infiltrating tumors with increased mitotic activity; no necrosis or vascular proliferation	3
Glioblastoma	IV	Infiltrating glial neoplasm with necrosis and micro-vascular proliferation; high rate of mitosis	1 to 2

Table-3.1. WHO 2007 classification for diffuse gliomas(55)

Malignant gliomas are responsible for about 2.5% of death among individuals between 15-34 years of age but the peak incidence arises between 55 to 60 years (49) (53). Furthermore, higher GBM incidence is observed in the Western world compared to other parts, due to differences in diagnostic practice, reporting or access to health care. Several studies have shown that prevalence of this tumour is higher in specific ethnic groups such as Caucasians, Asians, Latinos while Africans are less likely to develop malignancy (Table-3.3)(49)(51).

Approximately 5-10% of cases are associated with genetic predisposition. Rare genetic diseases like neurofibromatosis type 1 and type 2, tuberous sclerosis and Fanconi's Anemia have been associated with GBM (49)(51). However, there have been 116 reported cases of GBM associated with exposure to high dose ionizing radiation since 1960 (49). Children undergoing low dose radiotherapy for treatment of *tinea capitis* and *skin hemangioma* have been reported to develop GBM (56). Patients receiving treatment for Acute lymphoid leukaemia (ALL) have been shown to have increased likelihood to develop GBM, possibly from effects of chemotherapeutics or complications from the disease itself (51).

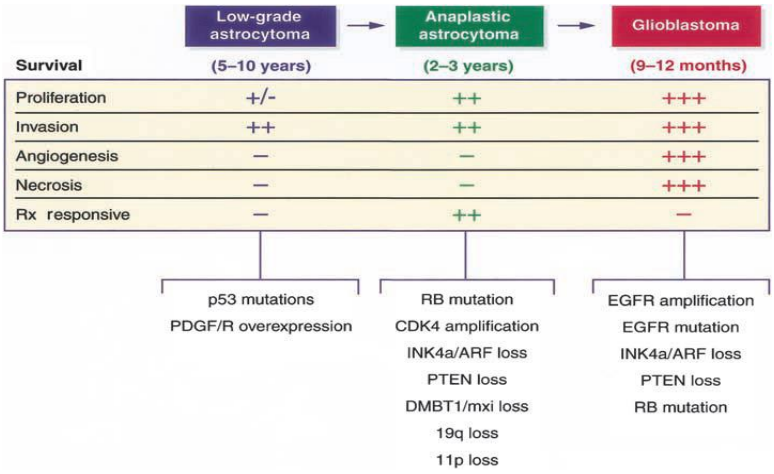

Table-3.2. The relationship between median survival, histological features, and major genetic lesions associated with each tumour(51)

Classification	Characteristics
Sex	High prevalence among males
Age	Common after 45 years of age
Race	Common among white people
Genetic disorder	Tuberous sclerosis (TSC), neurofibromatosis type 1 & 2, Turcot syndrome, Li-Fraumeni syndrome
Ionizing radiation	Grade II astrocytoma, grade III anaplastic astrocytoma

Table-3.3. Trends in the development of Glioblastoma Multiforme(57)

3.2. Molecular Classification of GBM

WHO classifies malignant gliomas according to histological and immunohistochemical properties associated with their cell of origin. Grading is based on histological structures and associated with biological aggressiveness: necrosis, mitotic figures, and vascular endothelial hyperplasia. Glioblastoma is classified into primary and secondary tumours based on their clinical features (Figure-3.1) (50).

Primary GBMs comprise about 90% of cases (50) and arise without the clinical or histological presence of existing lesions (49) while secondary tumours arise from low-grade astrocytoma and/or anaplastic astrocytoma (58). Changes in the EGFR/PTEN/Akt/mTOR pathway, epidermal growth factor receptor (EGFR) gene mutations and/or amplification, overexpression of human-orthologue of mouse double minute 2 (HDM2), deletion of p16 and loss of heterozygosity (LOH) of chromosome 10q (phosphatase and tensin homolog (PTEN)) and TERT promoter mutations(49) are implicated as drivers of the primary tumour. Hallmarks for secondary tumours include over-expression of platelet-derived growth factor A and platelet-derived growth factor receptor alpha (PDGFA/ PDGFRa), retinoblastoma (pRB), LOH of 19q and mutations of IDH1/2, TP53 and ATRX (58).

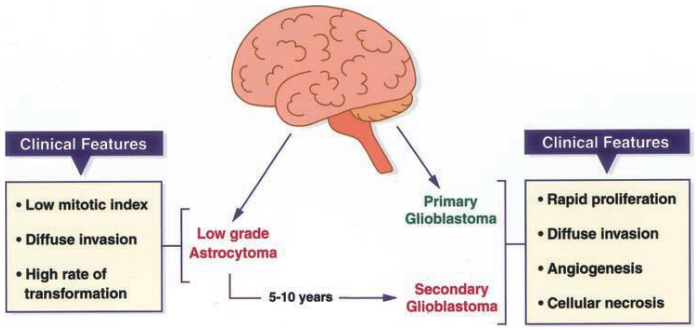

Figure-3.1. Two pathways to GBM. GBM can develop over 5–10 yr. from a low-grade astrocytoma (secondary GBM), or it can be the initial pathology at diagnosis (primary GBM). The clinical features of GBM are the same regardless of clinical route(51)

A third criterion may include H3F3 gene mutation status, although debate remains rampant on its inclusion. Further genetic variations, such as somatic mutations of the Wnt signaling regulator FAT1 (20% of GBMs) and, unexpected fusion transcripts such as the fibroblast growth factor receptor 3/transforming, acidic coiled-coil-containing protein (FGFR3/TACC) fusion have also been reported (59).

The Cancer Genome Research Atlas has used molecular classification to classify GBMs based on molecular pathogenesis and gene expression: *Classical, Mesenchymal, Proneural* and *Neural* subtypes. The *classical* subtype of GBM consists of epidermal growth factor receptor (EGFR) overexpression (97%) along with chromosome 7 amplification, loss of chromosome 10 and homozygous deletion spanning the INK4a/ARF locus (59)(58). Notch (NOTCH3, JAG1, and LFNG), Sonic hedgehog (SMO, GAS1, and GLI2) pathways and neural precursor and stem cell markers are highly expressed in this subtype (58).

The *mesenchymal* subtype includes expression of markers like CH13L1, MET, tumour necrosis factor superfamily pathway and NF-kB pathways, such as TRADD, RELB, and TNFRSF1A. Mutation of *PTEN* and focal deletion of a region at 17q11.2 containing *NF1* feature significantly in this subtype (50)(60).

The most common genetic aberrations characterized in the *proneural* subtype are mutations in *PDGFRA* and point mutations in isocitrate dehydrogenase 1 gene (*IDH1*). Other alterations include TP53 loss/mutation, chromosome 7 amplification paired with chromosome 10 loss (58), and high expressions of oligodendrocytic development genes, such as Sox genes, DCX, DLL ASCL1, and

TCF4 (59). The *neural* subtype includes expression of neuron markers such as NEFL, GABRA1, SYT1, and SLC12A5 (58).

3.3. Clinical presentation of GBM

Despite a great deal of research, there have not been any inroads in identifying specific diagnostic markers for detection of this disease. This deadly cerebral tumour is mainly detected when tumour progresses to an extensive stage and becomes visible for clinical presentation or the patient presents with unexplained neurologic dysfunction. GBMs are visualized and often diagnosed through magnetic resonance imaging (MRI) and other newer radiological techniques like diffusion-weighted imaging (DWI), perfusion-weighted imaging (PWI or perfusion MR), dynamic contrast-enhanced T1 permeability imaging (T1P), diffusion-tensor imaging(DTI), and MR spectroscopy (56).

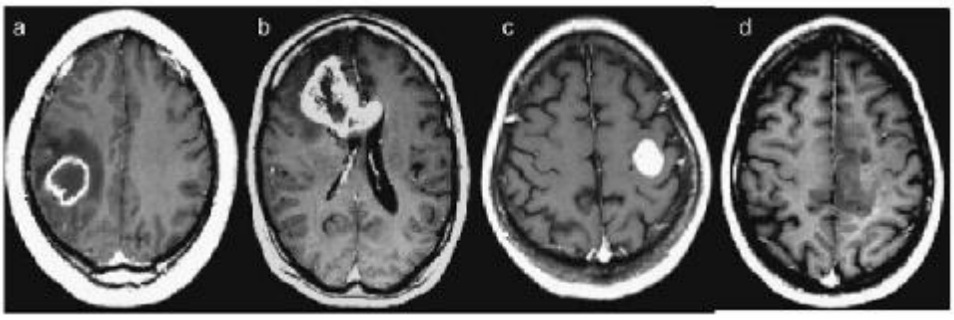

Figure-3.2. Different Patients with GBM representing heterogeneity in Anatomic Lesion. The contrast-enhanced axial T1-weighted (TR, 600 msec; TE, 14 msec) images demonstrate variegated appearance of GBM: (a) rim-enhancing mass with central necrosis in the right parietal lobe with surrounding edema; (b) irregularly enhancing mass that crosses the corpus callosum; (c) well-circumscribed homogeneously enhancing mass in the left frontal lobe with no associated edema; (d) ill-defined infiltrative mass in the left medial frontal lobe with no appreciable necrosis (49).

GBM tumours develop from low-grade astrocytoma and usually the clinical history is rather short, ~3-6 months, however; symptoms may develop quickly (51). Symptoms differ amongst individuals due to differences in the region of the brain being affected, but mechanisms remain the same. Signs and symptoms have been documented to arise from three major mechanisms (49). First, by the direct effect of GBMs, where brain tissue dies due to necrosis resulting in focal neural defects (40-60%) and cognitive impairments. Patients have a hearing and visual loss when tumours are in the temporal lobe while personality change, and impaired cognitive function attributed to

effects in the frontal lobe. Second, through secondary effects due to increased intracranial pressure resulting in a severe headache (30-50% of GBM patients) because of increased tumour size and edema in surrounding tissues. Third, seizure (simple, partial, generalized; 20-40% of GBM patients) attributed to the tumour location itself (49)(51).

3.4. Cell of origin

There are several theories regarding the cellular origin of gliomas, some of which remain highly controversial. Developmental studies of GBM formation have largely occurred in animal models in an effort to elucidate cell of origin (61). Neural stem cells (NSC) are found in the proliferative zones along the ventricles which differentiate into lineage-restricted progenitor cells. These progenitors intensify into neurons and glial cells (astrocytes and oligodendrocytes) (Figure-3.3) (60). NSCs show a level of plasticity that was previously unrecognized. Recent studies have led to the hypothesis that these NSCs or early glial progenitors can undergo a neoplastic transformation during gliomagenesis (51).

NSCs are at distinct brain regions where gliomas do not normally reside; indicating that a tumour may develop anywhere in the brain due to both the proliferative and migratory nature of these cell types. Tumour-associated mutations might trigger migratory signals in stem cells which allows them to drift from the subventricular zone into the striatum, septum, or cortex. In one animal study, tumour associated mutation has been observed in adult mice during embryogenesis (51)(62).

In normal brain development, glial progenitor cells give rise to are heterogeneous population. Some glia shows bipotent nature for both astrocyte and oligodendrocyte lineages while others may be restricted to specific zones like oligodendrocyte progenitor cells (OPCs) (61). NSC and glial progenitors continue to grow throughout an individual's lifespan, generating progeny cells and are thought to have initiating cell of origin potential for gliomas. Neural stem cells (NSC) express Nestin and GFAP markers and these are restricted to distinct brain regions like the subventricular zone (SVZ) of the lateral ventricles (62). Likewise, oligodendrocyte progenitor cells (OPCs) express markers Olig2, NG2, PDGFRα and are restricted to the oligodendrocyte lineage, however; glial progenitors although restricted to one lineage, but can express markers of another lineage leading to multiple differentiate such as astrocytes and oligodendrotes, during gliomagenesis, hence multiple potential cells of origin (Figure-3.3) (51)(61).

Clonal evaluation of a transformed cell of origin might give rise to a heterogeneous population but animal studies have shown that gliomas are able to recruit and proliferate non-neoplastic glia progenitors; the extent of which that this contributes to tumour growth and progression has yet to be recapitulated in humans (62). Other studies show that GBMs have a biphasic distribution with differentiation of astrocytes, oligodendroglia or gliomatous and mesenchymal differentiation. Thus, the presence of two biologically different cell types in a tumour suggests independent transformation events from unlike cells giving rise to each cell type or, different malignant transformation events from a common progenitor that gives rise to both cell types. A more detailed genetic analysis of these two cell types will more definitively elucidate the mechanism. The malignant transformation from a common progenitor will result in comparable generic profile (chromosomal level) amongst both cell types while independently-derived clones will reveal (subtle) genetic differences. Like the loss of heterozygosity (LOH) of 1p and 19q in oligoastrocytomas suggest that both oligodendroglial and astrocytic cells evolved to form a single precursor cell (51). Nevertheless, the complexity of malignant glioma has led to many theories for its cell of origin. As a definitive source has yet to be elucidated, a multidisciplinary approach may be required.

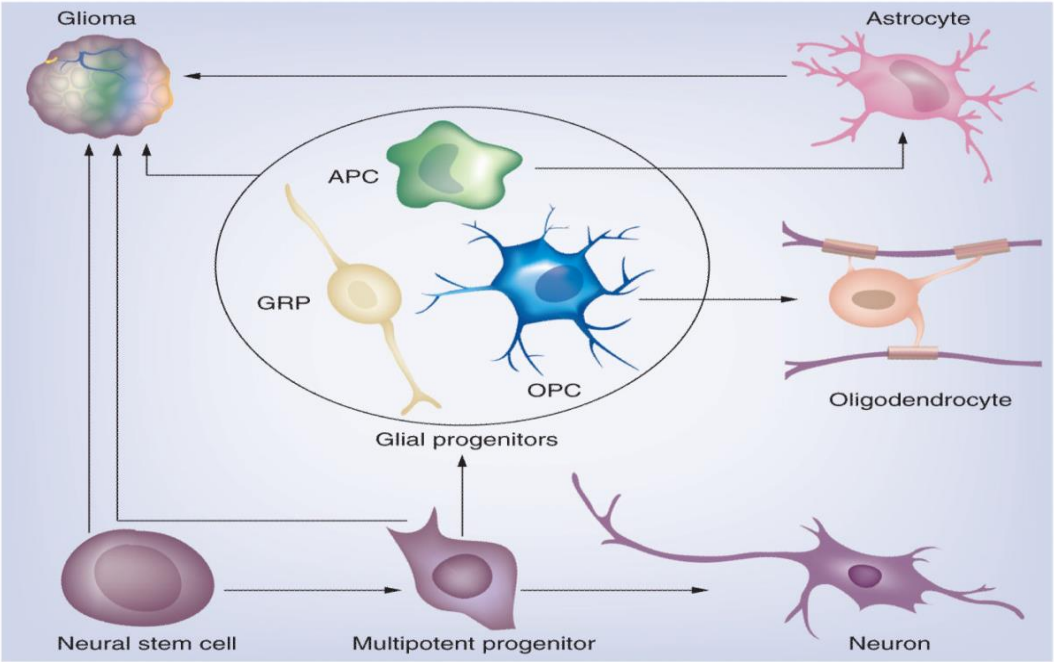

Figure 3.3. The gliomagenic potential of the different neural lineages
Neural stem cells and multipotent progenitors in the subventricular zone can give rise to cells of neuronal and glial lineage. Glial progenitors, which include a heterogeneous population of immature cycling cells, can give rise to astrocytes and oligodendrocytes. Glioma is a heterogeneous disease that can be divided into distinct subtypes. Different glioma subtypes arise from different cells of origin. APC: Astrocyte progenitor cell; GRP: Glial-restricted progenitor; OPC: Oligodendrocyte progenitor cell (62).

3.5. Current therapy

Unlike any other brain tumours, the standard of care for the clinical management of malignant glioma involves surgery followed by chemotherapy and radiotherapy. Despite significant research activity and advances in our molecular understanding very little clinically-relevant advancements have been achieved for GBM in the past few decades. Barriers for successful treatment for GBMs remain, primarily due to tumour heterogeneity, the inability of drugs to reach tumour cells (Blood Brain Barrier, BBB) which all contribute to relapse into more rapid and aggressive recurring tumours (56).

Surgery is a major, and oftentimes primary, therapeutic option for brain tumour treatment. Depending on the tumour type and location, surgical resection, whole or in part, is used to de-bulk the tumour mass, to offer immediate relief through seizure control and allaying neurological defects while also making the tumour site more amenable to anti-cancer drug therapeutics (49).

However, surgery alone cannot deal with the invasiveness of GBM as relapse is seen amongst 80% of patients within 2-3cm of the tumour margin. Location of tumour is important and limiting as tumours residing in the long brain stem, basal ganglia and cortex cannot be adequately removed via surgery, often leading to a worse prognosis. Thus, multimodal approaches are required for GBM management (63).

Radiotherapy plays an important role in the treatment of GBM following surgery to kill remaining tumour cells. However, ionizing radiation leads to radiation necrosis, radiation-induced permanent neuronal damage and radio-resistance of tumours (63)(64). Brachytherapy (insertion of radioactive implant directly into the tissues) and stereotactic radiosurgery has shown to be beneficial for relapsed GBM but not with newly diagnosed GBMs. In recurring GBM tumours, especially with multi-foci, whole brain irradiation can offer immediate but temporary secondary tumour control.

Chemotherapy has been long-used as an effective therapy to improve GBM patient survival. Among all anti-cancer drugs, alkylating agents like Temozolomide (TMZ), carmustine or BCNU (bis-chloroethylnitrosourea) and lomustine (CCNU) have shown favourable outcome. Of these agents, Temozolomide is the most promising and is used as the standard therapy for GBM patients. Temozolomide is given in oral form or as an adjuvant/concomitant with radiotherapy (57). A phase III trial by Roger Stupp and colleagues (2002) found that temozolomide, given with radiotherapy (65), produced much better patient outcomes with reduced overall toxicity. Currently, patients take temozolomide (Temodar) as a daily treatment consisting of a dose of 75 mg/m^2 for up to seven weeks (57).

Temozolomide (TMZ) is a DNA alkylating agent and acts as a prodrug (65). It is converted into its active metabolite monomethyl triazene 5-(3-methyltriazen-1-yl)- imidazole-4-carboxamide (MTIC). This metabolite then reacts with water to release 5 aminoimidazole-4-carboxamide (AIC) and reactive methyldiazonium cation. This reactive metabolite methylates DNA at *N7* positions of guanine in guanine-rich regions (*N7*-MeG; 70%), *N3* adenine (*N3*-MeA; 9%) and *O6* guanine residues (*O6*-MeG; 6%) (66). The main adduct is *O6* guanine residues and this lesion is resolved by methylguanine-DNA methyltransferase (MGMT). This enzyme directly repairs by removing the methyl adducts, hence reinstating guanine (Figure-3.4a)(67).

However, some of the lesion remains unrepaired and these unrepaired *O6*-MeG pairs with thymine instead of cysteine during DNA replication. DNA mismatch repair pathway (MMR) specifically recognizes mismatch pairing in DNA, such as mispaired thymine. MMR repairs damaged bases by using base complementarity to drive repair (66). MMR removes thymine while *O6*-MeG remain in the DNA strand blocking insertion of thymine during futile cycle resulting in formation of single strand breaks (Figure-3.4b). These single DNA strand breaks when collides with replication fork collapse form replication induced DSBs (68). Cell cycle arrest is triggered as part of a cellular DNA damage response (DDR) via ATR/CHK1-dependent signaling, at the G2/M phase. For a better clinical response from TMZ, efficient MMR pathway and reduced MGMT is required. Further, minor lesions such as *N7*-MeG and *N3*-MeA are repaired by single-strand break repair/ base excision repair (Figure-3.4c) (57).

Loss of MGMT gene at chromosome 10 is seen in 60-80% of gliomas and 45-70% of high-grade gliomas, due to mutations of MGMT (68). This loss is related to *MGMT* promoter methylation and is a common epigenetic factor in tumorigenesis. This occurs when there is methylation by 5`-methylcytosine methyltransferase on cysteine of cytosine of CpG islands and hypermethylation of CpG islands in *MGMT* promoter prevents transcription factor binding, thus silencing the gene (65).

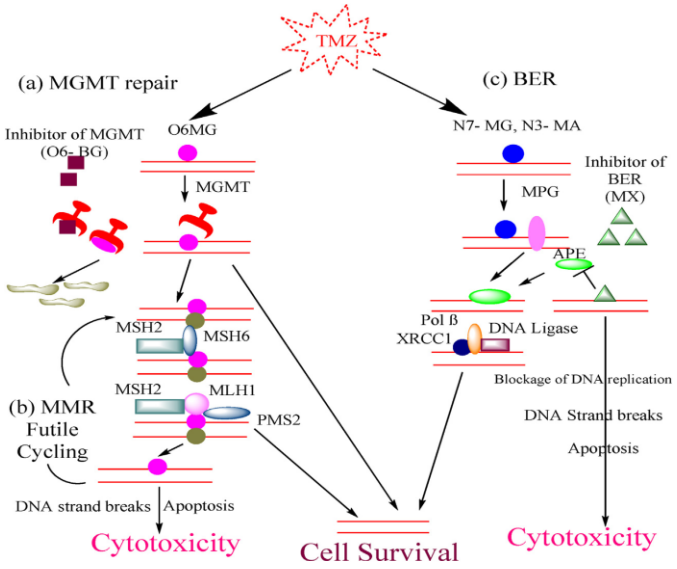

Figure-3.4. Mechanism of action of Temozolomide. TMZ is a cytotoxic prodrug which when hydrolyzed, inhibits DNA replication and destruct cancer cells by methylation of nucleotide bases through direct repair, Mismatch repair (MMR) and Base excision repair (BER) (57).

Before the advent of TMZ in GBM treatment, procarbazine and vincristine were often used in combination with lomustine (CCNU) but did not offer many benefits ss due to high toxicity (57). Second line GBM treatments currently include carboplatin, oxaliplatin, topoisomerase enzyme inhibitors such as etoposide (Topoisomerase 2) and irinotecan (Topoisomerase 1). These drugs are used in temozolomide resistant GBM. Other options include anti-angiogenic agents like anti-VEGF monoclonal antibodies (Bevacizumab), anti-FGF antibodies, monoclonal antibodies targeting EGFR (Erlotinib and Gefitinib) and tyrosine kinase inhibitors (49).

Despite invasive surgery, radiotherapy and chemotherapy regimens showing clinical gains in overall patient survival, patient quality-of-life is affected. Significant treatment-associated effects include cerebral edema, seizures, gastrointestinal tract disturbance, osteoporosis, venous thromboembolism, cognitive impairment and mood disorders (69).

Due to minimally-effective GBM therapy and dire prognoses, researchers have sought to better understand the molecular genetics of these deadly brain tumours. High-throughput and multidimensional profiling by The Cancer Genome Atlas project has revealed molecular subtypes of GBM characterized by varieties of genetic mutations. This approach has implicated numerous signaling pathways mitigating the aggressiveness of a tumour: pathways that offer opportunities as prognostic biomarkers involved in tumour growth and potentially new molecular targets for therapy. A future aim is to use this information to formulate specific targeted molecules for the personalized therapeutic approach (56).

3.6. Barriers to GBM treatment

Heterogeneity in GBM and among GBM may arise from clonal evaluation, that is some clones survive under selective drugs, incurring mutations, hence giving rise to resistant clones (Figure-3.5) (56). For example, mutation of the TP53 gene has been reported to give rise to the subclonal heterogeneity of GBM. Mutation of the MSH6 gene has been reported in GBM patients and is induced by TMZ (70).

Cancer stem cells (CSCs) are present in many tumours and this area of research has gained a lot of traction in recent years. CSCs are thought to be responsible for tumour initiation, progression, angiogenesis and differentiation into non-tumour cells. These stem cells are resistant to standard GBM therapy. Recent studies have found that chemotherapeutics developed to target brain cancer stem cells result in toxicities because they express CD133 and Nestin, just as normal brain stem cells. It is possible to selectively target these cells and so specific drugs are being designed to reduce toxicities (56).

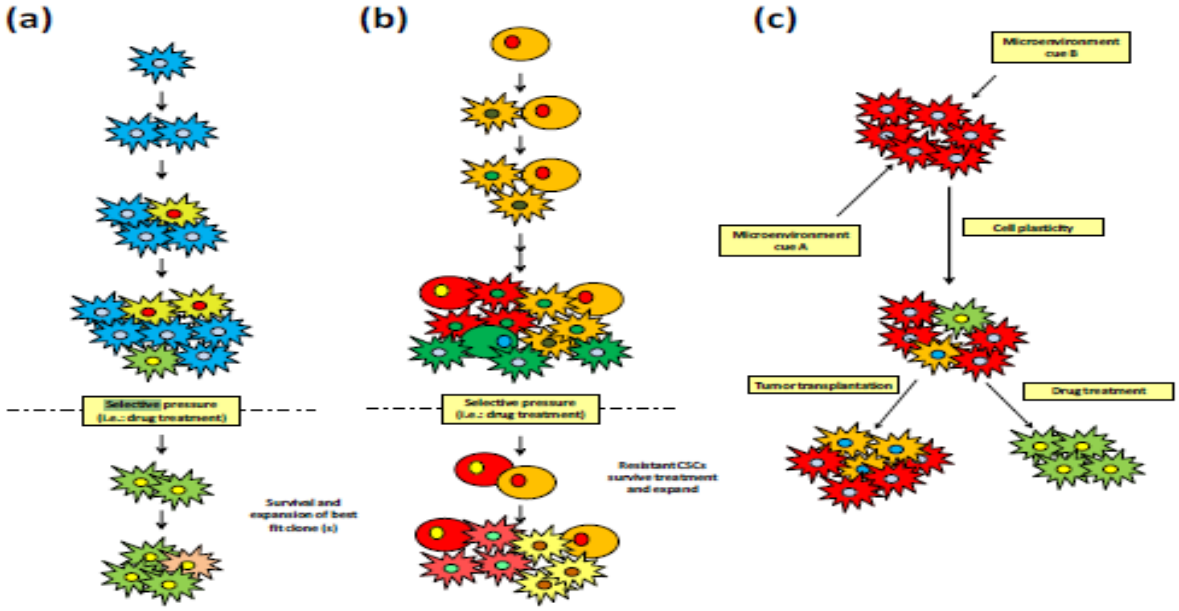

Figure-3.5. Models for the origin of intra-tumour heterogeneity. (**a**) Clonal evolution: tumour cells gain mutation under selective drug treatment and the fittet clone survives leading to tumour relapse (**b**) CSC model: CSCs divide generating asymmetrically differentiated tumour cells with mutations. Giving rise to resistant populations which survive with treatment resulting tumour relapse (70).

In the brain, the blood-brain barrier (BBB) is a major limiting factor in the penetration of chemotherapeutics to reach GBM tumour cells. The blood-brain barrier (BBB) is a lining of blood vessels of the brain that prevents penetration of harmful compounds or toxic xenobiotics from the bloodstream into brain tissues. This barrier does not allow many hydrophilic, protein-bound drugs and large molecular weight molecules (more than 400kDa) to enter brain tissues**.** The composition of the blood-brain barrier is transformed under pathological conditions like malignant glioma, giving rise to the blood-brain tumour barrier (BBTB)(65). Vascularization and function of this tumour barrier remain the same as blood-brain barrier in low-grade glioma but in high-grade

gliomas, the BBTB becomes leaky (disrupted). Overexpression of Vascular Endothelial Growth Factor (VEGF) and angiogenesis in high-grade glioma appears under hypoxic conditions due to increased metabolic demand. This overexpression is responsible for the formation of abnormal blood vessels leading to dysfunctional BBTB(71).

4.1. Medulloblastoma incidence and epidemiology

Pediatric medulloblastoma (MB) is an invasive cerebellar tumour (72) comprising of ~20% of all brain tumours; derived from the primitive neuroectodermal lineage. MB is commonly diagnosed in children younger than 19 years but affects individuals of all ages (73). Despite an overall stage-specific survival rate of about 80% (for patients with an average age of five years at diagnosis and treatment) survival is only about 55% for high-risk patients (74). Medulloblastoma is more common in males (3:1 M:F ratio)(73) with a higher incidence in early childhood (<5 yrs.). In fact, many MB tumours originate *in utero*, accounting for the high incidence at such young ages(75). The incidence of medulloblastoma peaks at 3-4 yrs and 8-9 yrs. Medulloblastomas do develop in adults but relatively infrequently; comprising only 1% of all primary adult CNS tumours that occur in patients <40 years of age (75).

Approximately 75% of all pediatric medulloblastoma arise in the cerebellar vermis projecting into the fourth ventricle (74); originating from immature or embryonal neuroprogenitors (76). Studies have shown that prognosis and treatment response are related to cellular pathways involved in MB tumour development and cell of origin (77). MBs metastasize through cerebrospinal fluid (CFS), forming tumours in ventricular surfaces, subarachnoid space and/or nerve roots; sometimes along the brain and spinal cord and of variable sizes. Distant metastasis is rare but is seen in bone marrow while individuals with ventriculoperitoneal shunts are prone to develop tumour cells in the peritoneal cavity (75).

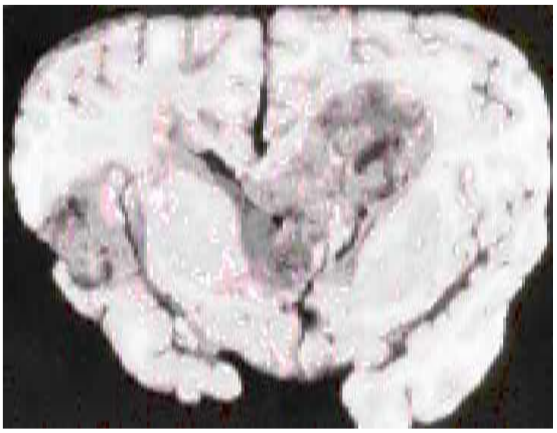

Figure-4.1. MRI of brain showing sagittal and horizontal views. Sagittal view shows a midline posterior fossa medulloblastoma with intermediate signal intensity. There is an obstruction to the flow of CSF, marked hydrocephalus and edema. Horizontal view shows a homogenous enhancing medulloblastoma arising from the right cerebellar hemisphere with displacement of the vermis (103).

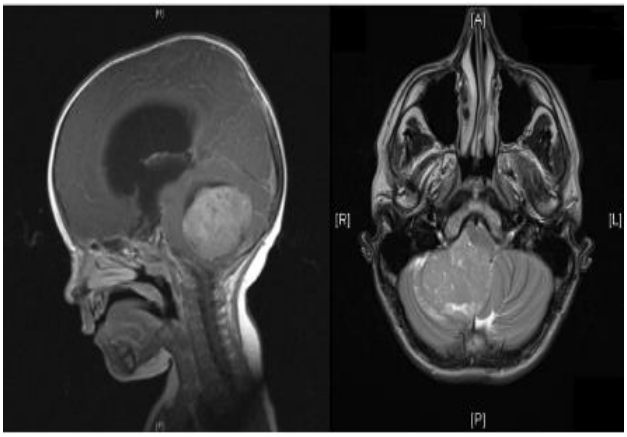

Figure-4.2. Coronal section of cerebrum showing multiple metastases from cerebellar primitive neuroectodermal tumour. Note growth along Ventricular surface with invasion of brain plus separate cortical metastasis (75).

Treatment of younger patients includes maximal surgical resection (76) along with craniospinal radiation therapy and adjuvant therapy with alkylators and/or microtubule inhibitors (73). Chemo-radiotherapy, in general, is toxic and results in physical and non-physical impairments, with physical defects such as neurological deficits, secondary malignancy, and endocrine dysfunction whereas non-physical impairments include cognitive difficulties, psychological and social problems (78). Patients often complain of headache, vomiting, lethargy, sometimes with increasing head circumference due to increased intracranial pressure and obstructive hydrocephalus. About 11-43% of patients have a worse prognosis and require systemic chemotherapy along with radiation resulting in decreased quality of life (79)**.**

These permanent sequelae make treatment of young children very challenging due to lifelong diminished functional capacity for gainful employment and family life (77)(78). Some studies have shown that children receiving craniospinal irradiation therapy have intellectual deterioration in children <7 years and less with lower doses (75). Although the survival rate in children with these therapies has improved in the past 20 years(78), however, 30-40% of patients die due to recurrence while survivors suffer significant permanent neurological defects, either due to effects elicited by the tumour or treatment (73).

Further study is required to better understand the biological characteristics of medulloblastoma including a cell origin and dysregulation of cellular signaling pathways (79) that are responsible for malignancy. This information will enable development of more targeted therapies, that will offer better risk stratification (80).

4.2. Cell of origin & histological classification

Medulloblastoma arises from fragments of the primitive neuroectoderm in the roof of the fourth ventricle, growing in the cerebellar vermis (81). This tumour is often found in the brainstem invading through the ependyma and in the floor of the ventricle. There are several theories for origin of MB tumour, one study indicates that the tumour arises from primitive neuroectodermal cells in the germinal matrix while others have shown that the tumour arises from external granular precursor cells as medulloblastoma expresses ZIC1 (usually expressed in the external granular layer of developing cerebellum) (82)(83). Other groups have suggested that there might be more than one cell type giving rise to this tumour or that cells from both locations are responsible (84).

Based on location within the central nervous system and histologic features, medulloblastoma along with other embryonal CNS tumours are classified into five histologic variants according to the World Health Organization, WHO (82). The first is *classical* (66%) which display features of neuroblastic differentiation (77) with apoptotic activity and are found in the midline (85). Second, *desmoplastic* (15%) where the cells represent neurocyte differentiation which (86) has a favorable prognosis (85). Third, *large cell anaplastic* (15%) which (84) is characterized by very high proliferative activity, apoptosis and associated with a poorer prognosis. *Melanotic* and *medullomyoblastoma* differentiation variants are additional but rare variants (Figure-4.3) (78).

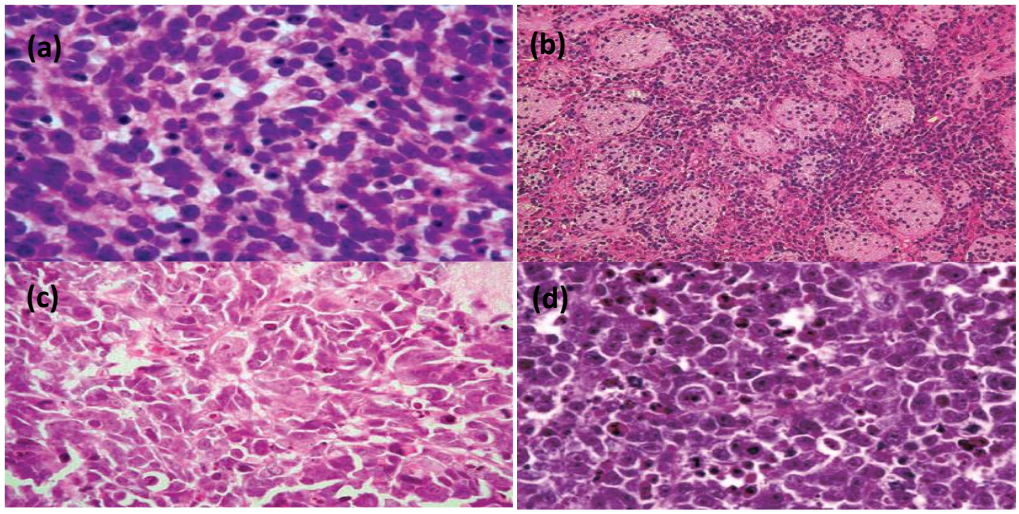

Figure-4.3. Histologic variants of medulloblastoma. (*a*) Classical Medulloblastoma subtype has small uniform cells with the high nuclear component. (*b*) Desmoplastic Medulloblastoma consists of a mixture of differentiated low growth neurocyte cells and high growth desmoplastic intermodular zones of pleomorphic cells (*c*) Anaplastic Medulloblastoma has contained pleomorphic cells with High growth fraction of polyhedral forms. (*d)* Large-cell medulloblastoma consists of large uniform cells with vesicular nuclei and a single nucleolus (83).

4.3. Molecular classification of MBs

Studies have shown that subgrouping for medulloblastoma is based on clinical prognostication and stratification which includes histological subgrouping, as mentioned earlier (classic, desmoplastic, large cell/anaplastic histology) (87). Also, clinical factors such as age, the extent of resection, metastases also figure in this stratification. Research has also suggested that transcriptional profiling of medulloblastoma cohorts have identified multiple distinct molecular subgroups differing in the transcriptome, genetic events, demographics along with clinical outcomes (Figure-4.4) (88). The finding of differences within a common tumour culminated in a meeting of MB researchers in Boston in fall of 2010, where based on the evidence presented, the participants came to a common consensus that medulloblastoma can be classified into four distinct subgroups: Wnt, Sonic Hedgehog-Shh, Group 3, and Group 4 (Figure-4.5) (84)(81).

Extensive study is being undertaken on the molecular aspects of signaling pathways that are involved in the development of these tumours. Identifying and targeting new signaling pathway targets will lead to more effective treatments with lower neurotoxic effects thus reduced life-impairing defects (78). Furthermore, studying the genetic mutations in these signaling pathways may illuminate critical information underpinning the development of brain tumours and their pathogenesis(84).

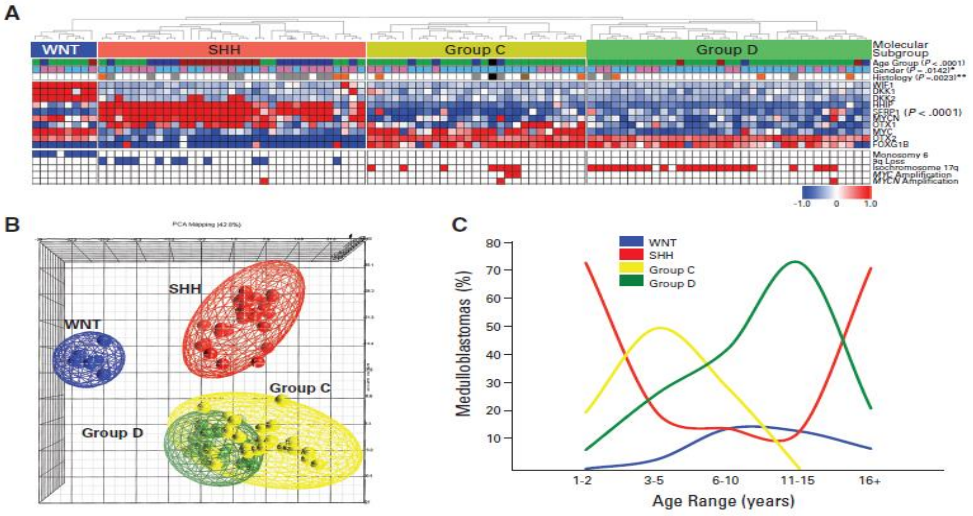

Figure-4.4. (A) Unsupervised hierarchical clustering of human 1.0 exon array expression data from 103 primary medulloblastomas using 1,450 high–standard deviation (SD) genes. Clinical features (age group, sex, and histology) for the 103 samples included in the study. Age groups include infants (< 3 years; blue), children (4 to 15 years; green), adults (< 16 years; red), and unknown (black). Sex includes males (blue) and females (pink). Histology includes classic (white), desmoplastic (gray), large-cell/anaplastic (orange), medulloblastoma with extensive nodularity (brown), and unknown (black). The heat map below the dendrogram shows the expression profile for 10 genes well characterized in medulloblastoma and demonstrates their significant pattern of differential expression among the four subgroups. Blue boxes indicate loss/deletion, red boxes indicate gain/amplification, and white boxes denote balanced copy number state for the specified genomic aberration. (B) Principal component analysis (PCA) of the primary medulloblastomas described in (A) using the same 1,450 high-SD genes used in clustering. Individual samples are represented as colored spheres (blue-WNT, red -SHH, yellow -group C, green -group D). (C) Age at diagnosis distribution for each of the four medulloblastoma subgroups(87).

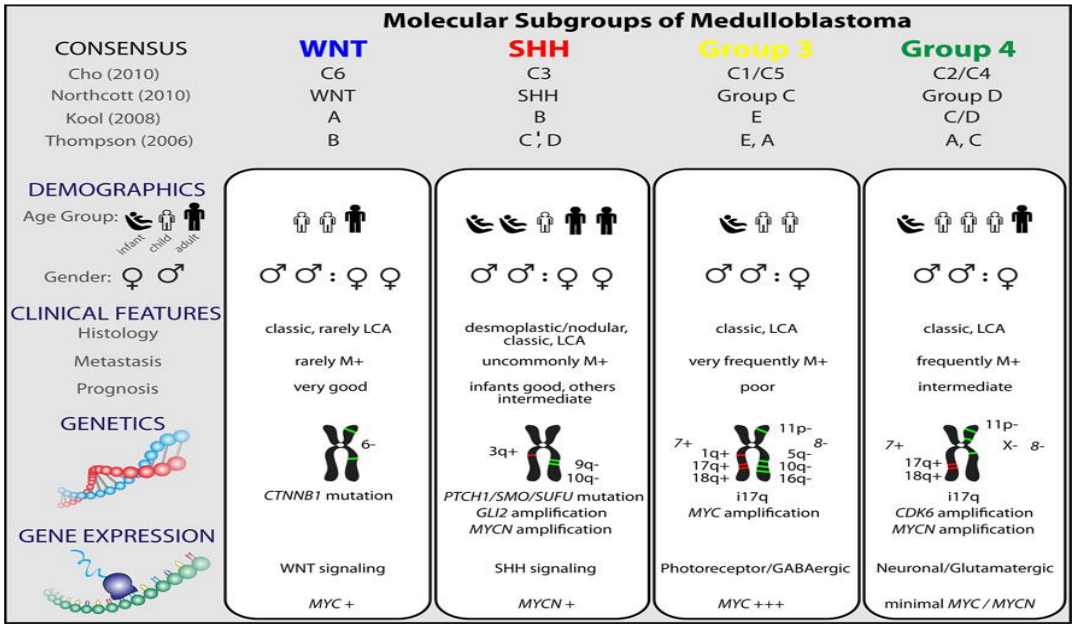

Figure-4.5. Molecular subgroups of Medulloblastoma including their gene expression profile and histological variants presented by each subtype(89).

4.3.1. Wnt subtype

Wnt medulloblastomas are a rare form, ~11% of all MBs, and has a more favorable long-term prognosis with 90% survival (78). While medulloblastoma is more common in males compared to females, the gender ratio for Wnt medulloblastoma is 1:1 (87). Mouse models developed to study Wnt medulloblastoma have shown that this type arises from the lower rhombic lip of the cerebellum(90). The WNT signaling pathway is involved in embryonal brain development with WNT signaling leading to the accumulation of β-catenin which binds to TCF-4/lef-1, involved in cell division, proliferation and cell adhesion (78)(88). Most of the genes involved in WNT MBs result in pathway hyperactivity and dysregulation.

Molecular analysis revealed mutations in *CTNNB1* (8%) (β-catenin), adenomatous polyposis coli (*APC*) (2%), *AXIN1* and *AXIN2* (3%) and overexpression of survivin (apoptosis inhibitor) (77)(78). Mutations of *CTNNB1* are associated with medulloblastoma development in older children and two studies have shown that these are curable(83). Several other genes overexpressed in the Wnt pathway are also overexpressed in Sonic hedgehog and Group 3 medulloblastomas (90).

4.3.2. Sonic Hedgehog (Shh) subtype

The Sonic Hedgehog (Shh) type comprises about 28% of medulloblastomas with an intermediate prognosis and is common in both infants (<4 years) and adults (>16 years). The SHH pathway is involved in the normal cerebellar development and plays a key role in the proliferation of neuronal cells (84)(75). Analysis of medulloblastoma identified germline inactivating mutations (9%) in Patched 1 (*PTCH1)* resulting in nevoid basal-cell carcinoma syndrome (NBCCS); also known as Gorlin syndrome. Patients with this syndrome develop basal cell carcinomas, bone cysts and are susceptible to several other tumours like medulloblastoma (4% risk of development) (83).

Molecular analysis of Shh tumours reveals mutation of Smo to about 30% (78)(84) along with Suppressor of Fused (SUFU) mutations which are a potent repressor of Gli1 activation(77). Upregulation of BMI1 leads to overactivation of the Shh pathway and overexpression of BMI1 in these tumours resulting in abnormal regulation of p53 and Rb pathway (90).

4.3.3. Group 3 and Group 4 subtypes

Group 3 tumours comprise 28% of medulloblastomas; considered classical medulloblastoma (90). This subtype primarily involves both MYCN and MYC amplification and overexpression, to an extent that sometimes it is referred to as an MYC group. This type of tumour is common in infants and children but not in adults. Little is known about the molecular pathogenesis of this tumour type and its classification occurs only after tumour transcriptional profiling (77). Group 3 medulloblastomas are categorized into 3α and 3β depending on Myc amplification status, where 3α involves Myc amplification with worse prognosis and 3β does not express Myc (78). These tumours have isochromosome 17q (abnormal chrosome 17 with two identical long q arms) (26%) (82) with a gain of chromosome 1q and loss of chromosomes 5q and 10q (77)(84). Overexpression of histone methylases/acetylases, such as HDAC5, HDAC9, MLL2, and MLL3 have been detected as well (78).

Group 4 medulloblastomas are the most common type comprising 34%. These tumours are associated with CDK6 and MYCN amplification with low Myc overexpression (90). Group 4 also has isochromosome 17q in ~66% of this tumour subtype. KCNA1 is considered as an immunohistochemical marker for Group 4 but requires further validation. Group 4 has documented the loss of chromosome X, primarily in 80% of females with this medulloblastoma subtype. OTX2 amplification and overexpression are only identified in Group 3 and Group 4 medulloblastomas (77).

Although this had been published in prior research studies, it was assumed that molecular classification based on transcriptional profiling will continue to diversify into larger cohorts as these subgroups continue to be studied in greater depth. More recently, refinements in epigenetic profiling and other molecular analyses have identified additional subgroups within these cohorts, as such, the number of groups continues to grow (Figure4.6)**.**

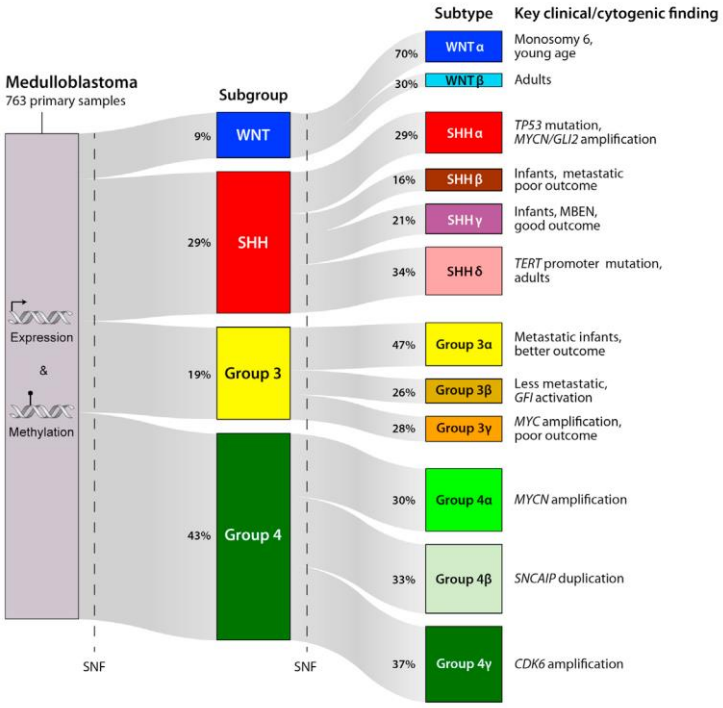

Figure-4.6. Intertumoural heterogeneity within Medulloblastoma reveals 12 subtypes of MB tumour(91)

4.4. Current Therapy

MBs are highly aggressive and heterogeneous with variations in cell types and numerous genetic discrepancy which makes it difficult to treat, especially in children, as there are inherent limitations in drug dosing and use of ionizing radiation (92). The current treatment regimen for medulloblastoma includes surgery supplemented with ionizing radiation followed by chemotherapy (92).

In younger patients, treatment includes chemotherapy and radiotherapy. However, radiotherapy is often avoided in children as radiation can be damaging to the developing brain. This extensively compromises tumour control and survival in patients under three years old (92)(93). These treatment protocols have a profound effect on long-term quality of life and are a major problem in children due to substantial neurological and cognitive defects (93). Survival of patients diagnosed with this cerebellar tumour has dramatically improved with continued advancements in treatment interventions and refinements to standard therapeutics (94).

Combination therapies using multiple drugs along with radiotherapy has proven to be effective in medulloblastoma. But novel therapeutic targets are lacking that offer fewer long-standing adverse effects (92). Therefore, new treatments are needed particularly in the treatment of younger patients. Furthermore, targeted therapy is required to eradicate therapy-resistant populations which arise as treatment progress (87).

Recognizing that medulloblastoma is comprised of multiple subtypes has created the pretext to identifying molecularly-targeted therapeutics. Enhancing the understanding of the biological traits of these subtypes has the potential of dramatically changing tumour stratification and treatment (90).

4.4.1. Surgery

Harvey and Cushing introduced the idea of surgical resection for brain tumours and established the treatment modal ~70 years ago (80). At the time, surgery was not successful due to excessive bleeding, poor wound healing and mortality rates of ~40%. Recent advances in surgical appliances and techniques have reduced the mortality rate to < 1%. The goal is maximal resection of the localized tumour without damaging the surrounding vital tissues and structures such as the lower cranial nerve and brainstem (95). As part of resection of the tumour, tissue for histological diagnosis along with resolution is collected for any type of obstructive hydrocephalus (94).

Following surgery, the degree of surgical resection is assessed by MRI of the brain, usually 48hrs post-surgery. It is not uncommon for small amounts of residual tumour to remain despite maximal resection, therefore, surgery is often accompanied by adjuvant chemoradiotherapy. Following tumour resection, patients often complain of a headache, vomiting, and lethargy due to increased intracranial pressure (96). These symptoms often referred to as mid-line syndrome usually appears within 6-7 weeks after surgery. Harper and Friedman recently demonstrated the connection between duration of symptoms and the stage at which the disease was initially diagnosed. They found a correlation with shorter duration of symptoms before diagnosis equated with more advanced disease progression (95).

Surgical complications can include air embolism, recovery issues from anesthesia, hemorrhage, posterior fossa mutism (decreased or absent speech), meningitis (bacterial or aseptic), pseudomeningocele, brainstem dysfunction, wound infection, stress ulcer, vascular stroke and

pain(93). A cerebrospinal fluid (CSF) shunt is required post-surgery if the patient is lethargic. About 40% of children require permanent CSF shunting after surgery to reduce the risk of metastasis (94).

4.4. 2. Radiotherapy

Radiation is the most effective non-surgical treatment modality in children (97). Radiotherapy is considered a primary treatment option in tumours that are highly radiosensitive (98). Several studies have demonstrated that maximum improvement in survival for newly diagnosed patients is observed when radiation is applied to the entire craniospinal axis regardless of the extent of disease at the time of diagnosis (99).

Radiation is given in the fractionated doses: 3500 to 4000cGy to the entire CNS axis and 5000 to 5500cGy to the posterior fossa at a rate of 800 to 1000cGy in five fractions per week. As medulloblastoma tends to metastasize to cerebrospinal fluid (CFS), an additional dose of 5000cGy is given. For children under 3 years of age, a 500cGy reduction of dose is used (96). This dosage regime has shown to prolong survival rates in children with medulloblastoma (82); with an overall 5-year survival (OS) rate at ~46% to 65% in the average-risk group and 50% in the high-risk group (85).

Despite this standard treatment for limiting residual tumour growth and prolonged survival rate, surviving patients suffer from pronounced neurological and endocranial complications along with secondary tumours (100). Radiation therapy can result in long-term devastating effects on intellect and growth (101), early puberty development and compromised spinal growth (82). Recently, chemotherapy has been introduced as an adjunct to radiotherapy with a goal of reducing the dose of radiation and an accompanying reduction in long-term side-effects in children (93). This combinatorial therapeutic modal of chemoradiotherapy has improved 5-year survival rate to about 55% to 76% for high-risk patients (patients with metastasis or local residual disease) and 70% to 80% for standard-risk patients (non-metastatic with poor prognosis) (92).

In a recent study, patients with medulloblastomas were treated with radiation followed by vincristine, cisplatin, and lomustine, this trial with children presented 5-year progression-free survival (PFS) with a rate of 90% ± 6% in patients with localized disease and 67% ± 15% in patients with metastatic disease. Although this trial presented good results, adverse effects were

reported, including grade 3 to 4 audiological toxicity in 32% to 47.6% of patients (with an accumulated dose of cisplatin of 225 to 272 mg/ml), grade 3 to 4 hematologic toxicity in 52.4%, grade 3 to 4 neurological toxicity in 25.4% and grade 3 to 4 renal toxicity in 17% to 20.6% along with sepsis in 9% of patients (85).

Another study of children with medulloblastoma treated with RT and vincristine, cisplatin and lomustine resulted in a 5-year progression-free survival (PFS) rate of 90% ± 6% in patients with localized disease and 67% ± 15% in patients with metastatic disease. The difference in these adjuvant chemotherapy protocols was studied in patients with average-risk (poor prognosis) medulloblastoma treated with RT plus randomly assigned lomustine, cisplatin, and vincristine or cyclophosphamide, cisplatin, and vincristine (102). In a similar study with adjuvant chemotherapy including cyclophosphamide, cisplatin and vincristine; outcomes for survival were reported to be 5-year OS rate in the average-risk group of 70.4% ± 9.5% and in the high-risk group of 49.7% ± 13.0%, with lower toxicities observed in patients compared to the first study mentioned in the previous paragraph. This difference in toxicities is due to the dose of chemotherapy used along with radiation in children (102)(103).

Despite these improvements in overall survival rate, 30-40% of patients encounter recurrence or progressive disease (104) and further reduction in morbidity and mortality is limited due to toxicities of standard treatments and occurrence of secondary tumours (86).

4.4.3. Chemotherapy

Medulloblastomas are chemotherapy-sensitive tumours. Several anti-cancer drugs are used to treat patients depending on the progression of the disease, stage, and dosage of the drug depends on age and health of the patient, as a high dose cannot be prescribed to younger patients due to toxicity issues (98). Chemotherapy results in long-term disease control but is not necessarily curative. Drug trials in various studies have either used single agent chemotherapeutics or drug combinations. Combinatorial therapeutics also include the use of drugs with radiotherapy, especially in post-surgical patients to reduce the burden of tumour mass (102).

4.4.3.1. Commonly-used MB chemotherapeutics

Single-agent trials have been shown with drugs like cyclophosphamide, methotrexate and platinum derivatives including carboplatin, cisplatin (in recurrent medulloblastoma). High dose cyclophosphamide (75) led to tumour shrinkage while cisplatin showed objective tumour response

in 75% of patients. Patients with recurrent medulloblastomas have shown positive results with vincristine and cisplatin (82).

❖ **Topoisomerase inhibitors-**

Topoisomerase I and Topoisomerase II inhibitors have been used in several recent medulloblastoma drug trials and have shown promising results. During replication, these enzymes help release the torsional strain by unwinding and rewinding the DNA molecule (92). Inhibiting these enzymes results in partial or complete inhibition of DNA replication leading to apoptotic death of tumour cells. Topoisomerase I inhibitors like Camptothecin (CPT), bind to the enzyme-DNA complex through hydrogen bonding thus forming a tertiary complex, hence stabilizing it (92). This prevents DNA break intermediates from re-ligating leading to S phase cytotoxicity along with DNA damage due to a collision between the Top I cleavable complex and replication fork giving rise to double-strand breaks which are known to be lethal, resulting in apoptosis of tumour cells (105).

Topotecan and irinotecan are CPT-related FDA approved Topoisomerase I inhibitors shown to be effective in many tumours like breast, prostate, colon, including brain metastases in several studies (Figure-4.7) (106). Clinical trials are now underway with these inhibitors in brain tumours, notably in medulloblastoma. Topotecan can freely cross the blood-brain barrier due to its low binding affinity in serum. A recent clinical trial of medulloblastoma with topotecan has shown prolonged survival in MB patients (107).

Topoisomerase II inhibitors, form stable tertiary structures with the Top II enzyme and transient DNA double-stranded breaks, resulting in persistence and collapse into frank DNA breaks leading to apoptosis (107). Top II drugs such as etoposide, doxorubicin and teniposide have been shown to be effective for treatment of brain tumours, including MB (80).

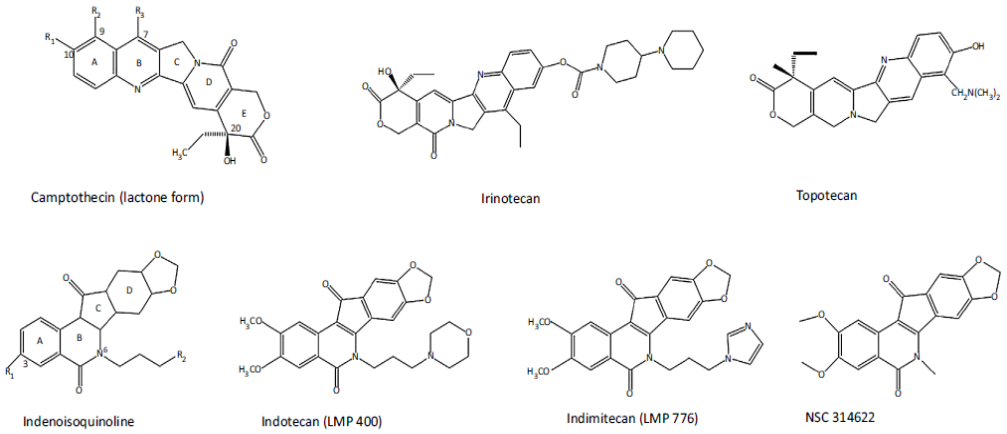

Figure-4.7. Chemical structures of Topoisomerase inhibitors(80)

❖ Tyrosine kinase inhibitors-

Tyrosine kinase inhibitors (TKi) target several oncogenic growth factors like Bcr–Abl, Her2, epidermal growth factor receptor (EGFR), platelet-derived growth factor receptor (PDGFR), vascular endothelial growth factor receptor (VEGFR), fibroblast growth factor (FGF), hepatocyte growth factor (HGF) and insulin-like growth factor 1 (IGF-I)(108). These pathways modulate cancer developmental pathways in medulloblastoma like differentiation, cell proliferation, death and metastasis (92). Many tyrosine kinase inhibitors are being used in clinical trials for MBs, including imatinib (targets PDGFRA and FIP1L1 genes) (109), gefitinib (targets EGFR gene) (110), lapatinib (GW-572016)(targets EGFR), canertinib (CI-1033) (targets EGFR), semaxinib (SU5416) (targets MPL) , vatalanib (PTK787/ZK222584), sorafenib (targets VGEF), sunitinib (targets PDGFRa, PDGFRb, VEGFR1, VEGFR2, VEGFR3), leflunomide (SU101), and erlotinib (targets EGFR) (92)(108)(110).

❖ Phosphoinositol 3 Kinase (PI3K) inhibitors-

PI3K signaling pathways are responsible for controlling cell proliferation, survival, and motility/metastasis, and present a potential therapeutic agent. Studies have shown that inhibiting the PI3K pathway in combination with the IGF-1R pathway has antiproliferative potential in MB and neuroblastoma cell lines (92)(111). This has been shown with humanized anti-IGF-1R antibody R1507 in conjunction with PIK75, a class IA PI3K inhibitor (92)(111).

Unlike any other therapeutic interventions, chemotherapy also induces toxicity to normal cells in addition to killing tumour cells. Cisplatin causes hearing loss and vincristine has several adverse drug reactions including hepatotoxicity, nephrotoxicity, neuropathy, resulting in a poorer long-term quality of life (80). Higher drug dosing results in more toxic effects leading to life-threatening issues. In younger patients, there is a constant need to manage side-effects and these children require more clinical care. Combinatorial treatment has proven to be more effective in reducing toxic effects in most cases. Numerous studies have demonstrated that a combination of surgery and chemotherapy result in improved outcomes compared to surgery with radiotherapy (93). However, drug-dosage must be considered in multi-drug regimen to reduce toxicity while maintaining beneficial therapeutic efficacy.

Research is being conducted more on understanding the molecular pathways of medulloblastoma which may provide potential targets based on individual patient's genetic composition. With the understanding of genetic abnormalities giving rise to Gorlin syndrome and Turcot syndrome (81), a means to dig more into the progression and development of medulloblastoma which may give rise to specific targeted therapeutics in the future.

4.5. Barriers to Medulloblastoma Therapy

For effective drug delivery to medulloblastomas, drug formulation must overcome several barriers. As medulloblastomas have different characteristics compared to peripheral tumours, factors such as tumour microenvironment, blood-brain barrier (BBB) and stem cells must be considered (92).
The blood-brain barrier (BBB) is a lining of blood vessels of the brain that evades penetration of harmful compounds or toxic xenobiotics from the bloodstream into brain tissues (110). This barrier does not allow many hydrophilic, protein-bound drugs and large molecular weight molecules (more than 400Da) to enter brain tissues. These characteristics must be taken into consideration when formulating drugs for medulloblastoma or any other brain tumours. Astrocytes along the BBB make it 98% impermeable to small molecules and 100% too large molecules (112). Drugs like topotecan cross BBB effectively and have proven to be promising in treating medulloblastomas (80).

As outlined above, medulloblastomas are chemo-sensitive but studies show that the sensitivity to chemotherapy varies among subtypes of medulloblastoma, not only due to molecular characteristics of the tumour itself but also due to differences in the composition of the blood-brain barrier (BBB) arising from differential gene expression. As shown by Phoenix and associates, the Wnt subtype is susceptible to chemotherapy due to perforations in BBB which allows enhanced accumulation of drugs inside the tumour resulting in better clinical outcomes (112). Other non-Wnt subtypes have intact BBB leading to impermeability of drugs, hence resistance (92).

Along with the natural brain-based blood-brain barrier (BBB), the tumour BBB is another physiological barrier that mitigates therapy in medulloblastoma. The tumour BBB forms between endothelial cells and tumour tissues. Tumour cells invade between astrocytes and brain endothelial cells disturbing their connectivity. The BBB is damaged as tumour cells are surrounding normal brain cells forming blood-brain tumour barrier (BBTB). BBTB possesses three hallmarks; low oxygen tension or hypoxia, high interstitial fluid pressure (IFP), and low extracellular pH(92). BBTB have altered characteristics from normal tissues and are exceedingly intact, thus not allowing most hydrophilic molecules from penetrating the tumour. The experimental data show the normal pore radii of BBB is to be 220A which is big enough for penetration of most drugs but due to mutations and formation of BBTB this pore size shrinks (110). For example, the pore size in solid malignant orthotopic RG-2 rat glioma microvasculature is about 12 nm, which is small enough for most drug molecules to reach the tumour cells. With disease progression, this BBTB become a greater barrier for drug delivery due to angiogenesis and further disruption of BBB (92).

Currently, a great deal of research is being conducted looking for high permeability of drugs across the BBB through strategies such as barrier disruption, blocking of efflux pumps, utilization of transporters and local drug delivery. Many transport drug delivery systems have been developed in recent years like absorption-mediated transcytosis (AMT), transporter-mediated transcytosis, receptor-mediated endocytosis, and nanoparticles. Albumin has proved to be a suitable drug delivery material for nanoparticles for its biodegradable and biocompatible properties. It interacts with the cell membrane and crosses BBB via absorptive transcytosis (Figure-4.8). Glutathione (GSH) responsive disulfide bond crosslinked bovine serum albumin (BSA) nanoparticles have been developed for camptothecin (CPT) delivery to medulloblastoma cells. Their effectiveness and cytotoxicity have been assessed *in vitro* in DAOY MB cell line (92).

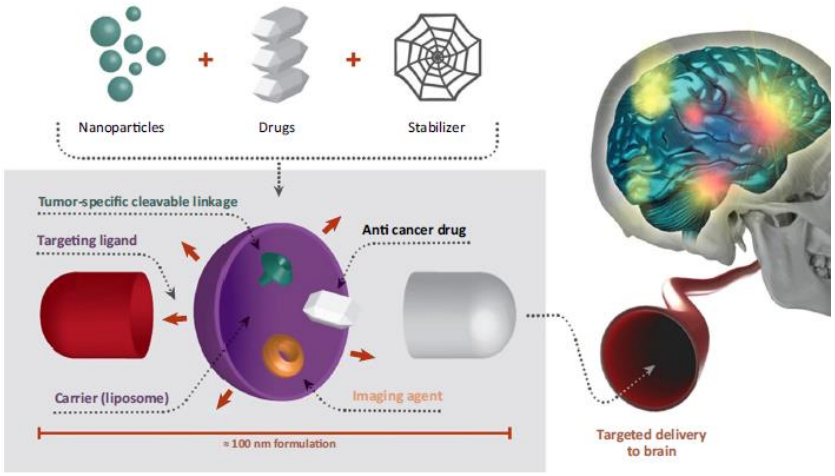

Figure-4.8. Drug formulation and targeted delivery to brain. The nanocarrier system has potential to enhance the circulation time of encapsulated drugs, allowing effective drug accumulation at the target site. Further receptor-mediated transcytosis can be an effective means of active transport for nanoparticle entry into the brain. Imaging and sensing agents can also be encapsulated to generate multifunctionality in the treatment of medulloblastoma (MB) (92).

Chemoradiotherapy generates DNA damage, mainly DNA double-strand breaks (DSBs) which are known to be lethal to the tumour as well as normal cells resulting in cytotoxicity. There are many DNA damaging agents used in cancer treatment that employs the idea of targeting DNA of tumour cells via induction of strand breaks and have proven to be effective in a wide range of cancers including brain tumours. For the past few decades, targeting tumour DNA repair pathways along with the development of new DNA damaging agents has been a major research focus. Advancements have been observed in breast, prostate, colon and ovary cancer and currently, this ideology is being employed in the treatment of brain tumours.

5.1. Cellular DNA Damage

DNA is the principle molecule with genetic information in a living organism and maintenance of its integrity is essential (20). However, DNA is not inert and is imperiled to stress. DNA damage occurs in cells due to various endogenous and exogenous factors (Table-5.1) (105). Every one of the ~10^{13} cells in the body undergoes tens of thousands of daily DNA lesions. DNA lesions emanate in various forms like base damage, DNA protein crosslinks, single strand breaks (SSBs), double-strand breaks (DSBs) and intra-interstrand crosslinks (Figure-5.1) (105). Although rare, DNA double strand breaks are deleterious and arises mainly from ionizing radiation. Studies have shown that one DSB occurs per 10^8 bp (20) in a genome of about 1.2x 10^7 bp and approximately 1% of SSBs are converted to DSBs per cell per cycle (113).

Environmental damage, such as ultra-violet (UV) light which induces 100,000 breaks per cell per hour, is amongst the common damage that affects DNA. Chemotherapeutic agents like cisplatin, cross-linking agents like mitomycin C, DNA alkylating agents like temozolomide (TMZ) and methyl methanesulfonate (MMS), topoisomerase drugs (camptothecin, etoposide), radio-mimetics like bleomycin are all induce DNA damage (113). Topoisomerase blocking agents induces SSBs and DSBs by trapping covalently linked topoisomerase-DNA cleaved complexes (113). Beyond exogenous insults, DNA damage arises from endogenous factors like metabolic reactions/byproducts (free radicals), replication stress and oxidative damage (20).

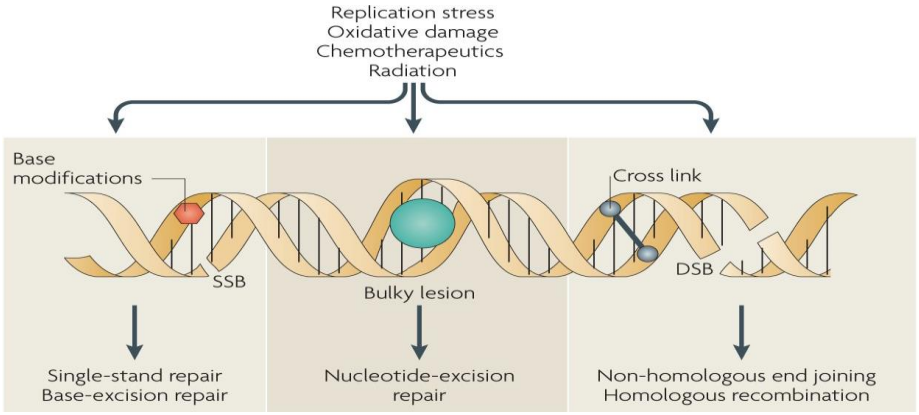

Figure-5.1. Different types of DNA damage(113)

Endogenous DNA Damage	DNA Lesions Generated	Number Lesions/Cell/Day	
Depurination	AP site	10000[a]	
Cytosine deamination	Base transition	100–500[a]	
SAM-induced methylation	3meA	600[a]	
	7meG	4000[a]	
	O^6meG	10–30[b]	
Oxidation	8oxoG	400–1500[c]	
Exogenous DNA Damage	Dose Exposure (mSv)	DNA Lesions Generated	Estimated Number Lesions/Cell
Peak hr sunlight	–	Pyrimidine dimers, (6–4) photoproducts	100,000/day[d]
Cigarette smoke	–	aromatic DNA adducts	45–1029[e]
Chest X-rays	0.02[f,g,h]	DSBs	0.0008[i]
Dental X-rays	0.005[f,g,h]	DSBs	0.0002[i]
Mammography	0.4[f,g,h]	DSBs	0.016[i]
Body CT	7[f]	DSBs	0.28[i]
Head CT	2[f,g]	DSBs	0.08[i]
Coronary angioplasty	22[h]	DSBs	0.88[i]
Tumor PET scan (^{18}F)	10[h]	DSBs	0.4[i]
^{131}I treatment	70–150[h]	DSBs	2.8–6[i]
External beam therapy	1800–2000[j]	DSBs	72–80
Airline travel	0.005/hr[f]	DSBs	0.0002/hr[i]
Space mission (60 days)	50[k]	DSBs	2[i]
Chernobyl accident	300[l]	DSBs	12[i]
Hiroshima and Nagasaki atomic bombs	5–4000[k]	DSBs	0.2–160[i]

Table-5.1. DNA lesions generated by endogenous and exogenous DNA damage(115).

5.2. Cell cycle checkpoint and DNA damage response (DDR)

The cell cycle comprises of four main stages whereby cells undergo cell growth and cell division. In G1 phase the cells are metabolically active and undergoes growth (114). Cell division takes place in S phase and cells continue to grow and synthesize proteins for cell division. The chromosomes divide into two daughter nuclei and cells divide into two daughter cells (114). This progression of cell division is guided by cell cycle checkpoints which ensures proper transfer of genetic information to the next generation (115). The movement of cells from one phase to the next during cell cycle is mediated by cyclin-dependent kinases (Cdks) which are bound by varying cyclin (proteins involved in cell cycle and DNA synthesis) , phosphorylation by specific protein kinases and dephosphorylation by Cdc25 family of phosphatases(Figure-5.2)(116).

Cell cycle checkpoints ensure successful DNA replication or DNA repair events. When cells are exposed to DNA damaging agents cell cycle progression is delayed by checkpoints with such response to ensure DNA repair events and successful DNA replication. Mutations in checkpoint components will fail this delay, thus in such case will allow tumour cell proliferation and survival resulting in cancer predisposition, immunodeficiency, and neurodegeneration (117)(118).

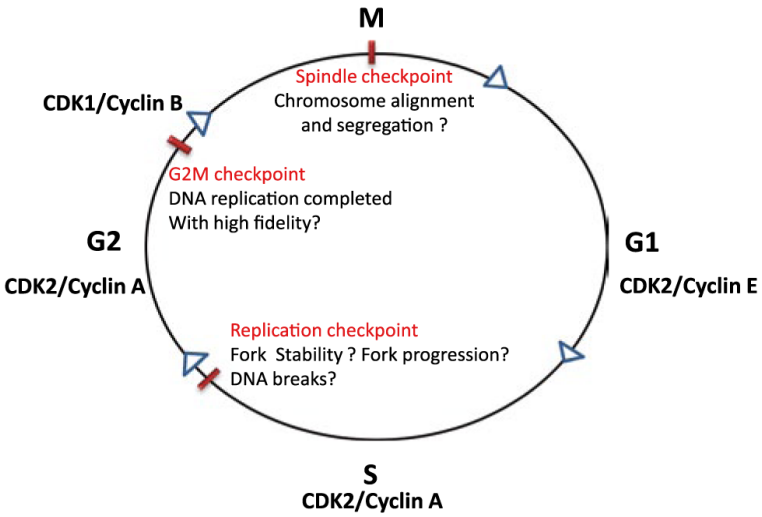

Figure-5.2. **Cell cycle checkpoints.** The cell cycle consists of G1, S, G2, and M phases which are directed by different cyclin/CDK complexes which monitor cell cycle progression from one phase to the next. S phase is regulated by replication checkpoint by conducting initiation of replication, replication fork stability, fork progression and DNA lesions. G2/M checkpoint verifies the completion of DNA replication with high fidelity. Spindle checkpoint monitors proper chromosome alignment and even distribution into two daughter cells (115).

Cells have their own unique signal transduction process to detect DNA damage, replication stress and induction of DNA repair through a plethora of cellular responses, collectively known as DNA Damage Response (DDR)(113)(119). In response to DNA damage, cell-cycle checkpoints integrate cell-cycle control with DNA repair (20). Cells that have encountered deleterious lesions that cannot be completely repaired undergo cellular senescence or elimination through cell death. For example, checkpoint kinase protein (Chk2) links apoptosis of thymocytes through p53 induced cell death (120).

5.3. DNA damage sensing and signaling

DNA damage engages DNA damage checkpoints with biochemical pathways to delay or arrest cell cycle progression. The first step is the activation of DNA damage checkpoint to identify the type of DNA damage. Rad9, Rad1, Hus1, and Rad17 are the key factors that are involved in activation of checkpoint signaling (115). Studies have shown that in both human and yeast cells, Rad9, Rad1, and Hus1 form a heterotrimeric complex, commonly known as the 9-1-1 complex (Figure-5.3) (115). Structure of this complex looks like a proliferating cell nucleus antigen (PCNA)-like sliding clamp and Rad17 interacts with four small replication factor (RFC) subunits, Rfc2, Rfc3, Rfc4 and Rfc5, to form a RFC-related complex (119), which acts as a clamp-loading complex and is associated to PCNA clamp loader (121).

When DNA damage is induced, sensor proteins like Rad9-Rad1-Hus1 (9-1-1) complex, Rad17–RFC complex (115) are recruited to the damage site and enables phosphorylation of protein kinases (119)(121). When DNA double-strand breaks (DSBs) are detected, the Mre11/Rad50/Nbs1 complex is the first to be recruited to the damage site which binds itself to the DNA ends (119). This binding leads to tethering of DNA end through a zinc hook in Rad50. There are several modulators of Mre11/Rad50/Nbs1 complex like MDC1 and 53BP1 in human cells and Sae2 in budding yeast (121).

The DDR process is mediated mainly by phosphatidylinositol 3-kinase-like protein kinase (PIKKs) family; Ataxia Telangiectasia Mutated (ATM), Ataxia Telangiectasia and Rad3-related protein (ATR) and DNA dependent protein kinase (DNA-PK) (Figure-5.3)(122). ATM and DNA-PK are activated upon recognition of double-strand breaks (DSBs) by sensor proteins; MRE11-RAD50-NBS1 (MRN) complex (in case of ATM) and Ku bound DSB ends (in case of DNAPK)(113). ATR activation is triggered by induction of single-stranded DNA (ssDNA) generated at stalled replication forks and double-stranded DNA (dsDNA) by its stable binding partner ATR interaction protein (ATRIP) (Figure-5.3)(123). ATR is also involved in activation of redundant DSBR pathways(123).

Single-stranded breaks are also detected and signaled by PARP proteins. While there are 16 members in PARP family, only two, PARP1 and PARP2, are functionally relevant for DDR. Both are activated during SSBs, and in some cases DSBs, by catalyzing the accumulation of poly (ADP-ribose) chains on proteins to facilitate recruitment of repair proteins (113).

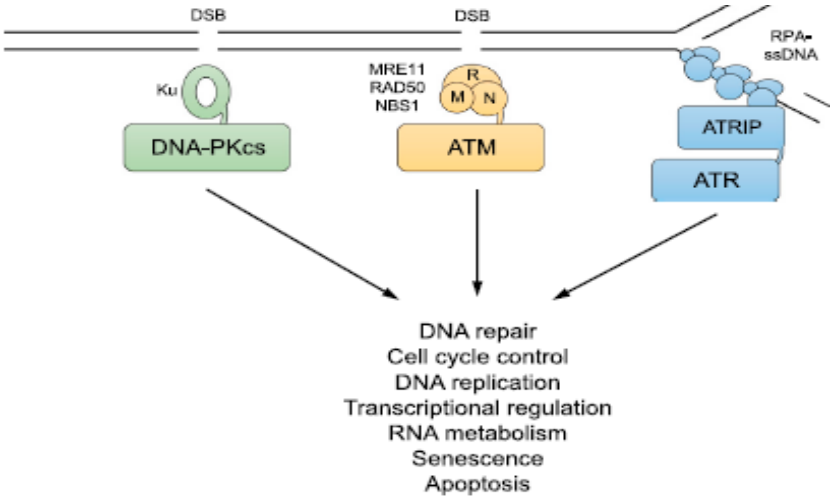

Figure-5.3. PIKKs protein recruitment and activation in response to DNA damage. DNA-PKcs is recruited and activated by Ku-bound DSB ends. ATM is activated and recruited to DSBs by the MRE11-RAD50-NBS1 (MRN) complex. ATR is recruited to RPA-coated ssDNA by its stable binding partner ATRIP(120).

Chk1 and Chk2 are effector proteins that relay downstream biochemical signals (124). These two checkpoint kinases are the targets of ATM/ATR and reduces the activity of cyclin-dependent kinase (CDK) (Figure-5.4) (120). Chk1 and Chk2 kinases regulate Cdc25, Wee1 and p53 which inactivate cyclin-dependent kinases (Cdks) leading to inhibition of cell-cycle progression (119). Blocking the activity of CDKs slows down or arrest cell cycle progression at the G1-S, intra-S and G2-M (118), allowing the cell to repair damaged DNA prior to replication and mitosis (20). Some of this cyclin-dependent kinase (CDK) are activated via p53 (120). Tumour suppressor p53 is activated by ATM/ATR through phosphorylation of Mdm2, this results in the reduced interaction of p53 with Mdm2 (Figure-5.4) (117). This activated p53 then transactivates the kinase inhibitor p21 resulting in inhibition of two cyclin-dependent kinases, Cyclin E/A-Cdk2 (125).

Parallel to this process, ATM/ATR signaling pathways induce DNA repair proteins transcriptionally or post-transcriptionally (115); by recruiting repair factors and activating DNA repair proteins to the damage site through post-translational modifications such as protein phosphorylation, acetylation, ubiquitylation or sumoylation (119). Also, changes in chromatin

structure during replication triggers DDR and the signal transduction is carried out through ATM/ATR/DNA-PK-mediated phosphorylation of serine-139 of the histone H2A variant, H2AX, on chromatin flanking DSB sites (120). This leads to ubiquitin-adduct formation and recruitment of DDR components along with chromatin-modifying components to induce DSB signaling and repair (118). Alternatively, if DNA repair fails then the DDR signal triggers p53 mediated cell death (anti-tumour activity) (116).

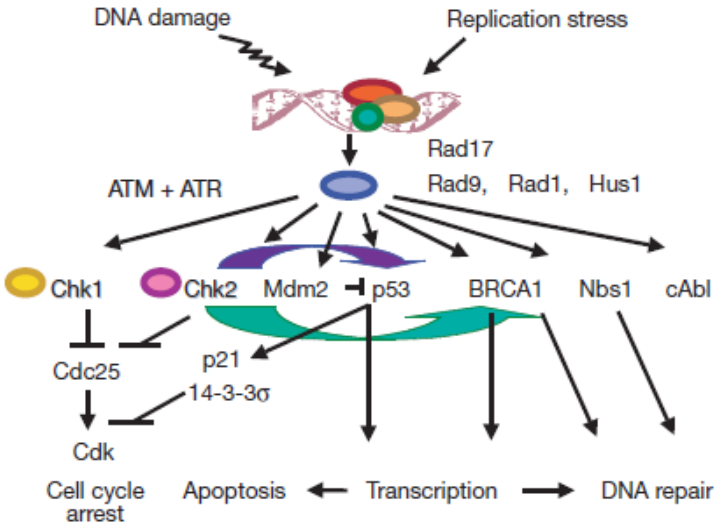

Figure-5.4. DNA damage response (DDR) and cell cycle checkpoint kinase pathway. Induction of DNA damage leads to replication stalling and is recognized by sensor proteins which then initiate cell cycle checkpoint signaling pathway via a plethora of cellular responses. (ROI) Reactive oxygen intermediate. Arrowheads represent positively acting steps while perpendicular ends represent inhibitory steps. Gene names are shown at the approximate positions where their encoded proteins function in the pathway. Although the general organization of the pathway is correct, some details are omitted, especially concerning the relationship between the ATR/ATM and Hus1/Rad17/Rad9/Rad1 proteins, which may participate in mutual regulation (117).

5.3.1. Sensing and signaling by Ataxia Telangiectasia Mutated (ATM) and Ataxia Telangiectasia and Rad3-related protein (ATR)

Ataxia Telangiectasia Mutated (ATM) and Ataxia Telangiectasia and Rad3-related protein (ATR), are very large polypeptides with a molecular weight of about ~300kD to 500kD (122). The catalytic domain of these PIKK family members are located near their carboxyl termini edged upstream by a FRAP-ATM-TRRAP (FAT) domain and downstream by a PIKK regulatory domain (PRD) and FAT C-terminal (FATC) motif(120). The FAT and FATC domains do not possess catalytic sequences (126). The N-terminus of the FAT domain is composed of helical solenoid HEAT-repeat domains of discrete lengths which promote protein-protein interactions (122).

Ataxia Telangiectasia Mutated (ATM) is a large protein (350kDa) composed of 3,056 amino acid residues. The PI3K domain in ATM comprises 10% of the protein consisting of regulatory and interaction domains which are responsible for activation and substrate specificity (127). Like ATM, Ataxia Telangiectasia and Rad3-related protein (ATR) is also a large protein with a molecular weight of about 303kD with 2,644 amino acid residues, and comprised of a similar general PIKKs structure (Figure-5.5) (120).

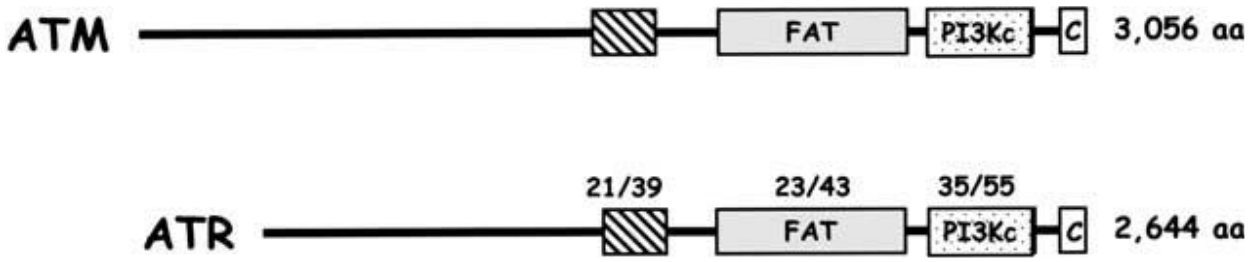

Figure-5.5. Schematic diagrams of ATM and ATR structures. Structural domains are shown for ATM and ATR with numbers above each domain indicating percent identity/similarity of a primary amino acid sequence of ATR compared with that of ATM. The numbers on the right indicate a total number of amino acids for each polypeptide. FAT and FATC (C) domains are aligned for ATM and ATR. The PI 3-kinase related catalytic domain (PI3Kc) is also shown for ATM (residues 2715–3011) and ATR (residues 2324–2627). The amino-terminal cross-hatched box indicates a functionally undefined region of homology between ATM (residues 1493–1773) and ATR (residues 1191–1463). (aa) Amino acids (119).

5.3.1.1. Ataxia Telangiectasia Mutated (ATM) activation

In non-irradiated cells, ATM is found throughout the nucleus in its non-phosphorylated homodimeric form. After formation of DSBs due to irradiation (or other damage), ATM is phosphorylated on Ser-1981 residue. The phosphorylation site, Ser1981 is present in the amino terminus of the FAT domain in the ATM structure (122). After exposure to radiation (0.5Gy), more than 50% of the cellular ATM is phosphorylated in less than 5 mins on Ser1981 residue. Phosphorylated ATM in cells can be detected with a low dose of 0.1Gy (induces about four DNA strand breaks per cell on average)(128). P-ATM coincides with separation into its monomeric form (129). This activated ATM is then recruited to DNA DSB sites. This activation mechanism of ATM is still being elucidated as the exact process by which ATM shifts from its inactive (dimeric non-phosphorylated) to its active (monomeric phosphorylated) form is unclear (130).

Recruitment of ATM to DSB sites is mediated via Nbs1(127), a sensor protein that is recruited to the break site and is usually found in complex with Mre11 and Rad50, Mre11–Rad50–Nbs1 (MRN) complex(129). Inhibiting Nbs1 or Mre11 hinders conversion of ATM from its inactive, non-phosphorylated form to its active, phosphorylation form (Figure-5.6)(128). *In vitro* studies have also shown that ability of ATM to phosphorylate downstream substrates increases in presence of MRN complex. This evidence suggests that MRN complex is critical for activation of ATM and its recruitment to the DSBs site(130).

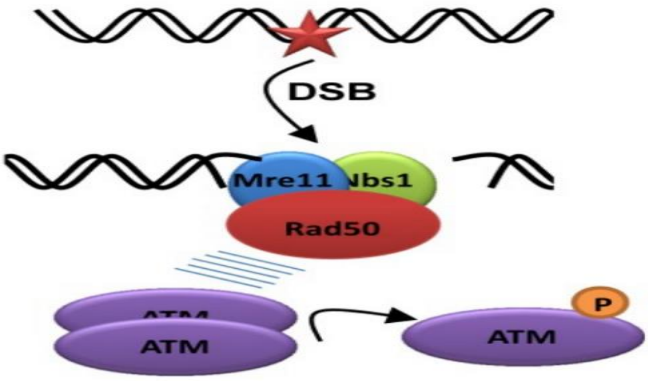

Figure-5.6. Mechanisms of ATM activation. DSBs (red asterisk) are detected by the MRN (Mre11-Rad50-Nbs1) complex which phosphorylates ATM from its inactive to active state, from an inactive dimer to an active monomeric form (131).

Further studies have revealed that ATM activation is not only limited to DNA DSBs but is also responsive to changes in chromatin structure resulting in activation of this protein kinase (127). Damage-independent chromatin structure alteration has been shown to auto-phosphorylate ATM (130). Furthermore, it has been documented that active ATM not associated with DSB sites can activate an inactive ATM molecule into an active monomeric form. Apart from DSB induction and altered chromatin structure, 53BP1 has also been found to be involved in activation of ATM; suppression of 53BP1 results in reduced ATM autophosphorylation (129).

5.3.1.2. *ATM substrates and its role in the checkpoint response*

There are over 1100 ATM-kinase substrate, impacting many cellular processes such as metabolism, stress response, and others. Although these can dramatically alter the cell in many ways, one major outcome of ATM activity is modulation of the DDR through phosphorylation of key DDR substrates. Two noteworthy targets mediate the cell cycle, Checkpoint kinase 2

(Chk2)(120) and tumour suppressor p53, while two targets are critical for cell survival are, SMC1 (structural maintenance of chromosomes 1) (129) and histone H2AX(118). Chk2 amplifies the DNA damage signal once phosphorylated by ATM on threonine-68 (130). Chk2, in turn, phosphorylates Cdc25A at Ser123, Cdc25C on Ser216, BRCA1 at Ser988 and p53 at several sites, including Ser20. Cdc25A and Cdc25C are two main protein phosphatases (117). Under normal cell cycle processes, Cdc25A activates Cdk2 promoting progression through S phase (120), whereas Cdc25C activates Cdc2 promoting progression from G2 into mitosis (124). During times of cellular DNA damage when Cdc25A and Cdc25C are phosphorylated by Chk2, their function is repressed, and cell cycle progression is delayed at S phase or arrests in G2(121) (Figure-5.7).

Tumour suppressor, p53 is phosphorylated by both Chk2 and ATM during DDR and inhibits cell cycle progression through the G1 phase by inducing expression of p21/waf1, a Cdk2 inhibitor(129) (Figure-5.7). p53 is also a transcription factor and is responsible for expression of genes involved in apoptosis (p53 mediated DNA damage-induced cell death) like in the hematopoietic system, where p53 can induce apoptosis rather than cell cycle arrest(119). Activated Chk2 diffuses out of the nucleus to phosphorylate its targets while transcriptionally-active p53 induces changes in gene expression(120)(128). In both cases, neither of these substrates accumulate at the damage site, unlike SMC1 and histone H2AX which are actively involved in the damage/repair process (129). H2AX is integrated with chromatin and when phosphorylated at ser-139 (γH2AX), recruits chromatin remodeling complexes to DNA DSB sites(118). SMC1 is a chromatin-associated protein active at sites of DSBs upon protein phosphorylation(126). Like many proteins involved in DDR, SMC1 does not impact the cell cycle but is required for DNA repair (115) (Figure-5.7). A mutant form of SMC1 and ATM-deficient cells are radiosensitive; in the former, ATM was unable to phosphorylate SMC1 and while in the latter ATM was absent(129).

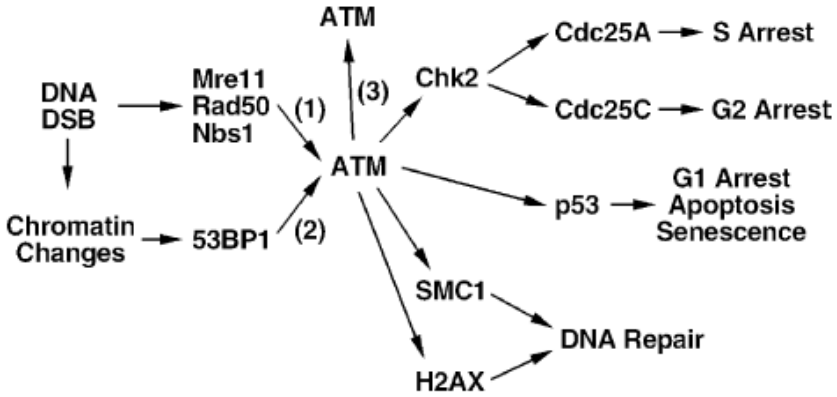

Figure-5.7. **ATM activation and signaling**. ATM is activated by the Mre11–Rad50–Nbs1 complex or 53BP1. The former is thought to be recruited at the DNA double-strand break (DSB), whereas the latter is recruited at chromatin regions flanking the DNA DSB and extending up to a few megabases from the DSB. ATM activated at sites of DNA DSBs may also phosphorylate and activate ATM in the nucleoplasm. A subset of ATM substrates (Chk2, p53, SMC1 and histone H2AX) and their function are also indicated (125).

In response to DNA damage, ATM is released from the DNA damage site to phosphorylate other distal molecules, including chromatin-associated histone (130), H2AX (γH2AX) (113). ATM interacts with Mediator of DNA damage checkpoint 1 (MDC1) and this MDC1-ATM complex is recruited to the damage site(132). H2AX phosphorylation occurs along a 1-2 megabase region in an ATM-MDC1 mediated manner. H2AX Ser139 is bound to MDC1 via direct binding to its C terminal BRCT domain(113). With γH2AX bound to this complex, the MDC1-ATM complex is stabilized to the DSB break site(126). ATM then amplifies this process by recruiting more H2AX to MDC1 molecules. This ongoing process builds a scaffold of phosphorylated H2AX which acts as a recruitment platform for more DNA damage repair proteins (128).

5.3.1.3. Ataxia Telangiectasia and Rad3-related protein (*ATR)* activation

Studies have shown that Ataxia Telangiectasia and Rad3-related protein (ATR) is activated mostly by induction of single-stranded DNA (ssDNA) but further research suggested that along with ssDNA, double-stranded DNA (dsDNA) also triggers ATR activation (126). Single-stranded DNA (ssDNA) are intermediates formed during DNA replication, stalled replication fork and DNA repair pathways (123).

Induction of ssDNA results in binding of these intermediates with ssDNA-binding protein complex RPA (replication protein A) and ATR interacting protein (ATRIP) binds with RPA coated ssDNA (133) (Figure-5.8.i). ATRIP is necessary for ATR stabilization and function and acts as a mediator to localize ATR-ATRIP complex onto damage sites and stressed replication forks(119). ATR

along with interacting with ATRIP also forms a complex with TEL2 (telomere maintenance 2; also called HCLK2)(123). Rad17–RFC complex and the Rad9–Rad1–Hus1 (9-1-1) complex are two regulators of ATR that detects single-stranded DNA and double-stranded DNA(134). Rad17–RFC complex acts as a loader at the ssDNA–dsDNA junctions bound with RPA, to recruit 9-1-1 complex onto DNA. RAD9 in the 9-1-1 is constantly phosphorylated at Ser 387 by ATR-ATRIP complex(119)(130)(Figure-5.8iii).

Along with RPA, RAD17–RFC, 9-1-1 complexes, ATR also requires DNA topoisomerase II binding protein 1 (TOPBP1) for complete activation(123). TOPBP1 activates the kinase activity of ATR-ATRIP complex through its eight BRTC proteins and ATR activation domain (AAD)(135). TOPBP1 BRCT domains interact with phosphorylated Ser387 of RAD9 and the AAD domain interact with ATR–ATRIP(136)(135) (Figure-5.8.iii).

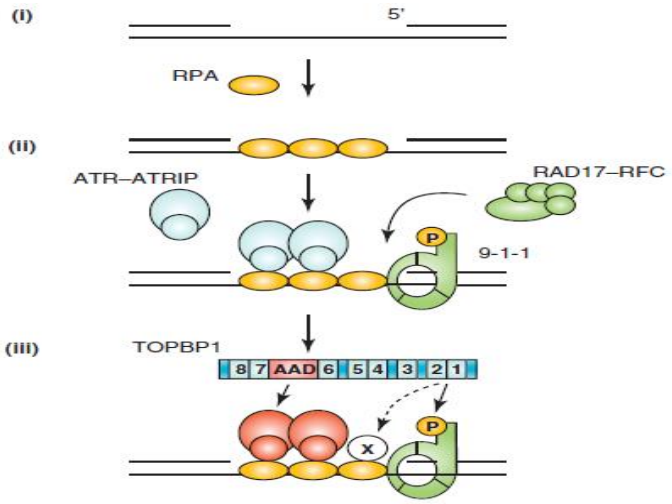

Figure-5.8. ATR–ATRIP activation by DNA damage. ssDNA and junctions of ssDNA and dsDNA trigger ATR–ATRIP activation. (i) ssDNA is recognized and coated by RPA (gold ovals). (ii) ssDNA coated by RPA (RPA–ssDNA) recruits the ATR–ATRIP kinase complex (blue ovals) to sites of DNA damage. In the presence of ssDNA–dsDNA junctions and RPA, the Rad17–RFC complex (green ovals) recruits the 9-1-1 complex (green circle) onto DNA. (iii) RAD9 in the 9-1-1 complex is constitutively phosphorylated at Ser 387. TOPBP1, the stimulator of the ATR–ATRIP kinase, contains eight BRCT domains (light blue boxes 1–8 in TOPBP1) and an ATR-activation domain (AAD; red box in TOPBP1). The TOPBP1 BRCT domains 1–2 interact with the phosphorylated Ser387 of RAD9 and the AAD domain interacts with ATR–ATRIP (121).

5.3.1.4. ATR substrates and role in checkpoint kinase

Upon induction of UV- induced DNA damage, several proteins are phosphorylated by ATR in an ordered manner(105). Cell division control 25 (Cdc25) phosphatases are downstream substrates in DDR and are important in cell cycle checkpoints(124). This family of phosphatases is a target for ATR in cell cycle arrest(117). After ATR activation, ATR phosphorylates its effector kinase CHK1 at Ser317/345 which then phosphorylates C-terminal portion of Cdc25A(120) (Figure-5.8). ATR-mediated Chk1 phosphorylation is mediated by claspin which binds and stabilizes activated Chk1(116). This phosphorylation of Cdc25A by kinases CHK1 and NEK11 indorses ubiquitylation and degradation of Cdc25A resulting in reduced cyclin-dependent kinase 2 (CDK2) activity in S phase, thus slowing or arresting cell cycle progression(116)(119). CHK1 also phosphorylates Cdc25C, providing a binding site for 14-3-3 proteins which in turn inhibits Cdc25C function preventing activation of CDK1–cyclin B kinase and mitotic entry(120)(Figure-5.9). This provides more time for DNA repair or for activation of apoptotic pathways if the damage is too extensive(20). For the DNA replication to be continued, ATR signaling pathway is required to be repressed.

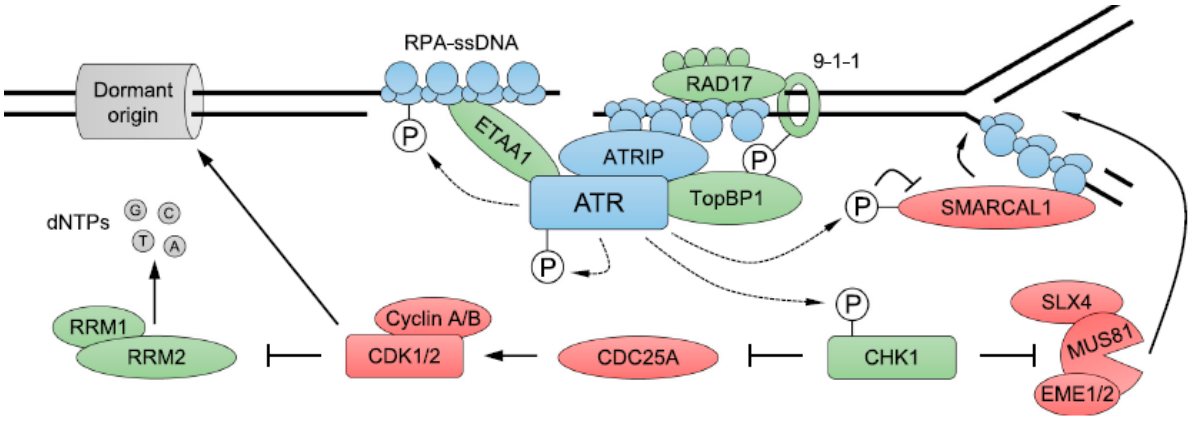

Figure-5.9. ATR recruitment and activation of S-phase checkpoint signaling. ATR is recruited to RPA-ssDNA and activated by TopBP1 or ETAA1. ETAA1 is recruited directly to RPA-coated ssDNA. TopBP1 is recruited via mechanisms that are not yet clear, but its role in ATR activation requires interaction with the RAD9-HUS1-RAD1 (9-1-1) clamp complex, which is loaded onto ds/ssDNA junctions by the RAD17/RFC2-5 clamp loader. ATR signaling activates the CHK1 kinase and restrains fork processing enzymes such as SMARCAL1. CHK1 activation causes CDC25A degradation, leading to inhibition of CDK activity, slowing of cell-cycle progression, inhibition of late-origin firing, and increased nucleotide availability, in part by upregulation of RRM2. ATR and its recruitment factors

are shown in blue. Factors with a positive role in ATR stimulation or that are activated by ATR are in green, while those that are inhibited by ATR are in red (120).

ATR prevents replication fork collapse via the following mechanism; ATR signaling confines replication origin firing through inhibition of CDKs, limits collapsing of replication fork by directly binding with helicases like SMARCAL1, which produces fork configurations that are recognized and cleaved by SLX4/MUS81 nuclease complexes(122). ATR signaling has its own unique targets for DNA repair at stalled replication forks and one of these is the Fanconi Anemia (FA) pathway(122)(126).

FA is a genetic disorder related to hypersensitivity to DNA cross-linking agent (123) and presents with bone marrow failure, cancer predisposition along with microcephaly and dwarfism features. The FA signaling pathway initiates repair of DNA interstrand crosslinks (ICLs) (122). FA protein are divided into three groups; the FA core complex and associated proteins (FANCA, -B, -C, -E, -F, -G, -L and -M), the FANCD2–FANCI complex and the BRCA-related FA proteins [FANCD1 (also called BRCA2), FANCN (also called PALB2) and FANCJ (also called BACH1)] (123). Mono-ubiquitination of FANCD2 is the key step for ICL repair followed by phosphorylation of the protein by ATR and this event plays a role in replication stress response by regulating dormant origin firing (122).

5.3.1.5. DNA damage repair effector molecule-p53

Tumour suppressor protein, p53 plays an essential role in cell cycle arrest and apoptosis (120). Transcriptional activity of this protein is initiated by post-translational modifications such as phosphorylation, sumoylation, neddylation, and acetylation (129). Under normal conditions, transcriptional activity of p53 is low due to Mdm2-mediated ubiquitylation and degradation of the protein via the proteasomal pathway. In response to DNA damage, p53 is activated via phosphorylation by several proteins on its transactivation domain (115). ATM and ATR phosphorylates p53 at Ser15, while Chk2 does so at Ser 20(134)(Figure-5.10). Phosphorylation at these sites inhibits contact of p53 with Mdm2, while phosphorylation of Mdm2 by ATM on Ser395 reduces its ability to induce nucleocytoplasmic shuttling(129)(Figure-5.10) (117). After activation, p53 phosphorylates p21 Cdk inhibitor (p21CKI) which impedes cyclin E Cdk2 activity, hence

inhibiting G1/S transition(118). p21CKI inhibits RB/E2F pathway by preventing phosphorylation of Rb, by binding to cyclin D–Cdk4 complex (120).

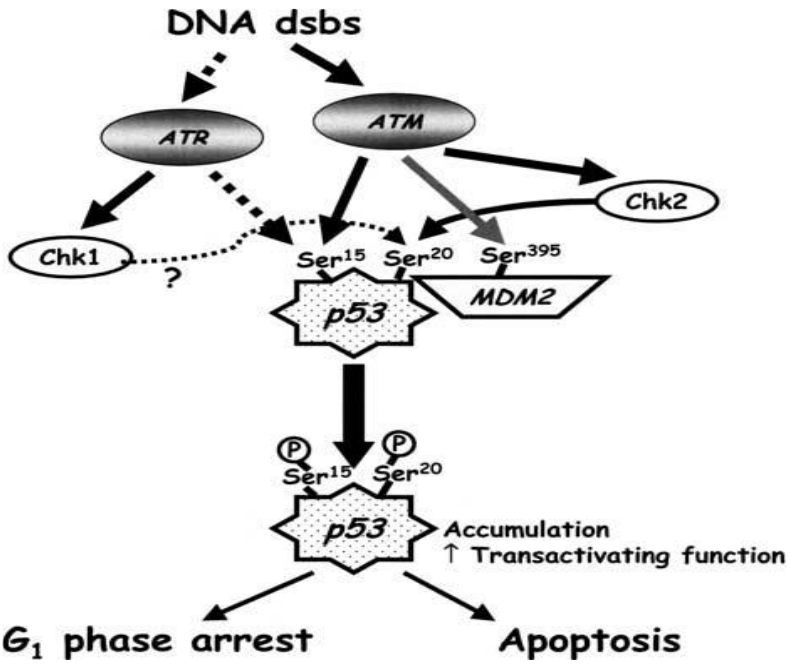

Figure-5.10. ATM/ATR-dependent p53 signaling through the G1 checkpoint. Activation of p53 is heavily dependent on the ATM-mediated pathway in response to DNA double-strand breaks (DSBs) but activation is also induced by ATR. ATM regulates p53 accumulation by indirect pathways involving the Chk2-mediated phosphorylation of Ser 20 on p53 and by directly phosphorylating MDM2 on Ser 395. ATR phosphorylates p53 at Ser 20 and mediates cell cycle arrest or apoptosis through activation of Chk1 (119).

5.4. DNA repair pathways

Cells can maintain genomic integrity through various cellular processes to prevent erroneous DNA lesions to pass across generations. Cells have developed their own specific repair mechanisms to repair DNA lesions (105)**.** Any DNA damage is resolved by DNA damage response (DDR) and repair pathways since unresolved DNA breaks are harmful to cells because they alter the content and organization of genetic material (137). There are two types of DNA strand breaks: single strand breaks (SSBs) and double-strand breaks (DSBs), which are resolved specifically by dedicated repair pathways (105). A wide variety of DNA lesions activate distinct DNA repair mechanisms. Some damage can be resolved by a direct protein-mediated process while others require a complex sequence of catalytic events mediated by multiple proteins (135). The table shown below gives an overview of these pathways (Table-5.2).

DDR mechanism	Prime lesions acted upon	Key protein components
Direct DNA-lesion reversal	UV photo-products O^6 alkylguanine	Photolyase O^6-methylguanine methyltransferase (MGMT)
Mismatch repair (MMR)	DNA mismatches and insertion/deletion loops arising from DNA replication	Sensors MSH2-MSH6 and MSH2-MSH3 plus MLH1-PMS2, MLH1-PMS1, PLH1-MLH3, EXO1, polymerases δ and e, PCNA, RFC, RPA, ligase I
Base excision repair (BER) and single-strand break repair (SSBR)	Abnormal DNA bases, simple base-adducts, SSBs generated as BER intermediates, by oxidative damage or by abortive topoisomerase I activity	DNA glycosylases (sensors), APE1 endonuclease, DNA polymerases (β, δ, e) and associated factors, flap endonuclease FEN1, ligase I or ligase III. SSBR can also involve polymerase β lyase activity, XRCC1, PARP-1, PARP-2, polynucleotide kinase (PNK) and aprataxin (APTX)
Nucleotide excision repair (NER)	Lesions that disrupt the DNA double-helix, such as bulky base adducts and UV photo-products	Sensors elongating RNA polymerase, XPC-HR23B and DDB1/2, plus XPA, XPE, XPF/ERCC1, XPG, CSA, CSB, TFIIH (containing helicases XPB and XPD), DNA polymerases and associated factors, RPA, ligase I
Trans-lesion bypass mechanisms	Base damage blocking replication-fork progression	"Error-prone" DNA polymerases, including polymerases eta, iota, kappa, REV3 and REV1; plus associated factors
Non-homologous end-joining (NHEJ)	Radiation- or chemically-induced DSBs plus V(D)J and CSR intermediates	Sensors Ku and DNA-PKcs plus XRCC4, XLF/Cernunnos and ligase IV. Can also employ the MRE11-RAD50-NBS1 complex, Artemis nuclease, PNK, Aprataxin and polymerases μ and λ
Homologous recombination (HR)	DSBs, stalled replication forks, inter-strand DNA cross-links and sites of meiotic recombination and abortive Topoisomerase II action	RAD51, RAD51-related proteins (XRCC2, XRCC3, RAD51B, RAD51C, RAD51D, DMC1), RAD52, RAD54, BRCA2, RPA, FEN1, DNA polymerase and associated factors. Promoted by MRN, CtIP, BRCA1, and the ATM signalling pathway
Fanconi anaemia (FANC) pathway	Inter-strand DNA cross-links	FA-A, C, D1/BRCA2, D2, E, F, G, I, J, L, M, N plus factors including PALB2 and HR factors
ATM-mediated DDR signalling	DSBs	ATM, MRN and CHK2. Promoted by mediator proteins such as MDC1, 53BP1 MCPH1/BRIT1, and by ubiquitin ligases RNF8, RNF168/RIDDLIN and BRCA1
ATR-mediated DDR signalling	ssDNA, resected DSBs	Sensors ATR ATRIP and RPA plus the RAD9-RAD1-HUS1 (911) complex, RAD17 (RFC1-like) and CHK1. Promoted by MRN, CtIP and mediator proteins such as TOPBP1, Claspin, MCPH1/BRIT1 and BRCA1

Table-5.2. DNA repair pathways and key protein components activated upon prime lesions (20)

5.4.1. Double strand break repair (DSBR) pathways

A single DSB can be lethal to the cell. DSBs are formed when both strands of the DNA are broken (138). DSBs are induced by ionizing radiation and radiomimetic agents like bleomycin, neocarzinostatin and topoisomerase poisons like etoposide, and doxorubicin. DSBs are also formed due to collapsed replication fork, during V(D)J recombination and class switch recombination (CSR)(139).

DSBs activate complex and multiple DSBR pathways, least four independent pathways are activated; Homologous Recombination (HRR), Non-Homologous Recombination (NHEJ), alternative-NHEJ (alt-NHEJ), and single-strand annealing (SSA) (Figure-5.11) (113). One of the major factors among these four independent repair pathways is the extent of DNA end processing. Classical NHEJ (C-NHEJ) is not dependent on DNA end resection but HRR (extensive), alt-NHEJ (limited) and SSA (extensive) requires DNA end processing (140). There are four independent sensors for DSB detection: PARP, Ku70/Ku80, MRN, and Replication Protein A (RPA) (138).

NHEJ occurs throughout the cell cycle and is coordinated by the DNA dependent protein kinase (DNA-PK) and the Ku70/86 heterodimer which joins the broken DNA ends via Xrcc4 and DNA ligase 4 (141) (Figure-5.11). In contrast to C-NHEJ, there is another NHEJ DSB repair pathway which is Ku-independent; known as microhomology-mediated end-joining (MMEJ) or alternative end-joining (AEJ) and is involved in sequence deletions. C-NHEJ and MMEJ are both error-prone processes and are activated despite phases of cell cycle (20).

HRR is is denoted as ‘error-free’ repair process and is a RAD51-BRCA2-XRCC2 recombinase-driven process occurring during DNA replication (G1-S) using a complementary sister chromatid for repair. This pathway is also involved in restarting stalled replication forks (141) and in repairing inter-strand DNA crosslinks (Figure-5.11) (20). It is important to know pathways by which DSBs are repaired as single unrepaired DSBs can trigger apoptosis. (105).

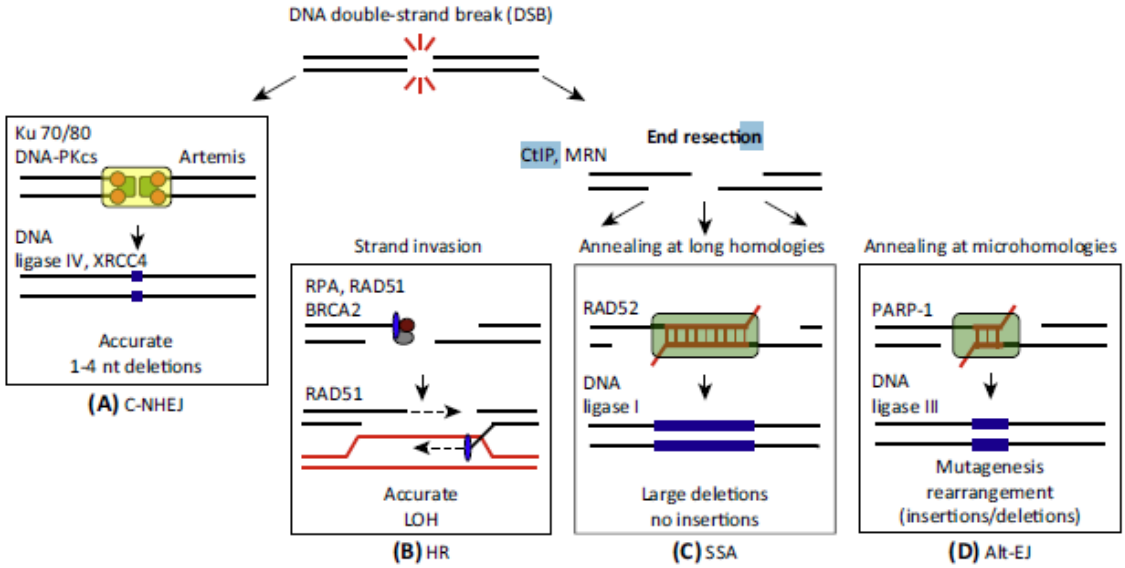

Figure-5.11. Four independent DNA double-strand breaks (DSB) repair pathways. (A–D) DSB repair profoundly depends on DNA end resection. When this resection is hindered, Classical NHEJ is preferred but three repair pathways are activated upon DNA resection, HR, alt-EJ, and SSA which competes for DSBR. Abbreviations: NT, nucleotides; LOH, loss of heterozygosity; C-NHEJ, classical nonhomologous end joining; HR, homologous recombination; alt-EJ, alternative end joining; SSA, single-strand annealing (144).

5.4.1.1 Non-Homologous End Joining

One of the major repair proteins orchestrating the NHEJ repair pathway is the DNA-dependent protein kinase (DNAPK). It is activated by double-stranded DNA ends and serves as a sensor as well as a transducer of DNA DSB damage signal (126). DNAPK is a member of phosphatidylinositol 3-kinase-like protein kinases (PIKKs) and has its catalytic subunit on C-terminal. It is a nuclear serine/threonine kinase which consists of about 470kDa catalytic subunit (DNAPKcs) and a DNA-end binding component, Ku(142). Ku is a heterodimer of two proteins, 70kDa and 80kDa, called Ku70 and Ku80 (also called Ku86). Apart from playing a critical role in DSB repair, DNAPK is involved in other cellular processes, for example, components of DNAPK complex are present at telomere where they cap chromosomal ends so that they are not mistaken as DSBs during repair. This protein is also involved in immune response to bacterial DNA and viral infection and mediates cell death/apoptosis(122) (Figure-5.12).

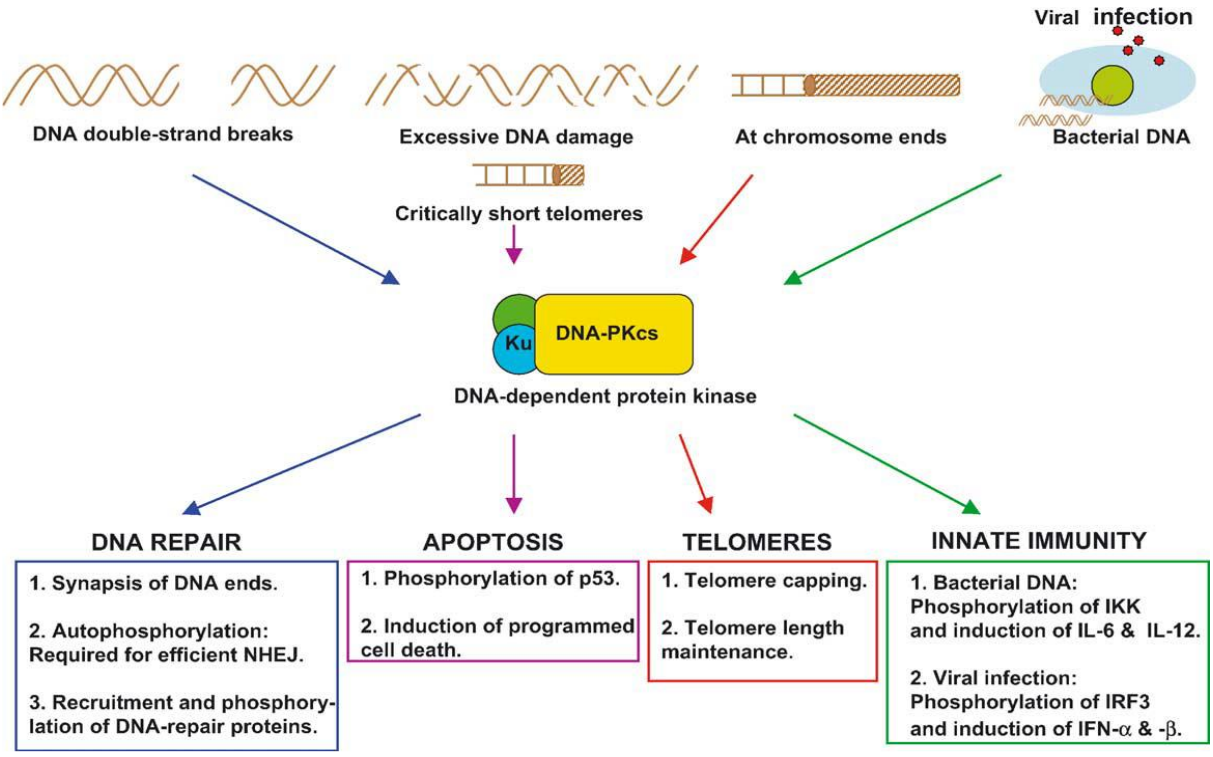

Figure-5.12. Different roles of DNAPK in mammalian cells. DNAPK serves as both a sensor and a transducer of DNA-damage signal. DNAPK is localized at DSBs and phosphorylates itself and other repair proteins to promote NHEJ. In case of severe DNA damage or extremely shortened telomeres, DNAPK triggers apoptosis. DNAPKcs and Ku are also present at the telomere where they are involved in capping telomeres and maintaining telomere length. DNAPK also plays an important role in mounting an innate immune response to viral infection or bacterial DNA (146).

The NHEJ repair pathway, resolves DSBs in a sequential manner; (I) DNA end recognition with repair protein assembly and stabilization of DNA ends at DSB, (II) Joining of DNA end and stability, (III) DNA end processing and gap filling, (IV) DNA Ligation (143).

After induction of DSB sensor protein, the Ku heterodimer is recruited to the break site and binds to DSBs for stabilization and preventing them from non-specific end processing (138) (Figure-5.13). Ku heterodimer has a toroidal structure with a hole through which it loads on to DSB ends. The ability of Ku heterodimer to localize to DSBs is due to its high affinity (binding constant of 2×10^{9} M^{-1}) for DNA ends (144). Ku acts as a scaffolding protein for recruitment of other NHEJ repair component to the DSB site and then directly or indirectly load(145) and activate the catalytic subunit of DNA-PK, known as DNA-PKcs, to initiate NHEJ repair process. Other repair proteins

like X-ray cross-complementing protein 4 (XRCC4), DNA Ligase IV, XRCC4-like factor (XLF), and Aprataxin-and-PNK-like factor (APLF) are recruited to the DSB site(144) (Figure-5.13).

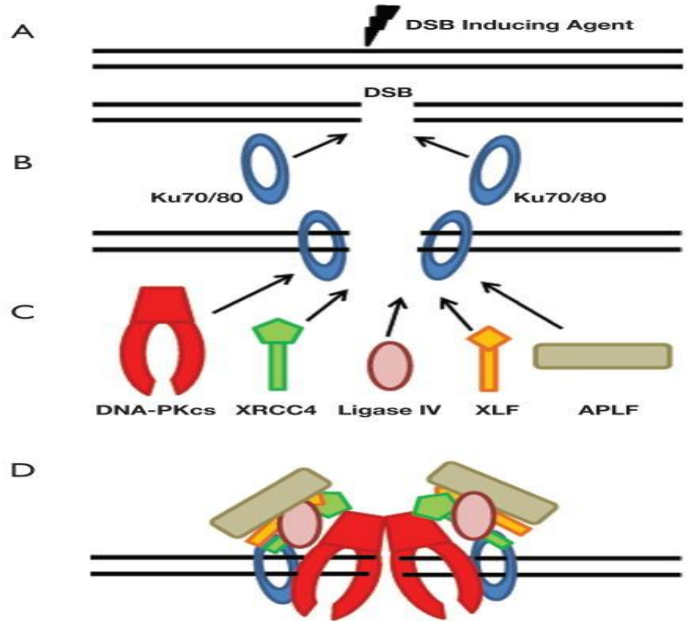

Figure-5.13. DNA end recognition with repair protein assembly and stabilization of DNA ends at DSB. A. DNA double-strand break (DSB) is induced; B. Ku is recruited and quickly binds to the ends of the broken DNA; C. Ku serves as a scaffolding protein to recruit the core NHEJ machinery to the DNA DSB. DNA-PKcs, XRCC4, XLF, DNA Ligase IV, and APLF are independently recruited to the Ku-DNA complex; D. The core NHEJ factors interact with each other to form a stable complex at the DSB (148).

XRCC4 and DNA ligase IV binds together, forming a complex and Ku directly interacts with this complex for recruitment to the DNA ends(146). XRCC4 interacts directly with Ku70 of the Ku heterodimer and DNA ligase IV interacts with the heterodimer through its BRCA1 C-terminal (BRCT) domains. XLF binds with Ku heterodimer through its C-terminal region from amino acids 270–299, for localization to the DSB site(138). *In vitro* studies showed that XRCC4 binds with XLF and this complex forms a filament (Figure-5.14) which is involved in joining DNA ends for stabilization. It has also been suggested that joining of DSB broken ends is mediated through both Ku-DNA-PKcs and XRCC4-XLF filament complexes(144). Casein kinase 2 (CK2) phosphorylates XRCC4, after which PNKP can interact with XRCC4 through its forkhead-associated (FHA) domain. PNKP is phosphorylated by ATM on serine 114 and on serine 126 by both ATM and DNA-PKcs(143)(144).

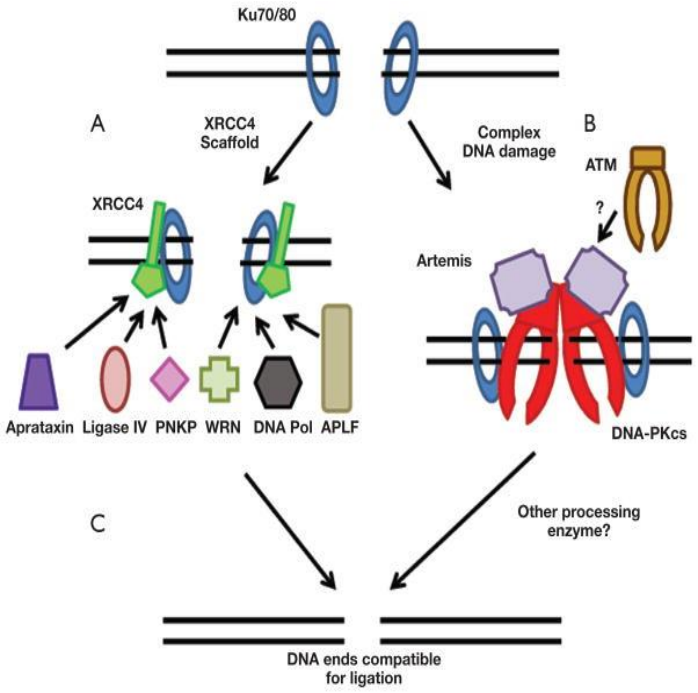

Figure-5.14. Joining of DNA end and stability. A. Ku heterodimer binds with DSB and stabilizes the DNA ends; B. DNA-PKcs then tether DNA ends through the formation of a synaptic complex; C. XRCC4 and XLF can form a filament which can link the two portions of the broken DNA molecule and stabilizes them; D. XRCC4-XLF filament in complex with DNA-PKcs and Ku produces a tightly regulated DNA end protection complex (148).

Proteins involved in trimming DNA ends in NHEJ are Artemis, WRN, and APLF. Artemis enzyme has nuclease activity such as 5′ endonuclease to nick a 5′ overhang leaving a blunt duplex end and, a 5′ to 3′ exonuclease on single-strand DNA and the ability to remove 3′-phosphoglycolate groups from DNA ends (144). In NHEJ, Artemis is activated upon phosphorylation by DNA-PKcs or ATM (or both) and this is required for its endonucleolytic activity (145) (Figure-5.15). APLF is an endonuclease and a 3′ to 5′ exonuclease(144). This protein resects 3′ overhangs to allow ligation of DNA substrates by XRCC4-DNA Ligase IV. 3′ to 5′ exonuclease of WRN is activated by interaction of WRN with Ku heterodimer and XRCC4 (143).

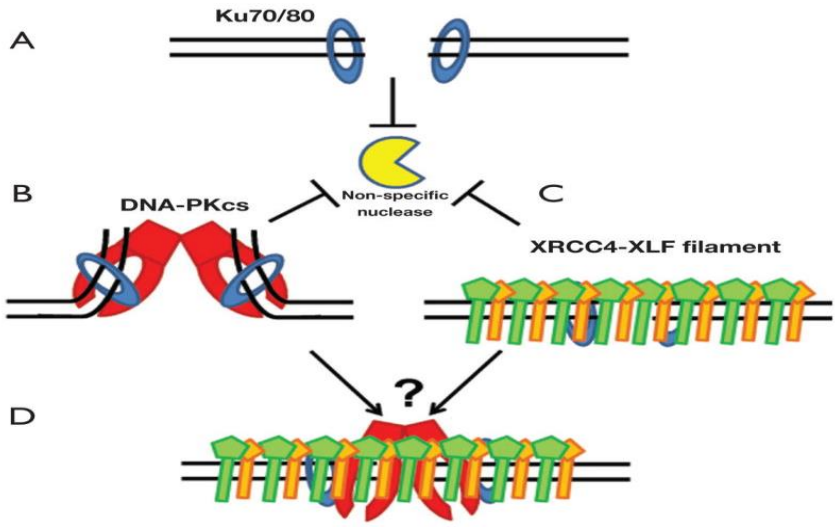

Figure-5.15. DNA end processing and gap filling. A. XRCC4, in combination with Ku heterodimer, serves as a scaffolding complex for recruitment of specific DNA end processing enzymes. The XRCC4-Ku scaffold has the liberty to choose enzymes for repair depending on the extent and nature of DSB; B. Complex DNA DSB have repaired via nuclease Artemis and the processing may require ATM; C. DNA end processing makes the ends ligatable (148).

After recruitment of all the repair proteins at the DSB site, DNA end-processing is required to make the DNA ends ligatable (147). For this, the proteins recruited at the damage site depend on the extent and type of DSB, such as those that respect DNA ends, fill in gaps, remove blocking end groups and make the ends ligatable(144). DNA ligation profoundly depends on DNA ligase IV. XRCC4 stabilizes this enzyme at the DSBs and activates its ligase activity through adenylation(143). DNA ligase joins mismatched DNA ends (143) (Figure-5.16). DNA gap filling is carried out by DNA polymerases μ and λ. DNA polymerase μ is localized to the break site in presence of both Ku and XRCC4-Ligase IV and polymerizes across the discontinuous template strand. Polymerase λ removes the damaged base(144).

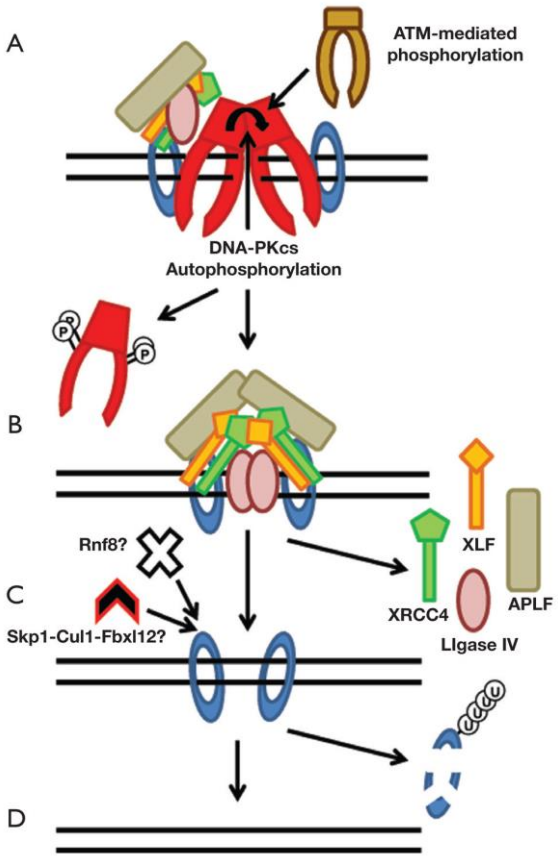

Figure-5.16. DNA ligation. A. Phosphorylation of DNAPK by ATM leads to conformational change in DNAPKcs resulting in its release from DSB.; B. Ligation of broken DNA occurs through DNA-Ligase IV activity and this process is mediated by XRCC4, XL, and APLF; C. Ku is released from repaired DSB by ubiquitylation through either Rnf8 or SCF complex of Skp1-Cul1- Fbx112 resulting in degradation of Ku; D. DNA DSB is repaired (148)..

5.4.1.2 Homologous Recombination (HRR)

When sensor proteins recognize DSBs, the NHEJ pathway is first activated for repair as it has the advantage of repairing DSBs at any phase of cell cycle over Homologous Recombination Repair (HRR). This makes HRR less active compared to NHEJ in repairing radiation-induced DSBs(148). NHEJ repairs by joining two broken DNA ends and this process is often denoted as error-prone whereas HRR requires a sister chromatid to precisely resynthesize damaged or missing sequence at the break site(149).

DSBs are recognized by MRE11-RAD50-NBS1 (MRN) complex which then phosphorylates ATM to activate DSB repair pathways (129). Binding of MRN to DSBs activates ATM which phosphorylates BRCA1, involved in G1/S phase arrest. BRCA1 indirectly activates RAD51 (105) (Figure-5.17). Recognition of DSB by this complex is followed by 5'-3' resections to produce a

long ssDNA 3’ extension (148). MRN complex also interacts with CtIP (C-terminal region of adenovirus E1A-binding protein [CtBP]-interacting protein), which activates the endonuclease activity of Mre11 to promote MRN-dependent resection (Figure-5.17).

The DNA end resection step occurs in S/G2 phase when a sister chromatid is available(146). This step is processed by ATM via CtIP, which then further interacts with BRCA1 and MRN in the BRCA1-C complex. CtIP binds with BRCA1 which ubiquitinates CtIP thereby loading it onto the DSB damage site(113). Before the strand invasion step can take place, the ssDNA binds with Rad51 to form a presynaptic filament. 3’-ssDNA extension of ssDNA binds with RPA protein for filament formation, thus also preventing premature strand invasion. During strand invasion, the 3’-ssDNA strand involves itself in the homologous sequence to form a D loop(146).

Multiple proteins are involved in stabilizing the filament and replace RPA with Rad51, such as Rad52, BRCA2 and the Rad51 paralogues (Rad51B, Rad51C, Rad51D, XRCC2, and XRCC3)(146). The 3’ DNA end is extended by DNA polymerase, pol β, and the second DSB end is captured by annealing to the extended D loop. This results in formation of Holliday junctions, which are one or more crossed strand structures. These Holliday junctions are resolved through crossover or non-cross over pathways in HRR(113) (Figure-5.17). Proteins that are involved in these steps include Rad54, WRN, BLM, p53 BLAP75, hMSH2-hMSH6, XPF, ERCC1, DNA polymerases, δ and ε, PCNA and DNA ligase I(113).

5.4.1.3. Alternative-Non-Homologous End Joining (Alt-NHEJ)

In DNA repair there are an abundance of redundant repair pathways, one of which is alternative NHEJ which functions as a backup repair pathway during dysfunction of classical NHEJ (150) (Figure-5.17). In this DSB repair pathway, PARP1/2 acts as a sensor to DSBs. PARP1 binds to broken DNA ends and facilitates synapsis (fusion of chromosomal pairs at meiosis) before ligation takes over which is mediated by XRCC1 and DNA Ligase III complex(151). During the active classical NHEJ process, Ku heterodimer inhibits PARP1, thus blocking alt-NHEJ(152).

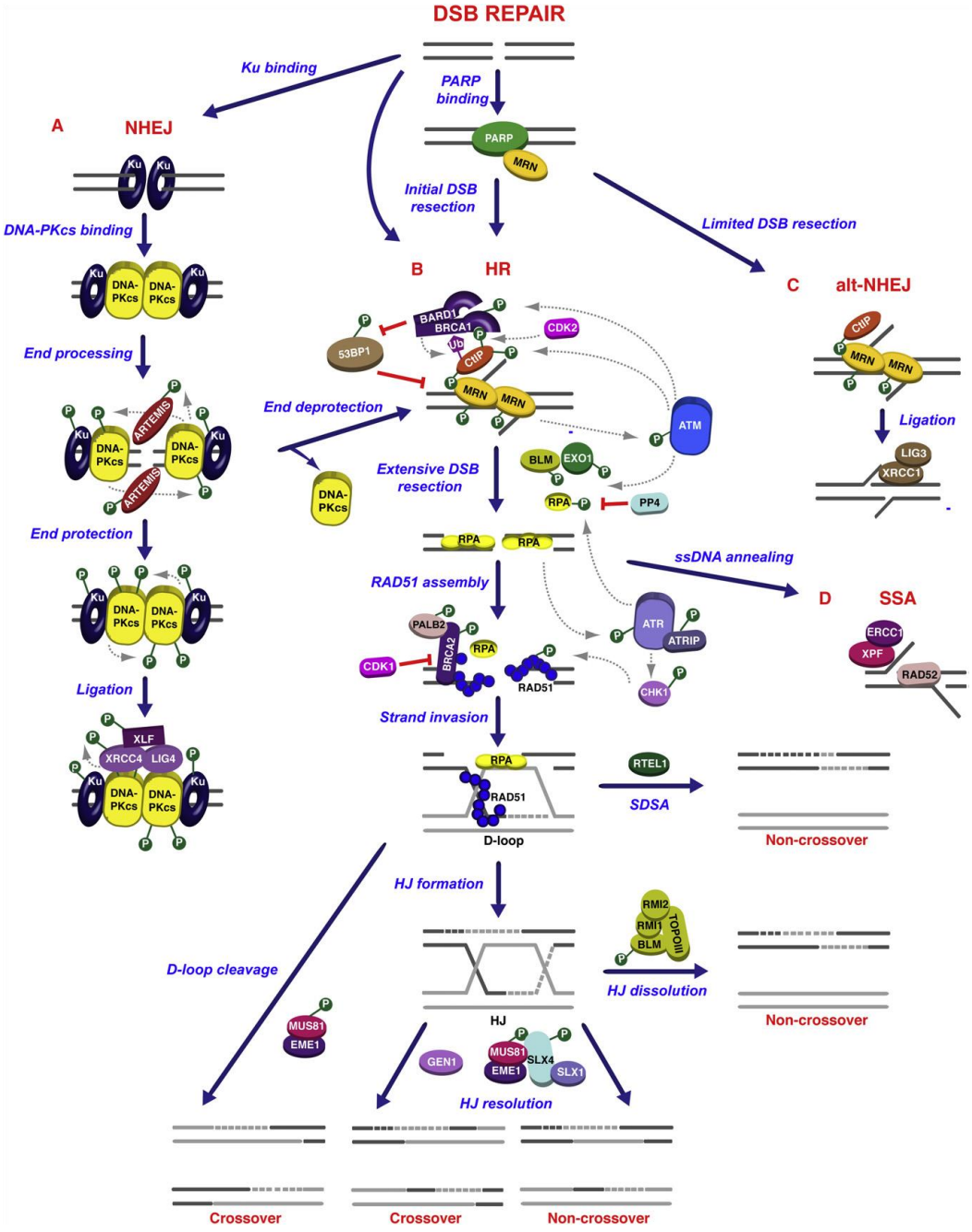

Figure-5.17. DNA repair pathways involved in the repair of double-strand breaks. (A) DSBs leads to recruitment of Ku which further localizes DNA-PK initiating NHEJ. Phosphorylation events on DNA-PKcs start DNA end processing by ARTEMIS. (B) MRN is also recruited at the DSB mediates DSB resection with CtIP and BRCA1, hence initiating homologous recombination in S and G2 phases of the cell cycle. MRN/CtIP/BRCA1 complex promotes DSB resection following deprotection of DNA ends when NHEJ fails. Formation of RPA coated ssDNA ends is induced by EXO1 and BLM after DNA resection. Removal of RPA by RAD51 is mediated by BRCA1, resulting in strand invasion into homologous DNA sequences. RAD51 is assembled on ssDNA by ATR pathway is activated by DNA resection step followed by formation of the D loop after strand invasion is cleaved by MUS81/EME1 or displaced by RTEL1 to generate cross-over or non-crossover events. Dissolution of Holliday junctions (HJs) by the BLM/TOPOIII complex results in non-crossovers while HJ resolution by the nucleases GEN1 and SLX1/SLX4

generate both crossover and non-crossover in association with MUS81/EME1. (C) Non-functional NHEJ and limited DSB resection by CtIP and MRN in G1 results in alternative NHEJ (113).

5.4.2. Single Strand Break Repair (SSBR) pathways

Single strand breaks are discontinuities in a single strand within a DNA molecule, which could arise due to loss of a nucleotide or damage at 5′- and/or 3′-termini. Reactive oxygen species (ROS) is one of the most common sources of SSBs and produces three times more SSBs than DSBs (153). SSBs are formed directly by the breakdown of oxidized sugars, indirectly by the formation of abasic sites (damaged or altered bases) and due to the abortive activity of cellular enzymes, DNA Topoisomerase I (TOP1) (154) (Figure-5.18). This enzyme relaxes DNA supercoils during DNA replication and transcription by generating 'cleavage complex' intermediates comprising a DNA nick (155). These DNA nicks are resealed by TOP1 but when faced with DNA or RNA polymerases or lesions, are rapidly converted into TOP1-linked SSBs (TOP1–SSBs) or TOP1-linked DSBs (TOP1–DSBs) (Figure-5.18). In both cases, TOP1 is bound to the 3′-terminus of the DNA strand break(153).

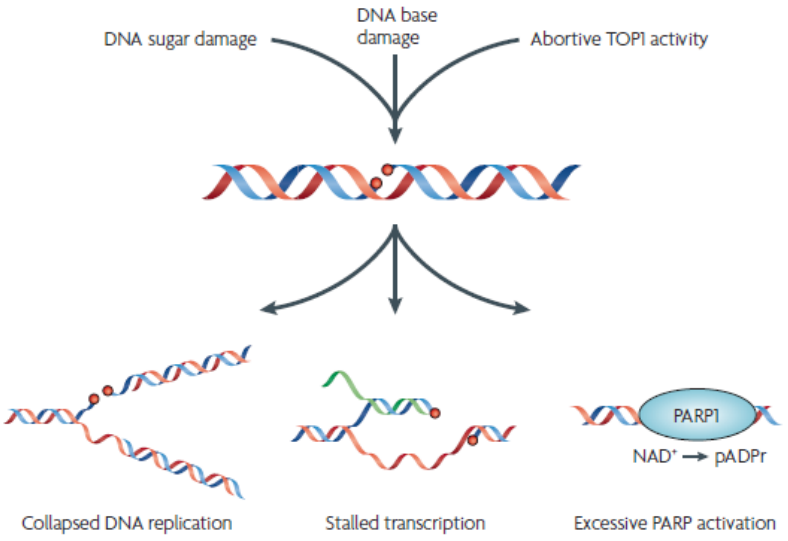

Figure-5.18. Single-strand breaks and cell fate. Single-strand breaks (SSBs) are induced due directly to the disintegration of deoxyribose, indirectly by the formation of abasic sites or as abortive intermediates of Topoisomerase I (TOP1) activity. If they are not repaired, SSBs can collapse replication forks, block transcription or activates SSB sensor protein poly(ADP-ribose) polymerase 1 (PARP1). Red circles denote damaged DNA termini. pADPr, poly(ADP-ribose) (157).

Formation of DSBs activate DSB repair pathways which efficiently repairs these DNA adducts but the continuous generation of SSBs saturates the HRR repair pathway resulting in genetic instability and cell survival (156). Studies have shown that acute increase in SSBs, if not restored, is associated with human genetic disease spinocerebellar ataxia with axonal neuropathy 1 (SCAN1)(154). In post-mitotic neurons (non-proliferating), SSBs result in stalling of RNA polymerases during transcription (Figure-5.18) (SSB blocks movement of RNA polymerase with damaged termini)(153). In most cases, SSBs are recognized by sensor protein poly(ADP-ribose) polymerase 1 (PARP1)(156) (Figure-5.18) and prolonged activation causes reduction of cellular NAD+ and ATP and/or release of apoptosis-inducing factor (AIF) from mitochondria. This type of cell death is similarly initiated by oxidative stress like diabetes, arthritis, and post-ischaemic brain or heart damage (153).

DNA SSBs interfere with DNA replication and transcriptional machinery resulting in persistent and numerous DNA nicks and conversion to DNA DSBs. DNA single-strand break repair (SSBR) includes base excision repair (BER) pathway, i.e. repairs base damage (157) . Poly (ADP-Ribose) PAR Polymerase (PARP) sits atop of this response by sensing the break and PAR-ylating the Xrcc1 scaffolding protein to DNA, bringing in DNA end-processing enzymes such as Tyrosyl-DNA phosphodiesterase 1 (TDP1), DNA polymerase beta (polβ), Polynucleotide Kinase 3'-Phosphatase (PNKP) and DNA ligases 1 and 3 to the break site. PARP1 is also involved in alternative DNA repair mechanisms. Furthermore, PARP1 inhibition leads to extensive SSB formation (105).

Induction and detection of DNA mismatches and insertion/detection loops activate single strand incision in mismatch repair (MMR). Repair proteins are then recruited at the single-strand incision site, such as nuclease, polymerase and ligase enzymes (20). Nucleotide excision repair (NER) identifies helix distorting base lesions and acts on it by two different pathways; transcription-coupled NER (TC-NER) and global genome NER (GG-NER). The damage is removed as a 22-30 base oligonucleotide forming ssDNA. This ssDNA is then modified by DNA polymerases and associated factors before ligation can take over (105) (Figure-5.19). All these ssDNA is not repaired, yet cell cycle is restarted, and unrepaired ssDNA are taken care of by polymerases as it requires less base-pairing requirements.

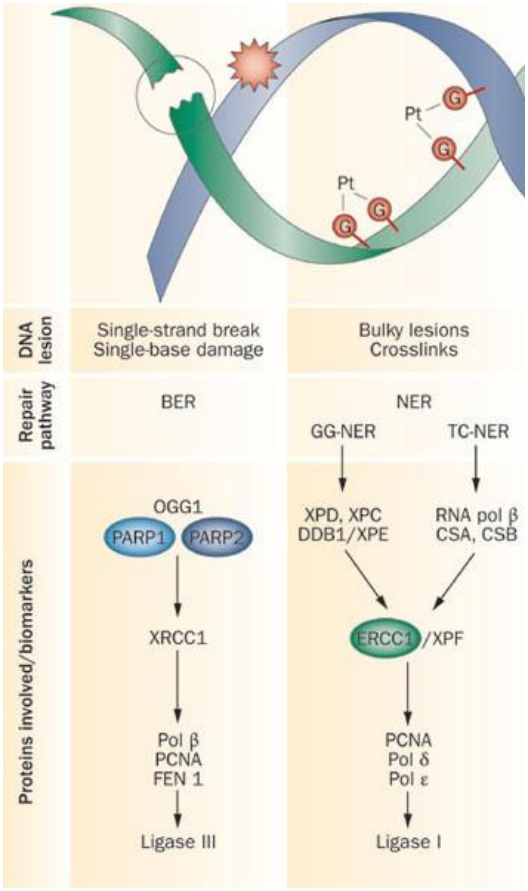

Figure-5.19. SSB repair mechanisms(141)

5.4.2.1. Role of poly(ADP-ribose) polymerase *(PARP) in DNA repair*

When SSBs are induced, one of the immediate response is activation of the sensor protein poly(ADP-ribose) polymerase (PARP) (156). Human PARPs consist of 17 enzymes(159) out of which PARP1 is the most abundant and is involved in the Base Excision repair (BER)/SSBR pathway, repairing SSBs(160). 85-90% of the PARP activity in cells is mediated by PARP1 and the rest by PARP2. Both enzymes are ubiquitously expressed in cells (159).

PARP1 comprises three major domains, NH2-terminal DNA-damage sensing and binding domain with three zinc fingers, an auto-modification domain, and a C-terminal catalytic domain. Zinc finger 2 has the highest affinity for DNA breaks while zinc finger 1 and zinc finger 3 are involved in DNA-dependent PARP-1 activation (160) (Figure-5.20). PARP1 activity is induced via phosphorylation, acetylation, sumoylation, and ubiquitination, while PARP1 is incapable of autophosphorylation, thereby inhibiting its activity to induce negative feedback (159). PARP1 is activated by SSBs resulting in cleavage of nicotinamide adenine dinucleotide (NAD) forming

nicotinamide and ADP-ribose. Addition of ADP-ribose units to form long and branched chains of poly (ADP-ribose) (PAR) form polymers adjacent to the DNA breaks which leads to covalent binding to acceptor proteins like PARP1, histone and other DNA repair proteins (160)(Figure-5.21).

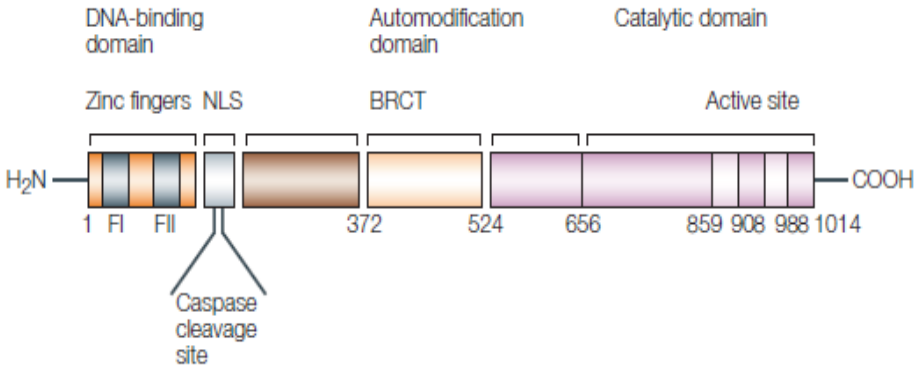

Figure-5.20. Structure of poly(ADP-ribose) polymerase-1 (PARP1). The amino (N)-terminal DNA-binding domain contains two zinc fingers and have an affinity for DNA binding and some protein-protein interactions. A DNA-nick sensor, which is a nuclear-localization signal (NLS) in the caspase cleavage site (DEVD) can be found in this DNA-binding domain. The auto-modification domain is a central regulating segment with a breast cancer-susceptibility protein-carboxy (C) terminus motif (BRCT), serves protein-protein interactions. The C-terminal contains the catalytic domain of PARP. The PARP catalytic fragment (CF), contains the active site and comprises of residues 655–1,014 and is composed of two parts: a purely α-helical N-terminal domain (NTD) from residues 662 to 784 and a C-terminal domain is found between residues 785 and 1,010, which includes the NAD+ binding site (161).

PAR structures provide a platform for recruitment of DNA repair proteins onto damage sites. There are three PAR binding domains; the macrodomain, PAR-binding zinc finger (PBZ) and an amino acid basic residue-rich cluster. Proteins such as PARP9, PARP14, PARP15, the histone variant macro H2A1.1 and the chromatin remodeling factor ALC1 comprises this macrodomain (113). Studies have shown that macro H2A1.1 and ALC1 are located to the damage site in a PAR-dependent manner and are involved in the reorganization of chromatin structure (113)(161).

Many DDR components like p53, XRCC1, LIG3, MRE11, and ATM have the acid-basic residue-rich cluster, on the other hand, nucleases APLF, SNM1, cell-cycle checkpoint protein CHFR contain PBZ motifs (113). DNA repair proteins like XRCC1 and LIG3 are recruited to the damage site in a PARP-dependent manner for repair of SSBs followed by DNA end-processing by DNA polymerase β, PNKP, and nucleases such as APE1, APTX, and APLF (154). Recruitment of these proteins to the DNA damage site is PBZ dependent (113).

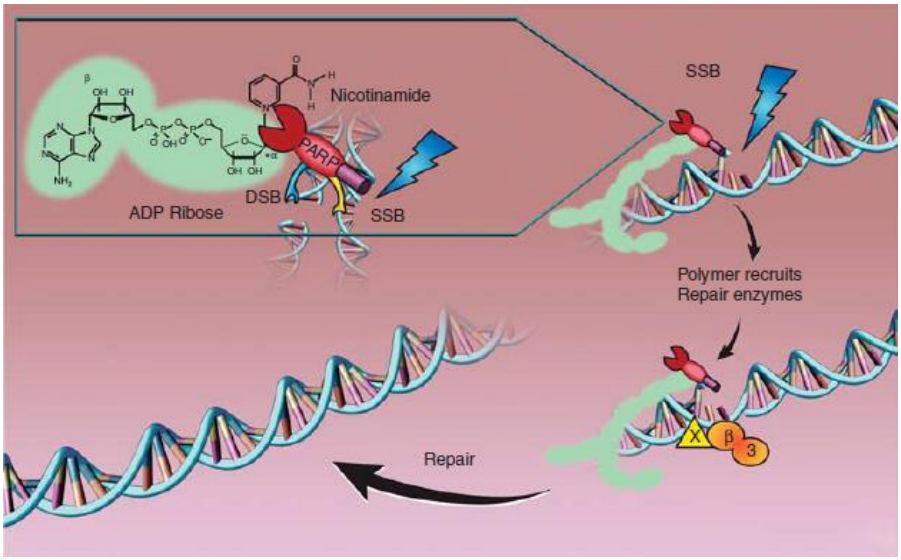

Figure-5.21. The catalytic activity of PARP-1 and role in DNA BER/SSBR. PARP cleaves NADþ and releases nicotinamide; the ADP-ribose polymers are covalently attached to acceptor proteins, like PARP and histones. This action leads to recruitment of other DNA break repair proteins (162).

5.4.2.2. Base Excision Repair (BER) pathway (SSBR)

SSBR is usually divided into four basic steps; Detection of SSBs, DNA end processing, DNA gap filling and DNA ligation(153).

❖ ***Detection of SSBs***

For SSB, the sensor protein poly (ADP-ribose) polymerase-1 (PARP-1) and poly (ADP-ribose) polymerase-2 (PARP-2) detects the DNA damage and immediately binds to the damage site(156) (Figure-5.22b). Once these enzymes are activated, they covalently modify themselves and target proteins with long chains of negatively charged poly ADP-ribose (PAR). This activation and binding of PARP1 to the damage site is temporary(161). When PARP1 is autoribosylated they detach from DNA due to charge repulsion and PAR is degraded by poly ADP-ribose glycohydrolase for reactivation of PARP1 at the break site. PARP1 then further recruits other DNA repair proteins to the SSB site through a plethora of cellular responses(162). In indirect SSB, abasic sites are formed during BER ("AP"), to which APE1 binds and cleaves the site(Figure-5.22a) (163).

❖ ***DNA end processing***

This is the most diverse step in SSBR involving various enzymes due to a variety of termini that arises upon SSB induction. Normally, the most common SSBs results in the formation of 3' – 5' termini, which must be repaired to 3' hydroxyl and 5' phosphate moieties for SSBR process to

continue and completely repair the damage (153). Enzymes involved include polynucleotide kinase (PNK), AP endonuclease-1 (APE1), DNA polymerase β (Pol β), tyrosyl phosphodiesterase 1 (TDP1), and flap endonuclease-1 (FEN-1) (162). SSBs produces AP endonuclease sites APE1 which forms 5'deoxyribose phosphate (dRP). This is usually removed by 5' dRP lyase activity of Pol β (Figure-5.22c) (154). Direct SSBs form 3' phosphate or 3' sugar fragments and both are removed by APE1 in association with the scaffolding protein, XRCC1. XRCC1 interacts with and stimulates polynucleotide kinase phosphatase (PNKP) which has both 3' DNA phosphate and 5' DNA kinase activity, hence repairing 3' phosphate and 5' hydroxyl termini (Figure-5.22d). FEN1 is usually responsible for removing the displaced 5' residue as a single-stranded flap (164).

❖ ***DNA gap filling***

SSBs usually form a single nucleotide gap at the break site and DNA polymerase, Pol β fills the gap by introducing a single nucleotide (short patch repair) or continues to fill in about 2-15 nucleotides (long patch repair)(162). In gap filling different DNA polymerases are involved depending on the type of SSB damage and the length of repair. Direct and indirect SSSR involves DNA polymerase, Pol β but in certain cases, both Pol β and Pol ε participates(Figure-5.22e,f) (154).

❖ ***DNA ligation***

In indirect SSBR/BER, DNA ligation initiates with XRCC1 interacting with DNA polymerase, Pol β. This interaction helps localize DNA ligase III to the damage site, which then further interacts with XRCC1, repairing the damage via short patch repair (Figure-5.22g). In long patch repair process DNA ligation is employed through PCNA interacting and stimulating of DNA ligase I(Figure-5.22h) (162).

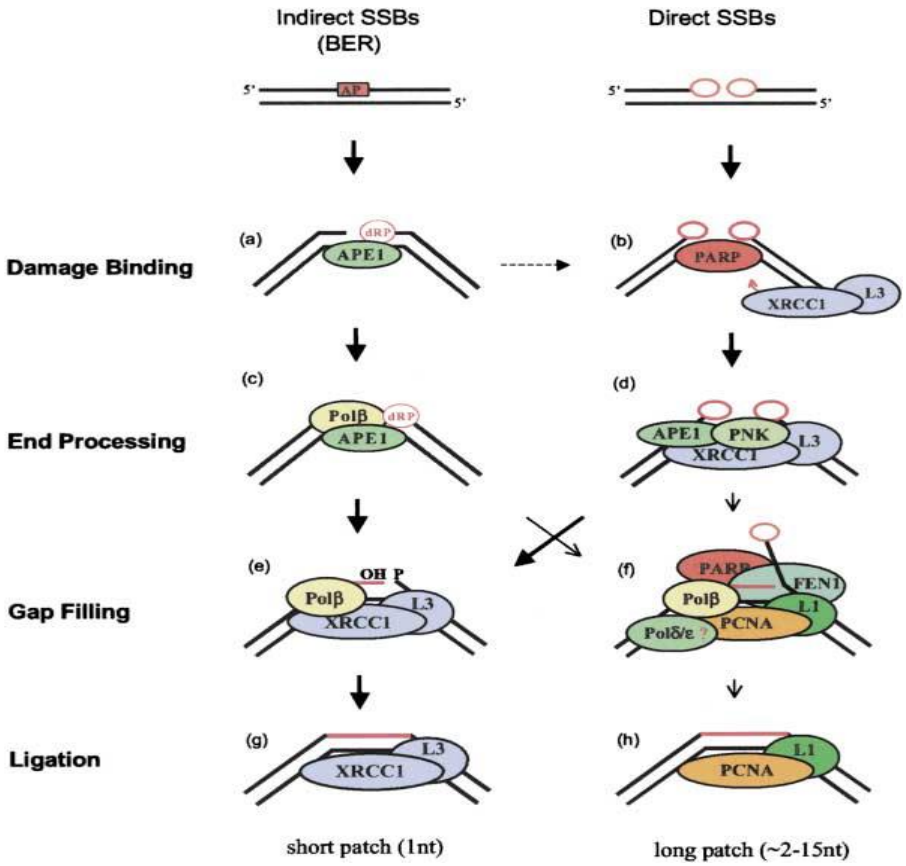

Figure-5.22. SSBR at direct breaks and indirect breaks during BER. At indirect SSB, abasic sites are formed during BER ("AP"), to which APE1 binds and cleaves the site (a), recruiting Pol β (c), this DNA polymerase then introduces a single nucleotide and repairs 5' deoxyribose phosphate termini ("dRP") (e). This makes the DNA ends ligatable and DNA ligation is carried out by the interaction of XRCC1 with DNA ligase 3 (g). In some cases, like indirect SSBs Pol β cannot remove 5' dRP (oxidized or reduced) so PARP (b), PCNA and FEN1 (d) is recruited at stalled DNA ends for extension by introducing 2-15 nucleotides for cleavage of the flap (f) and ligated by DNA Ligase 1 (h). DNA polymerase Pol β and ε participates in long patch repair. Indirect SSBs, PARP1, and PARP2 are recruited to the damage site which is then activated and automodified. This automodified PARP then recruits scaffolding protein XRCC1-Lig III. (d) Damaged 3' and 5' termini are replaced with 5' phosphate and 3'hydroxyl by APE1 or PNK (158).

❖ ***Repair of abortive TOP1 SSBs***

Topoisomerase I (TOP1) enzyme relaxes supercoiling of the DNA by producing nicks in DNA, during transcription and replication, thus; generating SSBs during its catalytic cycle (154). TOP1 attaches itself to the 3' terminus of the break and seals them. This ligation activity of the enzyme can be blocked by DNA lesions resulting in abortive TOP1 SSB (162). DNA SSBR is required to rectify these transient breaks. PARP1/PARP2 is recruited at the break site along

with TDP1. TDP1 removes TOP1 complex from the 3' terminus of abortive TOP1 DNA strand breaks, resulting in the formation of 3' phosphate and 5' hydroxyl termini (153). PARP then further recruits XRCC1-Lig III complex, which displaces PARP and localizes PNKP at the break site to repair 3' and 5' termini (Figure-5.23) (154). After this, the break ends become ligatable by DNA ligase IIIα (162). This repair process takes place when the abortive TOP1 SSB have not encountered replication fork. Replication fork collapse converts SSBs to DSB and this leads to activation of DSBR pathway and Homologous recombination repair (HRR) predominates (113).

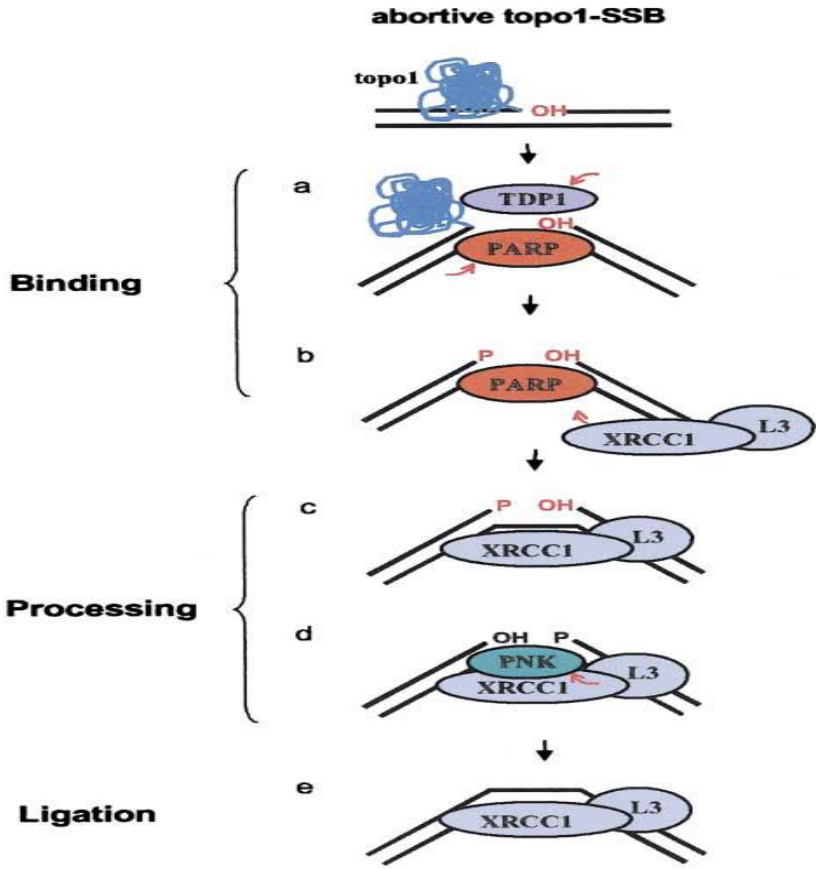

Figure-5.23. Model for the repair of abortive TOPI SSBs. PARP1/PARP2 is recruited at the break site along with TDP1. TDP1 removes TOP1 peptide from the 3' terminus of abortive TOP1 DNA strand breaks, resulting in the formation of 3' phosphate and 5' hydroxyl termini. PARP then further recruits XRCC1-Lig III complex, which removes PARP and localizes PNKP at the break site to repair 3' and 5' termini. After this, the break ends become ligatable which is carried out by DNA ligase IIIα (158).

5.4.3. DNA Damage response and human disease

Damage to DNA triggers DDR which in association with DNA repair pathways maintain genomic integrity(113) but in human pathophysiology, this DDR implements various genetic deficits from mutations in DDR and DNA repair genes. These mutations affect the nervous system, immune system, reproductive system and is associated with predisposition to cancer and premature aging(165). For the context of this thesis/research, focus on neurodegeneration and cancer will be the focus.

5.4.3.1. Defective DNA repair and neurodegenerative disease

Neurons do not possess the ability to regenerate unlike other cells in the body, so are profoundly dependent on DDR to prevail any DNA damage (113). DNA base lesions and DNA breaks are common damage in neurons from oxidative stress due to high consumption of oxygen from mitochondrial respiration(166). In non-proliferating cells like neurons about 10^8 purines are lost because of depurination in a neuron's lifespan. Neurons are very sensitive to reactive oxygen species (ROS) (167) and nitrogen species (RNS) because they induce DSBs, SSBs and AP sites. Neurons generate about 20,000 to 40,000 daily DNA-SSBs (168). Active DNA repair pathways are required to resolve these damages to maintain the neuron's lifespan. So, defects in repair mechanism and regulation of oxidative stress will result in neuronal death giving rise to neurodegenerative disease (167) (Table-5.3).

Most syndrome arising from DDR defects affect the cerebellum which comprises of 50% of the CNS' neurons: specifically granule neurons, Purkinje cells, and interneurons (113). Any defect or degeneration in this tissue often results in cerebellar ataxia (impaired motor coordination), oculomotor apraxia (eye movement defect)(169) and dysarthria (speech disorder). Ataxia Telangiectasia (AT) signifies these symptoms and occur due to a mutation in *ATM* (170). A-T patients show extensive ataxia and are restricted to a wheelchair before 10 years of life due to progressive loss of granule and Purkinje cells from the cerebellum(113). Studies have shown that ATM-deficient cells have excessive reactive oxygen (ROS) levels, linking ATM to resolving oxidative stress, hence mutations in ATM gene are associated with increased reactive oxygen species (ROS) in neurons following DNA damage leading to neurodegeneration(170).

There are two syndromes that overlap with AT which arise from mutation in the MRN complex (168); ataxia-telangiectasia-like syndrome (A-TLD), which develops from mutations in MRE11 and results in slower progression of ataxia compared to A-T patients(113) and; Nijmegen breakage syndrome (NBS) which arises due to mutations in NBS1(171). Mutations associated with these syndromes results in partial loss of the gene function (hypomorphic), disabling some but retaining the DNA replication and cell survival(168). The mechanism by which these mutations are responsible for these syndromes remain controversial (113). NBS mutations are usually associated with microcephaly rather than neurodegeneration and can lead to medulloblastoma development (171).

Axonal neuropathy (SCAN1) and Ataxia with oculomotor apraxia 1 (AOA1), are two ataxia associated neurodegenerative disorders acquainted with SSB repair defects induced by ROS in DNA. Both are caused by mutation of DNA end-processing enzymes, TDP1 (SCAN1) and APTX (AOA1) (165). TDP1 is involved in SSB repair and is frequently induced by abortive TOP1 (171). This enzyme repairs altered 3’ DNA ends from Topoisomerase I (168) DNA covalent complexes and oxidative damage. However, the AMP-lysine hydrolase activity of APTX is crucial for repairing altered 5’ AMP intermediates from abortive DNA ligation processes (113).

Disease or syndrome	Gene	Neurological symptoms	Extraneurological symptoms
DNA DSB repair deficiency			
Ataxia telangiectasia	*ATM*	Ataxia, neurodegeneration, telangiectasia and dysarthria	Immunological defects, malignancy and sterility
Ataxia telangiectasia-like disorder	*MRE11*	Ataxia, neurodegeneration, dysarthria and oculomotor apraxia	Mild immunological defects
Nijmegen breakage syndrome	*NBS1*	Microcephaly	Immunological defects and lymphoid malignancy
ATR-Seckel syndrome	*ATR*	Microcephaly and mental retardation	Growth defects
LIG4 syndrome	*LIG4*	Microcephaly	Developmental/growth delay, immunodeficiency and lymphoma
Human immunodeficiency with microcephaly	Cernunnos	Microcephaly	Immunodeficiency
Fanconi anaemia	*BRCA2*	Microcephaly and medulloblastoma	Bone marrow and congenital defects
DNA SSB repair deficiency			
Spinocerebellar ataxia with axonal neuropathy	*TDP1*	Ataxia, neurodegeneration, peripheral axonal motor and sensory neuropathy, and muscle weakness	Hypercholesterolaemia and hypoalbuminaemia
Ataxia with oculomotor apraxia 1	*APTX*	Ataxia, neurodegeneration, oculomotor apraxia and peripheral neuropathy	Hypercholesterolaemia and hypoalbuminaemia
NER deficiency			
Xeroderma pigmentosum	*XPA–XPG*	Neurodegeneration and microcephaly	UV sensitivity and skin cancer
Cockayne syndrome	*CSA, CSB, XPB, XPD and XPG*	Microcephaly and dysmyelination	Progeria and otherwise variable presentation
Trichothiodystrophy	*XPD, XPB and TTD-A*	Neurodevelopmental defects and dysmyelination	Brittle hair and otherwise variable presentation
DNA cross link repair			
Fanconi anaemia	*FAA–FAL*	Microcephaly and medulloblastoma (brain tumours in FANCD2 and FANCN subtypes)	Anaemia, developmental defects and cancer
Helicase deficiency			
Werner syndrome	*WRN*	?	Severe progeria and cancer
Rothmund Thomson syndrome	*RTS*	?	Cancer
Bloom syndrome	*BLM*	?	Proportional dwarfism and cancer
Ataxia with oculomotor apraxia 2	*SETX*	Ataxia, neurodegeneration and oculomotor apraxia	Absent or minimal

APTX, aprataxin; ATM, ataxia telangiectasia, mutated; ATR, ataxia telangiectasia and RAD3-related; BRCA2, breast cancer associated 2; DSB, double strand break; LIG4, ligase IV, NHEJ1, non-homologous end joining 1; SSB, single strand break; TDP1, tyrosyl-DNA phosphodiesterase 1; UV, ultraviolet; ?, neurological deficits are not clearly defined.

Table-5.3. Human DNA repair-deficient syndromes (175)

5.4.3.2. DNA repair and Cancer Development

Human DNA undergoes various damage from endogenous and exogenous sources and studies have shown that dysregulation, loss or gain of DNA repair genes are responsible for the accumulation of DNA lesions which confers to cancer cells growth and survival advantages(172). Dysregulated DNA repair results in mutations, disrupting the defined balance between oncogenes (activated) and tumour suppressor genes (inactivated), promoting malignant transformation and cancerous growth(173) (Figure-5.24).

Activated oncogenes, such as MYC and RAS, stimulate replication fork firing which stalls these replication fork resulting in collapse, hence forming DSBs (multiple collision of forks on the same chromosome). Formation of DSBs activates DDR and cell cycle checkpoints for repair, thereby halting the cell cycle(166). It has been shown in studies that for the precancerous lesion to advance into mature tumours, DSB signaling molecules like ATM, ATR, and p53 shut down and with dysfunctional cellular processes, stalled replication forks are not repaired efficiently, and the cell continues to proliferate with DSB lesions, hence incorporating unresolved mutations(174).

Germline mutations in cell cycle checkpoint or DNA repair genes incline to hereditary cancers while, somatic mutations(172) like epigenetic silencing of DNA damage response genes predispose to cancers with no inherited association. DNA repair genes in different pathways (BER, NER, NHEJ, HRR, MMR) can predispose to different types of cancers(173). For example, mutations and epigenetic silencing of DNA repair components in homologous recombination are associated with both sporadic and familial cancers.

Breast, ovarian and pancreatic cancer are related to loss of function mutation in *BRCA1*, *BRCA2*, *PALB2*, *ATM*, *RAD51C* and *RAD51D*(175). On the other hand, it is predicted that >90% of all tumours incur at least one defect in the DNA damage response (DDR)(113), thus tumour cells enhance the activity of other DNA repair pathway(135) resulting in tumour cells adapting and acquiring highly active DNA repair pathways along with redundancy among these repair processes with which they utilize to proliferate(175).

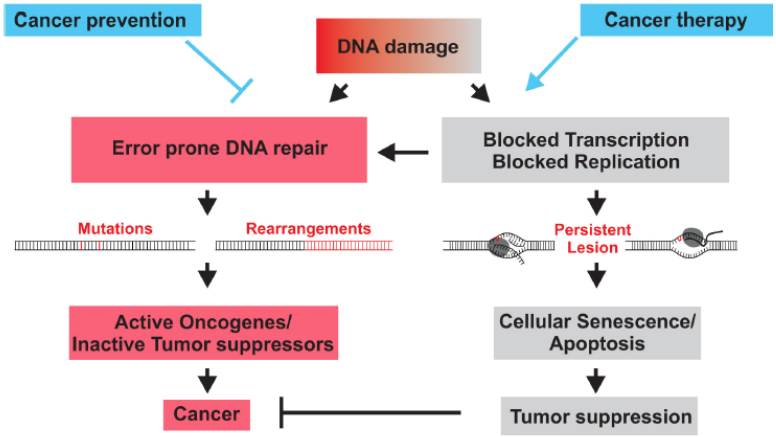

Figure-5.24. Dysfunctional DNA repair causes the development of cancer due to mutations in DNA damage response and repair genes resulting in activation of oncogenes and inactivation of tumour suppressors (169).

5.4.4. DNA Damaging agents in tumour therapy

Cancer therapy gained attention after the Second World War when multiple cases of bone marrow suppression and lymphoid aplasia were reported; the cause being exposure to chemical warfare agent - sulfur mustard(173). A therapeutic link was apparent decades later when physicians detected reduced white blood count in autopsies from affected individuals. This provided evidence for physicians that nitrogen mustard could be used to treat leukemias(173). After a few years, alkylating agents were developed in combination with nitrogen mustard and cisplatin for the induction of tumour cell death (175). This led to the notion that DNA damage is not only involved in tumour development but could be manipulated against tumour growth and tumour cell death(176).

5.4.4.1. Topoisomerase Inhibitors

Topoisomerase inhibitors are a class of DNA damaging agent for anti-cancer therapy which renders tumour cell death by blocking topoisomerase I enzyme during DNA transcription and replication (177). The first drug developed was Camptothecin (CPT) which has been approved for colorectal cancer in the United States. A 13-32% response rate was reported in clinical trials with CPT (singly and in combination with 5-fluorouracil) (178) along with dose-limiting toxicities such as myelosuppression and dual phase diarrhea. Afterward, synthetic derivatives of camptothecin were developed with increased efficacy, potency and ability to cross the blood-brain barrier (BBB) (179). Topotecan was approved for use in cisplatin-refractory ovarian carcinoma and clinical trials are underway with different tumour types (175). Other derivatives of CPT are in clinical trials; these newer drugs are designed to give more therapeutic benefit when used both singly and in combination(177) (Table-5.4). The common toxicity observed in patients is myelosuppression.

Camptothecin derivative	Status	Remarks	Indications
Topotecan hydrochloride (Hycamtin)	FDA approved (GlaxoSmithKline)	Intravenous infusion (water-soluble)	Metastatic ovarian cancer (second line); SCLC (second line)
Irinotecan hydrochloride (Camptosar)	FDA approved (Pfizer*)	Intravenous infusion (water-soluble)	Metastatic colorectal cancer (first line with 5FU/leucovorin)
9-NC; Rubitecan (Orathecin)	Phase II/III (SuperGen)	Oral administration; converted to 9-AC	Pancreatic cancer
9-AC; IDEC-132	Phase II	Intravenous infusion; oral; intraparenteral	Ovarian cancer (intraparenteral)
Exatecan mesylate (DX-8951f); DE-310[¶]	Phase II/III (Daiichi)	Intravenous infusion	Various carcinomas (sarcomas?)
Lurtotecan GI-147211 NX 211	Phase II (Gilead[‡])	Intravenous infusion; liposomal (NX 211)	Ovarian and other carcinomas
Gimatecan (ST-1481)	Phase I/II (Novartis[§])	Oral administration; lipophilic	Glioblastoma, SCLC and solid tumours
PEG–camptothecin; Prothecan	Phase II (Enzon Inc.)	PEGylated derivative; intravenous infusion (water-soluble)	NSCLC and other solid tumours
Karenitecin; BNP-1350	Phase II (Bionumerik Pharmaceuticals)	Oral administration; lipophilic	Glioblastomas, melanomas and NSCLC
Silatecan; DB-67	Preclinical	Lipophilic	Glioblastomas
Diflomotecan; BN 80915	Phase II (Ipsen)	Intravenous infusion	Advanced metastatic cancers: colon, breast and prostate

Table-5.4. Camptothecin derivatives in clinical trials(175)

There are non-camptothecin TOPI poisons like Indolocarbazoles derivatives, Nitidine, and phenanthridine derivatives and these drugs are now in clinical trials (179). Recently indenoisoquinolines have been selected for further clinical development and these drugs have several advantages over others (178), as they are more chemically stable because indenoisoquinolines are less reversible compared to camptothecin (179). Pharmacokinetics of indenoisoquinolines produces persistent TOPIccs resulting in shorter infusion times (178).

There are two major topoisomerase enzymes in mammalian cells, Topoisomerase I and Topoisomerase II. TOPI reseals a strand of DNA while TOPII cleaves both strands of DNA (179). TOPI relaxes DNA supercoil during DNA replication and transcription by generating 'cleavage complex' intermediates comprising a DNA nick (Figure-5.25) (155). TOP1 is bounded to 3′-terminus of DNA strand break (153). These DNA nicks are resealed by TOP1 but when blocked by TOPI inhibitors, are rapidly converted into TOP1-linked SSBs (TOP1–SSBs) or TOP1-linked DSBs (TOP1–DSBs)(153). TOPI inhibitors bind irreversibly to TOPI enzymes and so prolonged inhibition of this enzyme leads to irreversible DNA replication (175) defects resulting in cell cycle arrest and cell death. This cytotoxic effect of TOPI inhibitors highly depends on the length of exposure and not on the concentration of the drug, hence the time of administration of the drug is directly proportional to response (179).

Etoposide and doxorubicin are known Topoisomerase II inhibitors which inhibits the catalytic activity of Top II enzyme resulting in increased formation of DNA covalent cleaved complexes, hence mediating DNA damage.

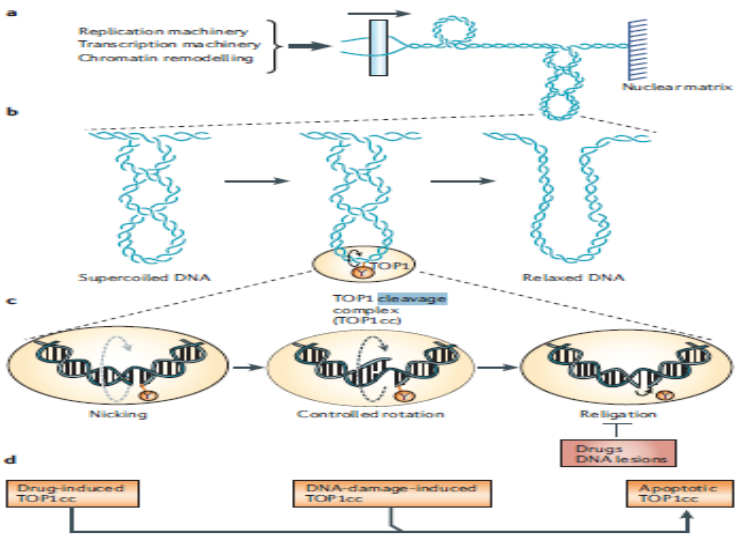

Figure-5.25. Relaxation of DNA supercoiling by TOP1-mediated DNA cleavage complexes and trapping of TOP1 cleavage complexes by drugs, DNA modifications and during apoptosis. (a) DNA supercoiling by DNA replication, transcription and chromatin remodelling (b) Formation of DNA single-strand breaks (nicks) by TOP1 provides swivel points that enable the rotation of the intact DNA strand around the break and facilitate DNA relaxation (c) The nicking step (on the left) is the transesterification reaction taking place where the tyrosine links to 3' DNA. In the middle step, the torsional stress from DNA supercoiling drives the 5' end of nicked DNA strand around the intact DNA and TOP1 slows this rotation, known as controlled rotation. In the last step (on the right) resealing of DNA strand takes place, where 5' end of the nicked DNA is relegated with 3' end. Drugs and DNA lesions blocks this relegation steps forming single and double-stranded TOP1ccs (d) TOP1ccs can be stabilized by drugs like camptothecin, DNA lesions which produce mismatched DNA strand and TOP1 modifications during apoptosis (181).

5.4.4.2. DNA alkylating agents

Alkylating agents are one of the common anti-cancer drugs used to treat several types of cancer. Most of the alkylating agents are monofunctional such as temozolomide (TMZ), *N*-methyl-*N*-nitro-*N*-nitrosoguanidine (MNNG), and dacarbazine; while some methylating agents are bifunctional such as nitrogen mustards (chlorambucil and cyclophosphamide) and chloroethylating agents (nimustine [ACNU], carmustine [BCNU], lomustine [CCNU], fotemustine)(180).

Alkylating agents add s methyl group at N- and 0- atoms in DNA bases forming various adducts with variable stabilities, for example *N*-methylation (comprises 80% of methylated bases), *N*7-methylguanine (*N*7MeG) (most stable), *O*6-methylguanine (*O*6MeG), *O*4-methylamine (*O*4MeT)(181), *O*-alkylations (e.g., *O*6alkylG and *O*4alkylT) and *N*-alkylations (*N*3alkylA and *N*1alkylA). These adducts are removed by DNA repair processes, like *N*-alkylated purines (*N*7MeG, *N*3MeA, *N*3MeG) are resolved by base excision repair(Figure-5.26d) while human AlkB homologous (hABH) (Figure-5.25e) repair *N*1MeA, *N*3MeC, *N*3MeT, and *N*1MeG(182).

*O*6MeG is repaired by the DNA repair protein *O*6-methylguanine- DNA methyltransferase (MGMT) and involves the transfer of an alkyl group from the oxygen in the guanine to a cysteine residue in the catalytic pocket of MGMT(Figure-5.26a). In absence of this DNA repair protein, *O*6MeG mismatches during DNA replication. DNA replication with *O*6MeG lead to the formation of *O*6MeG:T or *O*6MeG:C mismatch and in next cycle of replication this become an A:T transition mutation(181)(Figure-5.26a). This activates the mismatch repair (MMR) pathway which resolves the mismatched pair. This creates SSBs which convert to DSBs when faced with the replication fork(175)(Figure-5.26b). Also, *O*6MeG in the DNA strand form DSBs because of futile repair loop(182). DSBs activate DSBR pathways; Non-homologous end joining (NHEJ) and Homologous recombination (HRR)(174) (Figure-5.26c). Bifunctional alkylating agents produce chloroethyl adducts at *O*6G which are repaired by MGMT and secondary interstrand cross-links (ICLs) are repaired by Nucleotide Excision repair (NER) followed by homologous recombination to complete repair(181).

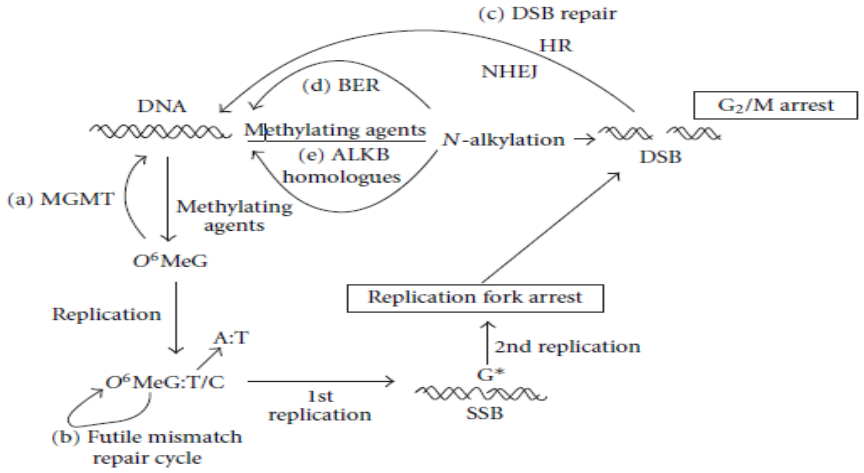

Figure-5.26. Pathways for DNA damage induced by methylating agents. (a) O6-methylguanine-DNA methyltransferase (MGMT) removes the methyl adduct from O6MeG. Unresolved O6MeG:C or O6MeG:T mismatch pairs form during replication. In the next round of replication, O6MeG: T pairs can become A: T transition mutations. (b) O6MeG:T and O6MeG:C pairs are recognized by the mismatch repair (MMR) system, which creates a single-strand break (SSB), cause replication arrest, and forms double-strand break (DSB). O6MeG: T/C induces G2/M arrest in the second cell cycle. (c) Homologous recombination (HR) and nonhomologous end joining (NHEJ)are activated upon formation of DSBs. N-alkylations are repaired by either (d) base excision repair (BER) or (e) AlkB homologs otherwise DSBs occur (182).

Temozolomide which is the first line drug for Glioblastoma Multiforme alkylates the O6 position of guanine and is repaired by alkyltransferase, O6-methylguanine-DNA methyltransferase (MGMT)(181). Topoisomerase inhibitors like camptothecin and etoposide block topoisomerase enzyme during DNA replication and transcription on double helix, blocking resealing of single-stranded DNA.

5.4.4.3. DNA crosslinking agents

DNA crosslinking agents introduce damage in DNA(183) when two nucleotide residues are covalently linked within DNA strands (intrastrand crosslinks, ICLs) or among opposite strands (interstrand crosslinks) (Figure-5.27). The N7 position of guanine or the exocyclic N2-amino group of guanines is the common target. ICLs completely block strand ligation during DNA transcription and replication and unresolved ICLs are lethal to tumour cells(184). ICLs are repaired by DNA repair pathways which render both inherent tumour sensitivity and acquired drug resistance. ICLs are mainly repaired by the Nucleotide Excision Repair pathway (NER) and unrepaired ICLs induces DSBs due to replication fork collapse activating DSBR pathways(183). DNA crosslinking agents are widely used anti-cancer drugs for its anti-tumour activity which include(184), the nitrogen mustards (melphalan, chlorambucil, cyclophosphamide, and ifosfamide), the platinum drugs (cisplatin and carboplatin), chloroethylnitrosoureas (carmustine and lomustine), the alkylalkanesuphonate busulfan, and the natural product mitomycin C(183).

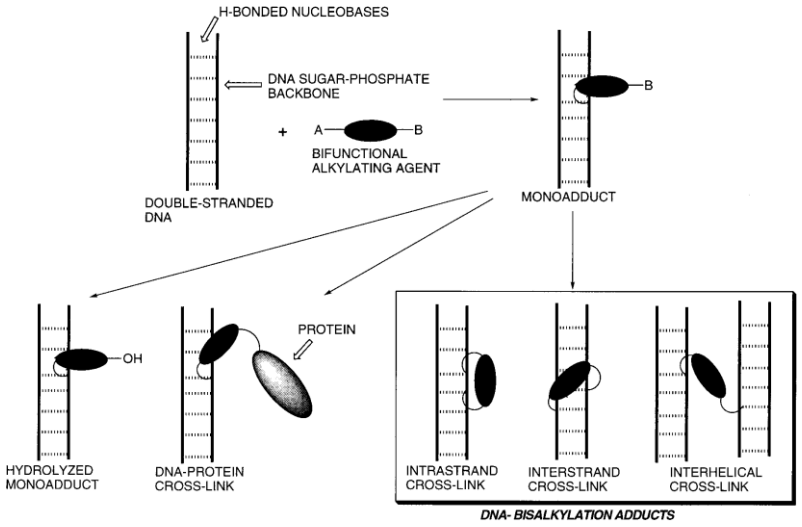

Figure-5.27. Formation of inter-strand crosslink (ICLs) by DNA crosslinking agents. A and B represent electrophilic moieties within the cross-linking agent of interest (187).

Chlorambucil has been used for chronic lymphocytic leukemia (CLL) but later was replaced by Fludarabine due to neural and bone marrow toxicity reported in children. Cisplatin is used for lung cancer, ovarian cancer, lymphoma, and testicular cancer (increased from 10% to 81% with adjuvant cisplatin therapy)(185). Cisplatin presents with nephrotoxicity, neurotoxicity and bone marrow suppression in cancer patients. Due to these toxicities, second generation platinum drugs were designed like carboplatin which has fewer side-effects in the kidney. Other platinum agents include oxaliplatin, satraplatin, picoplatin, nedaplatin, and triplatin. Ifosfamide is used to treat testicular, lung and breast cancer but shows similar side effect as chlorambucil (184).

DSB repair pathways are activated in the process of repairing ICLs so cancers with BRCA2 mutations, like breast and ovarian cancer which have deficient homologous recombination(183), respond better to DNA alkylating agents. This phenomenon has been seen in patients with a hereditary mutation leading ovarian cancer, who respond better to crosslinking drugs compared to patients with sporadic ovarian cancer(185).

5.4.4.4. Radiomimetic

Neocarzinostatin (NSC) and bleomycin are known antibiotics with anti-tumour activity. The ability of these drugs to sensitize tumour cells make them potential anti-cancer drugs. Bleomycins are glycopeptide antibiotics produced by Streptomyces verticillus while NCS are polypeptides produced by Streptomyces carzinostatcs(186). Both are capable of cleaving DNA and form single strand breaks and double-strand breaks of bacterial and mammalian tumour cells. These cleavages occur at specific nucleotides or nucleotide sequences(177). Studies have shown that incubation of cells at low concentration with these drugs released free thymine and adenine (186) suggesting that strand incision may occur at thymine and adenine residues. However, at higher concentrations, all the four bases were detected(177).

Radiomimetic like bleomycin induce DSBs which are repaired by NHEJ along with HRR repair during DNA replication (186). DNA base lesions and SSBs are induced by alkyl sulphonates and nitrosourea compounds; repaired by base-excision repair (BER) pathway or the nucleotide-excision repair (NER) pathway (187). Indirect DSBs are induced by replication inhibitors like hydroxyurea which form stalled replication fork and are repaired by HRR (178).

Chemotherapy and radiotherapy induce DNA damage in tumour cells and specific DNA repair pathways are activated (187). DNA damaging agent like antimetabolites (5-fluorouracil, thiopurines) block replication fork movement and nucleotide metabolism(177). The figure below gives an overview of the different types of DNA repair pathways activated by chemotherapy and radiotherapy (Figure-5.28).

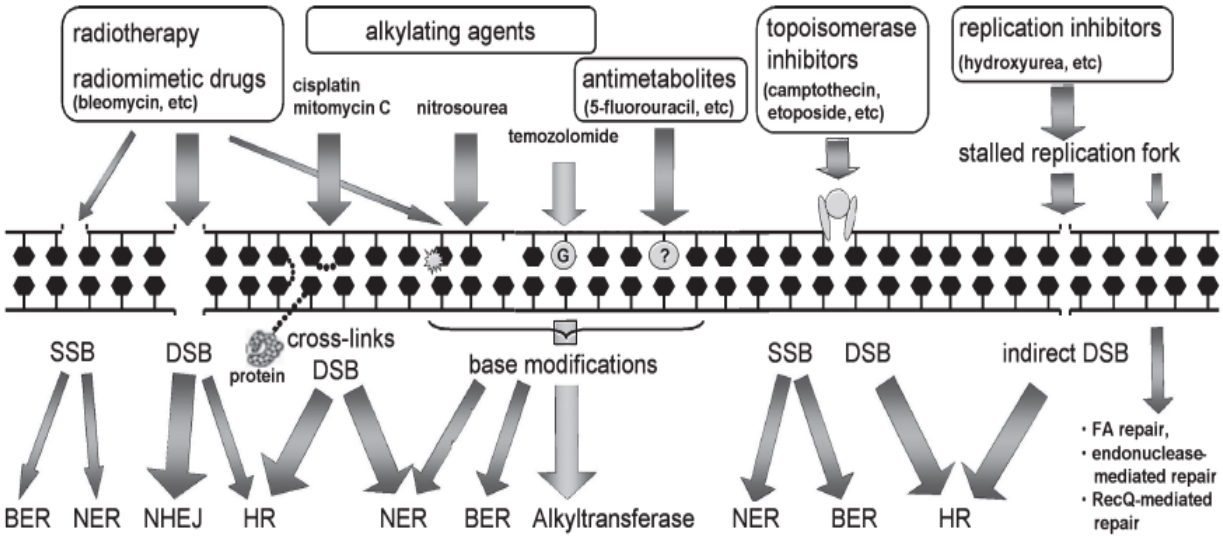

Figure-5.28. DNA damaging agents inducing different types of damage and activating different DNA repair pathways(189)

5.4.4.5. DNA repair inhibitors

Dysregulation in DDR and repair processes result in cell death along with mutagenesis leading to cancer development(188). In tumour cells, impairment in DNA repair genes causes upregulation of various DNA repair pathways, leading to resistance to DNA damaging anti-cancer therapy. Tumour cells have highly active DNA repair pathways; if one repair process is blocked they may use alternative repair pathways for recovery(172). Targeting the DDR components(188) and inhibiting repair proteins/enzymes of DNA repair pathways may have the potential to sensitize tumour cells to current DNA damaging agents(172), allowing tumour cell death and hindering cancer progression(188).

Some of the major DDR and DNA repair inhibitors are mentioned in the figure below alongside their cellular mechanism(188) (Fig 5.29).

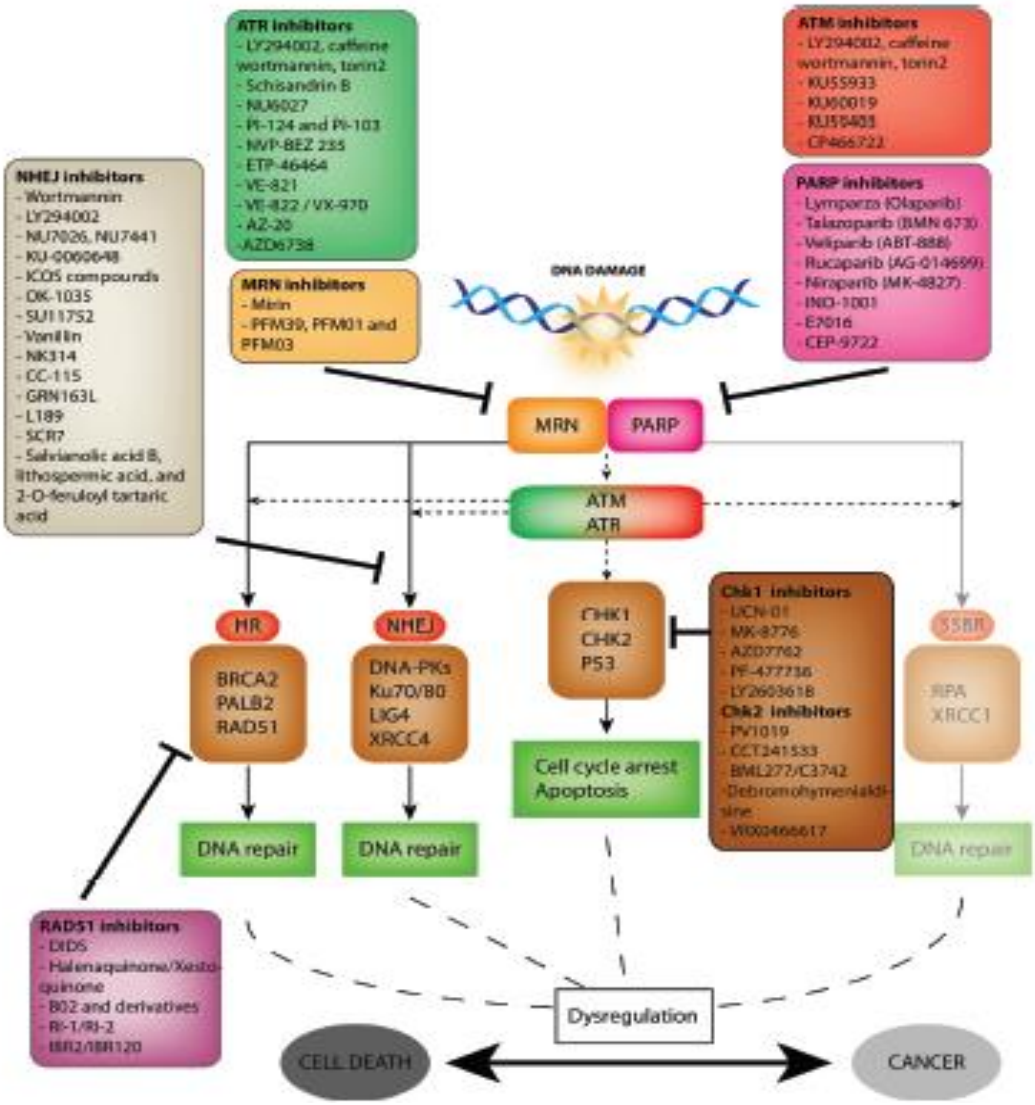

Figure-5.29. The DNA damage response and DNA repair pathways and their inhibitors(190)

a. PAPR Inhibitors

PARP inhibitors came into consideration as a therapeutic agent, with the observation that nicotinamide, a component of PARP catalytic activity, is a weak PARP inhibitor (175) and >90% of PARP activity must be blocked to hamper DNA repair. This led to the development of first-generation PARP inhibitors(189), 3-aminobenzamide (IC_{50}=10μM)(190). This produced an off-target effect of impaired differentiation of lymphocytes and muscle cells denoting that this particular inhibitor was not specific enough (189). Further study on PARP inhibitors then

eliminated this property from the compound and (175) added specificity along with increased potency (190). Second generation PARP inhibitors include, benzimidazole-4-carboxamide NU1025 (175) with IC_{50}=400Nm (190) while third generation inhibitors include tricyclic lactam indole, (AG014699) and phthalazinones, AZD2281-Olaparib (175). These PARP inhibitors have benzamide and purine structures and are designed to compete with NAD+ at the enzyme active site. As they target NAD+ they also inhibit other members of PARP family like mono-ADP-ribosyl-transferases and sirtuins (189).

PARP is considered as an effective DNA repair inhibition target due to its synthetic lethality potential in tumours with defective HRR and cytotoxic effects resembling chemo-radiotherapeutics (160). PARP acts as a sensor protein and binds to SSBs and DSBs upon DNA damage. PARP activity enhances (500 times) in response to DNA damage and under normal condition this activity is minimal. PARP1 is involved in several key DNA repair pathways, such as base excision repair (BER), nucleotide excision repair (NER), mismatch repair (MMR) and repair of double-strand break through homologous recombination (HR) and alternative non-homologous end-joining (Alt-NHEJ). Therefore, inhibition of PARP1 results in global failure of DNA repair pathways and the repair the DNA lesions in tumour cells(190).

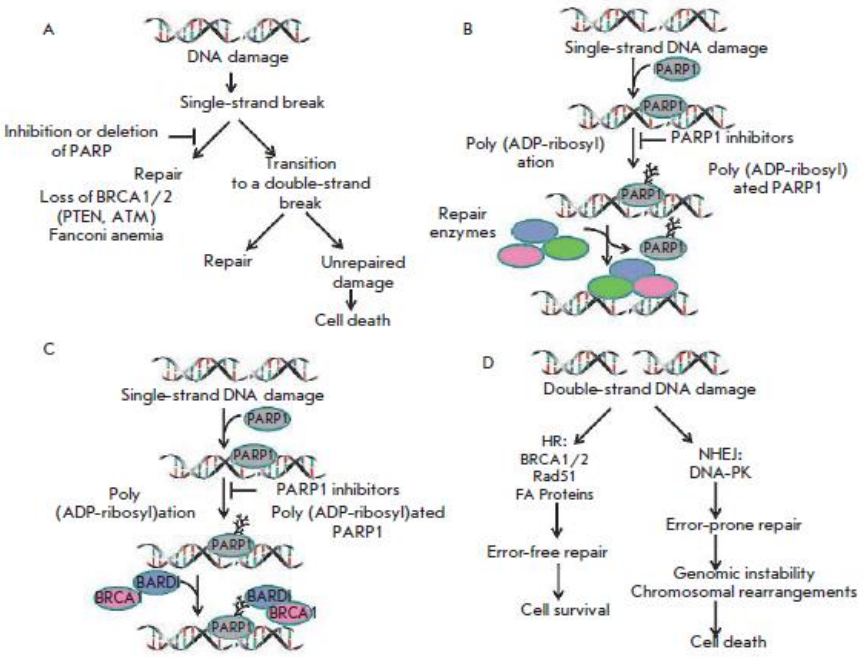

Figure-5.30. Direct cytotoxic effect of PARP1 inhibitors. *A*-blocking PARP1 results in failure of repair pathway and accumulation of SSBs which leads to the formation of DSBs *B* – due to inhibition of PARP1, PARP1 is attached to damaged DNA and cannot dissociate and clear area for PARP1-dependent repair enzymes. *C* – in the presence of PARP inhibitors, mutant BRCA1 is less accumulated at the DNA damage site D – when double-strand breaks occur in HR-deficient cells, NHEJ is activated resulting in errors in repair leading to genomic instability and cell death (192).

In 2005, synthetic lethality in tumours with hereditary mutations in HRR factors was observed with PARP inhibitors(190) (Figure-5.31). Synthetic lethality is the term used to describe when mutations in either of two genes have no effect individually but when combined results in cytotoxicity. This effect arises from gene-gene interaction, like two genes in the co-operating or same pathway where loss of both or one gene affect the stability of the pathway(191). Two groups showed the effect of PARP inhibitors in HRR defective cell lines and tumour xenograft or allograft. HRR is known as the 'error-free' double-strand break repair pathway and is frequently found to be defective in most tumours(160). Mutations in BRCA1 and BRCA2 genes are found in about 10-15% of ovarian cancers and these repair proteins function in HRR. HRR defects also arise from mutations in *RAD51*, *DSS1*, *RPA1*, or *CHK1* and tumours with these HRR defects are also sensitive to PARP inhibition(190).

When SSBs are induced in tumour cells, the principal pathway activated is base excision repair (BER) pathway(160). PARP1 inhibitors cause PARP1 to remain attached to the damaged DNA, hence preventing dissociation and hindering recruitment of repair proteins or scaffolding proteins in the BER repair process to the break site(190) (Figure-5.30B). This leads to the formation of DSBs upon collision with the replication fork (Figure-5.30A). DSBs attempt to activate the error-free homologous recombination (HRR) pathway, but it is defective due to mutation in several genes, mainly BRCA1 and BRCA2, thus DSBs cannot be repaired (Figure-5.30C). This, in turn, activates NHEJ, alternative NHEJ pathways, and single-strand annealing (SSA) repair process, delineating error in repair resulting in genomic instability and cell death(160) (Figure-5.30D).

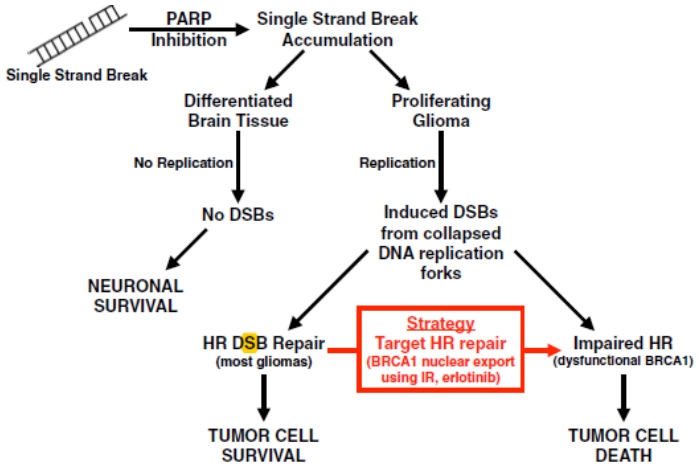

Figure-5.31. Synthetic lethality with PARP1 inhibitors in defective cells with Homologous recombination (HRR) repair (113).

Studies have shown that ionizing radiation, DNA methylating agents, and topoisomerase inhibitors activate PARP1; thus incentivizing the study of PARP1 inhibitors in combination with DNA damaging agents (189). Extensive preclinical studies have shown that PARP inhibition enhances the cytotoxicity of DNA damaging agents (methylating agents, topoisomerase inhibitors, alkylating agents) and ionizing radiation in tumour cell lines along with xenografts in a different type of tumours. This introduced PARP inhibitor (AG014699) to clinical trials along with DNA alkylating agent, temozolomide (160). Data from this trial verified that this combination reduces marrow suppression, a common effect seen with DNA alkylating agent. Reduction of this toxic effect is dose limiting when PARP inhibitor blocks pADPr synthesis by >90%. There are several ongoing clinical trials of PARP inhibitor with DNA damaging agents(Table-5.5) (190).

Temozolomide (TMZ) form SSBs(180) and PARP inhibitors prevents repair of these SSBs resulting in conversion to deleterious DSB which accumulate during replication(192). PARP inhibition enhances the cytotoxic effect of TMZ in the S phase of the cell cycle, denoting synergistic mechanism. PD128763 and NU1025 enhance the cytotoxic effect of TMZ by 4-7 times and with lower doses of TMZ, about 50-100 times compared to standard dose(190). Increased efficacy of TMZ has been reported (6 times) in 12 different human tumour lines (independent of p53 status)(192). Another PARP inhibitor, Velaparib, crosses the blood-brain barrier and has been reported to improve TMZ efficacy in human xenograft of the following tumours: lymphomas, ovarian, lung, pancreatic, breast, and prostate. Rucaparib has been seen to be useful in neuroblastoma and medulloblastoma xenografts in combination with TMZ (189).

Topoisomerase I inhibitors like camptothecin and topotecan inhibits topoisomerase preventing resealing of DNA strand. Unrepaired single-stranded DNA breaks are resolved by SSBR/BER during S phase(178). PARP1 localizes at the damage site and recruit other scaffolding proteins like XRCC1 and TDP1. Inhibiting PARP1 impairs this repair process and topoisomerase I continues forming single-stranded DNA breaks which are converted to lethal DSBs (stalled replication fork)(160), thus enhancing the cytotoxicity of TOPI inhibitors. Olaparib potentiated the toxicity of topotecan with a reduced dose by a factor of 8 while CEP-6800 enhanced irinotecan activity by 60% in mice with HT29 xenografts (190).

PARP inhibition enhances sensitization to ionizing radiation in actively replicating mammalian cells. Replication induced DSBs activates homologous recombination repair process which has been confirmed due to increased formation of γH2AX and RAD50 foci formation at stalled replication fork(160). This recovery of tumour cells after potentially lethal damage (PDL) is a key factor for radio-resistance. PARP1 inhibitors such as PD128763, NU1025, and AG14361 have been shown to prevent PLD in tumour cells. Velaparib improves radio-sensitization in a xenograft model of human colon, lung, and prostate cancers (190).

From these pre-clinical trials, it has been demonstrated that induction of PARP inhibition increases the efficacy of DNA damaging agents by two-fold and protected normal cells/tissues from toxic effects of anti-cancer therapy (192).

Name	Therapy	Tumors	CT phase
Rucaparib AG014699	Monotherapy	BRCA mutant lung cancer, ovarian cancer	2
Rucaparib	+temozolomide	Solid tumors, melanoma	2
Rucaparib	+carboplatin	Solid tumors	1
Olaparib	Monotherapy	Solid tumors, BRCA, TNBC/HGSOC carriers	2
Olaparib	+topotecan	Solid tumors	1
Olaparib	+dacarbazine	Solid tumors	1
Olaparib	+bevacizumab	Solid tumors	1
Olaparib	+paclitaxel	Ovarian Cancer	2
Olaparib	+paclitaxel	Stomach cancer	2
Olaparib	+cisplatin	Solid tumors	1
Veliparib ABT-888	Monotherapy	Solid tumors	1
Veliparib	+topotecan	Solid tumors	1
Veliparib	+carboplatin	Solid tumors	1
Veliparib	+temozolomide	Solid tumors, liver tumors, prostate cancer	2
Veliparib	+cyclophosphamide	Solid tumors and lymphomas	2
INO-1001	+temozolomide	Melanoma	1
MK4827	Monotherapy	Solid tumors and lymphoma	2
MK4827	+temozolomide	Ovarian cancer/glioblastoma	1
MK4827	+doxorubicin	Ovarian cancer/glioblastoma	1
CEP-9722	Monotherapy	Solid tumors	1
CEP-9722	+temozolomide	Lymphomas	1
BMN-673	Monotherapy	Solid tumors	1
Iniparib (BSI-201)	+gemcitabine +carboplatin	mTNBC	2
Iniparib	+gemcitabine +cisplatin	Lung cancer	2
Iniparib	+gemcitabine +carboplatin	mTNBC	3

Table-5.5. Clinical trials of PARP inhibitors (192)

b. ATM Inhibitors

Ataxia Telangiectasia Mutated (ATM) is a tumour suppressor and a sensor protein to DNA double-strand break damage(193). Activation of ATM starts a series of cellular responses, collectively known as the DNA damage response (DDR), where cell cycle arrest mediates detection of DNA damage leading to activation of specific DNA repair pathways to repair the lesion and cell cycle to be resumed. This sensor protein is frequently mutated in a variety of cancers (173) (lung, colorectal, breast, hematopoietic and brain cancer) (193) and tumour cells can use these active cellular mechanisms to repair any damage induced by chemotherapeutics. Thus, targeting ATM will block a plethora of cellular responses to repair damage leading them to cell death (173).

ATM inhibitors were first identified 15 years back and developed starting from non-specific compounds to selective inhibitors. Many of the inhibitors designed are now tested in pre-clinical studies(194). Caffeine has been found to be an ATM inhibitor. It is a methylxanthine which inhibits ATM and ATR. Studies have shown that caffeine sensitizes tumour cells to ionizing radiation and is more effective in p53 deficient tumours. Wortmannin is another drug in this class which impedes PI3K family members including ATM/ATR. Wortmannin has also been described as a radiosensitizer in the literature(193). KU-55933 is originally an ATP inhibitor but selectively inhibits ATM with low cytotoxicity. It sensitizes cells to ionizing radiation along with other DNA damaging agents like camptothecin, etoposide, and doxorubicin. Along with these drugs, there are several other compounds that have been designed as potent ATM inhibitors; being verified in laboratories against a variety of tumours(187) (Table-5.6).

Compound	Enzymatic activity	*In vitro* selectivity	*In vitro* efficacy	Pharmacology	*In vivo* activity	Development stage
Wortmannin	IC_{50} = 150 nM (irreversible)	–	R+/–	– (toxicity)	N.D.	Discontinued at optimisation stage
Caffeine	IC_{50} = 0.2 mM	–	R+/–	– (toxicity)	N.D.	Discontinued at optimisation stage
KU55933	IC_{50} = 12.9 nM K_i = 2.2 nM	+	R+/– C++	– (solubility, distribution)	N.D.	Discontinued at research stage
KU59403	IC_{50} = 3 nM	++	C+	+	+	Preclinical stage
KU60019	IC_{50} = 6.3 nM	++	R+ C+	+	+	Preclinical stage
CP-466722	IC_{50} = 20 nM	+	M+ R+	– (stability)	N.D.	Research stage
1	N.D.	++	R+	+	N.D.	Research stage
CGK733	N.D.	–	M+/–	N.D.	N.D.	Optimisation stage
NVP-BEZ235	N.D.	–	M+ R++ C+	+/–	+	Clinical trials[a] phase II
Torin-2	IC_{50} = 28 nM	–	M– R+ C++	+	+	Preclinical stage
2	IC_{50} = 0.6 nM	++	C++	+	++	Preclinical stage
SJ573017	IC_{50} = 0.48 μM	–	M++ R+ C+	N.D.	N.D.	Optimisation stage

Selectivity: "–": non-selective (<2 fold); "+/–": moderately selective (2–50 fold); "+": selective (50–100 fold); "++": very selective (>1000 fold). ***In vitro* efficacy**: "M": monotherapy, as a single agent; "R": radiosensitizer; "C": chemosensitizer; "–": inefficient (IC_{50} > 30 μM as single agent or sensitization ratio < 1.2 fold); "+/–": moderately active (2 μM < IC_{50} < 30 μM as single agent or sensitization ratio: 1.2–2 fold); "+": active (100 nM < IC_{50} < 2 μM as a single agent or sensitization ratio: 2–10 fold); "++": very active (IC_{50} < 100 nM as single agent or sensitization ratio > 10 fold). **Pharmacology**: "–": poor, main issues in brackets; "+/–": moderate, main issues in brackets; "+": good. ***In vivo* activity**: "+/–": moderate

Table-5.6. Properties of ATM inhibitors involved in clinical trials (196)

c. DNAPK Inhibitors

Non-homologous end joining (NHEJ) is considered one of the major DSB repair pathway in mammalian cells(135). It resolves 75% of DSBs in proliferating cells. NHEJ is divided into two sub-pathways; classical NHEJ (C-NHEJ) (DNA-PK-dependent pathway) and alternative NHEJ (Alt-NHEJ) (PARP1 dependent pathway)(188). NHEJ has a variety of repair components involved such as a nuclease, polymerase, and ligase activities; allowing a broad spectrum of DNA-end substrate configurations that may arise at a DSB site. This makes NHEJ pathway a prime target for anti-cancer therapy; enhancing tumour sensitivity to DSB inducing agents(188).

DNA-PK is the sensor and central DNA repair protein of this pathway(135) and previously it has been demonstrated that loss of this protein increases tumour sensitivity to ionizing radiation and chemotherapies, due to inefficient DSBs repair(195). DNA-PK inhibitors were designed to target

the ATP-binding site of the kinase catalytic subunit DNA-PKcs. Due to overlapping functional capabilities of DNA-PK with other PI3K proteins and poor pharmacokinetics being another challenge, proving to be difficult to design specific and selective DNA-PK inhibitors(196).

The first inhibitor to be designed and developed was Wortmannin which is a non-competitive inhibitor of PI3K that target both DNA-PK and ATM. It irreversibly alkylates Lys802 in the ATP-binding site of DNA-PKcs but due to lack of specificity and poor solubility, this compound was not approved for clinical trials. Later NU7026 was designed which is a competitive inhibitor having 60-fold selectivity towards DNA-PK(197). This inhibitor enhances the cytotoxicity of other DNA damaging agents like topoisomerase II poisons (used in leukemia), idarubicin, daunorubicin, doxorubicin, etoposide, amsacrine, mitoxantrone but not camptothecin or cytosine arabinoside(188)(197).

5.4.4.6. Drug resistance

Drug resistance is a major problem in cancer therapeutics as it reduces the pharmacological effects of the drug, preventing from exerting its effect on tumour cells. Drug resistance can be acquired during therapy by the drug itself or prior to treatment(198). Tumour cells were heterogeneous in nature, making it more challenging (199). Acquired resistance with results in cross-resistance among drugs with different mechanism of action limiting treatment options. Resistance is common and develops over time with 90% treatment reducing the survivability significantly in cancer patients. Treatment failure leads to metastatic cancer and development of resistant micro-metastatic tumour cells among patients (198). Along with heterogeneity between and within tumour cells, there are several other factors for drug resistance, such as increased drug efflux and decreased drug influx, drug inactivation, alterations in drug target, DNA damage repair and evasion of apoptosis (198)(199).

a. Role of Tumour Heterogeneity

Instability or disruption in cellular processes and mutation in tumour suppressor and oncogenes activate oncogenic pathways while inactivating tumour suppressors lead to tumour initiation and progression (200). Transformed cells continue to evolve into more dynamic malignant form even after complete transformation giving rise to a heterogeneous population with distinct molecular features and disparity in chemotherapeutic sensitivity (199). The heterogeneous population may arise from genetic, transcriptomic, epigenetic or phenotypic deviations (Figure-5.32). There are

two major types of heterogeneity observed among tumour cells, such as intratumoral and intertumoural heterogeneity (200). Intratumoral heterogeneity is amongst tumour cells in a common individual and arises due to dynamic genetic alterations in tumour cells over time, whereas intertumoural heterogeneity is between tumour type arising due to genetic variations, differences in somatic mutation profile and environmental factors (199)(200).

Increased mutation rate is a common phenomenon in cancer forming genetically-diverse tumour cell populations, giving rise to clonal evolution. Clonal evolution has been related to tumour progression in a branched or linear fashion (200), both denoting clonal diversity and adding further genetic heterogeneity within tumours (through further mutations). This intertumoural heterogeneity is responsible for phenotypic differences during tumour progression, thus chemotherapeutic resistance (199).

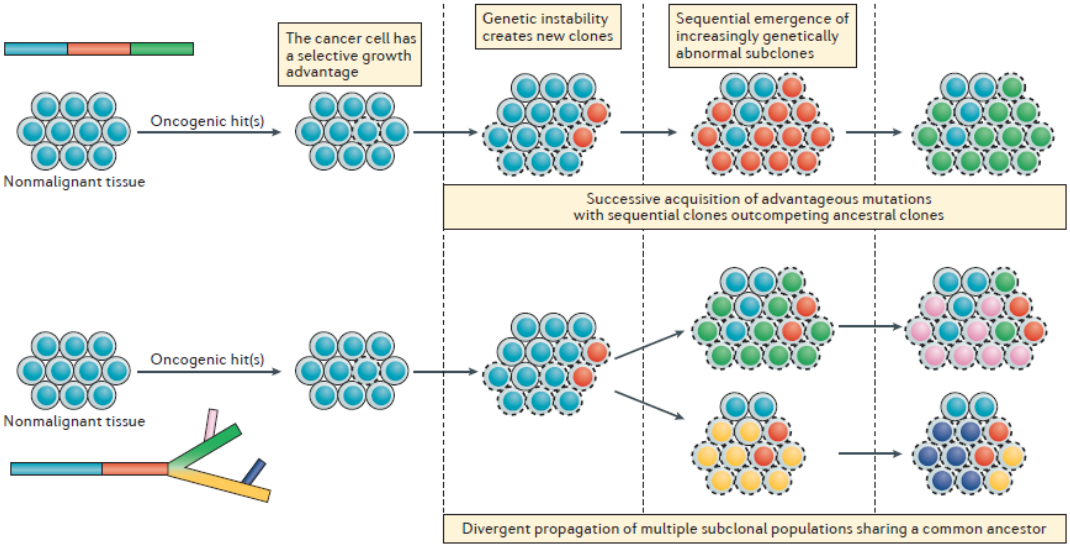

Figure-5.32. Linear and branched tumour evolution. For clonal evolution tow types of evolution, the manner as described (a) the linear evolution where the successive acquisition of advantageous mutations with sequential clones outcompete ancestral clones (b) branched evolution where the divergent progression of multiple sub-clonal populations shares a common ancestral clone (200).

b. Multidrug resistance (MDR)

Multidrug resistance (MDR) is a common phenomenon with anti-cancer therapeutics(201) between the cell line and human tumours(202). MDR is described as resistance among drugs with discrete structure and mechanism of action(201). MDR is related to increased drug efflux from the cells through transporters like ABC transporters such as P-glycoprotein (P-gp) and MDR-

associated protein (MRP)(202). Alterations in these transporter mechanisms are associated with multi-drug resistance. These transporters efflux drugs out of cells before they can exert their pharmacological action. Hydrophobic drugs are usually the main target, like taxanes, anthracyclines and vinca alkaloids. DNA damaging agents like Topoisomerase I inhibitor, irinotecan (CPT-11) along with its active metabolite SN-38, cisplatin and methotrexate are targets for the ABC transporter protein (198).

P-glycoproteins are found on plasma membranes of tumour cells and its overexpression of this transport protein mediates resistance to vinblastine, vincristine, doxorubicin, daunorubicin, etoposide, teniposide, and paclitaxel. P-gp overexpression has been reported in colon, kidney, adrenal cancer and in some solid tumours. Several factors trigger the increased activity of MDR1 such as anticancer drugs, DNA-damaging agents, heat shock, serum starvation and ultraviolet irradiation, as well as tumour progression (mutation of p53 and RAS activation)(202).

Transport protein inhibitors have been developed to counter drug resistance; p-gp inhibitors such as cyclosporin (first generation), valspodar (PSC-833) (second generation), tariquidar and zosuquidar (third generation). First generation drugs were not approved for trials due to unacceptable toxicities while the second generation had erratic pharmacokinetic interactions(198). Third generation drugs are highly specific for P-gp with high potency and are in phase III of a clinical trial. These drugs are being tested in combination with chemotherapeutics for therapeutic benefit (202).

c. Drug inactivation

Inactivation of drug reduces the efficacy of chemotherapeutics towards tumour cells by plummeting the amount of free drug in plasma (198), hence a reduced amount of drug reaches its target which is not enough to exert its pharmacological effect (202). Most of the drugs are inactivated by cytochrome P450 family of enzymes such as CPT-11, irinotecan (topoisomerase I inhibitor). The enzymes inactivate the prodrug along with its active metabolite, SN-38. This metabolite is subjected to glucuronidation by uridine diphosphogluronysl transferase 1A1 (UGT1A1)(203). Carboxylesterase (CE) converts CPT-11 into active metabolite SN-38 and level of CE in tumour cells confers CPT-11 sensitivity. This reduction in metabolite activation results in drug resistance (198)(203).

d. Drug targets

Mutation or alteration in drug targets such as receptors or enzymes results in drug resistance (202). Irinotecan (CPT-11) is a topoisomerase I inhibitor and its active metabolite SN-38 targets DNA topoisomerase I (TOPI). TOPI relaxes the supercoiled DNA during DNA transcription and replication by forming DNA nicks in one strand of DNA while passing the other strand through cleavage site and then re-ligating the cleaved complex (179). Topoisomerase I inhibitors stabilize cleavage complexes by blocking re-ligation of the cleaved strand, thereby; forming single-stranded DNA breaks. These single-stranded DNA breaks convert into lethal DSBs. It has been reported that in CPT-11 resistant colon cancer cell lines, there is a downregulation in TOPI mRNA(178). In several studies, mutations in TOP1 have been correlated with CPT-11 sensitivity in different colon cancer cell lines. Like TOPI, a mutation in TOPII enzyme activity leads to resistance towards for anthracyclines such as doxorubicin and epipodophyllotoxins such as etoposide (198).

e. DNA damage repair

DNA damaging agents are designed to directly exert its cytotoxicity to DNA with the notion of tumour cell death. The DNA damage signaling pathway halts the cell cycle in response to DNA damage through induction of the cell cycle checkpoint thus allowing time for repair; if the damage is too extensive then cells undergo apoptosis (135). Tumour cells have adapted the ability to induce hyperactive DNA repair mechanisms in comparison to normal cells through mutations/alteration in DNA damage response (DDR) and DNA repair components (113). Tumour cells use different DNA repair pathways along with alternative and redundant processes to resolve different types of damage induced by different DNA damaging agents, conferring chemotherapeutic resistance (196).

The ability of tumour cells to repair damage determines resistance to DNA damaging agents(202) that induce damage directly such as platinum drugs (cisplatin) or indirectly such as topoisomerase poisons(198). The platinum-based DNA adducts are resolved by nucleotide excision repair (NER) and this pathway is hypersensitive to cisplatin-induced damage. The NER repair process requires the involvement of 17 different enzymes to orchestrate proper repair; alterations in few of these components increases the tumour cell's capacity for NER(204). DNA repair pathway components represent suitable therapeutic targets in cancer(203).

To combine DNA damaging agents with DNA damage repair protein inhibitors has become one strategy for effective cancer therapy: to increase sensitization of DNA damaging agents in tumour cells(205). But this also brings the possibility that inhibition of one pathway may enable tumour cells to become dependent and upregulate alternative repair processes that are functionally redundant in normal cells(203). This phenomenon enables a synthetic lethality strategy to specifically target the redundant tumour-specific pathway (160).

Another example of resistance developed in DNA repair is of temozolomide (TMZ) (206). This drug adds methyl adducts at N7 guanine (70% of adducts), O6 guanine (5% of adducts) and N3 adenine (9% of adducts) but exert its cytotoxicity mostly through methylation at the O6 position of guanine(206). This O6 methylguanine pairs with thymine during replication activating mismatch repair process(206). Resistance to temozolomide has been reported in many cases and studied extensively. From several studies, two mechanisms of resistance evolved, 1. overexpression of the DNA repair protein, O6-alkylguanine-DNA alkyl transferase and, 2. deficiency in the DNA mismatch repair pathway, thus; developing tolerance to O6 methylguanine and allowing tumour cells to survive even in presence of consistent DNA damage(203).

6.1. Programmed cell death (PCD)

Programmed cell death (PCD) plays (207) a critical role in deciding a cell's fate(208) and occurs during organ development. There are several cellular processes by which cell death take place in mammalian cells from different stimuli like chemotherapeutics, ionizing radiation, growth factor deprivation and endoplasmic reticulum (ER) stress. There are three major types of programmed cell death; apoptosis (type I), autophagy (type II), and necrosis (type III). Apoptosis, also known as Type I PCD (207) is characterized by morphological changes (209) in cells such as nuclear condensation and fragmentation (208), cell shrinkage, loss of adhesion with surrounding cells and membrane blebbing. Apoptosis is mediated through activation of caspases and genotoxic stress activates apoptotic pathway which may be caspase-dependent or independent pathway (209).

Type II PCD is known as autophagy (207) which is triggered by inhibition of apoptosis (209) and is characterized by autophagosomes, double membrane-bound structures surrounding cytoplasmic macromolecules and organelles (208). During stress due to growth factor deprivation, autophagy plays a vital pro-survival role in maintaining cell homeostasis. It has been shown that autophagy controls cellular processes such as starvation, cell differentiation, cell survival and death (208).

Necrosis is denoted as the Type III PCD (207) with hallmarks such as cell swelling, organelle dysfunction, and cell lysis. This type of cell death process plays a vital role in the preservation of tissue homeostasis and elimination of damaged cells (having an effect on tumour cells) (208). Necrosis triggers inflammation and this cellular event can be programmed or accidental. Necrotic cell death occurs due to DNA damage in terms of reactive oxygen species, activation of poly(ADP-ribose) polymerase-1 (PARP-1) and Jun N-terminal kinase (JNK) in cell death(Figure-6.1) (209).

6.2. DNA damage and Apoptosis

DNA damage is a common phenomenon that occurs regularly, and cells have developed robust repair mechanisms to counter damage induced by various exogenous and endogenous factors (210). Cells have developed two approaches to deal with DNA damage, first to repair the DNA damage and second, is to eliminate the cell by activating cell death process, if the damage is too extensive to be repaired with full genomic integrity (211). Unresolved DNA damage is harmful to cells since it causes mutations along with chromosomal alterations leading to tumorigenesis and malignant transformation. Both these safeguards involves cellular and molecular mechanisms (211).

The DNA damage response (DDR) detects DNA damage and halts cell cycle progression by activating cell cycle checkpoints to properly resolve the damage via specific DNA repair pathways. After repair, cell cycle progression is resumed(20). In parallel, cellular death mechanisms play an important role. Cell death following DNA damage is not due to gene inactivation but rather a series of enzymatic reactions resulting in apoptosis, necrosis, autophagy and other forms of cell death (Figure-6.1) (211).

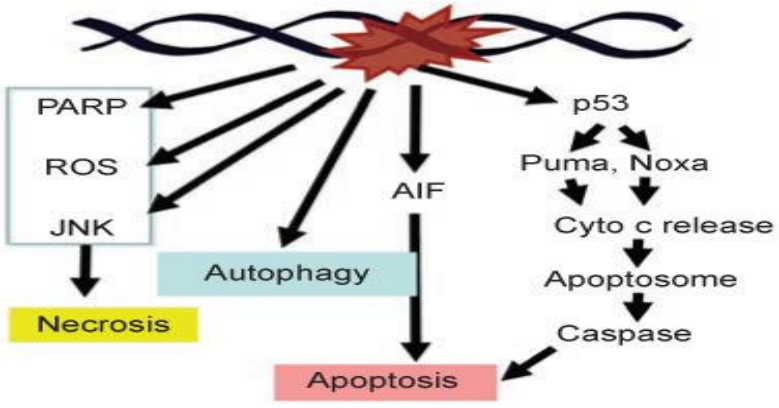

Figure-6.1. DNA damage-mediated cell death pathways. DNA damage induced DNA fragmentation triggers apoptosis through activation of caspases or through nuclear translocation of AIF. Necrotic cell death can be triggered

through production of reactive oxygen species (ROS), sustained activation of Jun-N terminal kinase (JNK) and activation of poly (ADP-ribose) polymerase 1 (PARP1) in response to DNA damage (210).

Most DNA damage-induced cell death results in an apoptotic response. This connection between DNA damage and apoptosis has been studied extensively and supported in literature. The link between DNA damage and apoptosis is mediated by the tumour suppressor, p53. Correlation between this two cellular mechanism involves a series of events including detection of lesion-sensors (MMR), signal transducers (ATM) and transcription regulation (p53, p73) (Figure-6.2) (210). The p53 mediated response to protect the cell or organism triggers another secondary response to growth arrest, therefore cells have a choice between p53-dependent growth arrest or p53-dependent apoptosis (212).

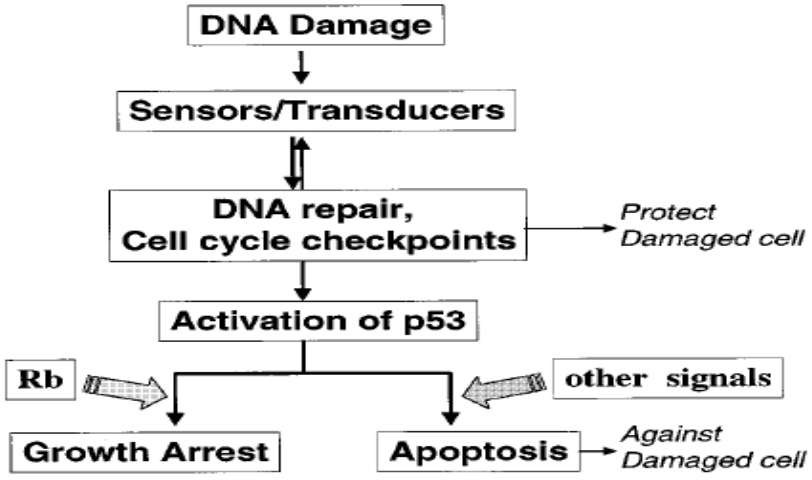

Figure-6.2. Correlation between DNA damage response and apoptosis. DNA damage induced p53 activation leads to cell cycle arrest for cells to repair the damage induced or the cell hits p53 mediated apoptosis in case of severe damage. (211)

6.3. p53-dependent apoptosis in response to DNA damage

Induction of DSBs via ionizing radiation activates MRN complex which acts as a sensor protein and reaches the DSB site. This, in turn, phosphorylates ATM which localizes to break site and phosphorylates effector proteins like CHK2, H2AX, BRCA1, NBS1, and MDM2 (211). ATM phosphorylates the ubiquitin protein, MDM2 which detaches itself from p53, thus activating the tumour suppressor, p53. p53 is phosphorylated by both Chk2 and ATM during DDR promoting cell cycle arrest in G1 phase by inducing expression of p21/waf1, a Cdk2 inhibitor, resulting in

cell cycle arrest (Figure-6.4b) (119). p53 is also a transcription factor and is responsible for expression of genes involved in apoptosis (NOXA, PUMA, BAX) like in the hematopoietic system, it induces apoptosis rather than cell cycle arrest(Figure-6.3b)(120). ATR is activated upon damage induced by UV and DNA damaging agents forming stalled DNA replication forks. ATR signals p53-mediated apoptosis through phosphorylation of CHK1(211) (Figure-6.4b).

Halting cell cycle mediated via ATM-ATR-p53 signaling gives time for cells to repair DSBs through activation of DSB repair pathways, Non-homologous end joining (NHEJ) and Homologous Recombination (HR) (118). Thus, repair of DSBs acts as an anti-apoptotic mechanism in terms of DNA damage (211). HR repairs damage during DNA replication phase of cell cycle (S/G2 phase) and NHEJ repairs damage at any phase denoting itself as the error-prone repair process(119). The repair pathways are activated depending on which phase the DSBs were formed. As mentioned above, NHEJ is the error-prone process and has been found to be involved in the generation of chromosomal rearrangement, genetic alterations hence DSBs repaired via NHEJ induce errors in cells and as a result cell death signals are stimulated (apoptosis) (Figure-6.4c) (211)(113).

At low DSB levels, a minor fraction of p53 is enough for p21 upregulation and cell cycle arrest (Figure-6.3b) (211). At a high level of DSBs, p53 activation and accumulation reaches a threshold which results in activation of proapoptotic genes (211) such as, BAX (BCL2-associated X protein), PUMA (p53 upregulated modulator of apoptosis) and First apoptotic signal (FAS) receptor(Figure-6.3a) (209). This proves that ATM-ATR-p53 mediated cellular responses are required to trigger DNA damage-induced apoptosis (212). However, this scenario differs among cell types such as cells with mutated ATM are more sensitive to ionizing radiation but is less prone to apoptosis compared to normal cells; thymocytes from ATM knockout mice show similar response to ionizing radiation as ATM mutated cells, but fibroblasts lacking p53 are more sensitive to UV-induced DSB-induced apoptosis compared to wild-type (211)(212). This indicates that not all cells types require p53 to trigger DSB-induced apoptosis, but that p53 activation may stand against it (212).

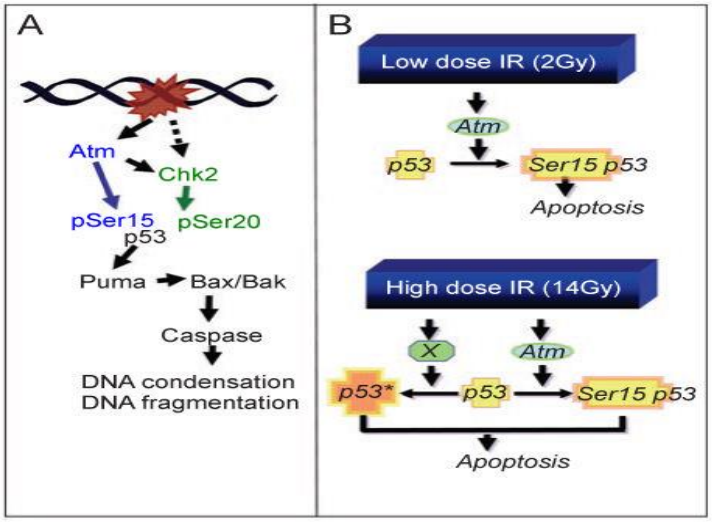

Figure-6.3. Role of ATM/p53 in IR induced apoptosis. (a) ATM directly and indirectly phosphorylates p53 through Chk2 kinase. Chk2 phosphorylates p53 at Ser 20 which mediates apoptosis through PUMA, BAX/Bak and caspase (210)

Cisplatin-induced DNA damage forms interstrand crosslinks that block DNA transcription and replication (213). These damage result in sustained activation of the c-Jun N-terminal kinase (JNK) and p38 kinase which in turn cause long-term activation and expression of activator protein-1 (AP-1)(209). It has been seen that high-level pf AP-1 triggers JNK and p38 mediated apoptosis in cells(212); JNK and p38 inhibitors show a reduction in cisplatin-induced apoptosis and cells treated with TPA (12-O-tetradecanoyl phorbol-13-acetate) enhanced cisplatin-induced apoptosis via activation of ERK (extracellular signal-regulated protein kinase) pathway mediated through PKC (protein kinase C) activation. Suramin, an EGF-receptor antagonist has also been seen to inhibit cisplatin-induced apoptosis(211). AP-1 transcriptionally activates FAS-L leading to activation of caspase 8. Sustained activation of caspase 8 accumulates caspase-cleaved products (Bid to tBid). These cleaved components activate caspase 3 and caspase 9 triggering apoptosis(212) (Figure-6.4a).

6.4. p53-independent apoptosis in response to DNA damage

DNA damage by DNA damaging agent like topoisomerase inhibitor (camptothecin, etoposide), activates ATM/ATR which phosphorylate CHK1 and CHK2(118). This phosphorylation event activates the transcription factor, E2F1 which triggers transcription of p73. p53 is required for p63 and p73 mediated apoptosis (although p73 is proapoptotic in absence of p53)(211). p73 mediated apoptosis includes upregulation of PUMA which stimulates BAX mitochondrial translocation, along with cytochrome c release resulting in apoptosis through activation of caspase 9 and caspase

3(212) (Figure-6.4d). p73 also stimulates transcription of NOXA which is involved in mitochondrial dysfunction. p73 is found to be overexpressed in tumours and so tumour cells are prone to be susceptible to DNA damaging agents even in absence of functional p53 (211).

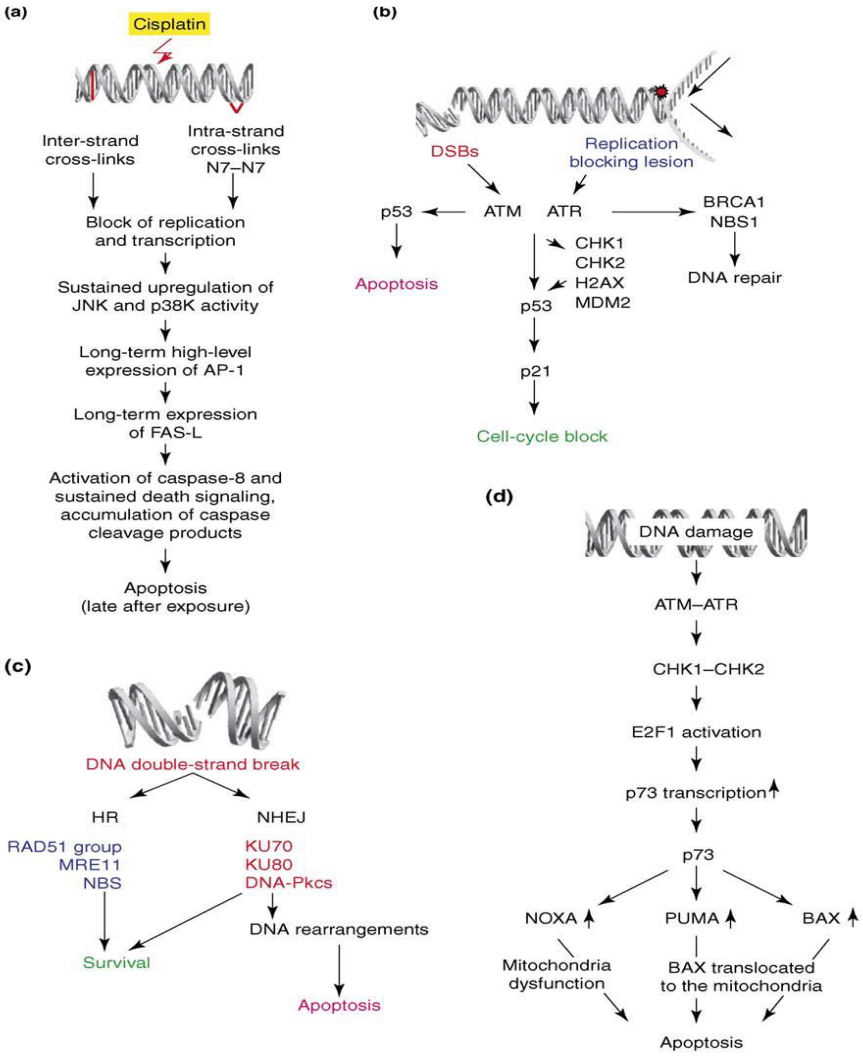

Figure-6.4. p53 dependent and independent apoptosis in response to DNA damage. (a) Cisplatin-induced apoptosis (b) Activation of ATM or ATR in response to DSBs (c) DSBs repair by HR and NHEJ resulting in survival or apoptosis (d) Mechanism of p53-independent apoptosis(212)

There are several processes that trigger p53 independent apoptotic signals like NF-kB (nuclear factor-kB), which is anti-apoptotic but in certain cases, it functions as a pro-apoptotic factor. Apoptosis in Jurkat T cells takes place due to transcriptional activation of FAS ligand-mediated by reactive oxygen species through NF-Kb pathway (211). The apoptotic signal is stimulated through the BCL-2 family of protein where degradation of BCL-2 takes place as phosphorylation of BCL-2 at Ser87 by MAP kinase protect cells against apoptosis (212).

6.5. Apoptotic signaling pathway

Anti-cancer therapeutics induce apoptosis to tumour cells by two mechanisms, death receptor-dependent (extrinsic) and death receptor-independent (intrinsic) pathway. Death receptor pathway includes stimulation of death receptors like Fas and TRAIL receptors (DR4, DR5)(207). Activation of death receptors mediates recruitment of Fas-associated death domain and procaspase 8 to death receptor forming death-inducing signal complex resulting in activation of caspase 8. Activation of caspase 8 activates caspase 3 resulting in apoptosis (Type 1 cell death)(209).

The death receptor-independent pathway (mitochondrial-dependent pathway) comprises of cleavage of Bid (proapoptotic protein) by caspase 8 to truncated Bid (tBid) in mitochondria. Cytochrome c is released from mitochondrial due to heterodimerization of tBid and Bak resulting in activation of caspase 9 and caspase 3 (type 2 cell death)(212)(209).

6.5.1. Activation of caspase-dependent apoptosis by DNA damage

Caspase 2 is the only procaspase that resides in the nucleus and is activated in etoposide-, cisplatin- and UV-light-induced apoptosis(209). The caspase 2 pathway is redundant in certain cell types and acts as a backup process for p53-dependent apoptosis. Caspase 2 is activation is stimulated upon Endoplasmic reticulum (ER) stress and reactive oxygen species (ROS)(214)(Figure-6.5). Caspase 2 is activated by PIDDsome complex or Disc (through caspase 8) and activated caspase 2 cleaves Bid to its truncated form, tBid(207). This action results in MOMP (major out membrane protein) and cytochrome c release from mitochondria. Cytochrome c is released from mitochondrial due to heterodimerization of tBid and Bak resulting in activation of caspase 9 and caspase 3(Figure-6.5) (215).

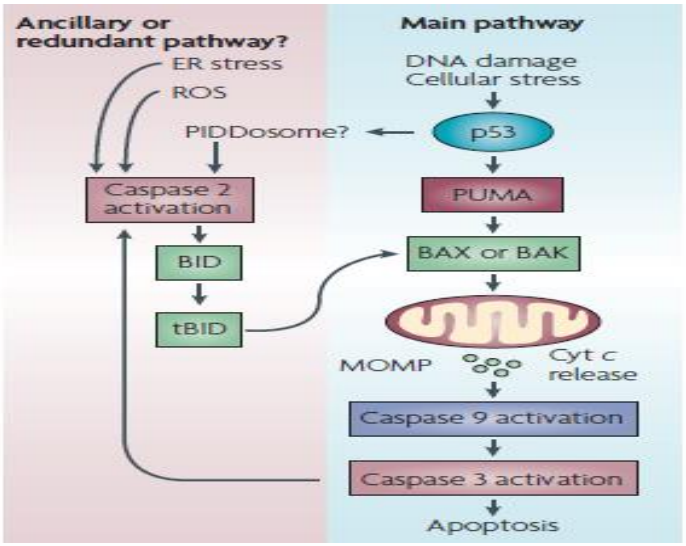

Figure-6.5. Caspase 2-mediated apoptotic pathway. In response to DNA damage, p53 activates cell death through the BH3-only protein p53 upregulated modulator of apoptosis (PUMA, also known as BBc3) and BAX/BAK activation, leading to mitochondrial outer membrane permeabilization (MOMP), cytochrome c (cyt c) release, formation of the APAF1 apoptosome, which in turn activates caspase 9, initiating the caspase activation cascade. In an alternative pathway caspase 2 acts upstream of MOMP and is activated by complexes such as the PiDDosome or Disc (through caspase 8). Once activated caspase 2 cleaves and activates BiD and this causes MOMP and cyt c release. Caspase 2 has also been shown to mediate the apoptosis induced by reactive oxygen species (ROS) and endoplasmic reticulum (ER) stress. The caspase 2 pathway is therefore likely to be redundant in some cell types, or it may function as an ancillary or backup mechanism of p53-dependent apoptosis in other cell types (215)

Studies have shown that there is a link between cell cycle and cell death through caspase 2(215). Caspase 2 is involved in regulation of cell cycle with the association between caspase 2 and cyclin D3 which stabilizes caspase 2 itself(214). Upon DNA damage and formation of DSBs, DSB repair pathway Non-homologous end joining (NHEJ) is activated. This repair pathway requires DNAPKcs which is a key DNA repair protein complex for resolving DSBs(212). In response to DSBs caspase 2 is activated by phosphorylation at S122 by DNAPKcs. This phosphorylation of caspase 2 is stimulated by the death domain receptor, PIDD(215). Caspase 2, p53 death domain protein 1 (PIDD) and DNAPKcs forms a nuclear complex called DNA-PKcs–PIDDosome where DNAPKcs acts as the adaptor protein for PIDD recruitment(214). PIDD binds with the N-terminal region of DNA-PKcs through its death domain(214). This active caspase 2 was seen to be involved in G2/M cell cycle arrest and DNA repair by non-homologous end joining (NHEJ)(212).

Caspases are responsible for DNA fragmentation and this is mediated through ICAD (Inhibitor of caspase-activated DNAase). ICAD causes activation of CAD (caspase-activated DNAase) from DFF (DNA fragmentation factor) complex through its caspase-mediated cleavage at D117 on N-terminal and cleavage at D224 on C-terminal retains CAD inhibitory function (usually mediated through caspase 3)(216). Caspase 3 cleaves Poly(ADP-ribose) polymerase (PARP) which is involved in DNA repair and maintenance of genomic integrity. PARP cleavage blocks DNA repair during apoptosis(217).

6.5.2. Activation of caspase-independent apoptosis by DNA damage

In response to death stimuli/apoptotic signals, toxic chemicals are released from intermembrane space of the mitochondria stimulated by permeabilization of the outer mitochondrial membrane(217). Proapoptotic Bcl-2 family proteins like Bax and Bak are activated to control outer mitochondrial membrane permeabilization. This process is also prevented by heterodimerization of Bcl-2 and Bcl-XL with Bax-like proteins(216). Other Bcl-2 proteins with a BH3 domain like Bad, Bid, Bim, Bmf, and Noxa hinders the inhibitory effect of Bcl-2 or Bcl-XL or activates Bax-like proteins(217). Cytochrome c is released from mitochondrial along with other proteins such as DNA Endonuclease G (EndoG, released by Bcl-2 family proteins) and Apoptosis-inducing factor (AIF) (Figure-6.6). Both proteins trigger apoptosis in a caspase-independent manner(212). Pro-apoptotic mitochondrial serine protease, A2 (HtrA2)／Omi is also involved in caspase-independent apoptosis and is released from mitochondrial upon death stimuli(217). HtrA2 accumulates in the nucleus upon damage which then activates transcription factor p73 through its serine protease activity. P73, in turn, activates pro-apoptotic genes such as Bax which then mediates apoptotic process(216)(217).

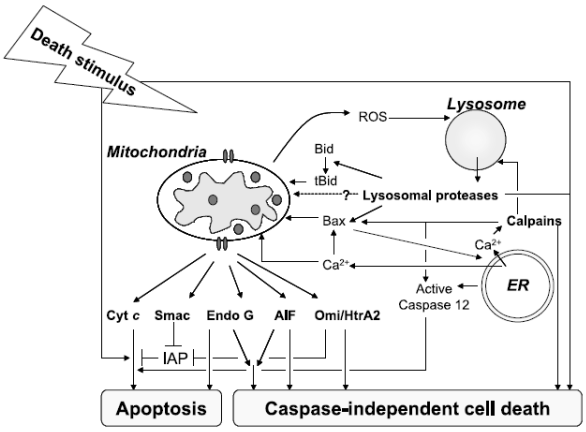

Figure-6.6. Caspase-independent cell death pathways (218)

II. Rational, Hypothesis and AIMS

a. Rational & Hypothesis

CNS tumours are known to be the most aggressive and lethal to individuals. Although brain tumours comprise a small percentage (~2%) of all cancer types but account for a high degree of cancer mortality with a survival time as 9 months to 5 years. Current methods to treat medulloblastoma (MB) and malignant glioma (MG) are highly intrusive leading to poor quality of life. Recurrence of these malignant tumours is pervasive due to resistance to anti-cancer therapeutics including activation and/or up-regulation of DNA repair pathways that resolve DNA damage elicited by chemoradiotherapeutics. We are targeting DNA repair pathways to enhance chemoradiotherapeutic strategies against MB and MG. DNA repair inhibitors like Poly (ADP-Ribose) Polymerase (PARP1i), DNA-dependent protein kinase (DNA-PKi) and Ataxia-Telangiectasia Mutated (ATMi) sensitize tumours to DNA damaging agents. In combination with chemotherapeutics, these sensitizers can significantly augment treatment success. However, differing tumours have variable expression of these enzymes, therefore; their identification and inhibition may enhance current treatment efficacy.

b. Hypothesis: Specific DNA repair enzymes are up-regulated in alternate DNA repair pathways in brain tumour cells that promote resistance to conventional DNA damaging therapeutics agents. Identification and inhibition of these repair enzymes will better sensitize tumour cells to such therapeutics thus overcoming chemo-radio resistance and enhanced tumour cell death.

c. Aims

This work will be carried out using three specific aims-

Aim-1. To develop novel high-throughput DNA damaging assay, Trevigen Comet Assay.

Aim-2. (a) Using the high-throughput comet assay to test cell lines of both tumours (MB & GBM) with DNA damaging agents and radiation in presence/absence of different DNA repair inhibitors.

(b) To select potential treatment combinations and cell lines for further analysis

Aim-3. Identify differentially expressed tumour-specific DNA repair enzymes via gene expression analysis (RNA-seq)

III. MATERIALS and METHODS

7.1. Reagents

Most chemicals were purchased from Sigma-Aldrich and ThermoFisher unless otherwise stated.

7.2. Cell culture Media

Dulbecco's Modified Eagle Media-high glucose (DMEM) was purchased from SIGMA-ALDRICH, Life Sciences and stored at 2-8 °C. Prior to use, the media was supplemented with 10% Fetal Bovine Serum (FBS) (Thermo-Fisher), 1% Penicillin/Streptomycin (10,000 units/ml Penicillin, 10,000µg/ml Streptomycin) (Life Technologies), 1% GlutaMax (200mM) (Life Technologies)/ Glutagro-L-ananyl-glutamine (200 mM) (VWR) and pre-warmed to 37°C.

7.3. Cell lines

Human brain tumour-derived cell lines were used for this study. Glioblastoma (GBM) lines, U251MG (Mesenchymal subtype) & U373MG are originally from Sigma-Aldrich (Saint Louis, MO) and these lines grow as adherent 2-D monolayers. Medulloblastoma (MB) lines, DAOY (Sonic Hedgehog, Shh) & D283MED (Group 3) are originally from ATCC. DAOYMB grow as flat adherent cells whereas D283MED cells are semi-adherent and grow in cell clusters. Hela cells are originally from ATCC and these cells grow as adherent 2-D monolayers. All the cell lines were cultured in DMEM (Sigma-Aldrich) supplemented with 10% Fetal Bovine Serum (FBS) (Thermo-Fisher), 1% Penicillin/Streptomycin (10,000 units/ml Penicillin, 10,000µg/ml Streptomycin) (Life Technologies), 1% GlutaMax (L-alanyl-L-glutamine, 200mM) (Life Technologies).

Primary Human Fibroblasts are from the Coriell Institute for Medical Research (Camden, USA) and these cells grow as adherent 2-D monolayers. These cells were cultured in DMEM (Sigma-Aldrich) supplemented with 15% Fetal Bovine Serum (FBS) (Thermo-Fisher), 1% Penicillin/Streptomycin (10,000 units/ml Penicillin, 10,000µg/ml Streptomycin) (Life Technologies), 1% GlutaMax (200mM) (Life Technologies). All cell lines were cultured in a humidified atmosphere in presence of 5% CO_2 at 37°C. All cells were passaged and detached using Trypsin-EDTA Solution (0.5g porcine trypsin and 0.4g EDTA, 100ML) (Sigma-Aldrich, USA).

GBM	MUTATIONS
U251	TP53, PTEN
U373	CDKN2A, NRAS, EGFR, BRAF, BIRC5

MB	MUTATIONS
D283 (Group 3)	TP53, c-myc amplification
DAOY (Sonic Hedgehog,Shh)	TP53, NF1, CDKN2A

Table-7.1. Mutations of oncogenes and tumour suppressor in MB and MG cell lines

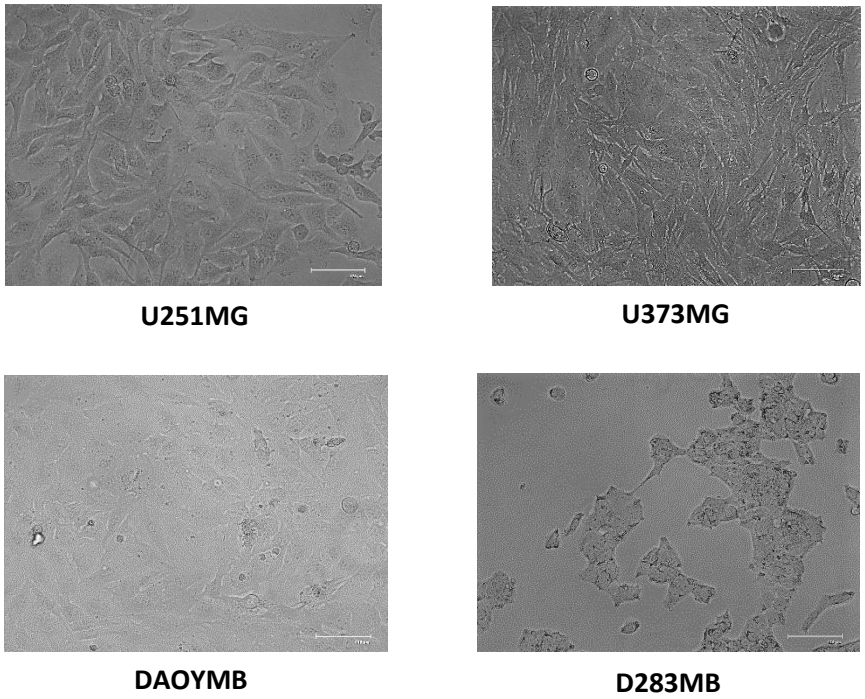

Figure-7.1. Morphology and structure of Glioblastoma Multiforme cell lines (U251MG& U373MG) and Medulloblastoma cell lines (DAOYMB & D283MB). These micrographs illustrate the unique morphology and structure peculiar to these two brain tumour types and within the same tumour.

7.4. DNA repair inhibitors and DNA damaging agents

Single strand brek (SSB) repair inhibitors, PJ34 (PARP1i, 5µM, EMD MILLIPORE Corp.) and Olaparib (PARP1i, 5µM), Cedarlane); DNA double-strand break (DSB) repair inhibitors, NU7026 (DNAPKi, 3µM, EMD MILLIPORE Corp.) and KU55933 (ATMi, 10µM, EMD MILLIPORE Corp.) was used for all experiments in this study. DNA damaging Topoisomerase-1 inhibitors, Camptothecin (14µM) (Calbiochem) and Topotecan (100nM) (Sigma-Aldrich, USA) were used to initiate DNA strand breaks (DSB) within tumour lines along with DNA alkylating agents, Methyl methanesulfonate (MMS), 0.2mg/ml (Sigma-Aldrich, USA-129925-54, 110.13g/mol).

7.5. DNA repair inhibitor, Drug treatment, and irradiation

For all experiments, cells were pre-treated with DNA repair inhibitors for 30 min at 37°C followed by 60 mins treatment with DNA damaging agents (Topoisomerase I inhibitors, Camptothecin (CPT) or Topotecan)/ 10 minutes treatment with DNA alkylating agent, Methyl methanesulfone (0.2mg/ml). Cells were irradiated using Irradiator (RS-2000/2000 Pro Owner's Manual, Rad Source Technologies, NC, Suwanee, GA, USA) at 20Gy immediately before the experiment to detect acute damage of tumour cells and 60 mins repair time was provided to observe the repair/damage effect of tumour cells in presence and absence of treatment.

7.6. Cytation ™ 5 cell imaging multi-mode reader

Cytation 5 is a microplate reader with automated microscopy which allows image-based analysis. The microscopy has up to 60X magnification in fluorescence, bright field, color bright field and phase contrast. This automated process provides temperature control up to 65°C, CO_2/O_2 gas control. The Cytation 5 platform is run by Gen 5™ software (version 3.04) which allows for data collection, processing, and analysis of all experiments (218).

7.6.1. Gen 5 ™ data analysis software

The accompanying Gen 5™ image analysis software enables automated image capture, analysis and processing. Before taking the reading or capturing images, image attainment is set up by image focusing and exposure control. Gen5 software provides a large range of processing tools for complex analysis like 3D images, montaged samples, and live cell kinetics. Image processing includes brightness/contrast adjustments followed by deconvolution and automated movies of

images when being taken during kinetic runs. Following image capture, the analysis program in the software allows automated quantitative data collection like cell count, confluence, signal translocation, subpopulation analysis, dual mask analysis, kinetic analysis and other customized methods. Augmented microscopy allows publication quality images, graphs (scatterplots, histograms, EC_{50} graphs etc.).

7.7. Alkaline comet assay (traditional method)

The alkaline comet assay (ACA) allows for real-time single-cell DNA damage quantification and analysis via electrophoresis of cellular DNA and microscopy. Cells are embedded into agarose, undergo lysis and alkali-mediated DNA unwinding. Upon gel electrophoresis, fragmented (damaged) DNA migrates away from undamaged nuclear DNA thus forming a comet-like shape which is visualized and quantified via fluorescence microscopy. Damaged DNA tails are quantified as "comet tail moments". Tail moment is the length from comet head to tail (Figure-7.5). Increasing cellular DNA damage present longer tail length denoting higher damage, hence higher tail moment values. Tumour cells in untreated condition has a comet tail moment of 1 to 2.5.

On day 1, cells are seeded in a 24 well plate (Corning, USA) (~$3x10^5$ cells/well), 500µl of complete media is added to each well in a 24 well plate (Falcon, Corning, USA, NY14831) and 4-6 drops of cell suspension is added per well so that the cells are 100% confluent on the day of the experiment. Lysis and electrophoresis buffer is made a day before (not completely) and kept at 4°C.

On day 2, MB & GBM cells were pre-treated (30 mins, 37°C) with NU7026 (3µM) and/or Olaparib (5µM) and/or Ku55933 (10µM), singly and in combination, followed by cotreatment with DNA damaging agent, Topotecan (14µM, 60 mins, 37°C) and/or Methyl methanesulfonate (MMS, 0.2mg/ml,10min, 37°C) or DMSO vehicle control. In addition to untreated controls, three treatment groups were used for each inhibitor: 1) Inhibitor(s) (or DMSO vehicle), 2) Inhibitor(s) +DNA damaging agent and 3) DNA damaging agent alone. In terms of radiation, cells will be pretreated (30mins, 37°C) with NU7026 (3µM) and/or Olaparib (5µM) and/or KU55933 (10µM), singly and in combination followed by irradiation at 20Gy, on a separate plate.

Fully frosted slides (Fisher, 12-544-5CY) are pre-coated with 0.6% normal agarose (Ultrapure Agarose, Invitrogen, 16500500) in PBS. 150µl of agarose were overlayed and covered with a square coverslip with 2 coverslips (Fisher, 12-544-10) per sample overlayed per slide. The agarose is dissolved in the microwave for 1-2 minutes, checking and mixing first after the 20s, then 5s and then every 3s until fully dissolved. The 0.6% agarose is maintained at 65°C until use. The agarose-coated slides are placed in the fridge, coverslips removed, and maintained at 4°C until use (~5-10 mins).

In the meantime, electrophoresis buffer and lysis buffer are kept at 4°C along with 1L ddH_2O. 1.2% low melting point agarose (Ultrapure LMP Agarose, Invitrogen, 15517-022) in PBS (0.12g in 10ml of PBS) is made in the same way as for normal agarose and kept at 42°C until use. Following cell treatments (damage), 5 drops of trypsin are added to each well in the 24 well plate and incubated for 4 minutes. 900µl of cold media is added, mixed well and transferred to a 15ml flacon tube on ice. This is repeated one more time. The cells are spun at 1000rpm for 5 minutes (Allegra, Beckman Coulter, USA 2955597) and resuspended in an appropriate volume in ice-cold PBS to give cell density around $3x10^5$ cells/well. Around 1-3 x 10^4 cells are needed to be mixed with agarose and overlayed under each coverslip.

The cell suspension is mixed well in the tubes and 150uL cells at ~1-3 x 10^5 cells/ml are transferred into pre-chilled black Eppendorf tubes for each sample. 150µl of 1.2% low melting point agarose is added to each 150µl sample one by one, mixing and immediately layering onto the first layer of chilled 0.6% agarose; placing a new coverslip on top of mixture. The slides are kept in the fridge, then coverlips removed followed by treatment with lysis buffer. Slides are held in a large glass rack (within a large Coplin jar) and gently lowered into this lysis buffer in a black glass box. The black box is maintained at 4°C for 1.25 hrs. After lysis, the slides are washed twice with cold H_2O for 1min and then once for 8min. Electrophoresis buffer is added to electrophoresis chamber (Aurogene) and slides are placed and equilibrated for 45 minutes followed by electrophoresis at 95mA for 25 min. The slides are removed and neutralized with 1ml, 0.4M Tris pH7 for at least 1 hour or overnight at 4°C.

On day 3, SYBR Green (Sigma Aldrich USA, S9430) dye is diluted at 1:10000 in 0.4M Tris pH 7.0 and 1ml is pipetted onto each slide to cover and incubated for 5 min before scoring the comets under a microscope. Only 6 slides are stained at a time. The comets are visualized via an epifluorescence microscope (Olympus BX51) and analyzed by Comet IV Assay software (Preceptive Instruments). This software calculates comet tail moments after manually clicking each cell within slides under the GFP channel. 110 cells/slide are manually clicked (in the dark) to get statistically-significant comet tail moment data for each single treatment (each slide representing one treatment/cell condition).

It takes about 3 days to do this manual comet assay and a full day to manually analyze 12 slides (which is equivalent to 12 treatments). In the need for multiple treatment groups or synergy experiments, these experiments would be enormous and highly onerous as it will take weeks to process and analyze data (and subject to user fatigue and error). To enable such research work in our lab, we collaborated with Trevigen (city, country) with their new 96 well-based comet slide system with which we developed a novel high-throughput (HT) comet assay workflow utilizing the new automated high content imaging Cytation 5 system with its built-in GEN 5 software for automated analysis.

7.8. High-throughput (HT) DNA damaging assay (Trevigen Comet Assay)

The alkaline comet assay is performed manually with each treatment/cell type being embedded on individual slides and "read" by the user clicking on individual comets visualized using epifluorescence microscopy. It is not uncommon to read a minimum of 100-200 comets per slide thus making the entire process and output cumbersome. Furthermore, "reading" comets can be subject to inadvertent user bias thus skewing the results.

We have developed a newer method in combination with an advanced analysis system to generate an automated, high throughput and unbiased assay technique. The high density 96 well comet slides (Trevigen-425309603), enables expanded sample analysis; more cell lines, conditions or treatment combinations can be compared simultaneously. In the high throughput 96-well slide, upon lysis, electrophoresis and DNA staining, automated imaging of each well is performed using Cytation V plate reader and analysis by GEN 5 using a specific algorithm, that we co-developed with Biotek Instruments, for comet analysis embedded within the built-in software (Figure-7.2).

This powerful combination provides a precise and robust system for measuring DNA damage among cell lines.

Cells were seeded in 96-well (Sigma Aldrich, St. Louis, USA) flat-bottomed plates (DAOYMB, U251MG, U373MG, 10.000 cells/well & D283MB, 15,000 cells/well). MB & GBM cells were pre-treated (30 mins, 37°C) with NU7026 (3μM) and/or Olaparib (5μM) and/or Ku55933 (10μM), singly and in combination, followed by co-treatment with DNA damaging agent, Topotecan (14μM, 60 mins, 37°C) and/or Methyl methanesulfonate (MMS, 0.2μg/ml,10min, 37°C) or DMSO vehicle control. Three treatment groups were used for each inhibitor: 1) Inhibitor(s) (or DMSO vehicle), 2) Inhibitor(s) +DNA damaging agent and 3) DNA damaging agent alone. In terms of radiation, cells were pretreated (30mins, 37°C) with NU7026 (3μM) and/or Olaparib (5μM) and/or KU55933 (10μM), singly and in combination followed by irradiation at 20Gy. For the control group (no drug, no inhibitor), DMSO (Sigma Aldrich, USA, D8418-250ml) was used, as all the DNA damaging drugs and DNA repair inhibitors were diluted in DMSO. Cells were treated in the dark at room temperature (RT). Cellular DNA damage imaging and quantification will be done with Cytation 5 (Biotek) high-content imaging system (HCS) at 2,5x magnification and image analysis software.

Following cells treatments, were trypsinized and re-suspended in PBS (30μl/well) followed by mixing with 1% LMP agarose (300μl/well) (Invitrogen) dissolved in PBS at 1:100 ratio. The mixture was then transferred onto the 96 well comet slide (Trevigen). The cells were then placed for 10 mins at 4°C for the agarose/cell mixture to settle and adhere onto the slide. Cells were then lysed for 60 mins at 4°C in lysis buffer (5M NaCl, 0.5M EDTA,1M Tris pH 7, 10M NaOH, TRITON X 100, 10ml of ≥99.5% DMSO). After lysis, the comet slides were placed in alkaline unwinding solution (pH >13). 50ml alkaline unwinding solution contains 0.4g of NaOH pellets, 200mM EDTA and 49.75ml ddH_20. DNA could unwind for 20 mins at room temperature (RT).

Electrophoresis was conducted in a solution containing 0.5M EDTA, 10M NaOH, 10ml of ≥99.5% DMSO at 4°C for 40 mins at 21V in an electrophoresis tank (Trevigen-425-0050-ES). The slides were then washed with distilled water (ddH_2O) for 5 mins (2x) followed by 70% ethanol. The slides were kept overnight for the agarose-cell slides to completely dry. Next day the slides were prepared for imaging by adding SYBR GREEN (20μl/well) (Sigma-Aldrich) fluorescent dye in 0.4M Tris pH 7 (1: 10,000) for 10 mins in dark at room temperature.

Slides were then washed with distilled water (ddH_2O) for 60 mins, dried and imaged. To prevent additional DNA damage, all steps were conducted in the dark at room temperature (RT). The experiment was performed in triplicate comet slides and 150 cells were counted in each well. Two-way ANOVA was used applied for statistical significance.

Automated imaging of each well is performed using the Cytation 5 high content imaging system (Bio-Tek) with analysis via the GEN 5 built-in software. Cytation 5^{TM} allows rapid imaging of each well in a 96 well CometSlide with a high degree of clarity to reproducibly detect and quantify comet tail moment measurements with a high degree of accuracy.

Built-in Gen 5^{TM} is an image software which automatically captures images along with analysis and processing. Before taking images, the image attainment is set up by image focusing and exposure control. DNA damage imaging and quantification is carried put at 2.5X magnification. Gen 5^{TM} software allows calculations such as "%DNA in tail" and "tail moment" to be automatically determined thus minimizing user bias and variability from data acquisition. Cellular analysis of comet head and tail is carried out separately by using dual mask analysis. Primary mask implies mask around comet head and secondary mask for comet tail. Three parameters are taken into consideration for analysis; tail length (measured for the edge of comet head), the percentage of DNA in the tail and tail moment (tail length). This also reduces false results and eliminates overlap, anomalies and other false parameters. The final analysis result includes comets with accuracy and consistency of a population along with individual comet analysis(218).

The combination of the assay, automated imaging and analysis represents a novel and robust method to determine genotoxicity of agents on the DNA integrity of various cells.

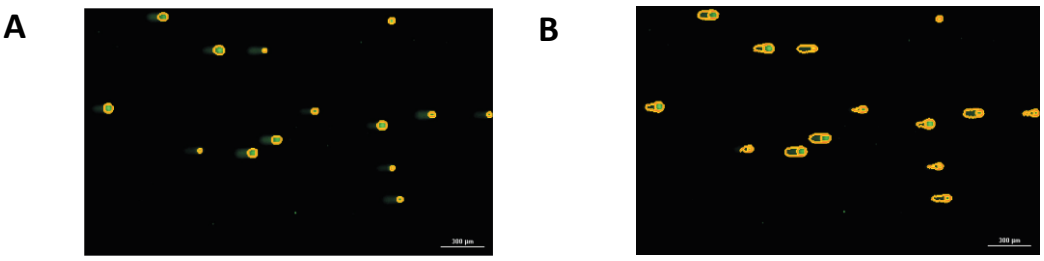

Figure 7.2. Automated comet assay analysis. 10µM camptothecin treated comet analyses based on user-programmed cellular analysis parameters. Primary and secondary cellular analysis object masks showing (A) comet head and (B) comet tail in relation to the comet head, respectively. Images captured using a 2.5x objective, 1x2 image montage, and GFP imaging channel(218).

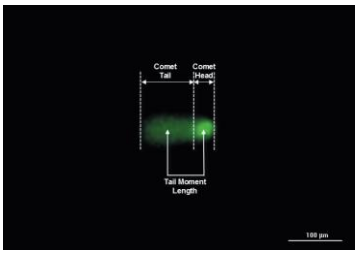

Figure-7.3. Comet areas included in tail moment calculation(218)

7.9. Cell proliferation assay (WST-1)

Cell proliferation assay is carried out to determine the number of viable cells using the WST-1 dye (Roche Diagnostics-11644807001) after 48 hrs following treatment with drugs/inhibitors. The stable tetrazolium salt WST-1 is cleaved to a soluble formazan and this bio-reduction is dependent on the glycolytic production of NAD(P)H in viable cells. Therefore, the amount of formazan dye that forms correlates to the number of metabolically active cells in the culture. This assay allows a direct, sensitive and accurate measurement of cell viability and proliferation(219).

Cells were seeded in 96 well flat-bottomed plates (Corning USA) to determine the relative sensitivity of tumour lines to specific treatment groups. U251 (GBM), U373 (GBM) and DAOY (MB) cells were seeded at a density of 500 cells/well and D283 MED (MB) 1000 cells/well. Cells were pre-treated (30 mins, 37^{o}C) with DNAPKi-NU7026 (3µM), PARP1i-PJ34 or Olaparib (5µM) and ATMi-KU55933 (10µM), singly and in combination, followed by co-treatment with Topoisomerase I inhibitor- Topotecan (100nM, 60 mins, 37^{o}C). DMSO vehicle control was included for all experiments. Three treatment groups were used for each inhibitor: 1) DMSO

vehicle, 2) Topotecan 3) Inhibitor(s) + Topotecan. For control group (no drug, no inhibitor) DMSO (Sigma Aldrich, USA, D8418-250ml) was used, as all DNA damaging drugs and repair inhibitors were diluted in DMSO. Following 48hrs incubation, the viability of cells was measured by WST-1 (10µl/well) using the Epoch plate reader (Bio-Tek). After one hour of adding the WST-1 dye, absorbance reading was taken at 450nm every hour for 3hrs. Experiments were performed in triplicate and *paired T-test* was applied for statistical significance.

7.10. Cell death assay (Trypan Blue)

Trypan blue (SIGMA-ALDRICH, Life Sciences) cell death assay is used to determine the percentage/number of dead cells in a cell suspension based on the principle that lives cells have intact cell membrane and do not allow trypan blue dye to enter the cytoplasm whereas non-viable cells have compromised cell membranes allowing the dye to enter and stain the cytoplasm blue.

Cells were seeded (DAOY-2x10^6 cells/ml, D283- 4x10^6 cells/ml) in a 6-well plate. The next day cells were treated the following combinations; DMSO, PARP1i (5µM), Topotecan (100nM), PARP1i+Topotecan and Etoposide (100µM) (serves as a positive control). Culture media was removed and kept aside while adding trypsin to detached cells. Collected media from each treatment group was used to collect cells in a tube. Cell pellets were then mixed with 200µl PBS. The cell suspension was transferred to fac tube (FALCON, Corning, USA). Trypan blue was added (DAOY- 2 µl/tube and D283-1µl/tube) and the percentage of dead cells was calculated by counting the number of blue cells in a population of clear cells via NovoCyte Flowcytometry (ACEA Biosciences, Inc). Cell death was measured at two different time points; 48hrs and 72hrs respectively.

Analysis of cells is performed by gating the cell population of interest using molecules visualized by fluorescence in an emission spectrum. The control-stained sample (Trypan blue) is compared with an unstained sample to observed non-specific binding and the interested cell population is selected, gated with other treated samples.

7.11. RNA extraction

Cells were grown in the 10cm dish until completely confluent. QIAGEN RNeasy Mini-extraction kit was used for extracting RNA from medulloblastoma cell lines (DAOY & D283) in triplicates (N=3). The RNA concentrations obtained from my NanoDrop analysis for both cell lines (preprared in triplicate) were as follows: DAOY: 1106ng/µl, 1095.2ng/µl,983ng/µl and D283: 332.8ng/µl, 268.6ng/µl, 1151.8ng/µl. RNA samples were run in a bioanalyzer to assess RNA quality prior to RNA sequencing. Each sample was diluted to 5ng/µl from original concentrations and 3µl/sample was used to run. RNA integrity Number (RIN) number obtained for each sample was between 9.8-10 for all samples denoting very high-quality RNA, suitable for RNA sequencing. After RNA extraction, the quantity extracted was assessed by ND-1000 spectrophotometer (Nano-Drop). The RNA sample was further run in a Bioanalyzer (DE13804420) using the Eukaryote Total RNA Pico assay. The sample was run on a gel and RNA Integrity Number (RIN) values were collected for each sample. RIN number is defined as an algorithm for determining integrity values to RNA measurements.

7.12. RNA sequencing

RNAs were sent to STEM CORE LABORATORIES (Ottawa Hospital Research Institute, OHRI, Ottawa) for RNA-Sequencing analysis. The samples were sequenced to identify differentially-regulated mRNAs within the DNA repair, DNA synthesis, and cell death/survival gene ontology (GO) profiles. The pooled DNA libraries will be denatured and normalized to achieve acceptable cluster density on the Illumina NextSeq 500 undergoing 1x75 bp cycles of single-end sequencing (100ng of total RNA).

7.13. Statistical Analysis

Raw data for comet assay were captured from GEN 5 3.03 software in Cytation 5, processed and analyzed. GraphPad Prism 5 (GraphPad Software, CA) was used for statistical analysis. All data values are reported are expressed as mean ± SEM. Mean values were compared using Two-way ANOVA for multiple group comparison. For cell viability assay multiple paired T-test has been used for multiple group comparison. $P<0.05$ was considered significant for all the experiments.

IV. RESULTS

8.1. Validation of High-Throughput Comet Assay vs Manual Comet assay

This experiment was the part of my development of the high-throughput (HT) comet assay in our laboratory, as per AIM-1 of my research project. The high-throughput Comet assay system allows for an expanded high density 96 well comet slide sample analysis; more cell lines, conditions or treatment combinations can be compared simultaneously. It takes about half a day to do the experiment and multiple experiments can be run in a day. Three 96 well comet slides can be run at the same time in an electrophoresis tank, hence three independent experiments can be run at once or one experiment with, N=3 (n=3), giving more statistically significant data. Automated imaging of each well is performed using the Cytation 5 high content imaging system where it takes ~5 minutes to read one plate. This powerful system provides a precise and robust system for measuring DNA damage among cell lines and enables new and highly detailed capability to evaluate new drug combinations for effective anti-tumour therapy. Furthermore, this system can be used to evaluate DNA damage and repair, in an unbiased manner, in several model systems or scientific contexts that requires detailed genotoxicity studies. On the other hand, the conventional method of performing comet assay analysis is very time-consuming and is not amenable to performing detailed combinatorial analyses.

HT- Comet assay and Manual Comet assay was carried out with medulloblastoma cell line DAOY under positive (no treatment, Control) and negative control (20Gy radiation). About 110 comets were considered. The average comet tail moment from both experiment was compared. The untreated DAOYMB cells have an average comet tail moment of 1.5 and with radiation around 12, in both comet assay techniques.

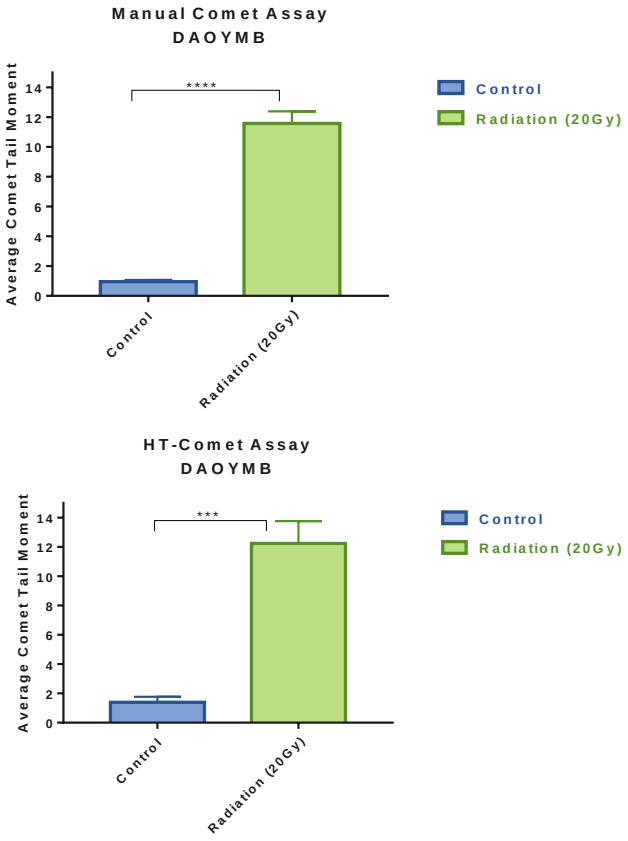

Figure-8.1. Validation of high-throughput comet assay vs manual comet assay. In both techniques the average comet tail moment is similar among both treatment groups. The error bar denotes standard deviation between three independent experiments, N=3. Paired T-test is used as a statistical test with $p<0.05$=****, $p<0.001$=***.

8.2. DNA damage increases with increasing concentration of Topoisomerase I poison, Camptothecin in Medulloblastoma (MB) and Glioblastoma Multiforme (GBM)

To further validate the HT comet assay, a dose response experiment was carried out on Medulloblastoma (MB) (DAOYMB, D283MB) and Glioblastoma Multiforme (GBM) (U251MG, U373MG) tumour lines to determine cellular DNA damage with the DNA damaging Topoisomerase I poison, Camptothecin, spanning a low dose (0.14µM) to a high dose (14µM). These tumour lines show progressively increasing damage amongst the tumour lines correlating with an increase in drug concentration. MB lines are more sensitive to the DNA damaging agent compared to GBM lines. Amongst GBM lines, U251MG possesses higher damage compared to the U373MG line, at 14µM with an average tail moment of 12 whereas U373MG has an average tail moment of below 10. Similarly, among MB tumour lines, higher cellular DNA damage is seen in DAOY (highest among all the four tumour lines) with an average tail moment of more than 15 at 14µM whereas D283 is below 15. Differential sensitization was observed between two brain tumour types and within the same tumour, indicating the variation amongst subtypes and the heterogeneous nature of tumour cells (one of the hallmarks of cancer).

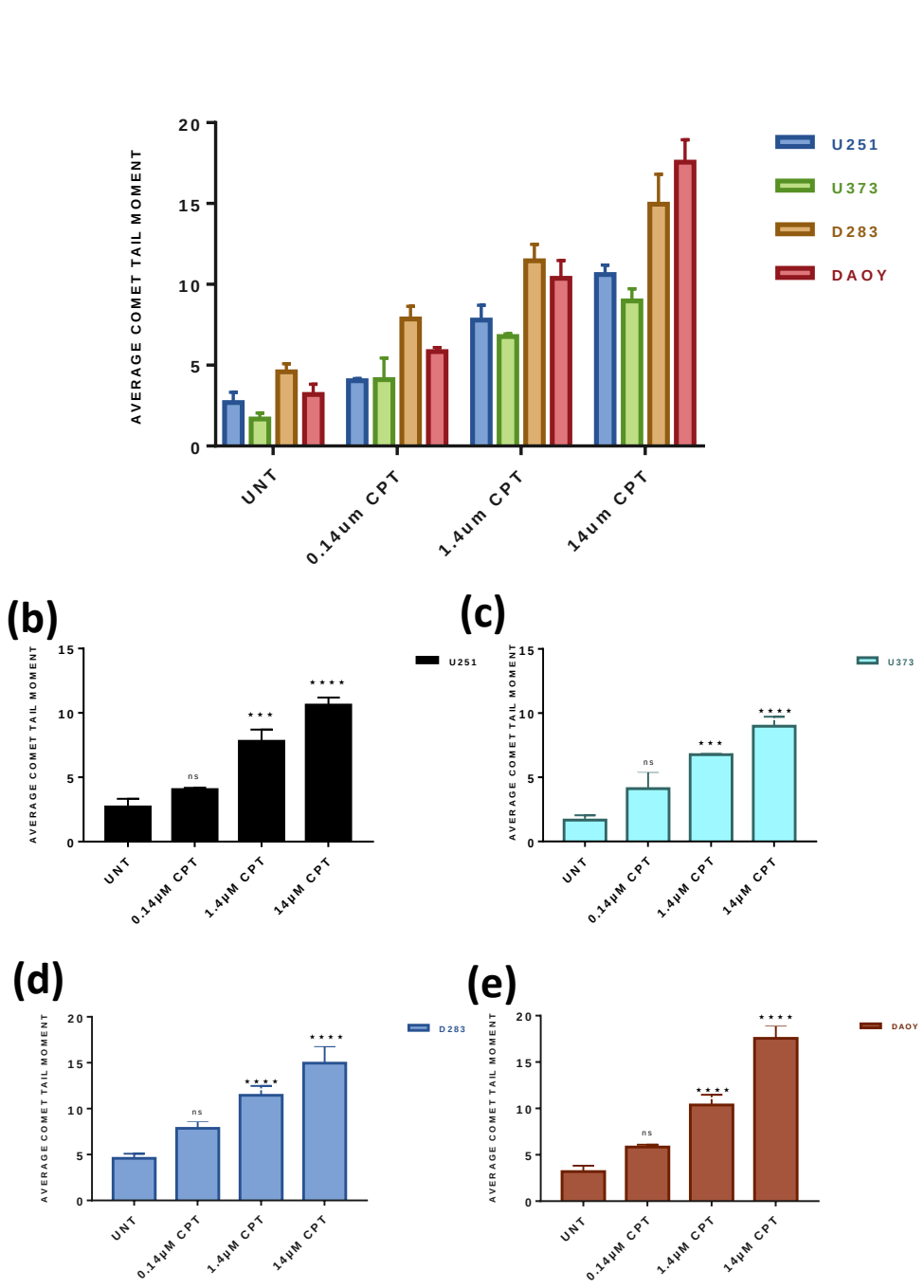

Figure-8.2. High-Throughput (HT) Comet assay carried out on both Medulloblastoma and Glioblastoma Multiforme cell lines with the Topoisomerase-I inhibitor, Camptothecin. In both MG (U251, U373) and MB (DAOY, D283) the damage increase correlates with higher drug concentrations. The error bar denotes standard deviation between two independent experiments, N=2 (n=3). Two-way ANOVA is used as a statistical test with $p<0.0001$=****, $p<0.0005$=***. Abbreviation: UNT-Untreated, Camptothecin-CPT

8.3. Resolution of Topoisomerase-I DNA damage is PARP/SSBR dependent in Medulloblastoma (MB) & Glioblastoma Multiforme (GBM)

It well known that different DNA damaging agents recruit distinct repair pathways and thus tumours would be expected to exhibit differential sensitivity based on adaptive responses through differential upregulation of DNA repair pathways. Topoisomerase inhibitors are generally used as a second line therapy in brain tumors and DNA repair inhibitors have been reported to enhance the toxicity of these agents to tumour cells. HT comet assay was carried out on MB (DAOYMB, D283MB) and GBM (U251MG, U373MG) tumour lines to asses the cellular DNA damage with Camptothecin in combination with DNA repair inhibitors. This experiment was carried out to determine the cellular DNA damage induced by DNA repair inhibitors in presence and absence of the DNA damaging agent in search of a synergistic effect (effect of two drugs producing greater effect than sum of their individual effect) with the combinatorial approach. The data presented was normalized with control to remove the basal damage and then with Camptothecin to bring forward the damage induced by DNA inhibitors only. The cellular DNA damage is presented in terms of 'fold change' to be synonymous with 'times', as in '3-fold larger' = "3 times larger.

Amongst both tumour types and within each tumour line, DAOYMB shows the highest sensitization to PARP1 inhibition alone in presence of Camptothecin. PARP1i alone has the highest cellular DNA damage level among all cell lines. Combination treatment groups in GBM such as PARP1i+ATMi and PARP1i+DNAPKi show a higher fold increase in damage compared to other treatment combinations. The case is quite different in MB lines, as the D283MB show >2-fold cellular DNA damage, denoting almost no sensitization whereas DAOYMB show almost 4-fold damage. From these data, it can be interpreted that the D283MB line show resistance compared to DAOYMB. Two different cell lines derived from same tumour type shows differential sensitization to anticancer drug classically illustrating the heterogenous nature of cancer.

Camptothecin induced damage in MB (DAOY, D283) & GBM (U251, U373)	Single Treatment Group	Double Treatment Group
	Control (+/- CPT)	Control (+/- CPT)
	PARP1i (+/- CPT)	PAR1Pi+ATMi (+/- CPT)
	DNAPKi (+/- CPT)	PARP1i+DNAPKi (+/- CPT)
	ATMi (+/- CPT)	DNAPKi+ATMi (+/- CPT)

Table-8.1. Treatment combinations with Topoisomerase-I inhibitor, Camptothecin, in presence and absence of DNA repair inhibitors, PARP1i, DNAPKi and/or ATMi

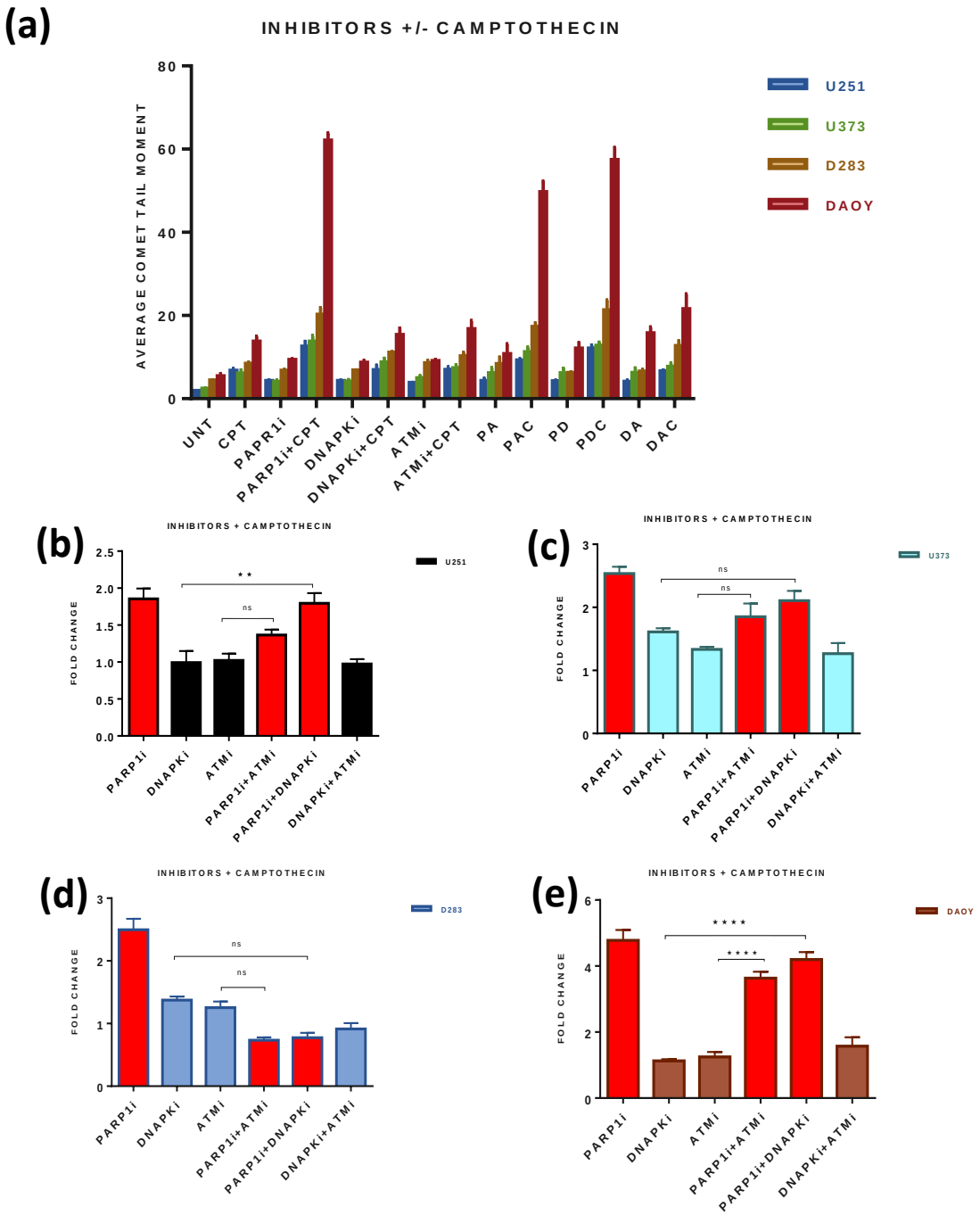

Figure-8.3. High-Throughput (HT) comet assay performed on both Medulloblastoma and Glioblastoma Multiforme cell lines with DNA repair inhibitors co-treated with the Topoisomerase I poison, Camptothecin. Cells were pretreated with DNA repair inhibitors for 30mins followed by 1hr treatment with camptothecin. The treatment groups presented are normalized with individual controls (no inhibitor, no drug). In both tumour types PARP1i, PARP1i+ATMi, PARP1i+DNAPKi (bars in red) combinations show the highest sensitization, with PARP1i treatment alone resulting in higher damage, indicating PARP1/SSBR-mediated repair (Base Excision Repair-BER). DAOY (MB) shows the most sensitization with PARP1i, PARP1i+ATMi, PARP1i+DNAPKi (bars in red) while D283 (MB) shows the least sensitization. The error bar denotes standard deviation between two independent experiments, N=2 (n=3). Two-way

ANOVA is used as a statistical test with p<0.0001=****, p<0.0005=***, p<0.005=**, p<0.03=*. Abbreviations: UNT-Untreated, PA-PARP1i+ATMi, PAC- PARP1i+ATMi+CPT, PD- PARP1i+DNAPKi, PDC- PARP1i+DNAPKi+CPT, DA-DNAPKi+ATMi, DAC- DNAPKi+ATMi+CPT

8.4. DNA alkylation in GBM is resolved co-operatively by DSB repair pathways and in MB by both PARP1/SSBR and DSBR pathways

Alkylating agents are used as a first-line therapy for highly aggressive tumours such as malignant glioma but have shown resistance overtime. Studies have shown that PARP1 sensitizes tumour cells for DNA alkylating agent in breast, prostate and some lymphomas. We wanted to observe this effect with MMS in MB and MG lines, with our treatment combinations. HT comet assay was carried out on MB (DAOYMB, D283MB) and GBM (U251MG, U373MG) tumour lines to assess the cellular DNA damage with DNA alkylating agent, Methyl methanesulfonate (MMS), in combination with DNA repair inhibitors. The cellular DNA damage is presented in terms of 'fold change' to be synonymous with 'times', as in '3-fold larger' = "3 times larger. The data presented was normalized with control to remove the basal damage and then with Camptothecin to bring forward the damage induced by DNA inhibitors only.

In GBM lines, the DNAPKi+ATMi (combination of two independent double-strand break sensing proteins) show the most cellular DNA damage with U373MG with about 15-fold more cellular damage than U251MG. This main difference between these two cell lines derived from same tumour type denotes the heterogenous property of classic glioblastoma. In MB lines we see a differential response. DAOYMB show similar pattern in DNA damage with all the treatment groups (both single/double combinations) whereas D283MB show 2-fold higher damage with PARP1i+ATMi and PARP1i+DNAPKi.

Methylmethanesulfonate (MMS) induced damage in MB (DAOY, D283) & GBM (U251, U373)	Single Treatment Group	Double Treatment Group
	Control (+/- CPT)	Control (+/- CPT)
	PARP1i (+/- CPT)	PARP1i+ATMi (+/- CPT)
	DNAPKi (+/- CPT)	PARPi+DNAPKi (+/- CPT)
	ATMi (+/- CPT)	DNAPKi+ATMi (+/- CPT)

Table-8.2. Treatment combinations with DNA alkylating agent, methyl methane sulfonate (MMS) in presence and absence of DNA repair inhibitors, PARP1i, DNAPKi and/orATMi.

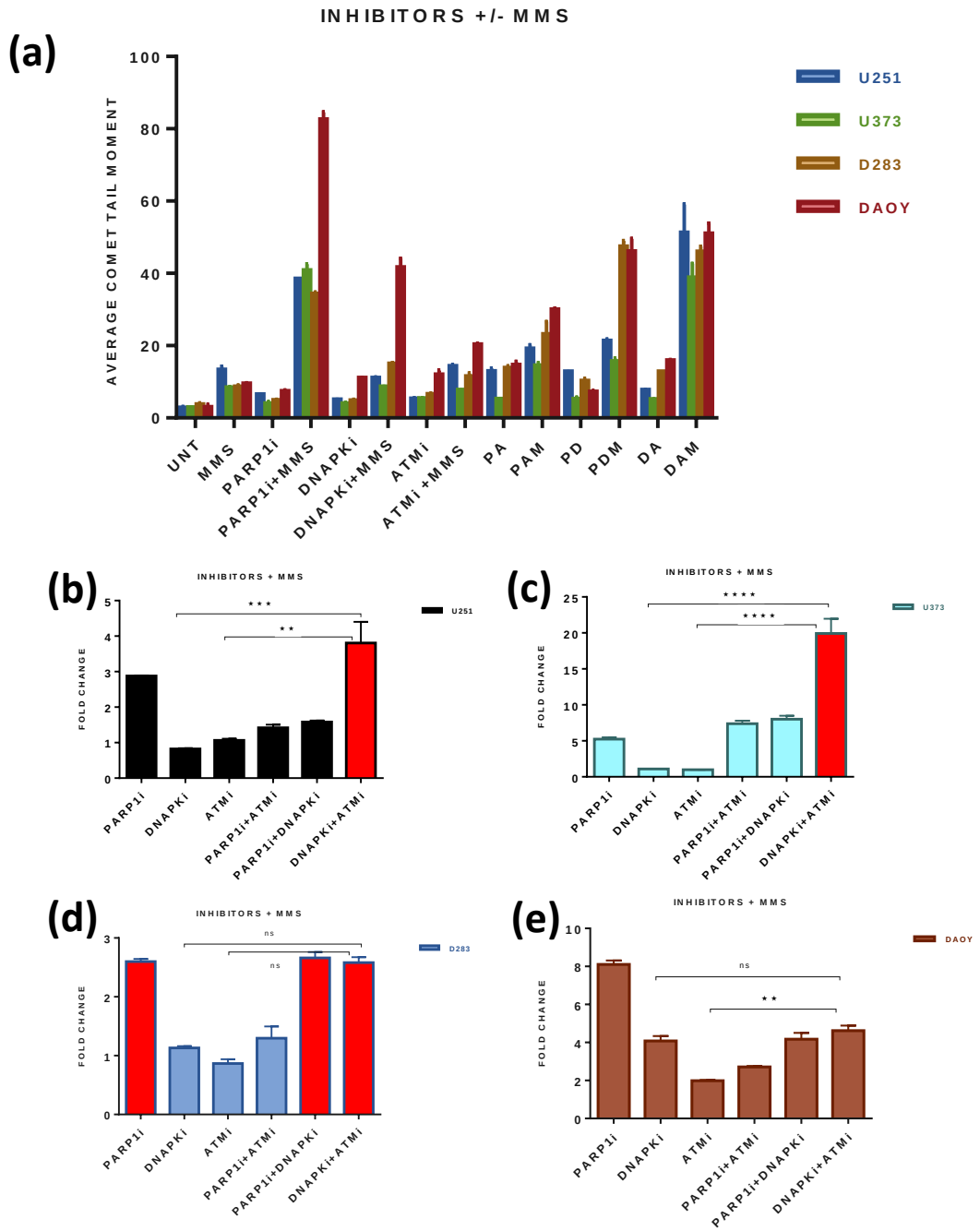

Figure-8.4. High-Throughput (HT) Comet assay carried out on both Medulloblastoma lines and Glioblastoma Multiforme cell lines with DNA repair inhibitors in presence of an alkylating agent, Methyl methanesulfonate. Cells were pretreated with DNA repair inhibitors for 30mins followed by 10mins treatment with MMS. Controls were placed in context to all tumour lines in the experiment and the treatment groups presented are normalized with individual controls (no inhibitor, no drug). Among GBM lines, both U373 and U251 show high sensitization in the DNAPKi+ATMi combination, with U373 showing 10-fold more damage than U251, indicating cooperativity with DSBR. Among MB lines, DAOY show more sensitization compared to D283 but damage in D283 is higher with PARP1i+ATMi and PARP1i+DNAPKi combinations. In GBM lines, sensitivity to MMS via PARP1i inhibition show greater cellular damage compared to other treatment groups. The error bar denotes standard deviation between two

independent experiments, N=2 (n=3). Two-way ANOVA is used as a statistical test with p<0.0001=****, p<0.0005=***, p<0.005=**, p<0.03=*. Abbreviations: UNT-Untreated, PA-PARP1i+ATMi, PAM-PARP1i+ATMi+MMS, PD- PARP1i+DNAPKi, PDM- PARP1i+DNAPKi+MMS, DA-DNAPKi+ATMi, DAM-DNAPKi+ATMi+MMS

8.5. DNA damage after radiation increases in the presence of PARP1 in both MB & GBM

HT comet assay was performed in MB (DAOYMB, D283MB) and GBM (U251MG, U373MG) tumour lines to asses the cellular DNA damage with 20Gy radiation followed by assessment of their repair kinetics after 60 mins recovery, in conjunction with combinations of DNA repair inhibitors. Radiation is used as a first-line therapy in cancer and studies have shown that DNA repair inhibitors sensitizes tumours to ionising radiation. We wanted to observe this phenomenon with our treatment combinations and whether off the repair time repairs or intensifies the damage. By comet analysis, 20Gy irradiation is fairly a high dose and serves as a well-documented positive control for damage. As such, this dose of irradiation was used on all cell lines *in vitro* as a relative yardstick for damage incurred in contrast to the drug/inhibitor treatments and conditions.

Upon treatment with ionizing radiation (IR, acute damage), a similar level of cellular DNA damage in all treatment groups was observed with some differences. In presence of DNA repair inhibitors, the cellular damage observed with IR treatment is higher compared to IR alone conditions. It has been previously noted that inhibiting PARP1 radiosensitizes tumours like breast and prostate; we observed a similar phenomenon in our brain tumour lines. After 60 minutes of repair time following IR, a decrease in cellular DNA damage in all treatment combinations (both single/double) was observed, except for treatments involving PARP1i.

After acute damage DAOYMB has the least cellular DNA damage (>1-fold change) but this scenario changes upon 60 minutes repair time as DAOYMB is observed to incur the highest damage in terms of fold change compared to all other cell lines within the same tumour type or between the two brain tumours.

Recovery time, increased cellular damage was noted in the following treatment groups; PARP1i, PARP1i+ATMi and PARP1i+DNAPKi, cellular DNA damage increased in all tumour lines. Among, GBM cell lines, following 60 mins repair, U251MG PARP1i, PARP1i+ATMi, and PARP1i+DNAPKi were all observed to show a 3-fold increase in residual damage (compared to no inhibitor controls) which is higher compared to U373MG (PARP1i:1-fold, PARP1i+ATMi:2-fold, PARP1i+DNAPKi:2-fold). Similarly, amongst MB lines, DAOYMB (PARP1i:3-fold, PARP1i+ATMi:4-fold, PARP1i+DNAPKi:3-fold) have increased damage compared to D283MB (PARP1i:2-fold, PARP1i+ATMi: 3-fold, PARP1i+DNAPKi:2-fold).

Radiation (20Gy) induced damage in MB (DAOY, D283) & GBM (U251, U373)	**Single Treatment Group**	**Double Treatment Group**
	Control (+/-Radiation)	Control (+/-Radiation)
	PARP1i (+ Radiation)	PARP1i+ATMi (+ Radiation)
	DNAPKi (+ Radiation)	PARP1i+DNAPKi (+ Radiation)
	ATMi (+ Radiation)	DNAPKi+ATMi (+ Radiation)
Radiation (20Gy) + 1hr Repair in MB (DAOY, D283) & GBM (U251, U373)	**Single Treatment Group**	**Double Treatment Group**
	Control (+/-Radiation +1hr repair)	Control (+/-Radiation +1hr repair)
	PARP1i (Radiation +1hr repair)	PARP1i+ATMi (Radiation+1hr repair)
	DNAPKi (Radiation+1hr repair)	PARP1i+DNAPKi (Radiation+1hr repair)
	ATMi (Radiation+1hr repair)	DNAPKi+ATMi (Radiation+1hr repair)

Table-8.3. Treatment combinations with acute radiation (20Gy) and 60 minutes post-IR repair time, in presence and absence of DNA repair Inhibitors: PARP1i, DNAPKi and/or ATMi.

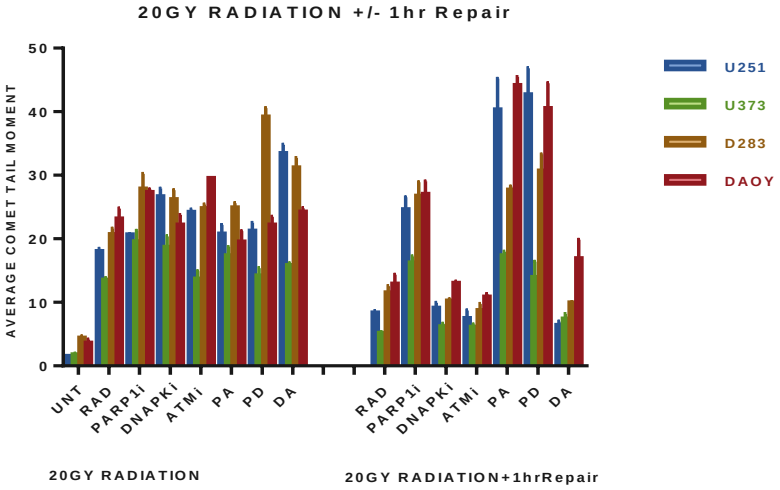

(a) DNA damage after 20GY acute treatment

(b) DNA damage after radiation increases in the presence of PARP1i in both MB & GBM

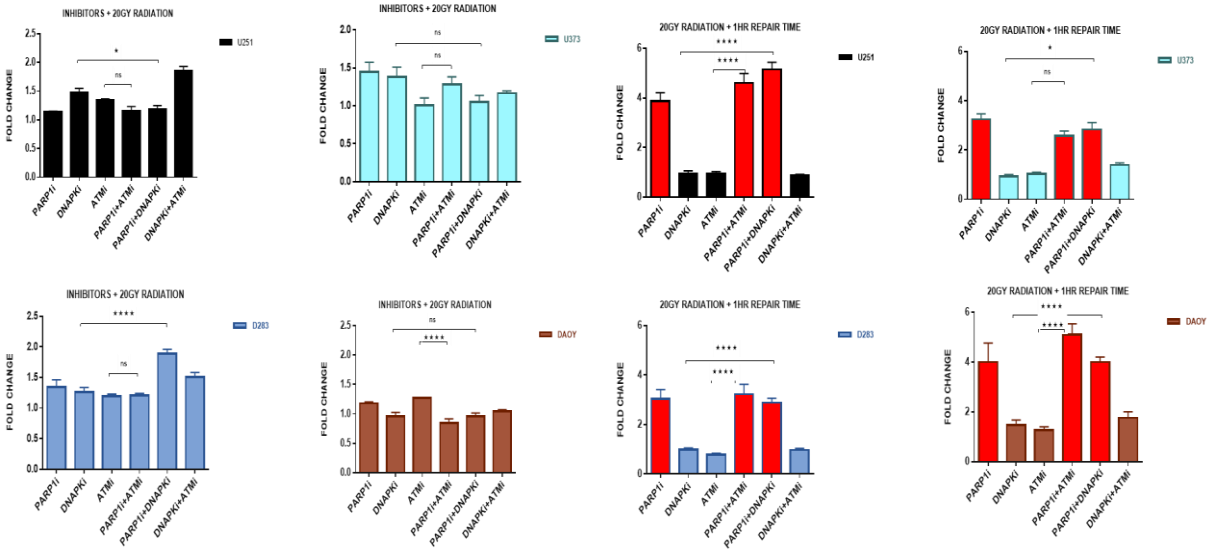

Figure-8.5. High-Throughput (HT) Comet assay carried out on both Medulloblastoma lines and Glioblastoma Multiforme cell lines with DNA repair inhibitors undergoing 20Gy radiation (a). Cells are pre-treated with DNA repair inhibitors for 30 mins and then radiation was applied. The results shown were normalized with control groups (no inhibitor, no radiation) to account for basal damage followed by normalization with the radiation group (no inhibitors added) to account for the DNA damage induced by specific DNA repair inhibitors. After acute damage with radiation, most treatment combinations show DNA damage however, DAOY (MB) shows low DNA damage compared to other cell lines. Abbreviations: UNT-Untreated, PA-PARP1i+ATMi, PD- PARP1i+DNAPKi, DA- DNAPKi + ATMi.

8.6. Selective Medulloblastoma (MB) cell lines show sensitization to Topoisomerase-I poisons in combination with PARP1i

We further wanted to investigate the significant difference within medulloblastoma cell lines in terms of drug treatment (Topoisomerase 1 + PARP1i). We wanted to find out why a Group 3 derived medulloblastoma cell line (D283MB) shows resistance towards a Topoisomerase I DNA damaging agent Sonic Hedgehog (Shh) group derived medulloblastoma cell line show sensitization; and it relates to DNA damage and repair kinetics. This led us to move forward with medulloblastoma in the follow-up study. We wanted to correlate our comet assay data with decreased cell survival, so we performed a WST-1 cell viability assay.

A dose-response was carried out with different concentration of the Camptothecin-related Topoisomerase I inhibitor, Topotecan (TPT, 0-10μM), in presence and absence of PARP1i, Olaparib (5μM), in MB lines. Topotecan has similar mechanism of action as that to Camptotthecin, with Topotecan being able to cross blood brain barrier (BBB). Differential responses were seen amongst the two MB cell lines. DAOYMB showed a decrease in relative cell survival with increasing concentrations of TPT with a drastic decrease at the 100nm concentration. In presence of PARP1i, there is 5-fold decrease in cell survival at the IC50. In case of D283MB, the scenario is opposite as there was no observed sensitization to TPT, either in the presence or absence of PARP1i.

Furthermore, when the cell viability assay was repeated with select treatment groups; PARP1i, PARP1i+ATMi, and PARP1i+DNAPKi, the DAOYMB showed sensitization to TPT (at 100nM) with an almost 2-fold decrease in relative cell survival in presence of PARP1i-Olaparib (5μM) for all treatment groups. On the other hand, D283MB showed limited sensitization with TPT, whether in presence or absence of PARP1i.

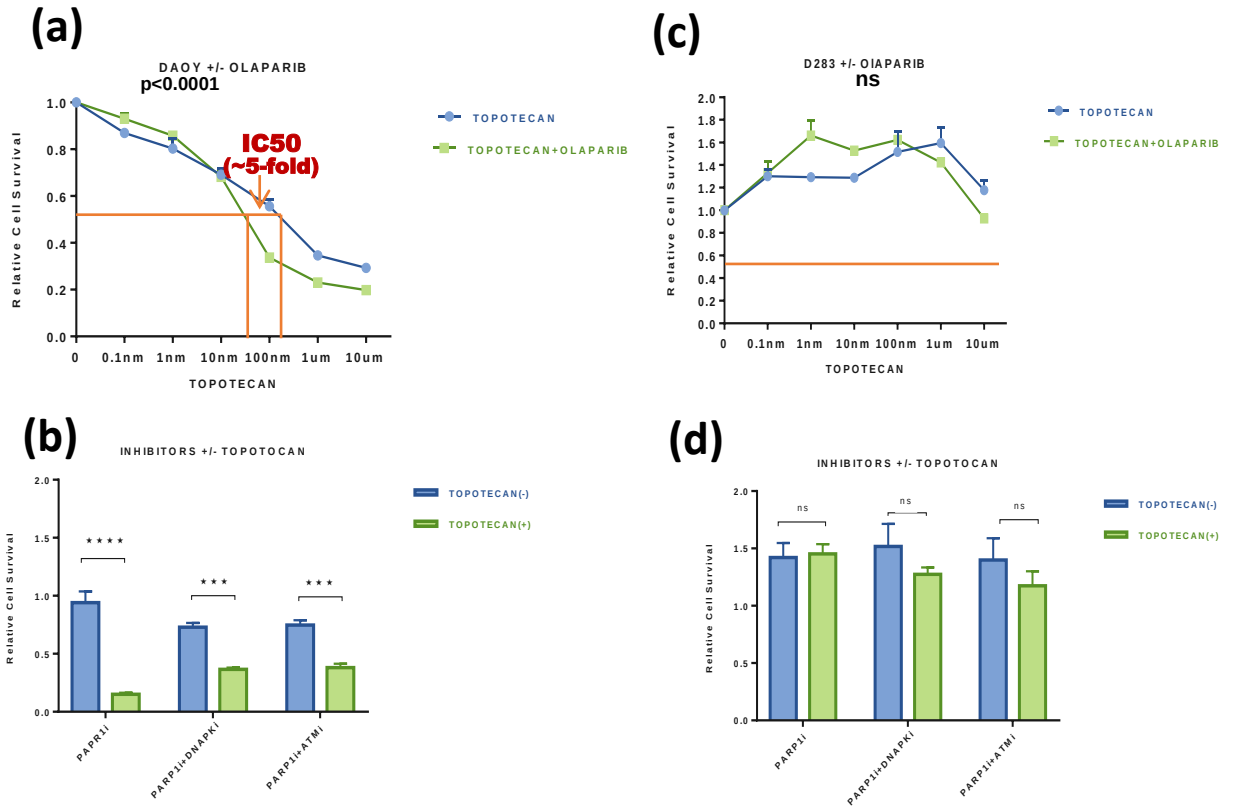

Figure-8.6. Cell viability assay on DAOYMB line, with PARP1i (Olaparib-5µM,) in presence and absence of Topotecan (100nM). Cells were pre-treated with PARP1i-Olaparib for 30 mins followed by treatment with Topotecan and incubated for 48 hrs. at 37ºC. In figure (a), DAOY(MB) showed a progressive decrease in cell proliferation with increasing concentrations of Topotecan, both in presence and absence of PARP1i. In presence of PARP1i, DAOY(MB) show 5-fold more sensitization at IC50. In figure (b) with PARP1i treatment, the proliferation of DAOY(MB) decreases to about half in all the treatment groups. On the other hand, in figure (c) and (d) D283(MB) show little to almost no sensitization. The error bar denotes standard deviation between two independent experiments, N=2 (n=3). Multiple paired T-test was used as a statistical test with p<0.0001=****, p<0.0005=***, ns=non-significant.

8.7. Selective Medulloblastoma (MB) cell lines show cell death with Topoisomerase-I poison

With the selected treatment combination of Olaparib + Topotecan, the DNA damage the data is consistent with the cell proliferation amongst MB lines. The goal for any drug treatment is to eradicate the tumour. Thus, we wanted to see whether this drug combination can elicit cell death. So, a cell death assay was carried out on both MB lines with Topotecan (100nM) at 48 hrs and 72 hrs, to characterize differences in susceptibility to Topoisomerase-1 inhibition and ensuing DNA damage amongst DAOYMB and D283MB on induction of tumour cell death.

Topoisomerase II inhibitor, Etoposide (100µM) served as the positive control in this experiment (as per literature). At 48hrs DAOYMB show 40% cell death and D283MB 20%. Similarly, at 72hrs, DAOYMB show 80% cell death and D283MB 60%. About 20% more cell death in DAOYMB compared to D283MB at both time points. Consistently, Topoisomerase I inhibitors are more amenable to killing tumour cells within the Sonic Hedgehog group (Shh) group of MBs (ie. DAOYMB) compared to the Group 3 subgroup (ie. D283MB). DMSO control showed only 10% death.

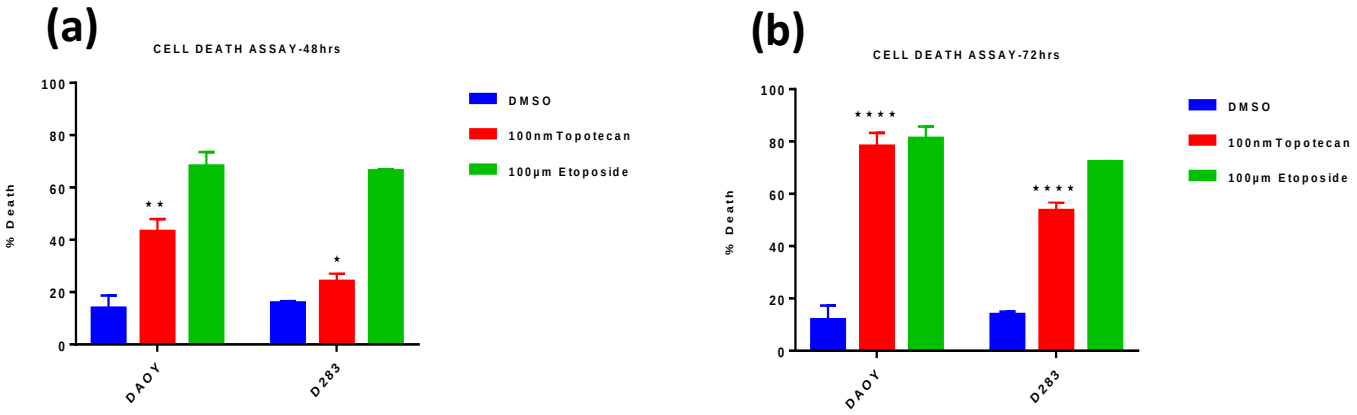

Figure-8.7. Trypan Blue cell death assay carried out on DAOY and D283, with Topotecan. Percentage cell death was taken at two different time points, 48 hrs and 72 hrs to observe tumour death over time. At 48 hrs (a), DAOY(MB) has twice the cell death as D283(MB) at 100nm Topotecan. At 72 hrs, while D283MB: DAOYMB cell death narrowed, the DAOYMB line showed 33% more cell death than D283MB. The error bars denote standard deviation between two independent experiments, N=2 (n=3). Two-way ANOVA is used as a statistical test with $p<0.0001$=****, $p<0.005$=**, $p<0.01$=*.

8.8. Specific Medulloblastoma (MB) lines show tumour cell death to Topoisomerase-I poisons in combination with PARP1 inhibitor

A cell death assay was performed on both MB lines with Topotecan (100nM) at 48hrs in presence of PARP1i-Olaparib (5µM), to characterize the differential susceptibility of MB tumour lines. The Topoisomerase II inhibitor, Etoposide (100µM) served as positive control in this experiment. At 48hrs, DAOYMB show higher percentage of cell death compared to D283MB. In the presence of PARP1i, DAOY (20%) showed twice the cell death as D283 (10%) while PARP1i+Topotecan treatment resulted in DAOY (60%) showing ~50% more cell death than D283 (40%).

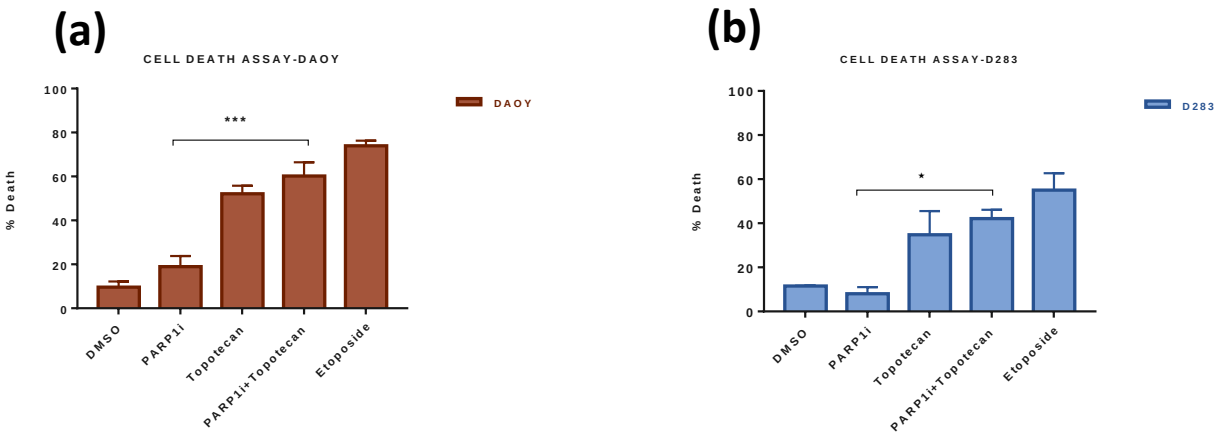

Figure-8.8. Trypan Blue cell death assay carried out on DAOY and D283 with Topotecan and the PARP1i, Olaparib. Percentage cell death was taken at 48 hrs to observe tumour cell death. At 48 hrs, DAOY(MB) **(Figure-8.7a)** has 50% more cell death compared to D283 (MB) **(Figure-8.7a)** upon co-treatment with Topotecan and PARP1i. The error bar denotes standard deviation between four independent experiments, N=4. Two-way ANOVA is used as a statistical test with $p<0.005$=***, $p<0.01$=*.

8.9. Treatment with Topoisomerase-I/ PARP1i sensitization is tumour-specific

A cell viability assay was performed on the non-neural tumour cell line, HeLa, and normal cycling human fibroblasts to determine if the observed anti-tumour effects the combined drug treatments, Topotecan and PARP1i-Olaparib, were specific to CNS tumours. HeLa and human fibroblasts were treated with different doses of Topotecan (0-10µM) in presence and absence of PARP1i-Olaparib (5µM). Both non-neural/tumour cell types showed little to no sensitization to the treatment combination, indicating that the treatment combination is tumour specific.

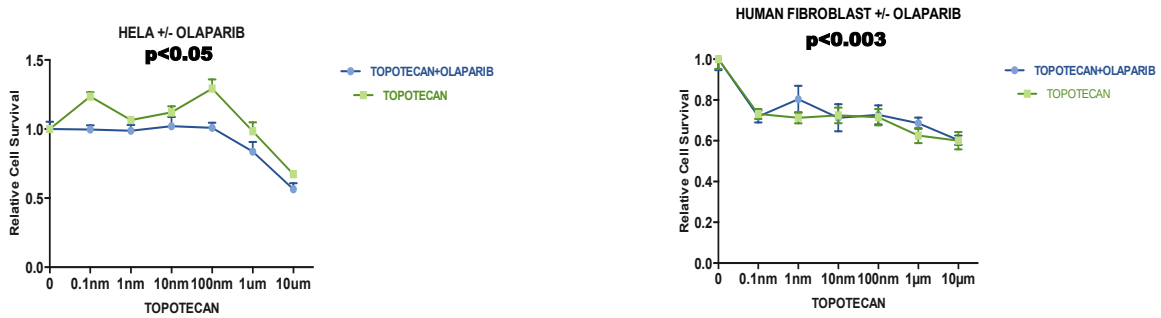

Figure-8.9. Cell viability assay-WST-1 carried out on HeLa and human fibroblasts with Topotecan. Cells were pretreated with PARP1i-Olaparib (5µM) for 30 mins followed by treatment with Topotecan and incubated for 48 hrs. Both cell lines show minimal sensitization with the treatment combination indicating that this combination is highly tumour-specific and has no effect on non-neural tumour types or normal cells. The error bar denotes standard deviation between two independent experiments, N=2 (n=3). Multiple paired T-test has been used as a statistical test with $p<0.05$=*, $p<0.0003$=***.

8.10. RNA extracted from Medulloblastoma lines (DAOY, D283) are of high quality for RNA Sequencing

In Comet assay analysis, since we identified differential DNA damage repair activity pertaining to both sensitivity to Topotecan and PARP1i, we sought to characterize differences in gene expression through RNA-Seq analysis comparing untreated samples of DAOYMB and D283MB to determine if there were marked differences in factors involved in DNA repair, cell proliferation and/or cell death that could account for the differential responses to the drug treatments. We extracted RNA using the Qiagen RNAase Kit, from untreated DAOYMB and D283MB samples (in triplicate) and ensured RNA quantity and quality via analysis.

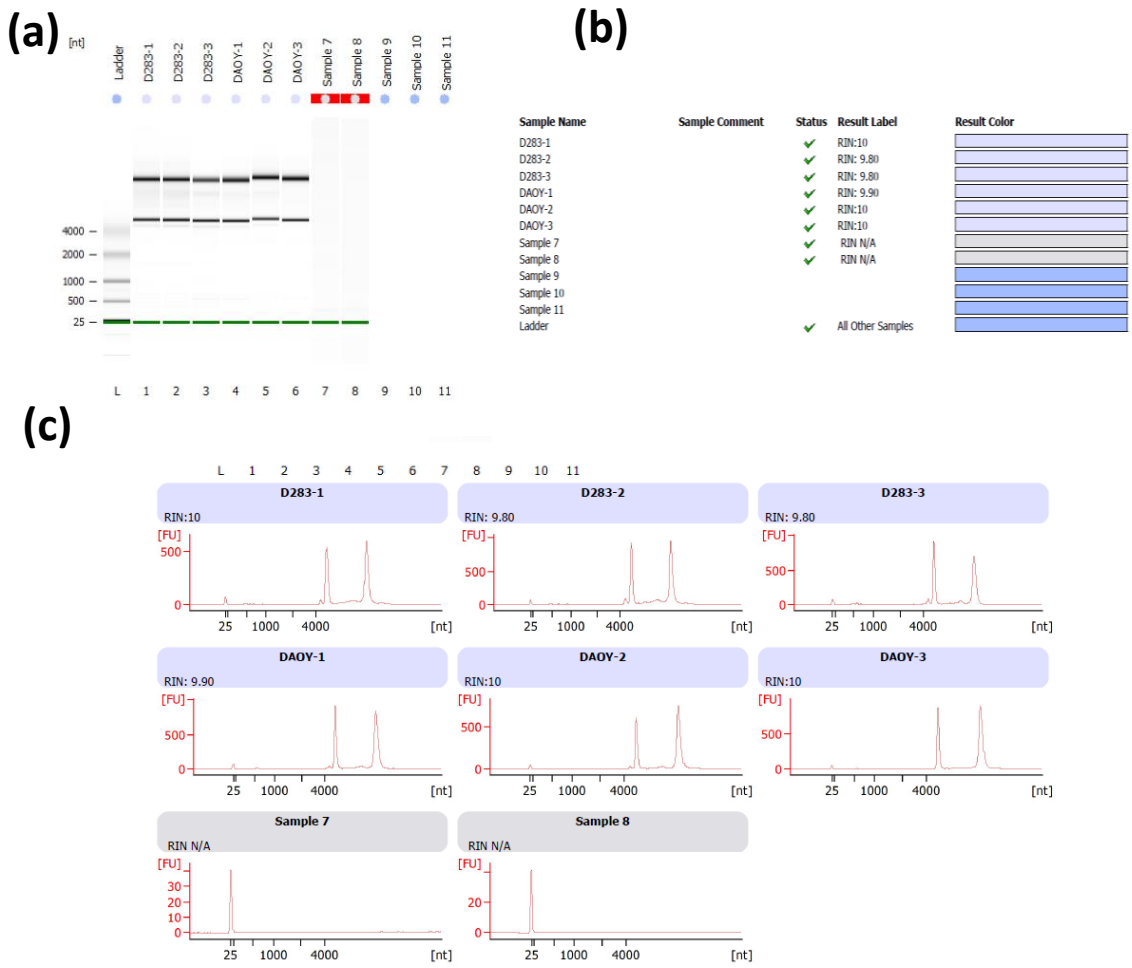

Figure-8.10. RNA quality assessment**.** Figure (a) shows the presence of considerable amount of RNA in the samples denoted by clear thick bands. Figure (b) represents bands for the two medulloblastoma cell lines with their replicates. Both cell lines show two peaks with no small peaks hence, indicative of an absence of impurities. Replicates for each cell line were highly consistent as indicated by similar band positioning (185,285). Figure (c) represent the RIN number which was consistently between 9.8-10 per sample for each cell line indicating very high-quality RNA.

8.11. Differentially-regulated DNA repair gene expression among Medulloblastoma cell lines

RNA-Seq (RNA sequencing) is used to determine the alternative gene spliced transcripts, post-transcriptional modifications, gene fusion, mutations/SNPs and changes/differences in gene expression in samples. Along with these, RNA-Seq also covers total RNA, small RNAs, such as miRNA, tRNA, and ribosomal profiling (220).

We wanted to see the differential gene expression for DNA repair gene products in the two MB cell lines to determine whether changes in DNA repair genes could explain the DNA damage responses with drug combinations. To decipher the potential molecular mechanism underlying this differential response in the two (untreated), DAOY and D283 MB lines, RNA-Seq was carried out. Amongst many differentially-regulated gene candidates, we narrowed our analysis to the 20 highest divergent DNA repair genes; selected based on their differential expression level in terms of 2log fold change.

We shipped our samples to STEM CORE LABORATORIES (Ottawa Hospital Research Institute, OHRI, Ottawa). Their analysis compares RNA abundance in our two MB cell lines (untreated), DAOY and D283, to determine which genes differ significantly in expression. The medulloblastoma samples underwent *Fragment Analyzer Run* to determine the presence and quality of RNA samples; matched my Bioanalyzer results. This was followed by library construction for sequencing. RNA-Seq libraries were prepared in triplicates.

After loading the matrix of reading counts, the resulting list of differentially-expressed genes candidates was filtered to retain only those with at least 5 reads in at least two samples (*i.e.* to remove genes with very low or no expression). This filtering approach resulted in 33,261 rows being removed from the original table of 60,498 genes. This means that 27,237 genes are retained for further analysis. Out of these 27,237 genes, 17,000 genes were filtered out by p-value (most significant fold changes). This large set of genes differentially regulated was then divided into the following categories: apoptotic processes, cell growth regulation, DNA damage response, DNA repair genes, DNA replication and regulation of proliferation.

The gene definitions used were derived from the GENCODE annotation and include not only protein-coding genes but also pseudogenes and various non-coding RNAs. Gene expression differences between the two cell lines were calculated as levels in D283 relative to levels in DAOY. Out of all potential differentially-regulated genes in all categories, the top 20 genes by p-

value (most significant fold changes) were used. From all these categories the DNA repair genes differentially-upregulated amongst the two MB cell lines (DAOY, D283) is presented in this section.

Fold change results are presented as a volcano plot, with the log2 fold change on the x-axis, and −log(p-value) −log(p-value) on the y-axis; thus, the larger the value on the y-axis, the smaller the p-value for that gene. The points in red indicate genes with an False Discovery Rate (FDR) <0.002 (adjusted p-value, calculated using the Benjamini-Hochberg method).

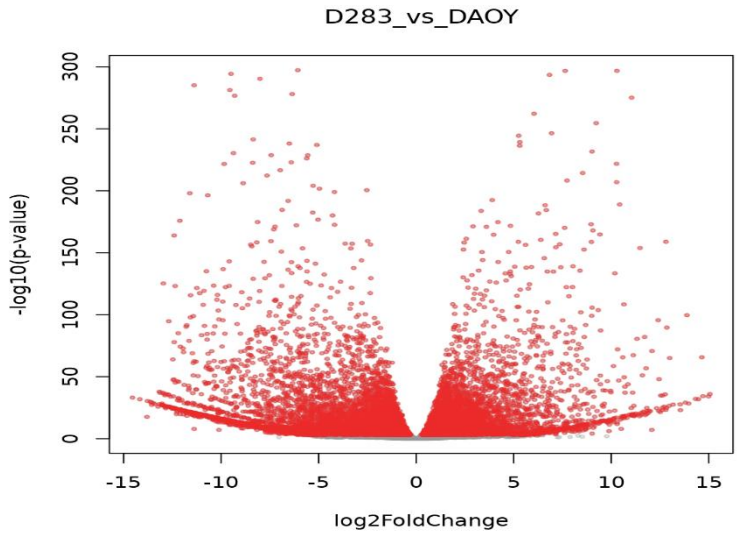

Figure-8.11. Volcano plot: Statistical significance of differentially expressed genes. This figure shows that not only were there many genes with small p-values for their expression differences but that the differences in expression level are themselves quite large. We see many genes with log2FoldChange values >3 (which is a fold difference of >8×). These results suggest that the expression differences between these two cell lines are extremely large. Selecting a subset of the differentially-expressed genes for further analysis will require some careful and strict filtering and any attempt to restrict the list to a more manageable set of genes will result in many genes with large highly significant fold changes being omitted from the analysis.

Of the 17,000 genes expressed in both cell lines (amongst 6 categories mentioned above) ~35 DNA repair genes were found to be differentially-regulated. The 20 most significant genes as sorted by p-value (most significant fold changes) were filtered out and represented as a heat map. Red (negative) denotes low expression of repair genes whereas green (positive) denotes higher expression. From the chart below, DAOYMB has lower expression of the following DNA repair genes; PARP1, ATM, BRCA1, RAD51C compared to D283MB. Concordantly downregulation of PARP1 in DAOY and upregulation in D283 supports the differential response of MB subtypes with the TopIi+PARP1i combination.

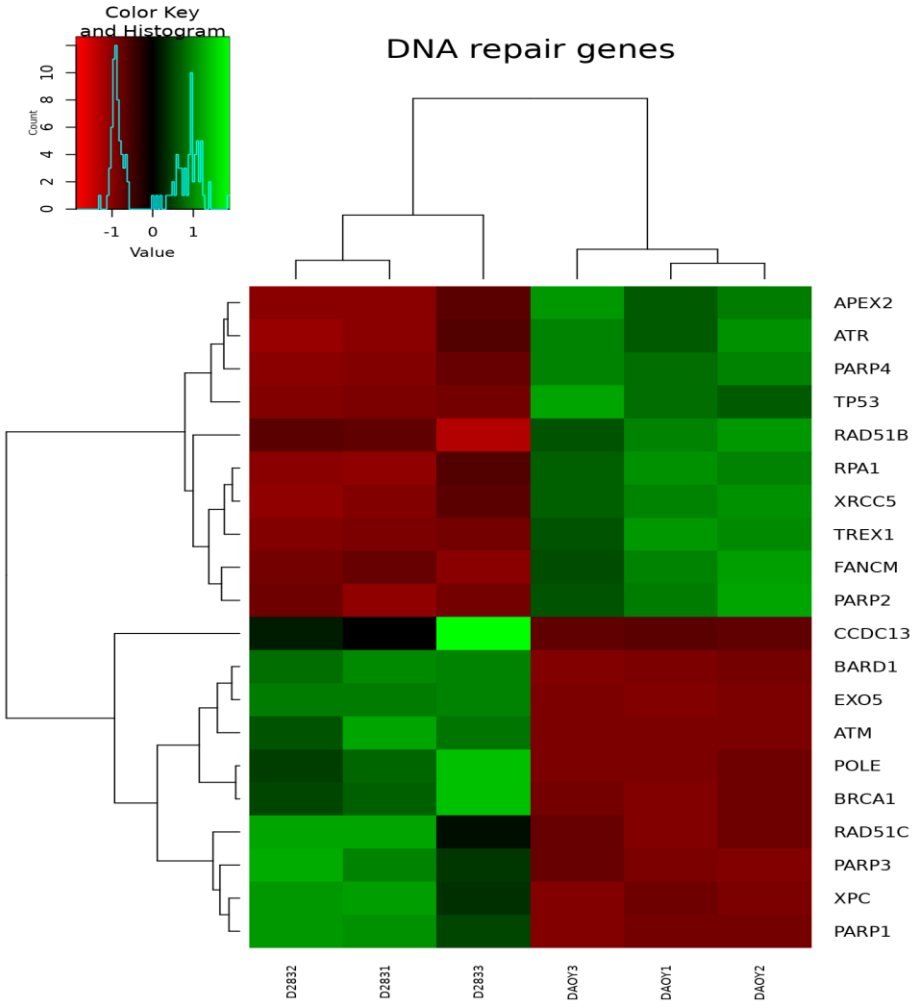

Figure-8.12. Top 20 DNA damage repair genes differentially regulated amongst in MB lines, D283 and DAOY. Red denotes repair genes with low expression levels in DAOY and high expression in D283 whereas green denotes repair genes with higher expression DAOYMB and downregulated in D283MB.

8.12. Validation of RNA-Seq data via Western Blot Analysis

Although ongoing work in the lab we validated the RNA-Seq data via western blot analysis. The results presented below is an N=1 and still requires replication for statistical significance. Eight target DNA repair genes selected from the RNA-Seq data for western blot analysis to validate expression levels. The following DNA repair genes were analyzed; TOPBP1, PARP1, ATR, ATM, RPA32, RAD51, Ku80 and p53. The protein expression level for all these DNA repair genes matched with that of RNA-Seq data. TOPBP1, RPA, ATR, p53 are upregulated in DAOYMB and downregulated in D283MB. On the other hand, ATM, Ku80 and PARP1 is downregulated in DAOYMB and upregulated in D283MB. These results represent corresponding factors/pathways that are mediating the differential response to TopI poisons and/or PARP1i.

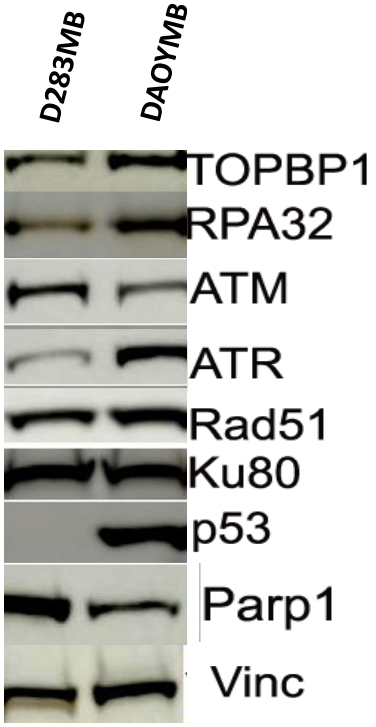

Figure-8.13. Validation of RNA-Seq data western blot Vinculin (Vinc) served as a loading control.

V. DISCUSSION

9.1. Summary of the key findings

DNA Damage Response (DDR) and DNA repair pathways are guardians of the cellular genome. Normal cells use these mechanisms to resolve DNA lesions. The inability to repair DNA lesions can interfere with DNA replication (resulting in replication fork collapse), transcriptional machinery, and other enzymatic functions, forming persistent SSBs and conversion to genotoxic DNA DSB lesion and/or aberrant gene expression. Combined, these genotoxic lesions can result in a variety of cellular pathology, including senescence, cancer and apoptosis (153) **.** It is known that the diverse mechanisms involving cell cycle regulation, DDR pathways, cellular metabolism, and cell death act in concert in response to DNA damage(221)(167). As such, cellular life and death decisions are balanced by these mechanisms as defective DDR in proliferating cells, including neuroprogenitors, can lead to cancer. Tumour cells tend to have more active repair mechanism, which makes treatment difficult.

One classic example of synthetic lethality is the utilization of the PARP1 inhibitor in Homologous Recombination (HR)-deficient cells. Tumour cells are highly replicative and the HRR pathway only functions during the S/G2 phase of cell cycle thus making HRR an important therapeutic target for effective treatment (222). PARP1 is a key mediator in SSB repair and BRCA1/2 (tumour suppressors) are required for DSBR via HRR. PARP1 inhibitors like Olaparib target BRCA-mutated cells and increases the sensitivity of tumour cells to chemotherapeutics ~1000-fold, thus increasing overall patient survival and progression-free survival with reduced toxicity in patients with BRCA-mutated breast cancer (189). DNA SSBs interfere with DNA replication and transcriptional machinery resulting in persistent and numerous DNA nicks and their conversion into lethal DNA DSBs. Unrepaired DSBs triggers apoptosis, therefore; inhibition of SSB repair combined with mutation and dysfunctional DSB repair can result in synthetic lethality specifically of the tumour whereas normal cells still retain ability to resolve DSBs.

The principal objective of my research was to evaluate differential regulation of DNA repair pathways in cancer cells, we reliably induced DNA damage using well known and characterized DNA damage causing agents (topoisomerase inhibitors and alkylating agents). These poisons are known to cause death of cancer lines, but also it is recognized that resistance to these agents is prominent, which we reasoned is due to upregulation of DNA repair pathways. Accordingly, we reasoned that specific tumour cell lines would vary in their response to DNA repair inhibitors in a

manner that reflects the differential regulation of DNA repair pathways in these cells (i.e. cell with upregulated PARP1 repair would be especially sensitive to PARP1i). To elucidate DNA repair mechanisms utilized by brain tumours, such as Glioblastoma Multiforme (GBM) and Medulloblastoma (MB), to repair DNA damage induced by chemo- and radio-therapeutics, along with identifying DNA repair proteins participating in parallel and/or redundant repair pathways involved in enhancing therapeutic resistance. It has been shown in studies that tumour cells induce upregulation of DNA repair pathways for repair of damage (135). It is also predicted that >90% of all tumours incur at least one defect in the DNA damage response (DDR), thus tumour cells enhance the activity of other compensatory DNA repair pathway which can modulate cellular responses to chemotherapeutics and promote tumour cell survival (20) . A combinatorial treatment strategy with DNA repair inhibitors along with DNA damaging agent has been used in this research project to augment the efficacy of anti-cancer therapy in these brain tumours. I developed new assay and analysis tools to systematically interrogate brain tumours cells with these different combinations in a high-throughput, reproducible and accurate manner. Furthermore, utilizing my data, I focused on identifying molecular modifiers underlying the therapeutic response to these therapeutics specifically in MB, using a responsive line (DAOY) and a relatively unresponsive line (D283) as a comparison for this analysis. This approach has identified many DNA repair factors which are differentially expressed amongst these tumours thus presenting a synthetic lethal opportunity to treat these tumours wherein specific DNA repair pathways, including parallel/redundant pathways, may be targeted in a tumour-specific manner.

To investigate the DNA repair mechanisms and to understand the differential cellular DNA damaging effect of combinatorial treatments on brain tumour cell lines, we developed a high-throughput DNA damage repair assay (HT-Comet). We have validated this new system by employing a dose-response curve of the DNA damaging Topoisomerase I inhibitor, Camptothecin. I have used a concentration gradient of the drug to asses the cellular damage induced in both MB and GBM tumour lines. As expected and validated by our system, low doses of camptothecin induced low levels of cellular DNA damage in both tumour types while high dose induced higher cellular DNA damage. I then employed a combinatorial treatment approach to these tumour cell lines. I used various combinations of treatments utilizing a variety of DNA damaging agents (CPT, MMs and IR), in the presence and absence of specific DNA repair inhibitors (ATMi, PAPRi, DNA-PKi). I have found that the combination of Topoisomerase-1 posion with PARP1 inhibitor induces

a high degree of cooperative unrepaired DNA damage, indicating that a major mode of DNA repair in these tumours is Topoisomerase-1- and PARP1/SSBR-dependent. Furthermore, I have found that DNA alkylation, via Methylmethanesulphonate (MMS) induced damage, is resolved co-operatively by DSBR pathways in GBM and by PARP1/SSBR with DSBR pathways in MB.

Based on my experimental data set, I have concluded that different cell lines have a differential sensitivity to therapy within a given tumour type and amongst different tumours as well, due to differential activity of DNA strand break repair pathways. Furthermore, PARP1 inhibition combined with DNA damaging agents may represent a profound therapeutic strategy to counteract brain tumours via induction of cellular DNA damage. Two cell lines from MB (D283MB, DAOYMB) have different response towards Topoisomerase I inhibition. D283MB show resistance while DAOYMB show sensitization (highest DNA damage compared to all four tumour lines). On the other hand, GBM lines (U251MG, U373MG) with DNA alkylation show a differential sensitization among tumour lines. U373MG show very high sensitization, despite the fact that this tumour line is considered to be a resistant and heterogenous GBM line.

To further elucidate the effect of cellular DNA repair in the context of repair following acute damage, I carried out HT-Comet analysis on MB and GBM tumour lines. I quantified the amount of acutely induced damage by radiation followed by residual damage following 60 min repair time also in the context of specific DNA repair inhibitors. Interestingly, I found that in some lines, DNA damage in fact increases after 60 min repair time in presence of PARP1 inhibition in both MB and GBM; the degree of which is tumour-specific.

After this comprehensive DNA damage repair analysis, comprising of various chemotherapies and DNA repair inhibitors, I focused my analysis on medulloblastoma, to further characterize the observed differential sensitization among the two tumour lines I used. I found that one MB cell line, DAOYMB, showed sensitization to Topoisomerase I poison in co-treatment with PARP1 inhibitor while D283MB did not. Cell proliferation and tumour cell death studies validated these conclusions. To further assess whether this effect is tumour-specific, I carried out similar combination studies (TPT+PARPi) in a non-neural tumour line, Hela and normal fibroblasts. These lines showed little to no sensitivity to these drug/inhibitor treatments indicating that this combination is tumour specific and has no effect on human fibroblast cell line.

To decipher the potential molecular mechanism underlying this differential response in the two MB lines, RNA Seq was carried out. Amongst a number of differentially-regulated gene candidates, we narrowed our analysis to the 20 highest divergent DNA repair genes; selected based on their differential expression level in terms of 2log fold change. In validating our cell studies, I found that PARP1 is upregulated in DAOYMB and downregulated in D283 and BRCA1/RAD51C is downregulated in DAOYMB and upregulated in D283MB, showing defective Homologous recombination (HRR) DSBR pathway. Previously, synthetic lethality in tumours with hereditary mutations in HRR factors was observed with PARP inhibitors in breast and ovarian cancer. We thereby, observe this synthetic lethality in MB cell line (DAOYMB) for the first-time, thus supporting the observed differential sensitization of these MB cells using the TOPIi+PARP1i combination.

Two groups showed the effect of PARP inhibitors in HRR defective cell lines and tumour xenograft or allograft. HRR is known as the 'error-free' double-strand break repair pathway and is frequently found to be defective in most tumours(160). Mutations in BRCA1 and BRCA2 genes are found in about 10-15% of ovarian cancers and these repair proteins function in HRR. HRR defects also arise from mutations in *RAD51, DSS1*, *RPA1,* or *CHK1* and tumours with these HRR defects are also sensitive to PARP inhibition(190).

9.2. Development of the High-Throughput comet assay

The alkaline comet assay (ACA) allows for real-time single-cell DNA damage quantification and analysis via electrophoresis of cellular DNA and microscopy. Classical alkaline comet assays are performed manually with each treatment/cell type being embedded on individual slides and "read" by the user clicking on individual comets visualized using epifluorescence microscopy. It is not uncommon to read a minimum of 100-200 comets per slide thus making the entire process and output cumbersome. Furthermore, "reading" comets can be subject to inadvertent user bias (false positive) thus skewing the results. It takes about 2 days to perform the experiments, and an additional 1-2 days to analyze 20 slides and approximately 1 week for 96 slides. This conventional method of performing comet assay analysis is very time-consuming and is not amenable to performing detailed combinatorial analyses.

The high-throughput Trevidgen Comet assay system allows for an expanded high density 96 well comet slide sample analysis; more cell lines, conditions or treatment combinations can be compared simultaneously. It takes about half a day to do the experiment and multiple experiments can be run in a day. Three 96 well comet slides can be run at the same time in an electrophoresis tank, hence three independent experiments can be run at once or one experiment with, N=3 (n=3), giving more statistically significant data. Automated imaging of each well is performed using the Cytation 5 high content imaging system where it takes ~5 minutes to read one plate. Comet analysis is carried out at the same time by GEN 5 software using our unique software algorithm for comet analysis which we embedded within the built-in software. This powerful system provides a precise and robust system for measuring DNA damage among cell lines and enables new and highly detailed capability to evaluate new drug combinations for effective anti-tumour therapy. Furthermore, this system can be used to evaluate DNA damage and repair, in an unbiased manner, in several model systems or scientific contexts that requires detailed genotoxicity studies.

9.3. Anti-tumorigenic agents overwhelm cellular DNA repair responses with lethal genotoxicity

The cellular consequences to DNA SSBs and base damage lend themselves well in the treatment of cancer. As tumour cells are highly proliferative, a combination of DNA damaging agents with specific DNA repair inhibitors may increase global genomic SSBs and base damage, and subsequent replication fork-associated DSBs, thus overloading the DNA repair machinery leading to persistent unrepaired DNA lesions and activation of cell death pathways. However, chemotherapeutic benefit in brain tumours can be offset either by failure of drugs to cross the blood-brain- barrier (BBB), enhanced activity/expression of drug efflux transporters (such as P-glycoprotein) and by the high degree of systemic toxicity associated with lethal doses of DNA damage to healthy tissue. Bone maroow suppression is a common side effect with DNA damaging agents and a study has shown that DNA alkylating agent with PARP1i inhibitor reduced bone marrow suppression in patients. PARP1 inhibitor enhanced the toxicity of alkylating agent, also reducing toxicity on normal cells.

Paradoxically, defects in DNA repair can also be tumorigenic through the accumulation of a range of genomic alterations during cell proliferation that allows for uncoupling of growth controls (223)(224). As such, tumours often show DNA repair defects and altered responses to DNA

damaging chemotherapeutics due to induction of other compensatory or redundant DNA repair pathways. These backup repair pathways are usually more active which enables resistance to DNA damaging radio- and chemotherapy.

In previous studies, it has been shown that PARP1 inhibition sensitizes tumour lines to Topoisomerase I poisons in breast, colon and prostate cancer. As tumour cells are highly replicative, the inhibition of topoisomerase I enzyme during replication leads to the formation of single-strand breaks which can turn into DSBs. These single strand breaks are normally resolved by activating dedicated SSB repair pathways. The base excision repair pathway is considered one of the major repair pathways where PARP1 acts as the key repair protein. Inhibition of PARP1 leads to disruption of this repair process, hence unresolved single strand breaks can collide with replication forks thus forming deleterious replication induced double-strand breaks. This activates error-prone DSB repair pathways such as NHEJ, alternate NHEJ and SSA which result in genomic instability hence activating cell death pathways.

I have employed combinatorial treatments using single (PARP1i) and double-strand (ATMi, DNA-PKi) break DNA repair inhibitors. ATM is a well-characterized DSB sensor ser/thr protein kinase that sits at the apex of the DNA damage-dependent cell cycle checkpoint pathway. Inhibiting ATM blocks activation of checkpoints that respond to DNA damage and can be useful to counteract tumour cells to suppress activation of DSB repair pathways. As the cells cycle continues, tumour cells can then replicate with the incurred damage thus resulting in enhanced genomic instability that induces cell death. However, there is inherent redundancy in the DNA damage response and with DNA repair pathways as DSB repair pathways can be activated through other means, such as DNA-PK. Thus, inhibition of DNA-PK blocks the NHEJ pathway from repairing DSBs. Through inhibition of selective repair pathways, the residual DNA repair machinery can become overloaded with persistent unrepaired DNA lesions leading to the activation of cell death pathways. Thus, blocking tumour cell repair processes is an effective mechanism to enhance the cytotoxicity of chemotherapeutics, such as Topoisomerase I poison.

A well-known example in colon cancer treatment involves the inhibition of FEN1, a protein involved in long-patch BER. Blocking long patch BER enhances the cytotoxicity of the DNA-alkylating agent, Temozolomide to colon cancer cells. Thus, in my study, the inhibition of PARP1, ATM and/or DNA-PK in Medulloblastoma (MB) and Glioblastoma Multiforme (GBM) resulted

in higher cellular DNA damage when given in combination (PARP1i+ATMi, PARP1i+DNAPKi) with Topoisomerase I compared to single inhibitor treatments alone, thus potentiating the anti-tumour effect of therapeutics through this DNA repair inhibition strategy.

Similarly, I found that the genotoxicity of the DNA alkylating agent, Methyl methanesulfonate (MMS) is enhanced in presence of DNA repair inhibitors PARP1i, ATMi and DNA-PKi. MMS induces damage by altering DNA alkylation leading to strand cleavage producing both SSBs and DSBs. Blocking repair of SSB via PARPi along with ATMi and DNA-PKi leads to a higher cellular damage in GBM tumour lines. Interestingly, U373MG is known to be a more resistant tumour line in malignant Glioma, however, my DNA damage study showed that U373MG tend to display much higher fold DNA damage compared to the U251 MG counterpart.

Studies have shown that ionizing radiation, DNA methylating agents, and topoisomerase inhibitors activate PARP1; thus incentivizing the study of PARP1 inhibitors in combination with DNA damaging agents (189). Extensive preclinical studies have shown that PARP inhibition enhances the cytotoxicity of DNA damaging agents (methylating agents, topoisomerase inhibitors, alkylating agents) and ionizing radiation in tumour cell lines along with xenografts in a different type of tumours. This introduced PARP inhibitor (AG014699) to clinical trials along with DNA alkylating agent, temozolomide (160). Data from this trial verified that this combination reduces marrow suppression, a common effect seen with DNA alkylating agent. Reduction of this toxic effect is dose limiting when PARP inhibitor blocks pADPr synthesis by >90%. There are several ongoing clinical trials of PARP inhibitor with DNA damaging agents.

9.4. Intratumoral heterogeneity in Medulloblastoma

Tumour biology plays a critical role in terms of therapeutic efficacy and this is seen with MB tumour lines conducted in this body of research. The two tumour lines used for this study, DAOYMB and D283MB, are derived from two different subtypes of MB. DAOYMB is derived from Sonic Hedgehog (Shh) and D283MB from the group 3 subtypes. Two different subtypes of the same tumour likely have different tumour biology. In this study, I have observed differences in DNA damage sensitivity and repair kinetics which I demonstrate can be further exploited through inhibition of DNA repair proteins in different repair pathways. DAOYMB show sensitization to Topoisomerase I poisons, whereas D283MB show limited sensitization to this

agent. However, D283MB shows significant sensitization with DNA alkylating agents, such as Methyl methanesulfonate (MMS). This phenomenon has been further validated through cell proliferation and cell death experiments. To identify potential mechanisms underlying this observation, we performed an RNA-Seq analysis to generate data to identify differentially regulated DNA repair genes amongst these two classical MB tumour lines. Amongst the wealth of data acquired through this method, we observed the down-regulation of PARP1 and BRCA1/RAD51C protein in DAOYMB and its up-regulation in D283MB.

Topoisomerase I induce cellular DNA damage in D283MB cells form DNA single strand breaks. PARP1 is involved in several key DNA repair pathways, such as base excision repair (BER), nucleotide excision repair (NER), mismatch repair (MMR) and repair of double-strand break through homologous recombination (HR) and alternative non-homologous end-joining (Alt-NHEJ). Therefore, inhibition of PARP1 results in global failure of DNA repair pathways and the repair the DNA lesions in tumour cells(190). Inhibition of all these pathways leads to activation of HRR, error-free DSBR process which begins to resolve induced DSBs. Downregulation of BRCA1/RAD51C in DAOYMB, suggest possible mutation in HRR process, denoting defective HRR. This phenomenon enables a synthetic lethality strategy. This explains the consistent sensitivity of DAOYMB seen with TOP1i+PARP1i.

On the other hand, up-regulation of PARP1 and BRCA1/RAD51C as seen in D283MB, is consistent with the observed insensitivity of the TOPI+PARP1 combination treatment, likely due to an up-regulation of BER and HRR repair activity in tumour cells consistent with augmented damage-induced. However, PARP1 is present in both lines yet PARP1i induced sensitization is only observed in DAOY thus suggesting that the abundance of PARP1 in D283 is not sufficiently counteracted by PARP1 inhibitors. Interestingly, my RNA-Seq data identified upregulation of PARP2 in DAOY compared to D283, worthy of further investigation.

9.5. Enhancement of cellular DNA damage in CNS tumour lines after acute radiation with recovery

In a DSB/cell/Gy basis, ionizing radiation causes DNA damage to about 850 pyrimidine lesions, 450 purine lesions, 1000 single-strand breaks (SSB) and 20-40 double-strand breaks, in conditions of low linear energy transfer (LET) gamma-radiation. About 2Gy of radiation is enough to form 3000 DNA lesions per cell and the damage increases with increasing dose. A higher dose of

ionizing radiation will increase the number of DNA lesions in tumour cells leading to complete eradication of tumour cells but the ratio of toxic to therapeutic dose, in terms of side effects and tolerance capability of the patient, must be considered which limits the use of a higher dose of radiation like any other anti-cancer treatment strategy (225).

Tumour cells are highly proliferative; front-line radiotherapy combined with chemotherapeutic drugs (chemoradiotherapy) are often used to increase global genomic SSBs and base damage, and subsequent replication fork-associated DSBs, thus overloading the DNA repair machinery leading to persistent unrepaired DNA lesions and activation of cell death pathways (226). Radiation is used to kill tumour cells by inducing apoptosis and recently, studies using kinase inhibitors have demonstrated an enhanced cytotoxic effect in combination with ionizing radiation (227). Based on this previous data, I tested whether I could enhance the genotoxicity of radiation with DNA repair/kinase inhibitors in combinatorial treatment, which would suggest improved cytotoxicity of brain tumour cells.

Previous work suggests that it takes 30-60 minutes to repair double-strand breaks formed by low dose radiation and <20% double-strand breaks undergo reduced reparability and can persist for >24hr (225). Using my combination treatments, I observe an increase in unrepaired DNA breaks following 60 minutes post radiation with specific DNA repair inhibitor combinations (PARP1i, PARP1i+ATMi, PARP1i+DNAPKi). When single strand breaks are formed by ionizing radiation, these are mainly resolved by BER and are mostly dependent on long patch repair process compared to short patch repair. Also oxidized abasic (AP) sites (apurinic/apyrimidinic site) induced by radiation are not repaired by short patch repair and are solely dependent on long patch BER repair. Inhibiting PARP1 will reduce proficiency of long patch BER thus increasing the number of DNA break sites leading to cellular DNA damage. Consistently, inhibition of long patch repair in mammalian cells has been found to result in enhanced formation of double-strand breaks (225). The presence of clustered DNA during the S phase increases the likelihood replication fork collisions; hence fork collapse-induced double-strand breaks. These unresolved DNA breaks can accumulate thereby overloading the repair process leading to activation of cellular apoptotic pathways.

9.6. Future Experiments

My study has showed that different DNA repair pathways are used by brain tumours (Glioblastoma multiforme and Medulloblastoma) to resolve damage instigated by chemotherapy and ionizing radiation. I found that, i. resolution of Topoisomerase I DNA damage is PARP/SSBR-dependent in both Glioblastoma Multiforme (GBM) and Medulloblastoma (MB) (between both brain tumour types and within these subtypes), ii. DNA alkylation in GBM is resolved co-operatively by double-strand break repair (DSBR) pathways, iii. both PARP1/SSBR and DSBR pathways resolve DNA alkylation damage in MB, iv. these treatment combinations do not have a profound effect on normal cells and are brain tumour specific, v. MB subtypes have differential responses to Topoisomerase I inhibitors in terms of DNA repair, cell proliferation, and cell death with the Sonic hedgehog subtype (DAOY) having enhanced sensitization in PARP1 inhibition and the Group 3 subtype (D283) showing resistance. This observed differential result put me on a path to identify DNA repair genes differentially regulated among the two cell lines. My RNA-seq data identified 20 potential DNA repair genes that are highly differentially regulated amongst these medulloblastoma subtypes, of which my protein expression and activity data confirmed that PARP1 is downregulated in DAOY and upregulated in D283 in addition to differential PARylation activity in these MB cell types.

Future work will involve further validation of PARP1's role in regulating Top1-induced DNA damage, likely through overexpression of PARP1 in DAOY (and/or knockdown/deletion of PARP1 in D283). Furthermore, many of the top DNA repair hits emanating from the RNA-Seq analysis will require further validation, either through qPCR or via Western Blot analysis using protein-specific antibodies (if available). Similarly, to the proposed study on PARP1, after validation target genes will be silenced via shRNA, CRISPR-CAS9 or chemical/drug inhibitors (if available) followed by validation via western blot or qPCR (if the suitable antibody is unavailable). The gene-inhibited lines will undergo treatment with drugs in presence/absence of DNA damaging agents/inhibitors to qualify their effect on overall cellular DNA repair. Repair of gene-modified cells will be measured by High-throughput Comet assay, γH2AX assay, WST-1 Cell Viability assay followed by Trypan Blue cell death assay. Furthermore, the mode of cell death is of interest; linking death to a cell death pathway would further elucidate mechanism (i.e. caspase, cytochrome c, etc.).

Based on my results in vitro, wherein I have observed candidate gene expression changes amongst cultured MB cell lines, *in vivo* tumour regression analysis, using mouse xenografts with these lines, comparing mock- and modified- tumour cell lines can be carried out. To make this study more clinically-relevant, we could compare my data/pathways with patient RNA-Seq data with the goal of identifying subtypes comprising of DNA repair enzyme expression signatures which would illuminate potential DNA damage repair-dependent treatment targets. Using clinical collaborators (i.e. Michael Taylor, Sick Kids Hospital, Toronto, ON), existing MB patient RNA-Seq data could be mined and corresponding MB tumours (with banked live cells) specifically showing DNA repair enzymes expression signatures like D283 and DAOY could be cultured and modified to develop new treatment modalities. These studies have the potential to elucidate novel drug/DDR-target combinations that will ultimately lead to the development of novel inhibitors.

During my research study, I focused on MB tumour lines. However, the wealth of data I generated using GBM lines is equally interesting and worthy of further study. The GBM lines U251MG and U373MG has been used for this project with U373MG previously documented to be representative of a resistant clonal population of GBM. I found that this tumour subtype shows remarkable damage to DNA alkylation (Methylmethane sulfonate, MMS) when co-treated with specific DNA repair inhibitors. Like the MB analysis, future experiments like WST-1 cell viability assay and cell death assay are required to correlate this drug/inhibitor combinatorial genotoxicity data with resulting cytotoxicity. Similarly, RNA-Seq could be carried out to identify target DNA damage repair enzyme/pathway candidates that underlie this sensitivity. Gene modulation experiments and *in vivo* tumour xenograft regression analysis, could be further used. Our lab has undertaken a recent complimentary GBM translational medicine collaboration (Sheila Singh, McMaster University, Hamilton, ON), wherein we have access to primary patient GBM transcriptomic data, tissue and cultures which will facilitate these studies.

9.7. Significance of the study

Topoisomerase I and PARP inhibitors are being used in a variety of clinical trials for a large complement of tumour types, including brain tumours, due their ability to enhance cellular DNA damage. Although their pharmacological action has profound effect on tumour cells, healthy cells are also subjected to toxicity. On the other hand, radiotherapy is used as the first-line cancer therapy and over time has proven to be effective in combination with DNA damaging agents.

However, tumour cells have developed innate cellular mechanisms to overcome these exogenous damages. These include decreased metabolic activation, mutations, alterations and molecular targets. One of the major abilities of tumour cells is to overcome exogenous chemo-radiotherapy associated DNA damage events through innate DNA damage response (DDR) linked with hyperactivity of DNA repair pathways.

My study involves blocking DNA repair through inhibition of specific DNA repair proteins in specific DNA repair pathways. By employing a combination of DNA damaging agents with DNA repair inhibitors, I have found that different cell lines within the same tumour and between tumours have unique therapeutic responses with specific DNA damaging agents; showing the classic intratumoral and intertumoral heterogeneity in brain tumours. With this study, I have found that with TOPI+PARP1i inhibition, Group 3 medulloblastoma confers resistance due to upregulation of PARP1 and BRCA1 in the tumour cell population while the Sonic Hedgehog (Shh) group show sensitization due to downregulation of PARP1 and BRCA1 at gene expression level. This combination has shown to be highly tumour specific in both a non-neural tumour line and normal fibroblasts which provides insight as to potential therapeutic benefit with minimal side effects. Also, radiation in combination with specific DNA repair inhibitors such as PARP1i, PARP1i+ATMi and PARP1i+DNAPKi, have shown to increase cellular DNA damage with repair. These combinatorial therapies confer their effectiveness in exerting damage to tumour cells with activation of cell death pathways confirming tumour cell death.

PARP1 inhibitors have shown promise in prostate, colon, breast cancer and are undergoing a variety of clinical trials, however; studies interrogating the combination of PARP1i with topoisomerase I inhibitors has not been performed in brain tumours. Further validation of DNA repair proteins expressed in medulloblastoma lines may highlight their role in chemo-radio-resistance and these DNA repair inhibitors may be subjected to as targeted pharmacological inhibitors for brain tumours. Employing this study from cell lines to preclinical and clinical studies, with patient samples, could help us understand the mechanism of heterogeneity among individuals. This could in the future lead to the development of precision medicine for brain tumour patients resulting in increased therapeutic efficiency with minimal side effects.

VI. REFERENCES

1. Sudhakar a. History of Cancer, Ancient and Modern Treatment Methods Akulapalli. J Cancer Sci Ther [Internet]. 2010;1(2):1–4. Available from: http://www.ncbi.nlm.nih.gov/pmc/articles/PMC2927383/pdf/nihms226784.pdf

2. Stratton MR, Campbell PJ, Futreal PA. The cancer genome. Nature [Internet]. 2009;458(7239):719–24. Available from: http://dx.doi.org/10.1038/nature07943

3. Hassanpour SH, Dehghani M. Review of cancer from perspective of molecular. J Cancer Res Pract [Internet]. 2017;4(4):127–9. Available from: http://linkinghub.elsevier.com/retrieve/pii/S2311300617300125

4. Canadian Cancer Sociey. Canadian Cancer Statistics Special topic : Pancreatic Cancers. Can Cancer Soc [Internet]. 2017;1–132. Available from: cancer.ca/Canadian-Cancer-%0AStatistics-2017-EN.pdf

5. Cancer mortality trends and projections: 2014 to 2025, All cancers combined - Australian Institute of Health and Welfare [Internet]. Available from: https://www.aihw.gov.au/reports/cancer/cancer-mortality-trends-and-projections-2014-to-2025/contents/all-cancers-combined

6. Lenoir GM. Genetic predisposition to cancer development. Rev Prat. 1995;45(15):1889–94.

7. Hanahan D, Weinberg RA. Hallmarks of cancer: The next generation. Cell [Internet]. 2011;144(5):646–74. Available from: http://dx.doi.org/10.1016/j.cell.2011.02.013

8. Hanahan D, Weinberg RA. The hallmarks of cancer. Cell [Internet]. 2000;100(1):57–70. Available from: http://www.ncbi.nlm.nih.gov/pubmed/10647931

9. Lazebnik Y. What are the hallmarks of cancer? Nat Rev Cancer [Internet]. 2010;10(4):232–3. Available from: http://dx.doi.org/10.1038/nrc2827

10. Wang M, Zhao J, Zhang L, Wei F, Lian Y, Wu Y, et al. Role of tumor microenvironment in tumorigenesis. J Cancer. 2017;8(5):761–73.

11. Gospodarowicz MK, Miller D, Groome PA, Greene FL, Logan PA, Sobin LH. The Process for Continuous Improvement of the TNM Classification. Cancer. 2004;100(1):1–5.

12. Boeker M, França F, Bronsert P, Schulz S. TNM-O: Ontology support for staging of malignant tumours. J Biomed Semantics [Internet]. 2016;7(1):1–11. Available from: http://dx.doi.org/10.1186/s13326-016-0106-9

13. Anderson MW, Reynolds SH, You M, Maronpot RM. Role of Proto-oncogene activation in carcinogenesis. Environ Health Perspect. 1992;98(9):13–24.

14. Bleich HL, Boro ES, Rowe JW. The New England Journal of Medicine Downloaded from nejm.org at UNIV OF MANITOBA LIBRARIES on November 15, 2014. For personal use only. No other uses without permission. From the NEJM Archive. Copyright © 2010 Massachusetts Medical Society. All rights res. N Engl J Med. 1997;

15. Sandoval J, Esteller M. Cancer epigenomics: Beyond genomics. Curr Opin Genet Dev [Internet]. 2012;22(1):50–5. Available from: http://dx.doi.org/10.1016/j.gde.2012.02.008

16. Land H, Parada LF, Weinberg RA. Tumorigenic conversion of primary embryo fibroblasts requires at least two cooperating oncogenes. Nature. 1983;304(5927):596–602.

17. Eliyahu D, Raz A, Gruss P, Givol D, Oren M. Participation of p53 cellular tumour antigen in transformation of normal embryonic cells. Nature. 1984;312(5995):646–9.

18. Parada LF, Land H, Weinberg RA, Wolf D, Rotter V. Cooperation between gene encoding p53 tumour antigen and ras in cellular transformation. Nature. 1984;312(5995):649–51.

19. Ortega S, Malumbres M, Barbacid M. Cyclin D-dependent kinases, INK4 inhibitors and cancer. Biochim Biophys Acta - Rev Cancer. 2002;1602(1):73–87.

20. Jackson SP, Bartek J. The DNA-damage response in human biology and disease. Nature [Internet]. 2009;461(7267):1071–8. Available from: http://dx.doi.org/10.1038/nature08467

21. Lane DP. Cancer. p53, guardian of the genome. Vol. 358, Nature. 1992. p. 15–6.

22. Kanwal R, Gupta S. Epigenetic modification in cancer. Clin Genet [Internet]. 2012;81(4):303–11. Available from: http://onlinelibrary.wiley.com/doi/10.1111/j.1399-0004.2011.01809.x/full

23. Dawson MA, Kouzarides T. Cancer epigenetics: From mechanism to therapy. Cell [Internet]. 2012;150(1):12–27. Available from: http://dx.doi.org/10.1016/j.cell.2012.06.013

24. Hassler MR, Egger G. Epigenomics of cancer - Emerging new concepts. Biochimie [Internet]. 2012;94(11):2219–30. Available from: http://dx.doi.org/10.1016/j.biochi.2012.05.007

25. Gay L, Baker A-M, Graham TA. Tumour Cell Heterogeneity. F1000Research [Internet]. 2016;5:238. Available from: http://f1000research.com/articles/5-238/v1

26. Dagogo-Jack I, Shaw AT. Tumour heterogeneity and resistance to cancer therapies. Nat Rev Clin Oncol [Internet]. 2018;15(2):81–94. Available from: http://dx.doi.org/10.1038/nrclinonc.2017.166

27. Visvader JE. Cells of origin in cancer. Nature. 2011;469(7330):314–22.

28. Canadian Cancer Society. Treatment - Canadian Cancer Society [Internet]. 2015. Available from: http://www.cancer.ca/en/cancer-information/diagnosis-and-treatment/treatment/?region=on

29. NCI; 2015. Research Areas: Treatment - National Cancer Institute [Internet]. Available from: https://www.cancer.gov/research/areas/public-health%5Cnhttps://www.cancer.gov/research/areas/treatment

30. Babcock M a, Kostova F V, Fountain J, Guha A, Packer RJ, Pollack IF, et al. Tumors of

the Central Nervous System: Clinical Aspects, Molecular Mechanisms, Unanswered Questions, and Future Research Directions. J Child Neurol. 2013;23(10):1103–21.

31. Gurney JG, Kadan-Lottick N. Brain and other central nervous system tumors: Rates, trends, and epidemiology. Curr Opin Oncol. 2001;13(3):160–6.

32. Mao Y, Demeules M, Semenciw RM, Hill G, Gaudette L, Wigle DT. Increasing brain cancer rates in Canada. Cmaj. 1991;145(12):1583–91.

33. Liu C, Zong H. Developmental origins of brain tumors. Curr Opin Neurobiol [Internet]. 2012;22(5):844–9. Available from: http://dx.doi.org/10.1016/j.conb.2012.04.012

34. Kaderali Z, Lamberti-Pasculli M, Rutka JT. The changing epidemiology of paediatric brain tumours: A review from the hospital for sick children. Child's Nerv Syst. 2009;25(7):787–93.

35. MacDonald SM. Central Nervous System Tumors in Children. Clin Radiat Oncol [Internet]. 2016;1389–1402.e3. Available from: http://linkinghub.elsevier.com/retrieve/pii/B9780323240987000678

36. Louis DN, Perry A, Reifenberger G, von Deimling A, Figarella-Branger D, Cavenee WK, et al. The 2016 World Health Organization Classification of Tumors of the Central Nervous System: a summary. Acta Neuropathol. 2016;131(6):803–20.

37. Imiela Anna PB, Polis Lech, Halina A. Novel strategies of Raman imaging for brain tumor research. Oncotarget. 2017;8(49):85290–310.

38. Ritzmann T, Grundy RG, Rahman R. The Molecular Era of Brain Tumour Research is upon us: But what now for our Patients? J Brain Tumors Neurooncology. 2016;1(3):1–2.

39. Perkins A. Primary Brain Tumors in Adults: Diagnosis and Treatment. 2016;93(3). Available from: www.aafp.org/afp

40. Stiles J, Jernigan TL. The basics of brain development. Neuropsychol Rev. 2010;20(4):327–48.

41. Pakkenberg B, Gundersen HJG. Neocortical Neuron Number in Humans : 1997;320(January):312–20.

42. Conde C, Cáceres A. Microtubule assembly, organization and dynamics in axons and dendrites. Vol. 10, Nature Reviews Neuroscience. 2009. p. 319–32.

43. Gage FH, Temple S. Neural stem cells: Generating and regenerating the brain. Neuron [Internet]. 2013;80(3):588–601. Available from: http://dx.doi.org/10.1016/j.neuron.2013.10.037

44. Gilbertson RJ, Gutmann DH. Tumorigenesis in the brain: Location, location, location. Cancer Res. 2007;67(12):5579–82.

45. Walker T, Huang J, Young K. Neural Stem and Progenitor Cells in Nervous System Function and Therapy. Stem Cells Int. 2016;2016.

46. Sylwester R. L Ecture 2 : T He N Ormal B Rain & T He D Isordered B Rain. 2003;(Rather 1978):37–66.

47. Vescovi AL, Galli R, Reynolds BA. Brain tumour stem cells. Nat Rev Cancer. 2006;6(6):425–36.

48. Brain Tumor Development - Brainlab.

49. Hanif F, Muzaffar K, Perveen K, Malhi SM, Simjee SU. Glioblastoma Multiforme: A Review of its Epidemiology and Pathogenesis through Clinical Presentation and Treatment. Asian Pac J Cancer Prev [Internet]. 2017;18(1):3–9. Available from: http://www.ncbi.nlm.nih.gov/pubmed/28239999%0Ahttp://www.pubmedcentral.nih.gov/articlerender.fcgi?artid=PMC5563115

50. Le Mercier M, Hastir D, Moles Lopez X, de Nève N, Maris C, Trepant AL, et al. A Simplified Approach for the Molecular Classification of Glioblastomas. PLoS One. 2012;7(9).

51. Maher EA, Furnari FB, Bachoo RM, Maher EA, Furnari FB, Bachoo RM, et al. Malignant glioma : genetics and biology of a grave matter Malignant glioma : genetics and biology of a grave matter. 2001;1311–33.

52. Carruthers R, Ahmed SU, Strathdee K, Gomez-Roman N, Amoah-Buahin E, Watts C, et al. Abrogation of radioresistance in glioblastoma stem-like cells by inhibition of ATM kinase. Mol Oncol [Internet]. 2015;9(1):192–203. Available from: http://www.sciencedirect.com/science/article/pii/S1574789114001859

53. Annovazzi L, Caldera V, Mellai M, Riganti C, Battaglia L, Chirio D, et al. The DNA damage/repair cascade in glioblastoma cell lines after chemotherapeutic agent treatment. Int J Oncol [Internet]. 2015;46(6):2299–308. Available from: http://www.ncbi.nlm.nih.gov/pubmed/25892134

54. Ahmed SU, Carruthers R, Gilmour L, Yildirim S, Watts C, Chalmers AJ. Selective inhibition of parallel DNA damage response pathways optimizes radiosensitization of glioblastoma stem-like cells. Cancer Res [Internet]. 2015;75(20):4416–28. Available from: http://cancerres.aacrjournals.org/cgi/doi/10.1158/0008-5472.CAN-14-3790

55. Vigneswaran K, Neill S, Hadjipanayis CG. Beyond the World Health Organization grading of infiltrating gliomas: advances in the molecular genetics of glioma classification. Ann Transl Med [Internet]. 2015;3(7):95. Available from: http://www.pubmedcentral.nih.gov/articlerender.fcgi?artid=4430738&tool=pmcentrez&rendertype=abstract

56. Kesari S. Understanding glioblastoma tumor biology: The potential to improve current diagnosis and treatments. Semin Oncol [Internet]. 2011;38(SUPPL. 4):S2–10. Available from: http://dx.doi.org/10.1053/j.seminoncol.2011.09.005

57. Anjum K, Shagufta BI, Abbas SQ, Patel S, Khan I, Shah SAA, et al. Current status and future therapeutic perspectives of glioblastoma multiforme (GBM) therapy: A review.

Biomed Pharmacother [Internet]. 2017;92:681–9. Available from: http://linkinghub.elsevier.com/retrieve/pii/S0753332217318942

58. Mischel PS, Shai R, Shi T, Horvath S, Lu K V., Choe G, et al. Identification of molecular subtypes of glioblastoma by gene expression profiling. Oncogene. 2003;22(15):2361–73.

59. Verhaak RGW, Hoadley KA, Purdom E, Wang V, Qi Y, Wilkerson MD, et al. Integrated Genomic Analysis Identifies Clinically Relevant Subtypes of Glioblastoma Characterized by Abnormalities in PDGFRA, IDH1, EGFR, and NF1. Cancer Cell [Internet]. 2010;17(1):98–110. Available from: http://dx.doi.org/10.1016/j.ccr.2009.12.020

60. Liang Y, Diehn M, Watson N, Bollen AW, Aldape KD, Nicholas MK, et al. Gene expression profiling reveals molecularly and clinically distinct subtypes of glioblastoma multiforme. Proc Natl Acad Sci [Internet]. 2005;102(16):5814–9. Available from: http://www.pnas.org/cgi/doi/10.1073/pnas.0402870102

61. Alcantara Llaguno SR, Parada LF. Cell of origin of glioma: biological and clinical implications. Br J Cancer [Internet]. 2016;115(12):1445–50. Available from: http://www.nature.com/doifinder/10.1038/bjc.2016.354

62. Ford JW, Mcvicar DW. NIH Public Access. Cancer [Internet]. 2010;19(1):38–46. Available from: http://www.pubmedcentral.nih.gov/articlerender.fcgi?artid=2886992&tool=pmcentrez&rendertype=abstract

63. Sundaresan R, Sheagren JN. Current understanding and treatment of Gliomas [Internet]. Vol. 12, Complications Surg. 1995. 261-268,274 p. Available from: https://books.google.com/books?id=_saoBQAAQBAJ&pgis=1

64. Grahovac G, Tomac D, Lambasa S, Zoric A, Habek M. Cerebellar glioblastomas: Pathophysiology, clinical presentation and management. Acta Neurochir (Wien). 2009;151(6):653–7.

65. Umar S, Baqvi A, Hammad M, Malik Z, Aziz A, Choudry UK. Understanding the current and evolving therapeutic drug regimes for Glioblastoma : A literature review iMedPub Journals Understanding the Current and Evolving Therapeutic Drug Regimes for Glioblastoma : A Literature Review Keywords : 2018;(January).

66. Mrugala MM, Chamberlain MC, Hutchinson F. Mechanisms of disease: Temozolomide and glioblastoma - Look to the future. Nat Clin Pract Oncol. 2008;5(8):476–86.

67. Zhang J, F.G. Stevens M, D. Bradshaw T. Temozolomide: Mechanisms of Action, Repair and Resistance. Curr Mol Pharmacol [Internet]. 2012;5(1):102–14. Available from: http://www.eurekaselect.com/openurl/content.php?genre=article&issn=1874-4672&volume=5&issue=1&spage=102

68. Erasimus H, Gobin M, Niclou S, Van Dyck E. DNA repair mechanisms and their clinical impact in glioblastoma [Internet]. Vol. 769, Mutation Research - Reviews in Mutation Research. Elsevier B.V.; 2016. p. 19–35. Available from:

http://dx.doi.org/10.1016/j.mrrev.2016.05.005

69. Gately L, McLachlan S, Dowling A, Philip J. Life beyond a diagnosis of glioblastoma: a systematic review of the literature. J Cancer Surviv. 2017;11(4):447–52.

70. Inda M, Bonavia R, Seoane J. Glioblastoma Multiforme: A Look Inside Its Heterogeneous Nature. 2014;226–39.

71. Van Tellingen O, Yetkin-Arik B, De Gooijer MC, Wesseling P, Wurdinger T, De Vries HE. Overcoming the blood-brain tumor barrier for effective glioblastoma treatment. Drug Resist Updat [Internet]. 2015;19:1–12. Available from: http://dx.doi.org/10.1016/j.drup.2015.02.002

72. Wong TT, Liu YL, Ho DMT, Chang KP, Liang ML, Chen HH, et al. Factors affecting survival of medulloblastoma in children: the changing concept of management. Child's Nerv Syst [Internet]. 2015;31(10):1687–98. Available from: http://link.springer.com/10.1007/s00381-015-2884-2

73. Martin AM, Raabe E, Eberhart C, Cohen KJ. Management of pediatric and adult patients with medulloblastoma. Curr Treat Options Oncol [Internet]. 2014;15(4):581–94. Available from: http://www.ncbi.nlm.nih.gov/pubmed/25194927

74. Padovani L, André N, Gentet JC, Muracciole X. Medulloblastoma. Eur J Cancer. 2011;47(SUPPL. 3):338.

75. Packer RJ, Cogen P, Vezina G, Rorke LB. Medulloblastoma: Clinical and biologic aspects. Neuro Oncol [Internet]. 1999;1(3):232–50. Available from: http://neuro-oncology.oxfordjournals.org/content/1/3/232.abstract

76. Wetmore C, Herington D, Lin T, Onar-Thomas A, Gajjar A, Merchant TE. Reirradiation of recurrent medulloblastoma: does clinical benefit outweigh risk for toxicity? Cancer [Internet]. 2014;120(23):3731–7. Available from: http://www.ncbi.nlm.nih.gov/pubmed/25080363

77. de Bont JM, Packer RJ, Michiels EM, den Boer ML, Pieters R. Biological background of pediatric medulloblastoma and ependymoma: a review from a translational research perspective. Neuro Oncol [Internet]. 2008;10(6):1040–60. Available from: http://neuro-oncology.oxfordjournals.org/cgi/content/abstract/10/6/1040%5Cnpapers3://publication/doi/10.1215/15228517-2008-059

78. DeSouza R-M, Jones BRT, Lowis SP, Kurian KM. Pediatric medulloblastoma - update on molecular classification driving targeted therapies. Front Oncol [Internet]. 2014;4(July):176. Available from: http://www.pubmedcentral.nih.gov/articlerender.fcgi?artid=4105823&tool=pmcentrez&rendertype=abstract

79. Brasme JF, Grill J, Doz F, Lacour B, Valteau-Couanet D, Gaillard S, et al. Long time to diagnosis of medulloblastoma in children is not associated with decreased survival or with worse neurological outcome. PLoS One. 2012;7(4).

80. Packer RJ, Vezina G. Management of and Prognosis With Medulloblastoma. Arch Neurol [Internet]. 2008;65(11):1419. Available from: http://archneur.jamanetwork.com/article.aspx?doi=10.1001/archneur.65.11.1419

81. Link C. Developmental Origins of Aggressive Medulloblastoma The Harvard community has made this article openly available . Please share how this access benefits you . Your story matters . 2013;

82. Rossi A, Caracciolo V, Russo G, Reiss K, Giordano A. Medulloblastoma: From molecular pathology to therapy. Clin Cancer Res. 2008;14(4):971–6.

83. Gibson P, Tong Y, Robinson G, Thompson MC, Currle DS, Eden C, et al. Origins. Nature. 2011;468(7327):1095–9.

84. Srivastava VK, Nalbantoglu J. The cellular and developmental biology of medulloblastoma: Current perspectives on experimental therapeutics. Cancer Biol Ther. 2010;9(11):843–52.

85. Sirachainan N, Nuchprayoon I, Thanarattanakorn P, Pakakasama S, Lusawat A, Visudibhan A, et al. Outcome of medulloblastoma in children treated with reduced-dose radiation therapy plus adjuvant chemotherapy. J Clin Neurosci [Internet]. 2011;18(4):515–9. Available from: http://dx.doi.org/10.1016/j.jocn.2010.08.012

86. Experience H. Medullob lastoma. 1954;56–60.

87. Northcott PA, Korshunov A, Witt H, Hielscher T, Eberhart CG, Mack S, et al. Medulloblastoma comprises four distinct molecular variants. J Clin Oncol. 2011;29(11):1408–14.

88. Parsons DW, Li M, Zhang X, Jones S, Leary RJ, Lin JC-H, et al. Supp: The genetic landscape of the childhood cancer medulloblastoma. Science (80-) [Internet]. 2011;331(6016):435–9. Available from: http://www.pubmedcentral.nih.gov/articlerender.fcgi?artid=3110744&tool=pmcentrez&rendertype=abstract

89. Taylor MD, Northcott PA, Korshunov A, Remke M, Cho YJ, Clifford SC, et al. Molecular subgroups of medulloblastoma: The current consensus. Acta Neuropathol. 2012;123(4):465–72.

90. Gibson P, Tong Y, Robinson G, Thompson MC, Currle DS, Eden C, et al. Subtypes of medulloblastoma have distinct developmental origins. Nature [Internet]. 2010;468(7327):1095–9. Available from: http://dx.doi.org/10.1038/nature09587

91. Cavalli FMG, Remke M, Rampasek L, Peacock J, Shih DJH, Luu B, et al. Intertumoral Heterogeneity within Medulloblastoma Subgroups. Cancer Cell. 2017;31(6):737–754.e6.

92. Kumar, V., McGuire, T., Coulter, D.W., Sharp, J.G., Mahato RI. Challenges and Recent Advances in Meulloblastoma Therapy. Cell Press. 2017;38(12):1061–84.

93. Hennika T, Gururangan S. Childhood medulloblastoma: current and future treatment

strategies. Expert Opin Orphan Drugs [Internet]. 2015;3(11):1299–317. Available from: http://www.tandfonline.com/doi/full/10.1517/21678707.2015.1087311

94. Whelan HT, Krouwer HG, Schmidt MH, Reichert KW, Kovnar EH. Current therapy and new perspectives in the treatment of medulloblastoma. Pediatr Neurol [Internet]. 1998;18(2):103–15. Available from: http://ac.els-cdn.com/S088789949700221X/1-s2.0-S088789949700221X-main.pdf?_tid=7588bc84-59af-11e3-936d-00000aacb35d&acdnat=1385809767_5b9584d5c068a4b676e8204044dc4a95

95. Mazza C, Pasqualin A, Da Pian R, Donati E. Treatment of medulloblastoma in children: long-term results following surgery, radiotherapy and chemotherapy. Acta Neurochir [Internet]. 1981;57(3–4):163–75. Available from: http://www.ncbi.nlm.nih.gov/entrez/query.fcgi?cmd=Retrieve&db=PubMed&dopt=Citation&list_uids=7282444

96. Evans AE, Jenkin RDT, Sposto R, Ortega JA, Wilson CB, Wara W, et al. The treatment of medulloblastoma. J Neurosurg [Internet]. 1990;72(4):572–82. Available from: http://www.ncbi.nlm.nih.gov/pubmed/2319316%0Ahttp://thejns.org/doi/10.3171/jns.1990.72.4.0572

97. Cumberlin RL, Luk KH, Wara WM, Sheline GE, Wilson CB. Medulloblastoma.Treatment results and effect on normal tissues. Cancer [Internet]. 1979;43(3):1014–20. Available from: http://doi.wiley.com/10.1002/1097-0142%28197903%2943%3A3%3C1014%3A%3AAID-CNCR2820430334%3E3.0.CO%3B2-9

98. Gudrunardottir T, Lannering B, Remke M, Taylor MD, Wells EM, Keating RF, et al. Treatment developments and the unfolding of the quality of life discussion in childhood medulloblastoma: A review. Child's Nerv Syst. 2014;30(6):979–90.

99. Sheline GE. Radiation therapy of brain tumors. Cancer [Internet]. 1977;39(2 Suppl):873–81. Available from: http://www.ncbi.nlm.nih.gov/pubmed/837351

100. de B, Beal K, de Braganca KC, Souweidane MM, Dunkel IJ, Khakoo Y, et al. Long-term outcomes of adult medulloblastoma patients treated with radiotherapy. J Neurooncol [Internet]. 2017;136(1):1–10. Available from: http://dx.doi.org/10.1007/s11060-017-2627-1

101. Van Dyk J, T. Jenkin RD, Leung PMK, Cunningham JR. Medulloblastoma: Treatment technique and radiation dosimetry. Int J Radiat Oncol Biol Phys. 1977;2(9–10):993–1005.

102. Packer RJ, Sutton LN, Elterman R, Lange B, Goldwein J, Nicholson HS, et al. Outcome for children with medulloblastoma treated with radiation and cisplatin, CCNU, and vincristine chemotherapy. J Neurosurg [Internet]. 1994;81(5):690–8. Available from: http://thejns.org/doi/10.3171/jns.1994.81.5.0690

103. Miralbell R, Bleher A, Huguenin P, Ries G, Kann R, Mirimanoff RO, et al. Pediatric medulloblastoma: Radiation treatment technique and patterns of failure. Int J Radiat Oncol Biol Phys. 1997;37(3):523–9.

104. Mori K, Kurisaka M. Brain tumors in childhood: statistical analysis of cases from the Brain Tumor Registry of Japan*. Child's Nerv Syst [Internet]. 1986;2:233–7. Available from: http://download.springer.com.ezp-prod1.hul.harvard.edu/static/pdf/62/art%253A10.1007%252FBF00272492.pdf?originUrl=http%3A%2F%2Flink.springer.com%2Farticle%2F10.1007%2FBF00272492&token2=exp=1491859086~acl=%2Fstatic%2Fpdf%2F62%2Fart%25253A10.1007%25252FBF00

105. Santivasi WL, Xia F. The role and clinical significance of DNA damage response and repair pathways in primary brain tumors. 2013;1–6.

106. Janss AJ, Cnaan A, Zhao H, Shpilsky A, Levow C, Sutton L, et al. Synergistic cytotoxicity of topoisomerase I inhibitors with alkylating agents and etoposide in human brain tumor cell lines. [Internet]. Vol. 9, Anti-cancer drugs. 1998. p. 641–52. Available from: http://www.ncbi.nlm.nih.gov/pubmed/9773809

107. Danks MK, Pawlik CA, Whipple DO, Wolverton JS. Intermittent exposure of medulloblastoma cells to topotecan produces growth inhibition equivalent to continuous exposure. Clin Cancer Res. 1997;3(10):1731–8.

108. Laird AD, Cherrington JM. Small molecule tyrosine kinase inhibitors: clinical development of anticancer agents. Expert Opin Investig Drugs [Internet]. 2003;12(1):51–64. Available from: http://www.tandfonline.com/doi/full/10.1517/13543784.12.1.51

109. Iqbal N, Iqbal N. Imatinib: A Breakthrough of Targeted Therapy in Cancer. Chemother Res Pract [Internet]. 2014;2014:1–9. Available from: http://www.hindawi.com/journals/cherp/2014/357027/

110. Pao W, Miller V, Zakowski M, Doherty J, Politi K, Sarkaria I, et al. EGF receptor gene mutations are common in lung cancers from "never smokers" and are associated with sensitivity of tumors to gefitinib and erlotinib. Proc Natl Acad Sci [Internet]. 2004;101(36):13306–11. Available from: http://www.pnas.org/cgi/doi/10.1073/pnas.0405220101

111. Baryawno N, Sveinbjörnsson B, Eksborg S, Chen CS, Kogner P, Johnsen JI. Small-molecule inhibitors of phosphatidylinositol 3-kinase/Akt signaling inhibit Wnt/β-catenin pathway cross-talk and suppress medulloblastoma growth. Cancer Res. 2010;70(1):266–76.

112. Phoenix TN, Patmore DM, Boop S, Boulos N, Jacus MO, Patel YT, et al. Medulloblastoma Genotype Dictates Blood Brain Barrier Phenotype. Cancer Cell [Internet]. 2016;29(4):508–22. Available from: http://dx.doi.org/10.1016/j.ccell.2016.03.002

113. Ciccia A, Elledge SJ. The DNA Damage Response: Making It Safe to Play with Knives. Mol Cell. 2010;40(2):179–204.

114. Barnum KJ. Cell Cycle Control. 2014;1170:1–11. Available from: http://link.springer.com/10.1007/978-1-4939-0888-2

115. Niida H, Nakanishi M. DNA damage checkpoints in mammals. Mutagenesis. 2006;21(1):3–9.

116. Patil M, Pabla N, Dong Z. Checkpoint kinase 1 in DNA damage response and cell cycle regulation. 2014;70(21):4009–21.

117. Walworth NC. Cell-cycle checkpoint kinases: Checking in on the cell cycle. Curr Opin Cell Biol. 2000;12(6):697–704.

118. Zhou BS, Elledge SJ. Checkpoints in perspective. Nature. 2000;408(November):433–9.

119. McGowan CH, Russell P. The DNA damage response: Sensing and signaling. Curr Opin Cell Biol. 2004;16(6):629–33.

120. Abraham RT. cell cycle checkpoint signaling therough the ATM an ATR kinases.pdf. Genes Dev. 2001;15:2177–96.

121. Lisby M, Rothstein R. DNA damage checkpoint and repair centers. Curr Opin Cell Biol. 2004;16(3):328–34.

122. Blackford AN, Jackson SP. ATM, ATR, and DNA-PK: The Trinity at the Heart of the DNA Damage Response. Mol Cell [Internet]. 2017;66(6):801–17. Available from: http://dx.doi.org/10.1016/j.molcel.2017.05.015

123. Flynn RL, Zou L. ATR: A master conductor of cellular responses to DNA replication stress. Trends Biochem Sci. 2011;36(3):133–40.

124. Weinert T. DNA Damage and Checkpoint Pathways. Cell [Internet]. 1998;94(5):555–8. Available from: http://linkinghub.elsevier.com/retrieve/pii/S0092867400815974

125. Bartek J, Bartkova J, Lukas J. DNA damage signalling guards against activated oncogenes and tumour progression. Oncogene. 2007;26(56):7773–9.

126. Durocher D, Jackson SP. DNA-PK, ATM and ATR as sensors of DNA damage: Variations on a theme? Curr Opin Cell Biol. 2001;13(2):225–31.

127. Shiloh Y, Ziv Y. The ATM protein kinase: Regulating the cellular response to genotoxic stress, and more [Internet]. Vol. 14, Nature Reviews Molecular Cell Biology. Nature Publishing Group; 2013. p. 197–210. Available from: http://dx.doi.org/10.1038/nrm3546

128. Kitagawa R, Kastan MB. The ATM-dependent DNA Damage Signaling Pathway The ATM-dependent DNA Damage Signaling Pathway. 2005;LXX:99–109.

129. Zgheib O, Huyen Y, DiTullio RA, Snyder A, Venere M, Stavridi ES, et al. ATM signaling and 53BP1. Radiother Oncol. 2005;76(2):119–22.

130. Shiloh Y. The ATM-mediated DNA-damage response. Mol Oncol Causes Cancer Targets Treat. 2015;31(7):403–22.

131. Signalling DNA Damage (Intech, 2012).

132. Kurz EU, Lees-Miller SP. DNA damage-induced activation of ATM and ATM-dependent signaling pathways. Vol. 3, DNA Repair. 2004. p. 889–900.

133. Zou L, Stephen J E. ATRIP Recognition of RPA-ssDNA. Science (80-). 2003;300(June):1542–8.

134. Kinases ATR. DNA Damage Sensing by the ATM and. 2017;1–18.

135. Harper JW, Elledge SJ. The DNA Damage Response: Ten Years After. Mol Cell. 2007;28(5):739–45.

136. Shiotani B, Nguyen HD, Håkansson P, Maréchal A, Tse A, Tahara H, et al. Two Distinct Modes of ATR Activation Orchestrated by Rad17 and Nbs1. Cell Rep. 2013;3(5):1651–62.

137. Kelley MR, Logsdon D, Fishel ML. Targeting DNA repair pathways for cancer treatment: what's new? Futur Oncol [Internet]. 2014;10(7):1215–37. Available from: http://www.ncbi.nlm.nih.gov/pubmed/24947262

138. Khanna KK, Jackson SP. DNA double-strand breaks: signalling, repair and the cancer connection. Nat Genet. 2001;27(march):247–54.

139. Chapman JR, Taylor MRG, Boulton SJ. Playing the End Game: DNA Double-Strand Break Repair Pathway Choice. Mol Cell [Internet]. 2012;47(4):497–510. Available from: http://dx.doi.org/10.1016/j.molcel.2012.07.029

140. Ceccaldi R, Rondinelli B, D'Andrea AD. Repair Pathway Choices and Consequences at the Double-Strand Break. Trends Cell Biol [Internet]. 2016;26(1):52–64. Available from: http://dx.doi.org/10.1016/j.tcb.2015.07.009

141. Lavin MF. Ataxia-telangiectasia: from a rare disorder to a paradigm for cell signalling and cancer. Nat Rev Mol Cell Biol. 2008;9(10):759–69.

142. Burma S, Chen DJ. Role of DNA-PK in the cellular response to DNA double-strand breaks. DNA Repair (Amst). 2004;3(8–9):909–18.

143. Weterings E, Chen DJ. The endless tale of non-homologous end-joining. Cell Res. 2008;18(1):114–24.

144. Davis A, Chen D. DNA double strand break repair via non-homologous end-joining. Transl Cancer Res [Internet]. 2013;2(3):130–43. Available from: http://www.ncbi.nlm.nih.gov/pmc/articles/PMC3758668/

145. Lieber MR, Ma Y, Pannicke U, Schwarz K. Mechanism and regulation of human non-homologous DNA end-joining. Nat Rev Mol Cell Biol. 2003;4(9):712–20.

146. Helleday T, Lo J, van Gent DC, Engelward BP. DNA double-strand break repair: From mechanistic understanding to cancer treatment. DNA Repair (Amst). 2007;6(7):923–35.

147. Haber JE. Partners and pathways - Repairing a double-strand break. Trends Genet. 2000;16(6):259–64.

148. Rothkamm K, Krüger I, Thompson LH, Kru I, Lo M. Pathways of DNA Double-Strand Break Repair during the Mammalian Cell Cycle Pathways of DNA Double-Strand Break Repair during the Mammalian Cell Cycle. Mol Cell Biol. 2003;23(16):5706–15.

149. Prakash R, Zhang Y, Feng W, Jasin M. Homologous Recombination and Human Health. Perspect Biol. 2015;1–29.

150. Nussenzweig A, Nussenzweig MC. A Backup DNA Repair Pathway Moves to the Forefront. Cell. 2007;131(2):223–5.

151. Dueva R, Iliakis G. Alternative pathways of non-homologous end joining (NHEJ) in genomic instability and cancer. Transl Cancer Res. 2013;2(3):163–77.

152. Chang HHY, Pannunzio NR, Adachi N, Lieber MR. Non-homologous DNA end joining and alternative pathways to double-strand break repair. Nat Rev Mol Cell Biol [Internet]. 2017;18(8):495–506. Available from: http://www.nature.com/doifinder/10.1038/nrm.2017.48

153. Caldecott KW. Single-strand break repair and genetic disease. Nat Rev Genet. 2008;9(8):619–31.

154. Caldecott KW. DNA single-strand break repair and spinocerebellar ataxia. Cell. 2003;112(1):7–10.

155. Xu Y, Her C. Inhibition of topoisomerase (DNA) I (TOP1): DNA damage repair and anticancer therapy. Biomolecules. 2015;5(3):1652–70.

156. Okano S, Kanno SI, Nakajima S, Yasui A. Cellular responses and repair of single-strand breaks introduced by UV damage endonuclease in mammalian cells. J Biol Chem. 2000;275(42):32635–41.

157. Bolderson E, Richard DJ, Zhou B-BS, Khanna KK. Recent Advances in Cancer Therapy Targeting Proteins Involved in DNA Double-Strand Break Repair. Clin Cancer Res [Internet]. 2009;15(20):6314–20. Available from: http://clincancerres.aacrjournals.org/content/15/20/6314.full.html#ref-list-1

158. Lieff J. The Many Ways Neurons Repair Their Own DNA. 2014. p. 1–6.

159. Bai P, Cantó C. The role of PARP-1 and PARP-2 enzymes in metabolic regulation and disease. Cell Metab. 2012;16(3):290–5.

160. D'Arcangelo M, Drew Y, Plummer R. The role of PARP in DNA repair and its therapeutic exploitation. DNA Repair Cancer Ther Mol Targets Clin Appl Second Ed [Internet]. 2016;105(8):115–34. Available from: http://dx.doi.org/10.1038/bjc.2011.382

161. Jagtap P, Szabo C. Poly(ADP-ribose) polymerase and the therapeutic effects of its inhibitors. Nat Rev Drug Discov. 2005;4(5):421–40.

162. Caldecott KW. Mammalian single-strand break repair: Mechanisms and links with chromatin. DNA Repair (Amst). 2007;6(4):443–53.

163. Vens C, Begg AC. Targeting base excision repair as a sensitization strategy in radiotherapy [Internet]. Vol. 20, Seminars in Radiation Oncology. 2010. p. 241–9. Available from: http://www.ncbi.nlm.nih.gov/pubmed/20832016

164. Fortini P, Dogliotti E. Base damage and single-strand break repair: Mechanisms and functional significance of short- and long-patch repair subpathways. DNA Repair (Amst). 2007;6(4):398–409.

165. Rass U, Ahel I, West SC. Review Defective DNA Repair and Neurodegenerative Disease. 2007;991–1004.

166. Hoeijmakers JHJ. Genome maintenance mechanisms for preventing cancer. Vol. 411, Nature. 2001. p. 366–74.

167. McKinnon PJ. DNA repair deficiency and neurological disease. Nat Rev Neurosci [Internet]. 2009;10(2):100–12. Available from: http://www.pubmedcentral.nih.gov/articlerender.fcgi?artid=3064843&tool=pmcentrez&rendertype=abstract

168. Rao KS. Mechanisms of disease: DNA repair defects and neurological disease. Vol. 3, Nature Clinical Practice Neurology. 2007. p. 162–72.

169. Woods CG V. REGULAR REVIEW DNA repair disorders. 1998;178–84.

170. Martin LJ. R EVIEW A RTICLE DNA Damage and Repair : Relevance to Mechanisms of Neurodegeneration. 2018;67(5):377–87.

171. Rolig RL, McKinnon PJ. Linking DNA damage and neurodegeneration. Trends Neurosci. 2000;23(9):417–24.

172. Broustas CG, Lieberman HB. REVIEW DNA Damage Response Genes and the Development of Cancer Metastasis. 2014;130:111–30.

173. Schumacher B. DNA repair mechanisms in cancer. 2015;6(April):1–15.

174. Dasika GK, Lin SJ, Zhao S, Sung P, Tomkinson A, Lee EYP. DNA damage-induced cell cycle checkpoints and DNA strand break repair in development and tumorigenesis. 1999;7883–99.

175. Lord CJ, Ashworth A. The DNA damage response and cancer therapy. Nature. 2012;481(7381):287–94.

176. Hansson J. INHERITED DEFECTS IN DNA-REPAIR AND SUSCEPTIBILITY TO DNA-DAMAGING AGENTS. Toxicol Lett. 1992;64–5:141–8.

177. Cheung-ong K, Giaever G, Nislow C. Perspective DNA-Damaging Agents in Cancer Chemotherapy : Serendipity and Chemical Biology. Chem Biol [Internet]. 2013;20(5):648–59. Available from: http://dx.doi.org/10.1016/j.chembiol.2013.04.007

178. Hematology-oncology P, Pharmacology C, Pharmacology C, Ii T. Topoisomerase I Inhibitors. 1997;359–64.

179. Pommier Y. Topoisomerase I inhibitors : camptothecins and beyond. 2006;6:789–802.

180. Kondo N, Takahashi A, Ono K, Ohnishi T. DNA Damage Induced by Alkylating Agents and Repair Pathways. J Nucleic Acids [Internet]. 2010;2010:1–7. Available from: http://www.hindawi.com/journals/jna/2010/543531/

181. Drabløs F, Feyzi E, Aas PA, Vaagbø CB, Kavli B, Bratlie MS, et al. Alkylation damage in DNA and RNA - Repair mechanisms and medical significance. DNA Repair (Amst). 2004;3(11):1389–407.

182. Fu D, Calvo JA, Samson LD. Balancing repair and tolerance of DNA damage caused by alkylating agents. 2012;12(February).

183. Mchugh PJ, Spanswick VJ, Hartley JA. Repair of DNA interstrand crosslinks : molecular mechanisms and clinical relevance. 44(0):483–90.

184. Manuscript A. NIH Public Access. 2013;2(3):144–54.

185. Rajski SR, Williams RM. DNA Cross-Linking Agents as Antitumor Drugs. 1998;

186. Andrea ADD, Haseltine WA. Sequence specific cleavage of DNA by the antitumor antibiotics neocarzinostatin and bleomycin. 1978;75(8):3608–12.

187. Hosoya N, Miyagawa K. Clinical importance of DNA repair inhibitors in cancer therapy. 2009;2:9–14.

188. Velic D, Couturier AM, Ferreira MT, Rodrigue A, Poirier GG, Fleury F, et al. DNA damage signalling and repair inhibitors: The long-sought-after achilles' heel of cancer. Vol. 5, Biomolecules. 2015. p. 3204–59.

189. Rouleau M, Patel A, Hendzel MJ, Kaufmann SH, Poirier GG. PARP inhibition: PARP1 and beyond. Nat Rev Cancer [Internet]. 2010;10(4):293–301. Available from: http://dx.doi.org/10.1038/nrc2812

190. Malyuchenko N V., Kotova EY, Kulaeva OI, Kirpichnikov MP, Studitskiy VM. PARP1 Inhibitors: Antitumor drug design. Acta Naturae. 2015;7(3):27–37.

191. Ashworth A. A Synthetic Lethal Therapeutic Approach : Poly (ADP) Ribose Polymerase Inhibitors for the Treatment of Cancers Deficient in DNA Double-Strand Break Repair. 2018;26(22):3785–90.

192. Tentori L, Graziani G. Chemopotentiation by PARP inhibitors in cancer therapy. Pharmacol Res. 2005;52(1 SPEC. ISS.):25–33.

193. Weber AM, Ryan AJ. ATM and ATR as therapeutic targets in cancer [Internet]. Vol. 149, Pharmacology and Therapeutics. Elsevier B.V.; 2015. p. 124–38. Available from: http://dx.doi.org/10.1016/j.pharmthera.2014.12.001

194. Martin AR. ATM, ATR, CHK1, CHK2 and WEE1 inhibitors in cancer and cancer stem cells. 2017;295–319.

195. Gavande NS, Vandervere-Carozza PS, Hinshaw HD, Jalal SI, Sears CR, Pawelczak KS, et al. DNA repair targeted therapy: The past or future of cancer treatment? [Internet]. Vol. 160, Pharmacology and Therapeutics. The Authors; 2016. p. 65–83. Available from: http://dx.doi.org/10.1016/j.pharmthera.2016.02.003

196. Sánchez-Pérez I. DNA repair inhibitors in cancer treatment. Clin Transl Oncol. 2006;8(9):642–6.

197. Davidson D, Amrein L, Panasci L, Aloyz R. Small molecules , inhibitors of DNA-PK , targeting DNA repair , and beyond. 2013;4(January):1–7.

198. Longley DB, Johnston PG. Molecular mechanisms of drug resistance. J Pathol. 2005;205(2):275–92.

199. Dagogo-Jack I, Shaw AT. Tumour heterogeneity and resistance to cancer therapies. Nat Rev Clin Oncol [Internet]. 2018;15(2):81–94. Available from: http://dx.doi.org/10.1038/nrclinonc.2017.166

200. Marusyk A, Almendro V, Polyak K. Intra-tumour heterogeneity: A looking glass for cancer? Nat Rev Cancer [Internet]. 2012;12(5):323–34. Available from: http://dx.doi.org/10.1038/nrc3261

201. Baguley BC. Multiple drug resistance mechanisms in cancer. Mol Biotechnol. 2010;46(3):308–16.

202. Tsuruo T, Naito M, Tomida A, Fujita N, Mashima T, Sakamoto H, et al. Molecular targeting therapy of cancer: drug resistance, apoptosis and survival signal. Cancer Sci [Internet]. 2003;94(1):15–21. Available from: http://doi.wiley.com/10.1111/j.1349-7006.2003.tb01345.x%5Cnhttp://www.ncbi.nlm.nih.gov/entrez/query.fcgi?cmd=Retrieve&db=PubMed&dopt=Citation&list_uids=12708468

203. Holohan C, Van Schaeybroeck S, Longley DB, Johnston PG. Cancer drug resistance: An evolving paradigm. Nat Rev Cancer [Internet]. 2013;13(10):714–26. Available from: http://dx.doi.org/10.1038/nrc3599

204. Florea A-M, Büsselberg D. Cisplatin as an Anti-Tumor Drug: Cellular Mechanisms of Activity, Drug Resistance and Induced Side Effects. Cancers (Basel) [Internet]. 2011;3(4):1351–71. Available from: http://www.mdpi.com/2072-6694/3/1/1351/

205. Brown JS, Carrigan BO, Jackson SP, Yap TA. Targeting DNA Repair in Cancer : Beyond PARP Inhibitors. 2017;(January):20–38.

206. Esteller M, Hamilton SR, Burger PC, Baylin SB, Herman JG. Inactivation of the DNA Repair Gene O 6 - Methylguanine-DNA Methyltransferase by Promoter Hypermethylation is a Common Event in Primary Human Neoplasia Advances in Brief Inactivation of the DNA Repair Gene O 6 - Methylguanine-DNA Methyltransferase by Prom. Cancer Res. 1999;793–7.

207. Kim R. Recent advances in understanding the cell death pathways activated by anticancer therapy. Cancer. 2005;103(8):1551–60.

208. Ouyang L, Shi Z, Zhao S, Wang FT, Zhou TT, Liu B, et al. Programmed cell death pathways in cancer: A review of apoptosis, autophagy and programmed necrosis. Cell Prolif. 2012;45(6):487–98.

209. Borges HL, Linden R, Wang JYJ. DNA damage-induced cell death. 2009;18(1):17–26.

210. Wang JY. DNA damage and apoptosis. Cell Death Differ [Internet]. 2001;8(11):1047–8. Available from: http://www.ncbi.nlm.nih.gov/pubmed/11687882

211. Roos WP, Kaina B. DNA damage-induced cell death by apoptosis. Trends Mol Med. 2006;12(9):440–50.

212. Norbury CJ, Zhivotovsky B. DNA damage-induced apoptosis. Oncogene. 2004;23(16 REV. ISS. 2):2797–808.

213. October TBS, Zamble DB, Lippard SJ. Ci @ atin # NA repair in c cer ch othe py. October [Internet]. 1995;20(Iv):435–9. Available from: http://www.ncbi.nlm.nih.gov/pubmed/8533159

214. Kumar S. Caspase 2 in apoptosis, the DNA damage response and tumour suppression: Enigma no more? Nat Rev Cancer. 2009;9(12):897–903.

215. Zhivotovsky B, Orrenius S. Caspase-2 function in response to DNA damage. Biochem Biophys Res Commun. 2005;331(3):859–67.

216. Kitazumi I, Tsukahara M. Regulation of DNA fragmentation: The role of caspases and phosphorylation. FEBS J. 2011;278(3):427–41.

217. Bröker LE, Kruyt FAE, Giaccone G. Cell death Independent of Caspases:A Review. Clin Cancer Res. 2005;11(9):3155–62.

218. Larson B, Instruments B. p p l i c a t i o n o t e Automated Comet Assay Imaging and Dual-Mask Analysis to Determine DNA Damage on an Individual Comet Basis. 2016;

219. Roche. Cell Proliferation Reagent WST-1. Cell Prolif. 2007;1(11):1–4.

220. Ozsolak F, Milos PM. RNA sequencing: advances, challenges and opportunities. Nat Rev Genet [Internet]. 2010;94(1):19–34. Available from: http://dx.doi.org/10.1038/nrg2934

221. Rev A, Hum G, Downloaded G, Mckinnon PJ, Caldecott KW. DNA Strand Break Repair and Human Genetic Disease. 2007;

222. Shiloh Y. The ATM-mediated DNA-damage response : taking shape. 2006;31(7).

223. Hoeijmakers JHJ. for preventing cancer. 2001;366–74.

224. Morandell S, Yaffe MB. Exploiting Synthetic Lethal Interactions Between DNA Damage Signaling , Checkpoint Control , and p53 for Targeted Cancer Therapy I . Introduction A . Targeting Cancer Genes in the Context of DNA Damage [Internet]. 1st ed. Vol. 110, Mechanisms of DNA Repair. Elsevier Inc.; 2012. 289-314 p. Available from: http://dx.doi.org/10.1016/B978-0-12-387665-2.00011-0

225. Lomax ME, Folkes LK, O'Neill P. Biological consequences of radiation-induced DNA damage: Relevance to radiotherapy. Clin Oncol [Internet]. 2013;25(10):578–85. Available from: http://dx.doi.org/10.1016/j.clon.2013.06.007

226. Rich JN. Cancer Stem Cells in Radiation Resistance. 2007;(19):8980–5.

227. Tichý A, Novotná E, Ďurišová K, Šalovská B, Sedlaříková R, Pejchal J, et al. Radio-sensitization of human leukaemic MOLT-4 cells by DNA-dependent protein kinase inhibitor , NU7026. Acta Medica Cordoba [Internet]. 2012;55(2):66–73. Available from: https://dx.doi.org/10.14712/18059694.2015.57

APPENDIX: ESTABLISHMT OF STABLE REPORTER LINES

1. Introduction

DNA comprises of genetic information and maintenance of the integrity of this molecule is essential for cell function, homeostasis and survival (1). However, DNA is not inert and is imperiled by constant endogenous and exogenous stress (2). Cells incur over 100,000 DNA lesions every day. DNA lesions emanate in various forms like base damage, DNA-protein crosslinks, single strand breaks (SSBs), double-strand breaks (DSBs) and intra/inter-strand crosslinks (1)(2).

DNA double strand breaks are considered the most deleterious, arising mostly from ionizing radiation and activates programmed cell death when the lesion is irreparable. Studies have shown that one DSB occurs per 108 bp (1) in a genome of about 1.2x 107 bp. Approximately 1% of SSBs are converted to DSBs per cell per cycle(3). The remaining 99% SSBs are repaired while the 1% DSBs produces 50 endogenous DSBs per nucleus during each cell cycle (4). Double strand breaks are formed during differentiation of reproductive cells or lymphocytes, oxidative stress and exogenous factors such as radiation, drugs and other environmental factors (5). These toxic DNA lesions, if not repaired, can lead to degeneration, pathogenesis and tumorigenesis. Mammalian cells have evolved inherent sensor proteins for recognition of specific damage, and effector proteins are activated to resolve DNA damage through functionally distinct repair mechanisms (4). Furthermore, these are linked with cell cycle checkpoints and mechanisms to ensure either cell repair or death prevails.

1.1. H2AX histone

Histones are alkaline proteins which are found in all eukaryotic organisms (6). In eukaryotes, there are four histone H2A subfamilies such as H2A1, H2A2, H2AZ, and H2AX (7). Eight histone molecules (two copies of each H2A, H2B, H3, and H4) binds with 145 base pair of DNA to form structural units called nucleosomes (6). Histones are subjected to post translational modifications such as acetylation, phosphorylation, methylation, ubiquitination, and ribosylation (8). These histone modifications are involved in cellular processes like DNA repair, gene regulation, chromosome condensation and spermatogenesis (6)(8).

Previous studies have shown that the level of nuclear histone H2AX varies from 2-25% of the total mammalian H2A pool but is highly dependant on the cell line or tissue (5). In human fibroblasts, 10% of pool of H2A is H2AX, consisting of 6106 molecules of H2AX per cell (4)(7). H2AX is found in eukaryotes as a C-terminal extension with a SQ (E/D) (I/L/F/Y) motif (5). H2AX is

integral for the cellular response to DNA repair, regulation of cell division, cell growth, immuno-receptor rearrangement. It is associated with a variety of DNA repair dysfunction syndromes and plays a major role in genomic instability in humans leading to cancer (7)(5).

1.2. γH2AX phosphorylation

A major step in repairing double-strand breaks is phosphorylation of the histone variant H2AX, known as γH2AX. This phosphorylation of H2AX takes place on the serine 139 residue in the mega basepair chromatin region surrounding the breaks. As multiple H2AX subunits are engaged with DNA at any corresponding break site, a DNA break will engage of protein signaling cascade that will induce phosphorylation of multiple proximal H2AX histones. Immune-detection of these phospho-H2AX sites using anti-phospho-ser-139 H2AX antibody along with a fluorophore-conjugated secondary antibody will stain these multiple proximal sites and under epifluorescence microscopy, these sites are visualized as a collection of immune-reactive nuclear sites often referred to as a distinct γH2AX foci (Figure-1.1b) (5)(4)(9). This γH2AX signal localizes to discrete foci-marked sites of cellular DNA damage with the number of foci correlating with the number of DNA break sites. Phosphatidylinositol 3-kinase-related kinases (PIKK) ataxia telangiectasia mutated (ATM), DNA-dependent protein kinase (DNA–PK) and ataxia telangiectasia and Rad3-related (ATR) phosphorylate H2AX (5)(4), in response to different DNA damaging stimulus. ATR phosphorylates H2AX during replication fork arrest and SSB induction, DNA-PK during hypertonic conditions and apoptotic DNA fragmentation (4). All three phosphatidylinositol 3-kinase-related kinases (PIKK) ATM, ATR and DNA-PK, phosphorylate H2AX in response to ionizing radiation (5).

In response to DSBs (Figure-1.1a), ATM is activated and interacts with Mediator of DNA damage checkpoint 1 (MDC1) where the MDC1-ATM complex is recruited to the damage site (Figure-1.1b)(10). ATM is then released from the site of damage to phosphorylate distant molecules like the chromatin-associated histone (11), H2AX on Ser139 (3). H2AX phosphorylation spreads to about 1-2 megabases in an ATM-MDC1 mediated manner. MDC1 directly binds to Ser139 via its C terminal BRCT domain (3). Phosphorylated H2AX, γH2AX, binds with this complex, hence stabilizing the attachment of MDC1-ATM to DSB site (12). ATM then recruits more H2AX in the process to bind to more MDC1 molecules. This ongoing process builds a driving force for phosphorylated H2AX to create a platform for recruiting more DNA damage repair proteins (13),

such as MRE11/NBS1/RAD50 (MRN complex), MDC1, 53BP1, and BRCA1 to the damage site where all these proteins colocalize and interact with γH2AX (4)(Figure-1.1c). These repair proteins recognize and bind specifically to the phosphorylated carboxy terminus of γH2AX, which then induces G2/M checkpoint arrest to allow repair of DSBs (4)(Figure-1.1d).

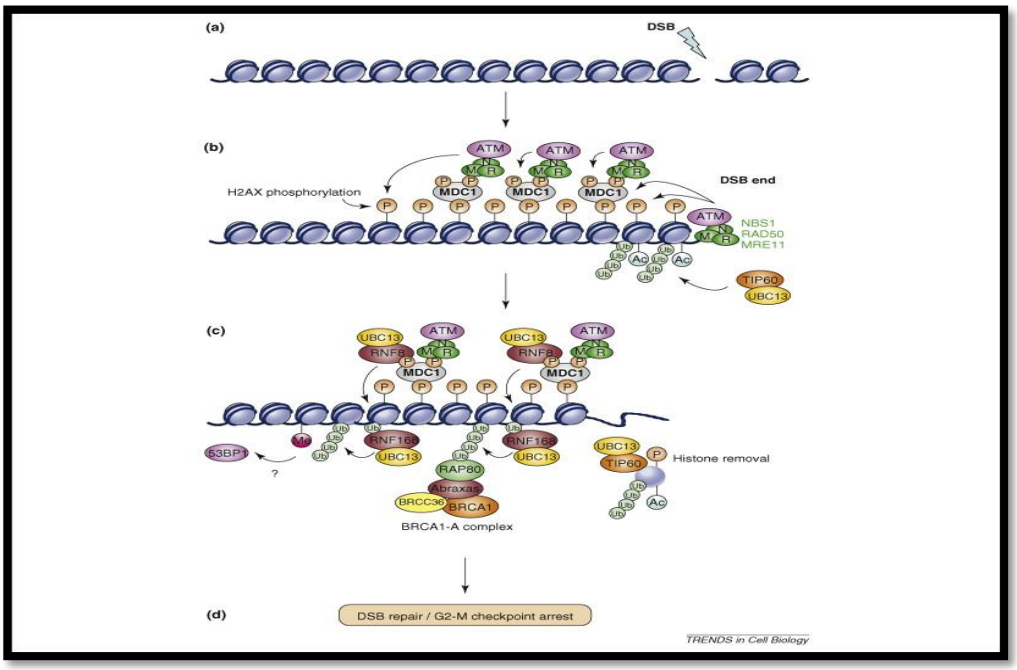

Figure-1.1. (a) Endogenous and exogenous DNA damage forms double-strand breaks (b) ATM recruitment to the damage site and formation of ATM-MDC1 complex which results in phosphorylation of H2AX to γH2AX (c) γH2AX mediated recruitment of other DNA repair proteins to the damage site (d) Double-strand break repair and G2/M checkpoint arrest.

1.3. The significance of γH2AX assay

In response to DNA damage, γH2AX is found in chromatin as discrete nuclear foci shortly after induction of DSBs (4). γH2AX binds specifically to DNA break site in a correlative manner (14). γH2AX signal localizes to discrete foci-mark sites (Figure-2.2) with each individual foci representing one break site (Figure-1.2). Therefore, an antibody specific to γH2AX will be able to detect DNA damage in individual cells. Formation of γH2AX provides for a sensitive, indirect determination of DNA damage (9). In our lab, γH2AX assay utilizes an antibody against phosphorylated histone variant H2AX and cells are labeled with a fluorescent-tagged version of secondary antibody, followed by nuclear DNA counterstaining (with DAPI or Hoescht) and

visualized via epifluorescence microscopy. Cells are visualized under two channels, DAPI channel (blue) to visualize counterstained nuclear DNA and Texas Red (red) to visualize γH2AX foci within the nuclei of each cell. Images are taken under both channels and individual foci are counted manually on a per cell basis within a population for analysis.

In addition, γH2AX foci can be measured by other means, such as flow cytometry as well as Western blotting of cell/tissue lysates, multiparameter flow or laser scanning cytometry. γH2AX signals can also be correlated with DNA content and induction of apoptosis. This immunostaining method is less cumbersome and more sensitive (4). Measurement of γH2AX serves as a surrogate marker for DSB induction with chemo-radiotherapy in order to track treatment efficacy, dose/scheduling estimation and to determine the efficiency of DNA repair in evaluating tumour sensitivity/resistance to DNA damaging anticancer agents (4)(7).

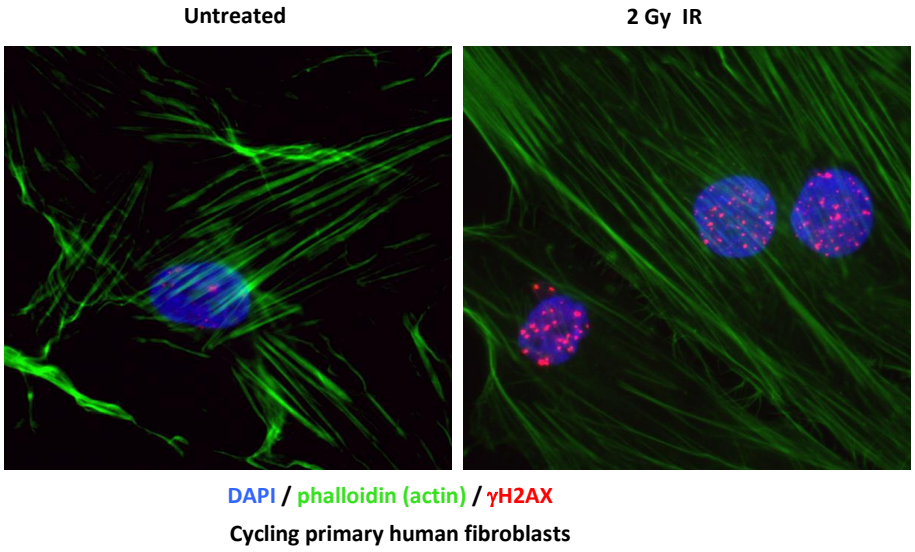

Figure-2.2. Primary Human Fibroblasts showing individual foci in nuclei following damage to DNA. Each of foci represents one DNA strand break or break site.

1.4. Antibody-free (less) γH2AX assay

The conventional γH2AX assay utilizes antibody against phosphorylated histone variant H2AX and the cells are tagged with the fluorescently labeled secondary antibody. The steps in fixing, permeabilizing and immuno-labelling cells for γH2AX analysis are long and cumbersome. We sought to develop an antibody-free method of detecting endogenous damage. Using unique

reagents, I developed 'stable cell lines' comprised of two constructs; mCherry-53BP1 (DNA damage marker) and H2B-GFP (nuclear marker) (detailed in Method & Material section). The usage of an endogenous mCherry-53BP1 labeling strategy provides for an antibody-less method to identify and track DNA breaks. It is also amenable to high-throughput analysis and screening and an effective real-time DNA break reporter functioning in a more dynamic and streamlined manner equivalent to the more cumbersome γH2AX immunostaining methodology.

The manual method involves growing cells on sterilized coverslips in each well of a 24 well plate. Cells are seeded onto the coverslips to attach, allowed to grow followed by cell treatments/experiments. One coverslip represents one treatment group. The cells are washed and fixed with paraformaldehyde, permeabilized with detergent followed by incubation with primary anti-γH2AX antibody, washed, treatment with fluorescent secondary antibody, more washing and then counterstained with a nuclear marker. Coverslips are then mounted onto microscope slides with mounting media. The analysis is carried out in dark room and cell images are taken for each coverslip/condition. The individual foci per cell are then counted, derived from the individual images. The innovation of the dual vector double-stable lines is the streamlining of the cell preparation following treatments. Cells can simply be visualized in realtime and kinectically, if microscopy is integrated with automated incubation. Alternatively, cells can undergo fixation with 1% paraformaldehyde and immediate visualization upon mounting onto slides. These cells are also amenable for incubation and visualization in 96/384-well imaging plates thus enabling the potential for drug screening studies.

2. Methods & Materials

2.1. ***Establishment and validation of stable mCherry-53BP1 (DNA damage marker) and H2B-GFP (nuclear marker) MB and GBM lines*** - Stable cell lines of both GBM and MB cells was established with the two nuclear markers mCherry-BP1-2 plPC-Puro (Addgene plasmid # 19835) and H2B-GFP (Addgene #11680). The mCherry-BP1-2 plPC-Puro (Addgene #19835) contains a fragment of p53 binding protein 1 (53BP1) fused to a fluorescent tag (mCherry). The 53BP1 fragment localizes to DNA break sites and appears as distinct nuclear foci. These foci are also comprised of DNA damage induced phosphorylated (S139) histone 2A.X variant (γH2AX) and are usually quantified using a highly specific rabbit monoclonal anti-γH2AX antibody (clone

17D3, Cell Signaling Technologies, USA) and a fluorescently-tagged anti-rabbit secondary antibody (Molecular Probes) via epifluorescence microscopy. Therefore, the mCherry-53BP1 labeling strategy is a high-throughput and effective real-time DNA break reporter functioning in a more dynamic and streamlined manner equivalent to the more cumbersome γH2AX immunostaining methodology. The H2B-GFP (Addgene #11680) fusion protein integrates into the cellular histone core to serve as a nuclear marker.

Cell lines were transfected with H2B-GFP and cells have undergone G418 (G418 Disulfate salt solution-10ml, 50mg/ml, SIGMA ALDRICH, USA) selection at 150µg/ml for 5 days. Highly expressing GFP+ colonies were isolated and expanded. Stable H2B-GFP cells were then transfected with mCherry-53BP1 and selected with puromycin (P9620, SIGMA ALDRICH, USA) at 1µg/ml for 5 days and then expanded. Epifluorescence microscopy was used to ensure cellular homogeneity of co-expressed H2B-GFP and mCherry-53BP1. Furthermore, ϒH2AX immunostaining (Alexa Fluoro 647 anti-H2AX,125µl, 25µg/ml, Cat# 92121, Biolegend, Santiago, CA 92121, USA) was used to validate the correct localization of mCherry-53BP1 fusion protein to DNA damage-induced foci.

2.2. Foci assay using stable reporter lines (pmCherry-53BP1) - Cells were seeded in a 96-well flat-bottomed imaging plate (Corning, USA). Cells are treated with Topoisomerase I inhibitor, Camptothecin (1µm, 5µm, 10µm) for 1hr. The cells are washed three times with PBS. The cells are fixed with 0.5ml 4% PFA at room temperature for 10 minutes. After fixation, the cells are washed three times with PBS. Cells are permeabilized by adding 0.5% TX100 in PBS for 4 minutes at room temperature and then washed three times with PBS and conjugated antibody (1:500) is added and kept overnight. The next day cells are again washed three times with PBS. Cellular 53BP1-mCherry DNA damage foci wias imaged under DAPI, Texas Red, Cy5 channels with Cytation 5 (Biotek) high-content imaging system (HCS) at 10x magnification and image analysis software.

3. Results

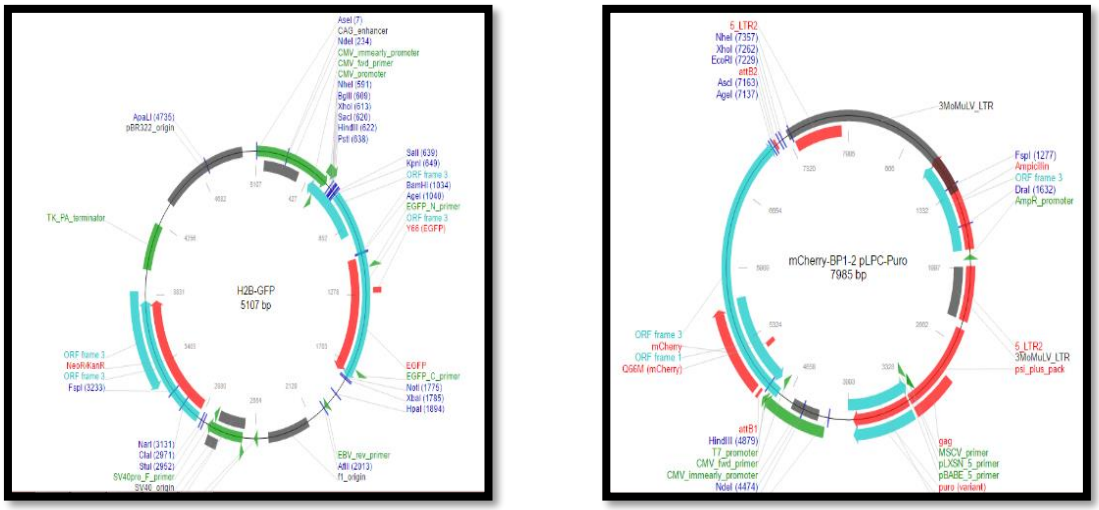

Figure-3.1. Plasmid construct for H2B-GFP, nuclear marker and mCherryBP1-2, endogenous DNA break marker

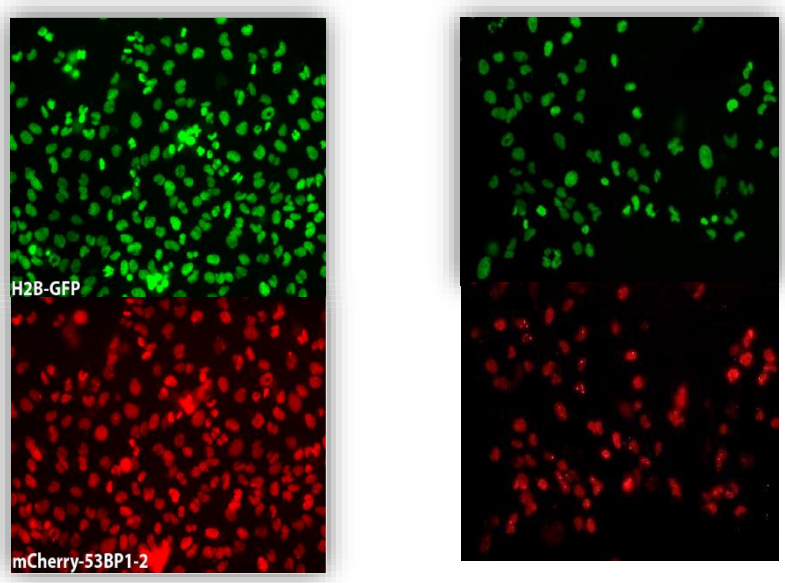

Figure-3.2. Established stable cell lines of Glioblastoma Multiforme (GBM). The green cells denote successful transfection and selection of H2B-GFP nuclear marker in GBM cells. Similarly, the same cell under Texas red channel denotes successful transfection and selection of mCherry BP1-2, endogenous DNA break marker in GBM cells.

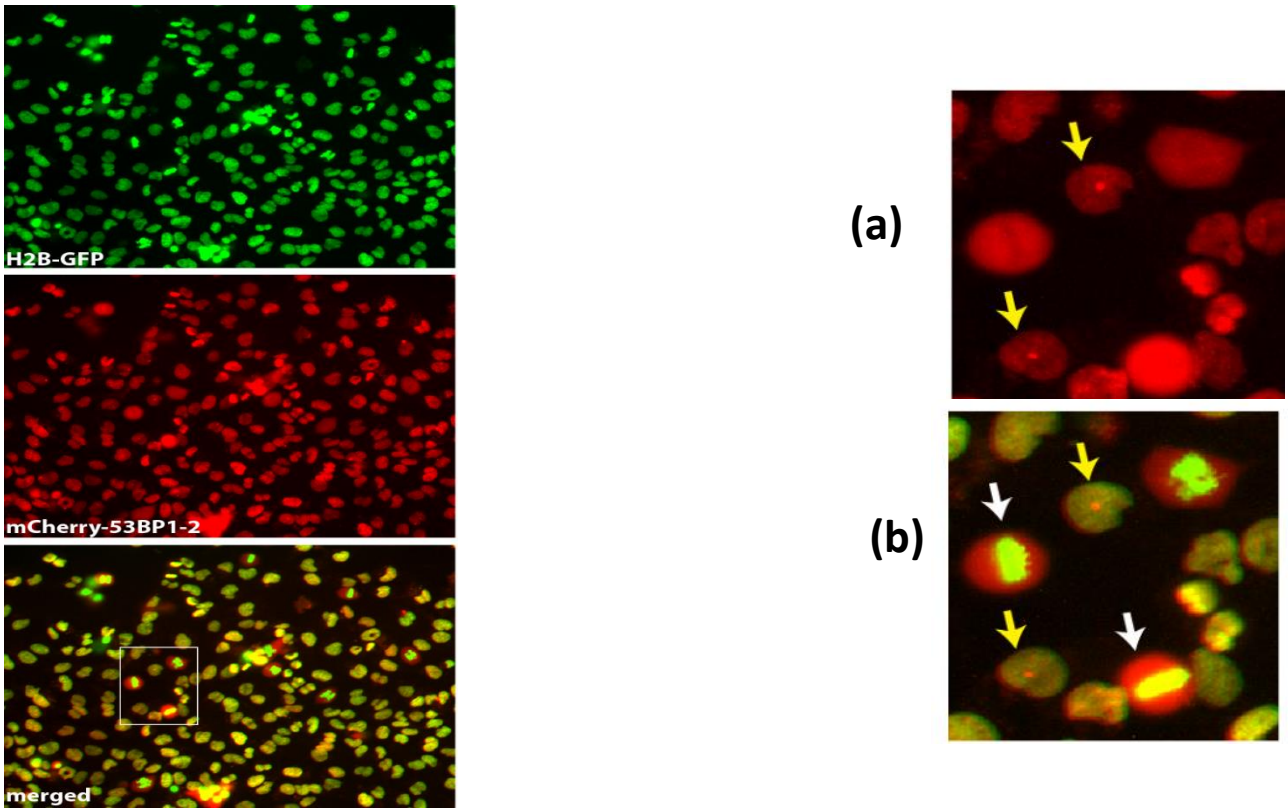

Figure-3.3. U251MG stable cell line integrated with H2B-GFP (nuclear marker) and mCherry BP1-2: a 53BP1 fragment which localizes to γH2AX-marked DNA break sites (endogenous break marker). The green one denotes H2BGFP marker and red one mCherry53BP1. (a) The cells pointed with a yellow arrow there indicates presence of foci which can be seen under red light and not under green light denoting that mCherry 53BP1 is serving as an endogenous damage marker (b) The cells pointed with white arrows denote that H2BGFP is labeling chromatin-associated histones only and mCherry BP1-2, as free proteins with no damage induced.

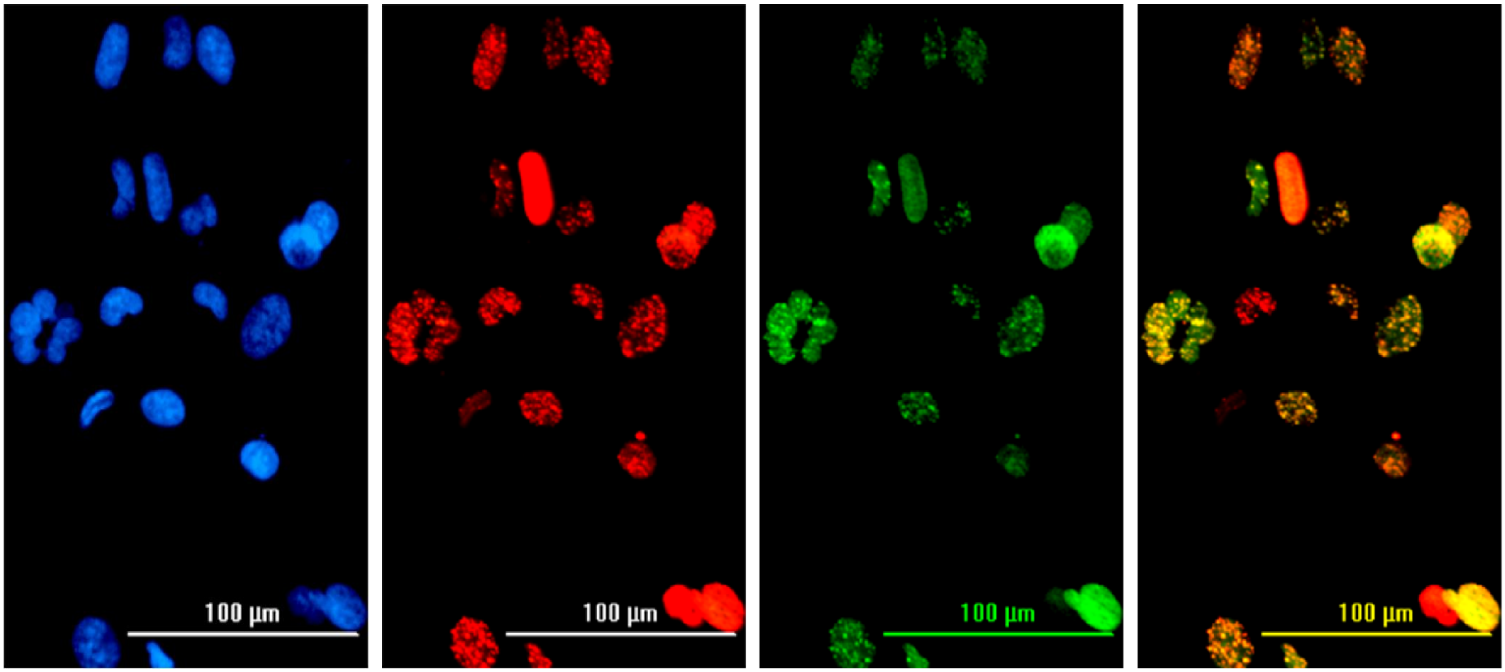

(a) DAPI **(b) mCherry -53BP1 Fragment** **(c) γH2AX AB** **(d) Merged**

Figure-3.4. Validation of stable reporter lines. The cells were treated with 5µm Topoisomerase I inhibitor, Camptothecin (a) DAPI (blue) channel represents the cell nucleus (b) Individual foci with endogenous DNA damage marker mCherry- 53BP1 fragment (c) Individual foci with conjugated γH2AX antibody (d) merged picture of (b) and (c) show the same localization of γH2AX foci with the γH2AX conjugated antibody and 53BP1 endogenous marker, denoting that both have the same localization on the break site.

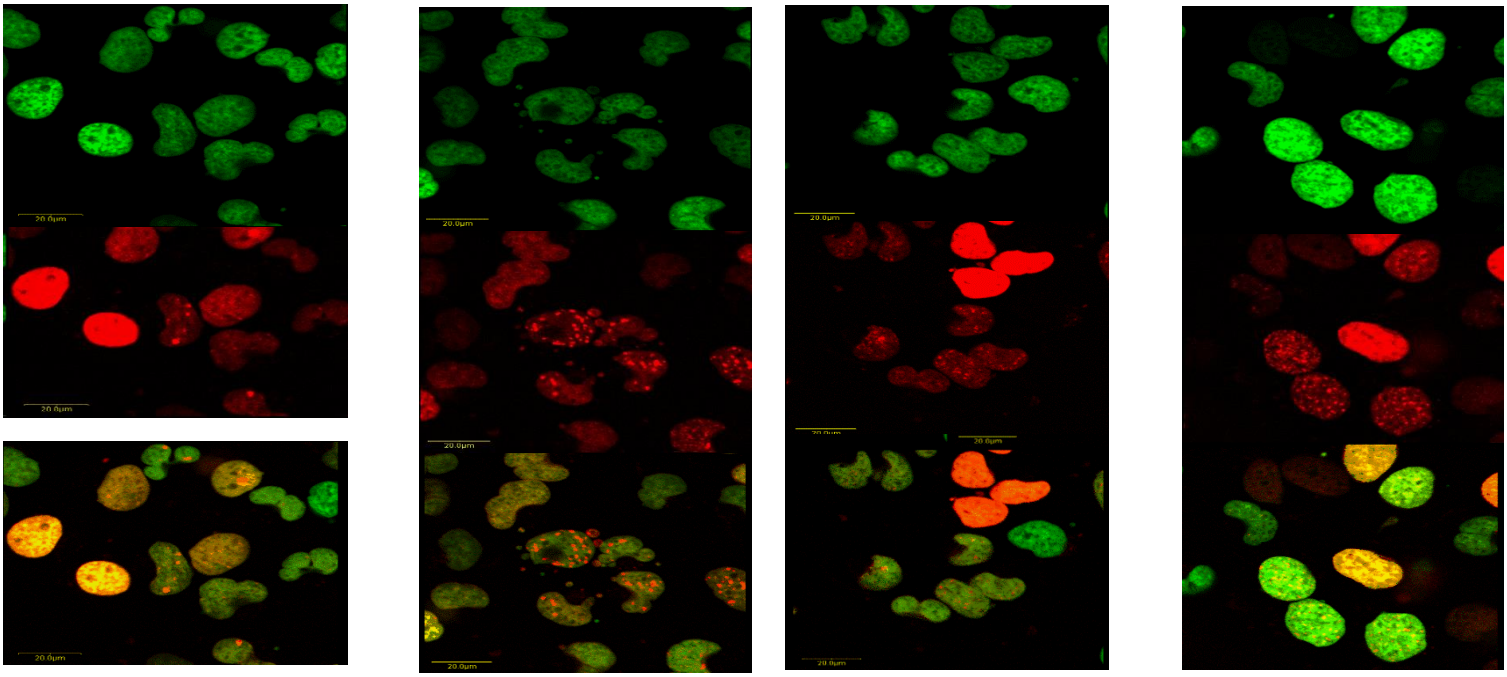

U251: No treatment | U251: 1µM | U251: 5µM CPT | U251: 10µM CPT

Figure-3.5. Foci assay with stable reporter line U251MG. Foci assay was performed with the Topoisomerase I inhibitor, Camptothecin. A dose-response curve was used with a concentration gradient of the drug (1µm, 5µm and 10µm). As the concentration of the drug increases, the number of foci per cell increases with the most number of foci at 10µm. Some of the cells at 10µm dose are highly damaged and appear to have a pan-nuclear γH2AX signal.

4. Future directions and significance

Using the coverslip method of traditional antibody-based gH2AX analysis, it takes one day to manually image and analyze ten slides; almost 10 days to analyze 96 slides. Thus, having multiple cells, conditions can make the entire process and output cumbersome. Furthermore, counting individual foci manually can be subject to inadvertent user bias and fatigue thus skewing the results. Recently, our lab has developed an automated method of γH2AX foci detection and analysis, utilizing our GEN5 high content imaging system afforded by our Cytation 5 system.

We have employed a dual mask analysis parameter for analysis of the γH2AX foci (15). The primary cellular mask will be used to first delineate each individual cell nuclei in the image (GFP-H2B) whereby a secondary cellular mask analysis will be applied demarcating each individual foci (pmCherry-53BP1). Using this method, the average number of individual foci per cell and within a cell population can be quickly and accurately analyzed and quantified (15). It takes about half an hour to image and analyze one 96 well plate, representing a 160-fold improvement in analysis time. Combined, this methodology and my double-stable cell lines enabled us to perform High-Troughput-γH2AX assays in an accurate and expedient manner; a highly unique capability that is currently one-of-its kind.

The double-stable cell lines have been developed with the expressed purpose of performing drug screening studies, using combinations of agents, drugs and/or inhibitors to identify new treatment combinations that impart increased tumor genotoxicity. Radiation can also be employed to quantify damage and repair kinetics of these tumour cells. These lines will also be screened against chemical libraries (i.e. FDA-approved drug library) to identify agents with unrecognized genotoxic and chemosensitizing functions thus enabling a powerful tool to repurpose known agents and increasingly the arsenal of anti-cancer therapeutics.

5. References

1. Jackson SP, Bartek J. The DNA-damage response in human biology and disease. Nature [Internet]. 2009;461(7267):1071–8. Available from: http://dx.doi.org/10.1038/nature08467

2. Santivasi WL, Xia F. The role and clinical significance of DNA damage response and repair pathways in primary brain tumors. 2013;1–6.

3. Ciccia A, Elledge SJ. The DNA Damage Response: Making It Safe to Play with Knives. Mol Cell. 2010;40(2):179–204.

4. Podhorecka M, Skladanowski A, Bozko P. H2AX Phosphorylation : Its Role in DNA Damage Response and Cancer Therapy. 2010;2010.

5. Meyer B, Voss KO, Tobias F, Jakob B, Durante M, Taucher-Scholz G. Clustered DNA damage induces pan-nuclear H2AX phosphorylation mediated by ATM and DNA-PK. Nucleic Acids Res. 2013;41(12):6109–18.

6. Rogakou E, Martin OA, Redon C, Pilch D, Rogakou E, Sedelnikova O, et al. Histone H2A variants H2AX and H2AZ . Curr Histone H2A variants H2AX and H2AZ. Curr Opin Genet Dev. 2016;(May 2002):162–9.

7. Takahashi A, Ohnishi T. Does γH2AX foci formation depend on the presence of DNA double strand breaks? Cancer Lett. 2005;229(2):171–9.

8. Bártová E, Kreǰcí J, Harničarová A, Galiová G, Kozubek S. Histone modifications and nuclear architecture: A review. J Histochem Cytochem. 2008;56(8):711–21.

9. Ivashkevich A, Redon CE, Nakamura AJ, Martin RF, Martin OA. NIH Public Access. 2013;327:123–33.

10. Kurz EU, Lees-Miller SP. DNA damage-induced activation of ATM and ATM-dependent signaling pathways. Vol. 3, DNA Repair. 2004. p. 889–900.

11. Shiloh Y. The ATM-mediated DNA-damage response. Mol Oncol Causes Cancer Targets Treat. 2015;31(7):403–22.

12. Durocher D, Jackson SP. DNA-PK, ATM and ATR as sensors of DNA damage:

Variations on a theme? Curr Opin Cell Biol. 2001;13(2):225–31.

13. Kitagawa R, Kastan MB. The ATM-dependent DNA Damage Signaling Pathway The ATM-dependent DNA Damage Signaling Pathway. 2005;LXX:99–109.

14. Kuo LJ, Yang L-X. γ-H2AX - A Novel Biomarker for DNA Double-strand Breaks. In Vivo (Brooklyn) [Internet]. 2008;22(3):305–9. Available from: http://iv.iiarjournals.org/content/22/3/305%5Cnhttp://iv.iiarjournals.org/content/22/3/305.full.pdf%5Cnhttp://www.ncbi.nlm.nih.gov/pubmed/18610740

15. Larson B, Instruments B. p p l i c a t i o n o t e Automated Imaging and Dual-Mask Analysis of γ H2AX Foci to Determine DNA Damage on an Individual Cell Basis.